

This electronic thesis or dissertation has been downloaded from the King's Research Portal at <https://kclpure.kcl.ac.uk/portal/>



## **Cationic lipid formulation of short interference RNA (siRNA) for delivery to respiratory epithelial cells**

Betkaoui, Radia

*Awarding institution:*  
King's College London

The copyright of this thesis rests with the author and no quotation from it or information derived from it may be published without proper acknowledgement.

### **END USER LICENCE AGREEMENT**



**Unless another licence is stated on the immediately following page** this work is licensed

under a Creative Commons Attribution-NonCommercial-NoDerivatives 4.0 International

licence. <https://creativecommons.org/licenses/by-nc-nd/4.0/>

You are free to copy, distribute and transmit the work

Under the following conditions:

- Attribution: You must attribute the work in the manner specified by the author (but not in any way that suggests that they endorse you or your use of the work).
- Non Commercial: You may not use this work for commercial purposes.
- No Derivative Works - You may not alter, transform, or build upon this work.

Any of these conditions can be waived if you receive permission from the author. Your fair dealings and other rights are in no way affected by the above.

### **Take down policy**

If you believe that this document breaches copyright please contact [librarypure@kcl.ac.uk](mailto:librarypure@kcl.ac.uk) providing details, and we will remove access to the work immediately and investigate your claim.

This electronic theses or dissertation has been downloaded from the King's Research Portal at <https://kclpure.kcl.ac.uk/portal/>



**Title:** Cationic lipid formulation of short interference RNA (siRNA) for delivery to respiratory epithelial cells

**Author:** Radia Betkaoui

The copyright of this thesis rests with the author and no quotation from it or information derived from it may be published without proper acknowledgement.

#### END USER LICENSE AGREEMENT



This work is licensed under a Creative Commons Attribution-NonCommercial-NoDerivs 3.0 Unported License. <http://creativecommons.org/licenses/by-nc-nd/3.0/>

You are free to:

- Share: to copy, distribute and transmit the work

Under the following conditions:

- Attribution: You must attribute the work in the manner specified by the author (but not in any way that suggests that they endorse you or your use of the work).
- Non Commercial: You may not use this work for commercial purposes.
- No Derivative Works - You may not alter, transform, or build upon this work.

Any of these conditions can be waived if you receive permission from the author. Your fair dealings and other rights are in no way affected by the above.

#### Take down policy

If you believe that this document breaches copyright please contact [librarypure@kcl.ac.uk](mailto:librarypure@kcl.ac.uk) providing details, and we will remove access to the work immediately and investigate your claim.

**Cationic lipid formulation of short interference RNA (siRNA) for  
delivery to respiratory epithelial cells**

**Radia Betkaoui**

October 2011

**A thesis submitted for the degree of  
Doctor of Philosophy**

Pharmaceutical Science Division

King's College London

Franklin-Wilkins Building

150 Stamford Street

London SE1 9NH

## **Certificate**

This is to certify that research work embodied in this thesis entitled “Formulation of short interference RNA (siRNA) for delivery to respiratory epithelial cells” has been carried out by me under supervision and guidance of Dr Benjamin Forbes and Dr Nilesh Patel.

Radia Betkaoui

# Abstract

Cationic lipids are commonly used and relatively safe vectors for plasmid (pDNA) delivery. In search for an optimal lipid-based formulation for siRNA delivery to the lungs, cationic lipid-based carriers were investigated for the delivery of siRNA in comparison with pDNA delivery. The aim was to determine whether the factors that influence cationic-lipid mediated pDNA delivery would similarly affect siRNA delivery.

Plasmid DNA encoding for luciferase and GAPDH siRNA were complexed using three model cationic lipid-based systems; DOTAP:DOPE, DOTAP:DOPE:DMPE-PEG<sub>5000</sub>, DOTAP:DOPE:protamine. Cationic lipid/pDNA (+/-) charge ratio of 2 or greater complexed pDNA most efficiently, while much higher ratios ( $\geq 10$ ) were still less efficient in complexing siRNA. pDNA complexes were larger (up to 4  $\mu\text{m}$ ) and formed aggregates in physiological buffer, compared to water, whereas siRNA complexes remained small (<300 nm). Gene silencing in bronchial and alveolar cell lines Calu-3 and A549 revealed a dependency on high lipid/siRNA (+/-) charge ratio ( $> 8$ ) compared to the delivery of pDNA complexes (0.5-1). Confocal microscopy and endocytic inhibitors studies indicated that the cellular uptake of siRNA/lipid complexes was via a temperature-dependent pathway, which lead to the vesicular localisation of siRNA in the peri-nuclear region. Gene silencing activity was not dependent on the endocytosis-mediated uptake of the complexes. In conclusion, important differences in the factors that affect of siRNA *versus* pDNA delivery were revealed: the optimal properties of gene silencing were different depending on the nucleic acid and the lipid used. DOTAP:DOPE:DMPE-

PEG<sub>5000</sub> and DOTAP:DOPE:protamine at charge ratios 8-10 delivered siRNA most effectively.

# Table of Contents

Abstract .....	3
Table of Contents.....	5
List of Figures.....	14
List of Tables .....	22
List of abbreviations .....	23
Publications .....	26
Acknowledgments .....	27
Chapter 1. Introduction.....	28
1.1. Nucleic acid therapy, gene expression and gene silencing.....	29
1.2. RNA interference (RNAi) .....	31
1.2.1. siRNA as a therapeutic tool .....	32
1.3. Delivery vectors for nucleic acids.....	35
1.3.1. Viral vectors.....	35
1.3.2. Non-viral vectors.....	36
1.3.3. Cationic lipids as gene delivery vectors .....	40
1.4. Delivery of pDNA vs siRNA using cationic lipids .....	41
1.4.1. Cationic lipid/nucleic acid complex formation.....	43
1.4.2. Structure of the complexes .....	43
1.4.3. Physicochemical properties .....	44
1.4.3.1. Complexation efficiency.....	45

1.4.3.2. Particle size .....	45
1.4.3.3. Zeta potential.....	46
1.4.4. Influence of charge ratio on physical properties .....	47
1.5. Challenges of gene delivery.....	48
1.5.1. Cellular binding and internalisation .....	48
1.5.2. Endosomal escape .....	49
1.5.3. Nuclear translocation and entry .....	50
1.5.4. Stability of the complexes .....	51
1.5.5. Toxicity.....	52
1.6. Cellular uptake mechanisms .....	53
1.6.1. Endocytic uptake pathways .....	53
1.6.1.1. Clathrin-mediated endocytosis.....	54
1.6.1.2. Caveolin-mediated endocytosis .....	55
1.6.1.3. Macropinocytosis .....	56
1.6.1.4. Caveolae and clathrin-independent endocytosis .....	57
1.6.2. Non-endocytic pathways .....	58
1.7. Formulation strategies to improve delivery of nucleic acids.....	59
1.7.1. Helper lipids.....	59
1.7.2. Polyoxyethylene glycol polymers .....	60
1.7.3. Pre-condensation with a polycation .....	61
1.8. Aims and objectives of the thesis.....	63



Chapter 2. The effect of physicochemical characteristics on cationic lipid-mediated DNA delivery <i>in vitro</i> .....	64
2.1. Introduction:.....	65
2.1.1. Cationic lipid formulation used in this study.....	66
2.1.2. Physicochemical characterization of pDNA complexes .....	68
2.1.3. Transfection of respiratory epithelial cells by pDNA .....	69
2.1.3.1. Calu-3 cells .....	69
2.1.4. Aim and objectives.....	71
2.2. Materials .....	72
2.3. Methods: .....	74
2.3.1. Plasmid DNA preparation.....	74
2.3.1.1. Plasmid pDNA amplification and purification .....	74
2.3.1.2. Plasmid pDNA verification and quantification.....	74
2.3.2. Liposome preparation.....	75
2.3.3. Preparation of cationic liposomes and pDNA complexes .....	76
2.3.4. Physicochemical characterization of cationic liposome/pDNA complexes ..	77
2.3.4.1. Assessment of complexation efficiency .....	77
2.3.4.2. Light scattering and zeta potential measurements.....	78
2.3.5. Cell culture.....	79
2.3.6. Transfection experiments.....	80
2.3.6.1. Luciferase activity .....	80

2.3.6.2. Protein Assay .....	81
2.3.6.3. MTT toxicity studies .....	81
2.3.6.4. Calibration curves for MTT test.....	82
2.3.6.5. Cytotoxicity of pDNA/lipid complexes.....	83
2.3.7. Statistical tests.....	83
2.4. Results .....	85
2.4.1. pDNA characterization.....	85
2.4.2. Complexation efficiency as a function of charge ratio.....	86
2.4.3. Changes in particle size and zeta potential as a function of charge ratio .....	92
2.4.4. Transfection efficacy .....	97
2.4.5. MTT toxicity study.....	101
2.5. Discussion.....	104
2.5.1. Effect of charge ratio on physicochemical properties of pDNA complexes	104
2.5.1.1. Characterization in water .....	104
2.5.1.2. Characterization at physiological salt concentration.....	107
2.5.2. Relationship between physicochemical properties and transfection.....	110
2.5.3. Transfection <i>versus</i> toxicity.....	113
2.5.4. Conclusion .....	114
Chapter 3 <i>In vitro</i> delivery of siRNA using cationic lipid delivery vectors.....	116
3.1. Introduction:.....	117

3.1.1.	siRNA assays using respiratory epithelial cells <i>in vitro</i> .....	118
3.1.2.	Aim and objectives .....	119
3.2.	Materials .....	120
3.3.	Methods .....	121
3.3.1.	GAPDH siRNA and negative control siRNA .....	121
3.3.2.	Preparation of cationic liposomes/siRNA complexes .....	121
3.3.3.	Characterization of cationic liposome/siRNA complexes .....	122
3.3.3.1.	SYBR green II intercalation assay .....	122
3.3.3.2.	Light scattering and zeta potential.....	123
3.3.4.	The optimisation of transfection conditions for the positive control .....	124
3.3.5.	Determining protein knock down and toxicity using KDalert assay kit .....	125
3.3.6.	Transfection of bronchial epithelial cell line, Calu-3 .....	126
3.3.7.	Transfection of alveolar epithelial cell line, A549 .....	127
3.3.8.	The effect of serum on gene silencing efficiency .....	127
3.3.9.	Data analysis and statistics .....	127
3.4.	Results .....	129
3.4.1.	SYBR green II intercalation assay .....	129
3.4.2.	Particle size and polydispersity of siRNA complexes .....	131
3.4.3.	Optimisation of the transfection conditions .....	133
3.4.4.	Transfection of Calu-3 cells with siRNA .....	136
3.4.5.	Transfection of A549 cells with siRNA .....	139

3.4.6. Cell viability.....	142
3.4.7. The effect of serum on the gene silencing efficiency.....	144
3.5. Discussion.....	145
3.5.1. Condensation efficiency as a function of charge ratio .....	145
3.5.2. Particle size as a function of charge ratio .....	147
3.5.3. Gene silencing efficiency of siRNA complexes: .....	148
3.5.3.1. Gene silencing efficiency and physical properties of the complexes .....	149
3.5.3.2. Gene silencing and cytotoxicity in Calu-3 vs A549 cells.....	150
3.5.3.3. Effect of serum on gene silencing .....	151
3.5.4. Delivery of pDNA <i>versus</i> siRNA .....	152
3.5.5. Conclusion .....	153
Chapter 4. The mechanism of cellular uptake of functional siRNA/lipid complexes.....	155
4.1. Introduction.....	156
4.1.1. Aim and objectives.....	160
4.2. Materials .....	161
4.3. Methods: .....	162
4.3.1. siRNA complex localization studies .....	162
4.3.2. Temperature adjustment .....	163
4.3.3. Colocalization of siRNA complexes with Alexa Fluor 488-transferrin and BODIPY-LacCer .....	164

4.3.3.1. Colocalization with Alexa Fluor 488-transferrin .....	164
4.3.3.2. Colocalization with BODIPY-LacCer.....	164
4.3.4. Optimisation of endocytosis inhibitors concentrations .....	165
4.3.4.1. MTT screening of the endocytosis inhibitors .....	165
4.3.4.2. Inhibition of transferrin uptake via the clathrin-mediated endocytosis....	166
4.3.4.3. Inhibition of BODIPY-LacCer via caveolae-mediated endocytosis .....	167
4.3.4.4. Effect of endocytosis inhibitors on the cell viability after 7 h exposure. .	168
4.3.5. Gene silencing in A549 cells with siRNA complexes after inhibition of endocytic pathways.....	168
4.3.5.1. Inhibition of the clathrin-mediated endocytosis.....	168
4.3.5.2. Inhibition of caveolae and macropinocytosis.....	169
4.3.6. Gene silencing in A549 cells after combined inhibition of endocytic pathways.....	169
4.3.7. Data analysis and statistics .....	170
4.4. Results .....	171
4.4.1. siRNA complexes subcellular localization.....	171
4.4.2. Functional siRNA complexes uptake is temperature-dependent .....	171
4.4.3. Optimisation of endocytosis inhibitors concentrations .....	176
4.4.3.1. MTT screening of endocytosis inhibitors .....	176
4.4.3.2. Inhibition of transferrin uptake via the clathrin-mediated pathway .....	179
4.4.3.3. Inhibition of BODIPY-LacCer via the caveolae-mediated endocytosis ..	182

4.4.3.4. Effect of endocytosis inhibitors after exposure to cells for a duration equivalent to the duration of transfection experiment .....	184
4.4.4. Role of Clathrin-mediated endocytosis in the uptake of functional siRNA	185
4.4.5. Role of Caveolae-mediated endocytosis and macropinocytosis in the uptake of functional siRNA.....	190
4.4.6. The effect of combined inhibition of endocytosis pathways on the silencing efficiency of siRNA complexes.....	194
4.5. Discussion.....	196
4.5.1. Peri-nuclear localization of siRNA complexes .....	196
4.5.2. siRNA complexes uptake is temperature-sensitive.....	197
4.5.3. The uptake of LPR and LpegR complexes is clathrin-dependent.....	198
4.5.4. Functional siRNA uptake is non-clathrin, non-caveolae mediated and does not depend on macropinocytosis .....	199
4.5.5. Conclusion .....	202
Chapter 5. General discussion .....	204
5.1. Introduction.....	205
5.2. Correlation between the physicochemical properties and transfection efficiency of pDNA complexes .....	207
5.3. Difference between siRNA and pDNA complexes.....	209
5.3.1. Physical properties .....	209
5.3.2. Transfection efficiency.....	211
5.4. The involvement of endocytic pathways in the uptake of siRNA complexes	213

5.5. Future challenges .....	215
Appendix. Standard Curves .....	216
References .....	220

# List of Figures

<b>Figure 1.1</b> The mechanism of RNA interference (RNAi) in mammalian cells induced by either (A) long dsRNA molecules expressed from DNA vectors or (B) directly enter the cell or (C) by small siRNAs (21–23 bp) which are directly delivered into the cell (Aigner, A., 2007). .....	34
<b>Figure 2.1</b> Chemical structures of the neutral lipid (DOPE), cationic lipid (DOTAP) and the PEG associated phospholipid (DMPE-PEG <sub>5000</sub> ). Avanti Polar Lipids, Inc website ( <a href="http://www.avantilipids.com/">http://www.avantilipids.com/</a> ).....	67
<b>Figure 2.2</b> Gel electrophoresis of a sample of pGL3 control vector after extraction and purification using Qiagen Endofree Plasmid Mega Kit. 1) Pure pGL3 obtained from (Sigma Pharmaceuticals) was used as a marker, 2) sample pGL3 control vector. ....	85
<b>Figure 2.3</b> A) Picogreen intercalation assay of LD complexes in water and HBSS. The percentage free pDNA represent the fraction of pDNA in the sample available for intercalation with picogreen reagent (n=3, mean $\pm$ SEM). B) Gel electrophoresis of LD complexes prepared at different charge ratios in water; pure pGL3 control vector was used as a marker (M).....	87
<b>Figure 2.4</b> A) Picogreen intercalation assay of LpegD complexes in water and HBSS. The percentage free pDNA represent the fraction of pDNA in the sample available for intercalation with picogreen reagent (n=3, mean $\pm$ SEM). B) Gel electrophoresis of LpegD complexes prepared at different charge ratios in water; pure pGL3 control vector was used as a marker (M) .....	89
<b>Figure 2.5</b> A) Picogreen intercalation assay of LPD complexes in water and HBSS. The percentage free pDNA represent the fraction of pDNA in the sample available	



for intercalation with picogreen reagent (n=3, mean  $\pm$ SEM). B) Gel electrophoresis of LPD complexes prepared at different charge ratios in water; purre pGL3 control vector was used as a marker (M)..... 91

**Figure 2.6** (A) Particle size, and (B) zeta potential of LD complexes prepared at the indicated charge ratios. The particle size (diameter) and zeta potential of the complexes was determined in water (clear) or after incubation in HBSS (filled) (n=3, mean  $\pm$ SEM)..... 93

**Figure 2.7** A) Particle size, and B) zeta potential of LpegD complexes prepared at the indicated charge ratios. The particle size (diameter) and zeta potential of the complexes was determined in water or after incubation in HBSS (n=3, mean  $\pm$ SEM). ..... 95

**Figure 2.8** A) Particle size, and B) zeta potential of LPD complexes prepared at the indicated charge ratios. The particle size (diameter) and particle size of the complexes was determined in water or after incubation in HBSS (n=3, mean  $\pm$ SEM). ..... 96

**Figure 2.9** Transfection of Calu-3 cells with LD complexes containing luciferase pDNA prepared at the indicated cationic lipid/pDNA charge ratios. Luciferease activity was measured 48 h post-transection and luminescence (RLU/mg) represents the level of luciferase gene expression. Lipofectamine/pDNA complexes were used as a (+) control and naked pDNA (charge ratio= 0) represent (-) control. (n=3, mean  $\pm$ SEM). \*Significant (p<0.05) difference from positive control. .... 99

**Figure 2.10** Transfection of Calu-3 cells with LpegD complexes containing luciferase pDNA prepared at the indicated cationic lipid/pDNA charge ratios. Luciferease activity was measured 48 h post-transection and luminescence (RLU/mg) represents the level of luciferase gene expression. Lipofectamine/pDNA

complexes were used as a (+) control and naked pDNA (charge ratio= 0) represent (-) control. (n=3, mean  $\pm$ SEM). \*\*Significant (p <0.01) difference from positive control. ....100

**Figure 2.11** Transfection of Calu-3 cells with LPD complexes containing luciferase pDNA prepared at the indicated cationic lipid/pDNA charge ratios. Luciferase activity was measured 48 h post-transfection and luminescence (RLU/mg) represents the level of luciferase gene expression. Lipofectamine/pDNA complexes were used as a (+) control and naked pDNA (charge ratio= 0) represent (-) control (n=3, mean  $\pm$ SEM). ....101

**Figure 2.12** Cytotoxicity of LD (A), LpegD (B) and LPD (C) complexes in Calu-3 as assessed by MTT assay. The relative cell viability as compared to untreated cells is presented as a function of charge ratios (n=3, mean  $\pm$ SEM). ....103

**Figure 3.1** SYBR green II intercalation assay for A) Lipofectamine/siRNA B) LR C) LpegR and D) LPR complexes prepared in DMEM. Complexes were prepared at the indicated charge ratios and the percentage of siRNA in the sample that is available for intercalation with SYBR Green II gel stain was determined. Naked siRNA was used as control and represents 100% free siRNA (n=3, mean  $\pm$ SEM). 130

**Figure 3.2** The changes in the particle size and size distribution of LR complexes as a function of the cationic lipid:DNA/siRNA charge ratio. The diameters (nm) and polydispersity of the complexes were determined 45 min after their preparation in serum-free cell culture media. (n=3, mean  $\pm$ SEM). ....132

**Figure 3.3** The changes in the particle size and size distribution of LpegR complexes as a function of the cationic lipid:DNA/siRNA charge ratio. The diameters (nm) and polydispersity of the complexes were determined 45 min after their preparation in serum-free cell culture media. (n=3, mean  $\pm$ SEM). ....132

<b>Figure 3.4</b> The changes in the particle size and size distribution of LPR complexes as a function of the cationic lipid:DNA/siRNA charge ratio. The diameters (nm) and polydispersity of the complexes were determined 45 min after their preparation in serum-free cell culture media. (n=3, mean $\pm$ SEM). .....	133
<b>Figure 3.5</b> The optimization of siRNA transfection in Calu-3 cells using Lipofectamine. GAPDH gene silencing (bar) and cell viability (line) were determined using KDalert assay either (A) 48 hours or (B) 72 hours post-transfection (n=3, mean $\pm$ SEM). .....	135
<b>Figure 3.6</b> GAPDH activity in arbitrary fluorescence units in Calu-3 cells measured 72h post-transfection with GAPDH and negative control siRNA complexes; A) LR, B) LpegR, C) LPR, D) Percentage specific GAPDH silencing for the three complexes (n=3, mean $\pm$ SEM). *Statistical significance as per independent t-test (p<0.05) **(p<0.01). .....	138
<b>Figure 3.7</b> GAPDH activity in arbitrary fluorescence units in A549 cells measured 72h post-transfection with GAPDH and negative control siRNA complexes; A) LR, B) LpegR, C) LPR, D) Percentage specific GAPDH silencing for the three complexes (n=3, mean $\pm$ SEM). *Statistical significance as per independent t-test (p<0.05) **(p<0.01). .....	141
<b>Figure 3.8</b> The percentage of cell viability in Calu-3 and A549 cells after transfection with A) LR, B) LpegR, and C) LPR complexes prepared at the indicated cationic lipid/siRNA charge ratios. Data represent the mean of 3 experiments with 3 replicates in each experiment (n=3, mean $\pm$ SEM). *Significant difference from control (100% cell viability) as per t-test (p< 0.05). .....	143
<b>Figure 3.9.</b> GAPDH activity measured after 72h exposure of A549 cells transfection with GAPDH and negative control siRNA complexes: LpegR and LPR at the	

indicated FBS concentrations. Data was presented as percentage GAPDH silencing (n=3, mean±SEM). \*Significant difference from control (0% serum) as per t-test (p<0.05). .....144

**Figure 4.1** Confocal images of fluorescent LPR and LpegR complexes in A549 cells 2 h post-transfection. Red fluorescence represents Cy3-GAPDH siRNA in the complexes. Blue DAPI stain was employed to highlight the nucleus. ....172

**Figure 4.2** Colocalization of Cy3 siRNA (red) and CF-DOTAP:DOPE (green) in A549 cells after 2 hour incubation with fluorescent LPR complexes. DAPI (blue) was used to stain the nucleus. Images on the lower panel are an enlarged version of images on the upper panel. ....173

**Figure 4.3** Confocal images of Cy3-GAPDH siRNA in A549 cells at 4°C. A549 cells were transfected with LpegR (A) and LPR (B) complexes for 2 hours at 4°C. The fluorescent complexes were prepared using red Cy3-GAPDH and blue DAPI was used to highlight the nucleus. ....174

**Figure 4.4** A) Gene silencing efficiency and B) cell viability of A549 cells incubated with LPR and LpegR complexes at different temperatures for 6 h. Cells were incubated at the indicated temperatures for 1 h pre-transfection and during transfection then incubated at 37°C post-transfection. Gene silencing and cell viability were measured after 72 h using KDalert assay (n=3, mean±SEM). \* Statistical significance (p<0.05, unpaired t-test). ....175

**Figure 4.5** Percentage viability of A549 cells after incubation with different concentrations of inhibitors; A) chlorpromazine, B) nystatin, C) amiloride and D) potassium depletion. Results are expressed as a percentage of the viability of untreated cells or cells treated with potassium containing buffer in the potassium

depletion experiment (Data represent mean $\pm$ SEM, n=3). \*Statistically significant (p<0.05, unpaired t-test).....178

**Figure 4.6** Uptake of Alexa Fluor 633-transferrin in A549 cells pre-treated with chlorpromazine. Confocal microscopy analysis following cell exposure to chlorpromazine at different concentrations: A) 0  $\mu$ g/ml, B) 4  $\mu$ g/ml, C) 8  $\mu$ g/ml, D) 10  $\mu$ g/ml. Cells were incubated with the inhibitor for 1 h before the addition of transferrin. Blue DAPI stain was used to highlight the nucleus. ....180

**Figure 4.7** Uptake of Alexa Fluor 633-transferrin in A549 cells pre-treated with non-clathrin inhibitors: Confocal microscopy analysis following cell exposure to A) no inhibitors, B) 25  $\mu$ g/ml nystatin, C) 10  $\mu$ g/ml cytochalasin D, D) 8 $\mu$ g/ml amiloride. Cells were incubated with the inhibitors for 1 h before the addition of transferrin. Blue DAPI stain was used to highlight the nucleus.....181

**Figure 4.8** Uptake of Alexa Fluor 633-transferrin in A549 cells exposed to (A) potassium containing buffer and (B) potassium depletion. Blue DAPI stain was used to highlight the nucleus. ....182

**Figure 4.9** Uptake of BODIPY-LacCer in A549 cells pre-treated with nystatin. Confocal images of uptake in cells treated with different concentrations of nystatin: (A) 0  $\mu$ g/ml, (B) 10  $\mu$ g/ml, (C) 20  $\mu$ g/ml, (D) 25  $\mu$ g/ml. Cells were incubated with the inhibitor for 1 h before the addition of green BODIPY-LacCer. Blue DAPI stain was used to highlight the nucleus. ....183

**Figure 4.10** Viability of A549 cells treated for 7 h with endocytosis inhibitors. Treatments were: nystatin (25  $\mu$ g/ml), cytochalasin D (10  $\mu$ g/ml), amiloride (8  $\mu$ g/ml) or chlorpromazine (7.5  $\mu$ g/ml – low, and 10  $\mu$ g/ml). Cell viability was measured using the MTT assay and results are expressed as a percentage of the

viability of untreated cells (Data represent mean $\pm$ SEM, n=3). \*Statistically significant (p<0.05, unpaired t-test).....184

**Figure 4.11** Co-localization of Cy-3 labeled LPR and LpegR complexes with Alexa Fluor 488-transferrin in A549 cells. Cells were co-incubated with fluorescent siRNA complexes and transferrin (green) for 2 h prior to analysis by confocal microscopy. Blue indicates DAPI-stained nucleus.....186

**Figure 4.12** (A) Gene silencing efficiency and (B) cell viability of A549 cells after exposure to potassium depletion and subsequent transfection with LPR and LpegR complexes. Cells transfected in the presence of potassium were used as control. Gene silencing and cell viability were determined 72 h post-transfection by KDalert assay. (Data represent mean $\pm$ SEM, n=3). .....188

**Figure 4.13** A) Gene silencing and B) cell viability of A549 cells after pre-treatment with chlorpromazine and subsequent transfection with LPR complexes, as well as C) Gene silencing and D) cell viability after transfection with LpegR complexes. Cells were exposed to chlorpromazine for 1 h, followed by incubation with complexes for 6 h in the absence (grey bars) or presence (white bars) of the inhibitor. Control represent cells transfected with LPR or LpegR complexes without treatment with inhibitors at all (Black bars) (Data represent mean $\pm$ SEM, n=3). \* Statistically significant (p<0.05, unpaired t-test).....189

**Figure 4.14** Colocalization studies of LPeg-Cy3-R complexes with BODIPY-LacCer in A549 cells. Cells were first incubated with BODIPY-LacCer (green) for 30 min at 4°C, followed by incubation with Lpeg-Cy3-R complexes for another 90 min at 37°C prior to analysis with confocal microscopy. Blue indicates DAPI-stained nucleus.....191

**Figure 4.15** A) Gene silencing and B) cell viability of A549 cells when exposed to LPR complexes after pretreatment with inhibitors of non-clathrin mediated endocytosis. Pre-treatment with nystatin 25 µg/ml, amiloride 8 µg/ml or cytochalasin D 10 µg/ml for 1 h, followed by transfection with LPR complexes in the absence (grey bars) or presence of the inhibitor (white bars) for 6 h. Gene silencing and cell viability were measured 72 h post-transfection using KDAlert assay. Data represent the mean of three independent experiments (mean±SEM). \*Statistically significant (( $p < 0.05$ , unpaired t-test) .....192

**Figure 4.16** (A) Gene silencing and (B) cell viability of A549 cells when exposed to LpegR complexes after pretreatment with inhibitors of non-clathrin mediated endocytosis. Pre-treatment with nystatin 25 µg/ml, amiloride 8 µg/ml or cytochalasin D 10 µg/ml for 1 h, followed by transfection with LpegR complexes in the absence (grey bars) or presence of the inhibitor (white bars) for 6 h. Gene silencing and cell viability were measured 72 h post-transfection using KDAlert assay. Data represent the mean of three independent experiments (mean±SEM). \*Statistically significant (( $p < 0.05$ , unpaired t-test) .....193

**Figure 4.17** A) Gene silencing and B) cell viability of A549 cells after pre-treatment with combinations of the endocytic inhibitors. Pre-treatment for 1 h, followed by transfection with LpegR complexes in the presence of the inhibitors. Gene silencing and cell viability were measured 72 h post-transfection using the KDAlert assay. (Data represent mean±SEM,  $n=3$ ). Statistically significant (\* $p < 0.05$ , \*\*\*  $p < 0.001$ , One-Way Anova, Tukey's test).....195

# List of Tables

<b>Table 1-1</b> Main differences between plasmid DNA (pDNA) and short interference RNA (siRNA). .....	42
<b>Table 2-1</b> A summary of the formulations used in this study.....	68
<b>Table 4-1</b> Description of the three major endocytic pathways and the chemicals used to inhibit them.....	159



## List of abbreviations

AD	Aerodynamic diameter
AFM	Atomic force microscopy
AMD	Age-related macular degeneration
ANOVA	Analysis of variance
CF	Cystic fibrosis
CFTR	Cystic fibrosis transmembrane conductance regulator
DAPI	4',6-diamidino-2-phenylindole
DMEM	Dulbecco's Modified Eagle's Medium
DMF	Dimethylformamide
DMPE	1,2-Bis(dimethylphosphino)ethane
DMRIE-C	1,2-dimyristyloxypropyl-3-dimethyl- hydroxy ethyl ammonium bromide) and cholesterol.
DMSO	Dimethylsulfoxide
DNA	Deoxyribonucleic acid
DOPE	1,2-Dioleoyl- <i>sn</i> -glycero-3-phosphoethanolamine
DOTAP	1,2 Dioleoyl-3-trimethylammonium-propane
DOTMA	N-[1-(2,3-dioleyloxy)propyl]-N,N,N-trimethylammonium chloride
DPI	Dry powder inhaler
DSPE	1,2-Distearoyl-phosphatidylethanolamine
EDTA	Ethylenediaminetetraacetic acid
EGFR	Epidermal growth factor
ER	Endoplasmic reticulum

FBS	Foetal bovine serum
GAPDH	Glyceraldehyde 3-phosphate dehydrogenase
GL	Genzyme lipid
HBSS	Hank's Balanced Salt Solution
HIV	Human immunodeficiency virus
IFN	Interferon
kD	kiloDalton
LB	Luria Bertani
LD	Lipid (DOTAP:DOPE)/pDNA
LDLR	Low density lipoproteins receptor
LPD	Lipid (DOTAP:DOPE)/polycation/pDNA
LPegD	Lipid (DOTAP:DOPE:DMPE-PEG <sub>5000</sub> )/pDNA
LpegR	Lipid (DOTAP:DOPE:DMPE-PEG <sub>5000</sub> )/siRNA
LPR	Lipid (DOTAP:DOPE)/polycation/siRNA
LR	Lipid (DOTAP:DOPE)/siRNA
MPG $\alpha$	N-methylpurine-DNA glycosylase-Alpha
MTT	3-(4, 5- dimethylthiazol-2-yl)-2, 5-diphenyl tetrazolium bromide)
NAD	Nicotinamide adenine dinucleotide
Nct	Nucleotides
ODN	Oligonucleotides
PBS	Phosphate buffered saline
pDNA	Plasmid DNA
PEG	Polyoxyethylene glycol

PEI	Polyethylenimine
PFA	Paraformaldehyde
RISC	RNA-Induced Silencing Complex
RLU	Relative light units
RNA	Ribonucleic acid
RNAi	Ribonucleic acid interference
SAXS	Small angle X-ray scattering
SDS	Sodium dodecyl sulphate
TAT	Trans-activator of transcription protein
TE	Tris and EDTA buffer
TEM	Transmission electron microscopy
TGN	Trans-Golgi network
VEGF	Vascular endothelial growth factor
VMD	Volume mean diameter

# Publications

## (A) Abstracts

Betkaoui, R., Patel, N., and Forbes, B., (2008). The use of lipid vectors for plasmid DNA to formulate siRNA for delivery to airway epithelial cells. Poster communication at the 7<sup>th</sup> International Conference and Workshop on Biological Barriers and Nanomedicine.

Betkaoui, R., Forbes, B., and Patel, N. (2009). Preliminary studies into the formulation of siRNA for inhalation. Poster communication at The Academy of Pharmaceutical Sciences Inhalation (Awarded prize for best poster).

Betkaoui, R., Forbes, B., and Patel, N. (2009). Adaptation of cationic lipid formulations for the delivery of short interference RNA (siRNA) to respiratory epithelial cells. Poster communication at the first Pharmaceutical Sciences Fair and Exhibition (PharmSciFair 2009).

## (B) Papers

The role of endocytic pathways in the cellular uptake of cationic lipid based-siRNA delivery vectors (Manuscript in preparation).

# Acknowledgments

First and foremost I offer my sincerest gratitude to my supervisors, Dr Benjamin Forbes and Dr Nilesh Patel who have supported me throughout all stages of this work and for their guidance and input into my thesis. I also thank the Algerian Government for funding this project.

Many thanks to my colleagues and friends, for all their help, support, and valuable hints. Especially I am obliged to Dr. Laila Kudsiova for her assistance with the confocal imaging and Dr Sara Ailane for her support in difficult times.

Last but not the least, I am deeply thankful to my family in particular my Mum and Dad for their unconditional love and support and from whom I get all my strength and motivation. I am also very grateful to my brother Brahim for his continuous encouragement and support.

# **Chapter 1. Introduction**

## **1.1. Nucleic acid therapy, gene expression and gene silencing**

Gene therapy involves the transfer of genetic information into cells to modify their function or behaviour and therefore altering the disease state or preventing the occurrence of a disease (Lasic, D.D. and N.S. Templeton, 1996, Tomlinson, E. and A.P. Rolland, 1996). Because inherited or acquired genetic diseases are often associated with a defect or absence of a particular gene, most gene therapy has been based on inducing gene expression by introducing nucleic acid that contains a specific gene to replace the defective or missing gene. Examples of such genetic diseases are cystic fibrosis, alpha 1-antitrypsin deficiency and sickle cell anaemia (Lasic, D.D. and N.S. Templeton, 1996). The genetic material is delivered to humans in two ways. One method consists of using modified viruses which contain the gene of interest and which are able to efficiently deliver their genomes in cells and express their content. The other approach consists of combining the gene of interest, in many cases by inserting it into a bacterial plasmid construct with a non-viral carrier. Plasmids are easily manipulated to include any gene of interest and the preparation of large quantities in the pure form is simple.

Studies in gene therapy have been ongoing for many years in order to improve transfection efficiencies to levels required for clinical trials. Meanwhile, there has been a growing interest in developing ways of altering cell function by the suppression of gene expression, and the idea of silencing pathogenic genes has become an attractive approach for the treatment of many diseases including viral infections, such as HIV and influenza, cancer and inflammatory diseases such as rheumatoid arthritis and Crohn's disease (Opalinska, J.B. and A.M. Gewirtz, 2002). The most widespread approach employed to downregulate gene expression consists

of the use of antisense oligonucleotides. Over 20 antisense drugs have entered clinical studies (Chan, J.H. *et al.*, 2006, Juliano, R. *et al.*, 2008). However despite the success of the antisense approach in studying gene function, this methodology is not the most attractive therapeutic gene silencing approach because it requires extensive experimental work to define effective target sites within the gene of interest, which is expensive and time consuming (Thomas, M. *et al.*, 2007, Behlke, M.A., 2006). Ribozymes are catalytically active RNA composed of three helices that chop single-stranded regions of their own or other RNAs by transesterification or hydrolysis. They haven't been highly investigated for therapeutic use due to their low stability in serum of only seconds to minutes (Reischl, D. and A. Zimmer, 2009, Dorsett, Y. and T. Tuschl, 2004).

The discovery of RNA interference (RNAi) in the 1990s opened up an entirely new field of gene silencing methodology. Although RNA interference was first observed in the early 90's in plants (Napoli, C. *et al.*, 1990), the mechanism remained unexplained until 1998 when Fire and co-workers showed that the injection of double stranded RNA (dsRNA) several hundred bases in length, caused an important gene silencing in *Caenorhabditis elegans*. They identified RNAi as a fundamental pathway in which sequence specific stands of RNA can target and induce the cleavage of complementary messenger RNA (mRNA). After the display of RNAi in mammalian cells (Elbashir, S.M. *et al.*, 2001) it was rapidly recognized that this highly specific mechanism of sequence-specific gene silencing might be explored to develop a new class of drugs that interfere with disease-causing or disease-promoting genes (Shrivastava, N. and A. Srivastava, 2008, Wu, S.Y. and



N.A. Mcmillan, 2009, Cejka, D. *et al.*, 2006) and therefore a lot of efforts have been made to understand the RNAi mechanism.

## **1.2. RNA interference (RNAi)**

RNAi is a naturally occurring gene silencing pathway. In eukaryotic cells this sequence-specific silencing mechanism is essential for the suppression of genes that determine cell differentiation and survival. In plants and microorganisms, this RNAi pathway protects the genome from viral infections (Tijsterman, M. *et al.*, 2002, Dykxhoorn, D.M. and J. Lieberman, 2006, Spelios, M. *et al.*, 2010). In mammalian cells, Elbasir et al (2001) showed that introducing synthetic 21-nucleotide siRNA duplexes to different cells specifically suppressed the expression of endogenous genes. RNA interference is initiated by long dsRNAs that are cleaved by the Dicer enzyme into short duplexes (~21-25 nucleotides) with 2-nucleotide 3'overhangs (Tijsterman, M. *et al.*, 2004). These are known as short interfering RNA (siRNA). RNA interference occurs when components of the RNAi machinery specifically recognize these short RNA duplexes and then integrate a single siRNA strand into a protein complex known as the RNA induced silencing complex (RISC (Angaji, S.A. *et al.*, 2010). RISC contains the endonuclease (Ago2) (Hammond Sm, B.S., Caudy Aa, Kobayashi R, Hannon Gj, 2001) that cleaves the target messenger RNA bearing a complementary sequence to the incorporated siRNA strand and the second strand of the duplex is degraded (Aigner, A., 2007, Angaji, S.A. *et al.*, 2010, Schroeder, A. *et al.*, 2010).

siRNA is a highly potent gene silencing tool compared to antisense oligonucleotides and riboenzymes, because it uses the physiological gene silencing

machinery (Figure 1.1). The observation that long dsRNAs are cleaved by the Dicer enzyme, encouraged researchers to identify endogenous interfering RNA that is encoded by the genome itself. Endogenous molecules termed microRNAs have been found and are the most characterised short RNA molecules. These are single stranded RNA (ssRNA) of 21-22 nucleotides and are effector molecules derived by the cytoplasmic processing of pre-microRNAs (~70 nucleotides) by the dicer enzyme (Cejka, D. *et al.*, 2006). These micro-RNAs suppress gene expression by cleaving mRNAs or inhibiting their translation (Scherer, L.J. and J.J. Rossi, 2003, Karagiannis, T.C. and A. El-Osta, 2005).

Introduction of long (>30 nucleotides) dsRNA into mammalian cells leads to the initiation of the antiviral interferon (IFN) response and global protein expression shutdown (Akhtar, S. and I.F. Benter, 2007). Short siRNA duplexes (21-23 nucleotides) avoid the non-specific activation and causes highly efficient gene silencing (Yadava, P. *et al.*, 2007). Therefore for safer therapeutic applications RNAi can be initiated through delivery of shorter siRNAs that are produced synthetically *ex vivo* and can result in highly specific and potent gene silencing in mammalian cells. Although siRNAs are expensive and the induced RNA interference is short lived this approach is simple and effective (Gary, D.J. *et al.*, 2007, Aigner, A., 2007).

### **1.2.1. siRNA as a therapeutic tool**

Because RNAi is present in all cells and any gene can be targeted with good specificity, siRNA has become an attractive strategy for the treatment of many diseases caused by over-expression of a gene or multiple genes such as cancer

(Takeshita, F. and T. Ochiya, 2006, Garbuzenko, O.B. *et al.*, 2009), neurological disorders (Davidson, B.L. and H.L. Paulson, 2004), inflammation and infections (Ponnappa, B.C., 2009). Before the discovery of RNA interference, antisense oligonucleotides were the primary tools for targeted gene silencing; but studies into the inhibitory effect of the different gene silencing nucleic acids have found that the effect of siRNA is more potent at low concentration than antisense oligonucleotides and ribozymes (Scherer, L.J. and J.J. Rossi, 2003). Bertrand *et al* (2002) also reported that siRNA is 1000-fold more effective than antisense ODNs in silencing target genes. In addition, gene silencing using siRNAs is cheaper and faster compared to the conventional gene silencing technologies (Thomas, M. *et al.*, 2007). Because of these advantages, pharmaceutical companies are now aiming to exploit this new molecule commercially and despite its recent discovery, the first siRNA-based drugs have already reached phase II clinical trials (Schroeder, A. *et al.*, 2010). Examples of such drugs include Bevasiranib and Cand5 siRNA, which targets the VEGF ligand for the treatment of age-related macular degeneration (AMD). However the therapeutic application of RNA interference is highly dependent on its delivery, since the siRNA sequences need to be delivered to the host in an efficient and safe manner (Sioud, M. and D.R. Sorensen, 2003).

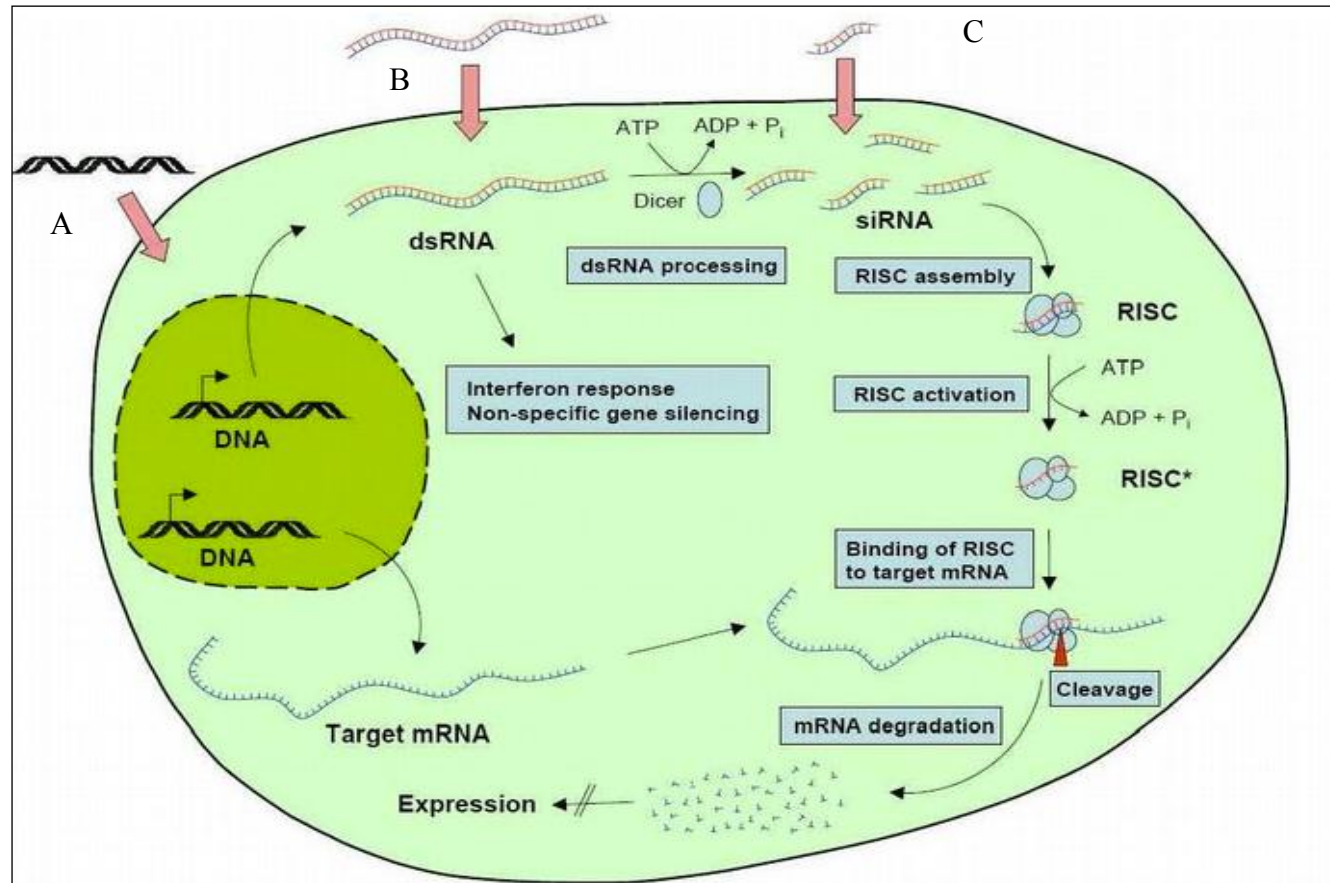


**Figure 1.1** The mechanism of RNA interference (RNAi) in mammalian cells induced by either (A) long dsRNA molecules expressed from DNA vectors or (B) directly enter the cell or (C) by small siRNAs (21–23 bp) which are directly delivered into the cell (Aigner, A., 2007).

### **1.3. Delivery vectors for nucleic acids**

The prerequisite for successful gene therapy or gene silencing is efficient and safe delivery of pDNA or siRNA to target cells. Due to their hydrophilic nature, the negative charge of the phosphate backbone and their susceptibility to degradation by nucleases, these molecules are not able to efficiently enter the cells due to the physical barriers of the negatively charged cellular membrane. Therefore carriers are necessary for delivery of pDNA or siRNA. Present delivery vectors for nucleic acids are divided into two major classes, viral and non-viral vectors.

#### **1.3.1. Viral vectors**

Viruses are highly efficient delivery vectors because they are extremely infectious and have very good endosomal escape mechanisms (Lasic, D.D. and N.S. Templeton, 1996); retroviruses, adenoviruses and adeno-associated viruses. Retroviruses infect only dividing cells and permanently integrate genes into the host chromosomal DNA, which makes it difficult to stop or modify therapy in case of intolerance to the side effects. In addition, permanent incorporation of genes may lead to the stimulation of oncogenes or inhibition of tumour suppressor genes leading to cancer (Kay, M.A., 2007, Lasic, D.D. and N.S. Templeton, 1996, Tomlinson, E. and A.P. Rolland, 1996). Another disadvantage of retroviruses is the inability to make high concentration of the virus and their low stability in blood (Kaneda, Y., 2001, Kay, M.A., 2007, Lasic, D.D. and N.S. Templeton, 1996). Unlike retroviruses, adenoviruses transduce non-dividing cells and have high titres, but they have been associated with immune and inflammatory responses, which prevents repeated

administration (Kovesdi, I. *et al.*, 1997). In addition, there is the risk of developing host resistance to transduction after repeated exposure to the viral vector as well as the generation of an infectious form of the virus during production or use. Adeno-associated viruses are safer when compared to other viruses because of the removal of all viral genes (Driskell, R.A. and J.F. Engelhardt, 2003), but due to its small transgene size there is a limit to the size of DNA that can be packaged (Kaneda, Y., 2001, Kay, M.A., 2007).

### **1.3.2. Non-viral vectors**

Despite the popularity of viruses as vectors for *in vitro* and *in vivo* gene delivery, in the past decade non-viral vectors have evolved as safer and effective gene delivery systems for *in vivo* applications. These systems include cationic lipids, polymers, and peptides (Martin, M.E. and K.G. Rice, 2007, Lasic, D.D. and N.S. Templeton, 1996). Cationic lipids and polymers are the most promising non-viral vectors (Zhang, Y. *et al.*, 2010) and despite their low transfection efficiency *in vivo* compared to viral vectors, they offer many advantages over viruses. They are easy to prepare and can carry an unlimited size of DNA, and they are less likely to cause immunogenic and inflammatory responses (Akhtar, S. and I.F. Benter, 2007). Moreover the risk of developing the infectious form or inducing oncogenic mutations is very low because the genes delivered have low integration capacity and are unable to replicate or recombine (Birchall, J.C. *et al.*, 1999).

There is massive literature on the different non-viral vectors used to deliver nucleic acids. Some recent examples include cationic lipids, Lipidoids, Polyethyleneimine, dendrimers, and polysaccharides. Although they have all been

successfully explored for pDNA and siRNA delivery, they all share the same major obstacles for in vivo application and these consist on physical and colloidal stabilities as well as toxicity.

*Cationic polymers.* Linear or branched cationic polymers including peptides readily bind pDNA to form a complex known as a polyplex capable of gene delivery. Unlike cationic lipids, they do not contain a hydrophobic moiety and are completely soluble in water. In addition they have the advantage of compacting pDNA into small nanoparticle which favourable for delivery (Lv, H.T. *et al.*, 2006). Their common feature is that they exhibit proton sponge effect, which allows endosomal escape and release of nucleic acid in the cytosol (Juliano, R. *et al.*, 2008). Polyethyleneimine (PEI) has been extensively and successfully used for both pDNA and siRNA transfection provided that the correct architecture and molecular weight polymer is selected to avoid high toxicity. It was shown that branched low molecular weight PEI (< 25 Kda), rather than linear are more transfection efficient and that high molecular weight PEI result in higher toxicity (Akhtar, S. and I.F. Benter, 2007, Tseng, Y.C. *et al.*, 2009). It has been shown that PEI have two types of toxicity, an immediate toxicity that occurs when free PEI enters the circulation and causes destabilisation of the plasma membrane. The delayed toxicity is associated with cellular processing of PEI/pDNA complexes, as after the release of the nucleic acid free PEI is restored and it interacts with cellular components resulting in the inhibition of normal cellular process. Some efforts are being made to tackle the toxicity challenge (Lv, H.T. *et al.*, 2006). In terms of siRNA delivery *in vivo*, microarrays of tumors treated with linear and branched PEI revealed that both architectures induced multiple gene changes *in vivo* that might contribute to off

target effects of siRNA and also have an effect on gene silencing activity ((Akhtar, S. and I.F. Benter, 2007, Tseng, Y.C. *et al.*, 2009).

Poly(l-lysine) polymers are linear polymers with the amino acid Lysine as the repeat unit. They were the first cationic polymers used for gene delivery and their biodegradable nature gives them an advantage for *in vivo* applications. However it has been shown that DNA condensation and transfection efficiency is favored by the use of high molecular weight polymers which was linked with high toxicity. Also their disadvantage is the rapid clearance from circulation due to interaction with plasma proteins leading to poor delivery efficiency. In addition they need the co-use of a lysosmotropic agent to minimise their lysosomal degradation, which has been associated with increased toxicity (Lv, H. *et al.*, 2006).

*Cationic polysaccharides.* Another group of cationic polymers desirable for nucleic acid due to their biocompatible, biodegradable and low toxic nature. Chitosan is a naturally occurring linear polysaccharide, which has been widely applied for pDNA delivery with encouraging results however limited research with siRNA ((Gary, D.J. *et al.*, 2007). These polymers have the ability to compact the nucleic acid in nano-sized polyplexes, but the stability and properties of the complexes depends on the structure and molecular weight of the chitosan. In addition, interactions of chitosan and nucleic acid is pH sensitive and decreases with increasing pH ((Akhtar, S. and I.F. Benter, 2007, Tseng, Y.C. *et al.*, 2009). So far, chitosan nanoparticles have been modified and stabilised in many ways to optimise gene delivery but one of the major obstacles is physical and colloidal stability in particular *in vivo*.



*Dendrimers.* The branched, nanometer sized, spherical modular structures can be engineered to have specific molecular weight and defined molecular shapes and sizes able to overcome biological barriers *in vivo*. Dendrimers of positive charge can be generated to bind to nucleic acid. This family of polymeric vectors were initially designed for pDNA delivery but are emerging as potential carriers for siRNA. The advantage with dendrimers is that the small sized siRNA can be positioned as a polyplex on a positively charged dendrimer surface or well hidden within the sphere, which prevents aggregation. Increasing efforts have been made to develop various dendrimers and dendritic structures for siRNA delivery. In parallel, various chemical alterations have been required to increase bio- compatibility and delivery efficiency, reduce toxicity and promote targeted delivery via surface group modification (Lv, H.T. *et al.*, 2006).

*Lipidoids.* A new class of delivery vectors, which have been generated recently to allow rapid synthesis of large libraries of lipid like carriers and therefore expand the diversity of delivery vectors. The range of the previous vectors is restricted due to the long multi-step process of their sythesis. Lipidoids are generated by conjugate addition of alkyl acrylamide or acrylacylate to primary or secondary amine groups, this reaction does not require the presence of solvent or catalyst and therefore skips the protection or de-protection step as well as concentration or purification. After the synthesis the library is screened for ability to deliver siRNA and a number of vectors with a certain characteristics were identified to be effective for gene delivery *in vitro* and *in vivo*, but further studies are necessary to characterise these systems (Mahon, K.P. *et al.*, 2010)

### 1.3.3. Cationic lipids as gene delivery vectors

Cationic lipids are amphipathic mono- or polycationic molecules made up of a positively charged head group attached to a hydrophobic moiety via a linker group (Brown, M.D. *et al.*, 2001, Wasungu, L. and D. Hoekstra, 2006). The hydrophobic anchor group is responsible for the formation of liposomes and interaction with the cell membranes, the positively charged head group (amine group) interacts with the nucleic acid, and the linker group is a determinant of lipid stability and biodegradability (Mahato, R.I. *et al.*, 1997). Because of their amphiphilic nature, cationic lipids easily form liposomes or micelles in aqueous media. Cationic lipids were introduced as carriers for DNA (Felgner, P.L. *et al.*, 1987, Zhang, S. *et al.*, 2007) and RNA (Malone, R.W. *et al.*, 1989) over 20 years ago. They have been extensively used as a transfection reagent *in vitro* and *in vivo* (Akhtar, S. and I.F. Benter, 2007, Tseng, Y.C. *et al.*, 2009) and some formulations have already been used in clinical trials (Brown, M.D. *et al.*, 2001). However generally, gene expression has been found to be at a low level and transient (Kay, M.A., 2007). 1,2-Dioleoyl-3-Trimethylammonium-Propane (methyl sulfate salt) (DOTAP), a double chain quaternary ammonium surfactant, is one of the most widely used cationic lipids. It is relatively cheap, and is efficient in both *in vitro* and *in vivo* transfection (Ciani, L. *et al.*, 2004, Felgner, P.L. *et al.*, 1987). DOTAP can be used alone as a cationic carrier for transfection (Birchall, J.C. *et al.*, 1999, Lasic, D.D. and N.S. Templeton, 1996) or in combination with an equal amount of the neutral lipids such as 1,2-Dioleoyl-*sn*-Glycero-3-Phosphoethanolamine (DOPE) or cholesterol to improve transfection.

#### **1.4. Delivery of pDNA vs siRNA using cationic lipids**

Plasmid DNA (pDNA) and siRNA share many similar characteristics; i.e. they are both double stranded nucleic acids, share the negative phosphodiester backbone structure and can both interact electrostatically with cationic lipids. However, there are a few key differences in their physicochemical properties and mode of action that are important when considering how they should be formulated for delivery to cells (Table 1.1). pDNA has a molecular topography which allows it to condense into small particles once the negative charge has been neutralised by the cationic lipid and. On the other hand, siRNA, which is shorter in length and has a more rigid structure, is not likely to condense. Interaction with cationic lipid may result in incomplete condensation and formation of large aggregates (Spagnou, S. *et al.*, 2004). Unlike pDNA, which contains the sugar deoxyribose, siRNA has a hydroxyl group in the second position of the pentose ring instead of hydrogen. The presence of hydroxyl groups makes the siRNA backbone more susceptible to hydrolysis by serum nucleases (Juliano, R. *et al.*, 2008, Keller, M., 2005, Schroeder, A. *et al.*, 2010). Adequate protection from nucleases is required for both nucleic acids. The difference in site of action gives siRNA an advantage as entry into the nucleus is not required since mRNA molecules are released from the nucleus following transcription (Bouxsein, N.F. *et al.*, 2007, Thomas, M. *et al.*, 2007).

**Table 1-1** Main differences between plasmid DNA (pDNA) and short interference RNA (siRNA).

	<b>pDNA</b>	<b>siRNA</b>
Physicochemical Characteristics	Large molecular weight (several kilobases) Deoxyribonucleic acid	Small molecular weight (21-23 nts) Ribonucleic acid
Cellular stability	Relatively stable	Unstable due to the presence of 2'OH groups
Site of action	Nucleus	Cytoplasm
Interaction with cationic lipids	Condensation into nanoparticles	Less condensation
Gene regulation	Upregulation	Downregulation

#### **1.4.1. Cationic lipid/nucleic acid complex formation**

Cationic lipid/nucleic acid complexes are self-assembling nanosystems, which are prepared by simply mixing cationic liposomes and nucleic acid in aqueous solution. Counterion release from the nucleic acid, a related decrease in hydration and increase in entropy are the driving force for the spontaneous electrostatic interaction between the negatively charged nucleic acid and the positively charged nucleic acid (Wasungu, L. and D. Hoekstra, 2006). As cationic lipid/nucleic acid complex formation is dependent on charge neutralization, the ratio of positive charges on the cationic lipid and negative charges of the nucleic acid generally defines the characteristics of the formed complexes (Zuhorn, I.S. *et al.*, 2002b).

#### **1.4.2. Structure of the complexes**

The spontaneous electrostatic interaction leads to the formation of supramolecular assemblies whose structure is difficult to determine, although extensive studies have been undertaken with this aim (Desigaux, L. *et al.*, 2007). A fairly uniform picture has emerged from different studies using small angle X-ray scattering (SAXS) where it has been found that pDNA complexes display a highly ordered lamellar structure or non-bilayer inverted hexagonal structure according to the co-lipid and the salt concentration used in the preparation (Prasad, T.K. *et al.*, 2003, Wasungu, L. and D. Hoekstra, 2006). The lamellar structure consists of aligned strands of helical pDNA sandwiched between bilayers of cationic lipid. However, when neutrally charged lipids such as DOPE are included a remarkable transition to the two-dimensional hexagonal phase occurs, where the buried apolar side chains of lipid extend outward from pDNA chain forming a uniform apolar coat around each strand of pDNA

(Tranchant, I. *et al.*, 2004). The transition to hexagonal structure is enhanced in the presence of physiological salts as it has been shown that in water complexes exist in lamellar phase but when suspended in salt solution of physiological concentration, the system converts to the hexagonal phase (Labatmoleur, F. *et al.*, 1996). The presence of salt or neutral lipids reduces the net charge density of the cationic bilayer and weakens electrostatic interaction between DNA and bilayer, which induces the order to disorder transition (Prasad, T.K. *et al.*, 2003). The hexagonal phase has been shown to possess higher transfection efficiency than the ordered lamellar phase as it facilitates nucleic acid release once inside the cells (Smisterova, J. *et al.*, 2001, Middaugh, C.R. and J.D. Ramsey, 2007, Hoekstra, D. *et al.*, 2007).

For siRNA, there are very few reports concerning interactions with cationic lipid and the resulting structures. Desigaux and colleagues (2007) reported the results of cryo-transmission electron microscopy (cryo-TEM) and SAXS experiments showing that self-assembled siRNA-lipidic complexes formed ordered lamellar domains with an even spacing.

#### **1.4.3. Physicochemical properties**

The physicochemical properties of cationic lipid/nucleic acid complexes such as size, charge and packing efficiency are believed to play a significant role in gene delivery efficiency. Therefore a lot of effort has been made using different methods to characterise these complexes.

#### 1.4.3.1. Complexation efficiency

Protection of nucleic acid against degradation by nucleases depends strongly on the positive/negative (+/-) charge ratio and is associated with high transfection efficiency (Eastman, S.J. *et al.*, 1997, Xu, Y. *et al.*, 1999). Displacement of intercalating dyes, such as ethidium bromide, from nucleic acid is one of the most commonly used techniques to determine the amount of unbound or uncondensed nucleic acid. Typically, the fluorescent dye used has the ability to intercalate between nucleic acid bases and therefore competes with cationic lipids. The reduction in fluorescence of the dye indicates inaccessibility of the dye to the nucleic acid, which is interpreted as condensation (Gershon, H. *et al.*, 1993).

#### 1.4.3.2. Particle size

The particle size of complexes can be characterized using dynamic light scattering, which is a well-established technique for measurement of particle size over a scale range of nanometers to micrometers. In suspension, particles scatter light, which fluctuates depending on size. Therefore the intensity of fluctuations in scattered light (due to Brownian motion of particles in solution) are analysed by an autocorrelation method to yield a diffusion constant and ultimately a particle size expressed as the mean hydrodynamic diameter (Yang, S.T. *et al.*, 1994). Although the polydispersity of cationic lipid/nucleic acid complexes make the analysis of the resulting data difficult, a mean diameter can still be obtained. The particle size (diameter) of a lipid/ nucleic acid complex has been reported to influence the deposition of the complexes after administration as well as their uptake by target cells (Wiethoff, C.M. *et al.*, 2004, Rejman, J. *et al.*, 2004). Because large molecules

are poorly endocytosed, it has been suggested that transfection complexes with small particle size ( $\leq 100$  nm) are more efficient for transfection and provide better extravasation to target cells. In contrast, more recent reports have shown that larger particles (micron range) are preferred for *in vitro* transfection (Zhdanov, R.I. *et al.*, 2002, Esposito, C. *et al.*, 2006, Boussein, N.F. *et al.*, 2007). This was associated with quicker sedimentation at the cell surface compared to smaller complexes and a suggestion that large complexes reach the lysosomes relatively slowly compared to smaller particles. Cationic lipid/siRNA complexes are usually smaller than cationic lipid/pDNA complexes (nano range, from  $\sim 50$  to 800 nm), however, transfection efficiency has not been restricted to small or large particle size as complexes of small size ( $< 200$  nm) or larger aggregates (500-800 nm) have both been reported to be efficient in delivering functional siRNA (Spagnou, S. *et al.*, 2004, Zhang, Y. *et al.*, 2010).

#### 1.4.3.3. Zeta potential

The surface charge of nucleic acid/lipid complexes is an important property that affects its interaction with cells and non-cellular components such as serum proteins (Wolff, J.A. and D.B. Rozema, 2008). Dynamic light scattering in the presence of an electrical field can estimate the zeta potential of the complexes, as particles in suspension will migrate toward the electrode of opposite charge with velocity proportional to zeta potential. The zeta potential is used to assess the charge stability of a disperse system as it can give an estimate of the surface charge of particles in suspension. It has been reported that complexes with positive charge are formed when the cationic lipid is in excess in comparison to the nucleic acid and at



these ratios the complexes are more transfection efficient *in vitro* (Tomlinson, E. and A.P. Rolland, 1996, Sakurai, F. *et al.*, 2000a). However, non-specific interactions between negatively charged components *in vivo* and the positively charged complexes affects the stability of the complexes. Several strategies have been developed to reduce these non-specific interactions, but the most common is the use of hydrophilic uncharged polymers such as polyoxyethylene glycol (PEG) attached to the lipid in order to shield the positive charge and provide a steric barrier (Lee, M. and S.W. Kim, 2005).

#### **1.4.4. Influence of charge ratio on physical properties**

All the physical properties discussed in the previous sections are strongly dependent on the +/- charge ratio. Both pDNA and siRNA complexes have been reported to follow a three zone model of colloidal stability; zone A which represents a region of colloidal stability for complexes with excess negative charge ratio (excess nucleic acid) and uncondensed nucleic acid surrounding lipids; one B which represents colloidal instability where complexes are uncharged and tend to form large aggregates; and zone C where colloiddally stable complexes of excess positive charge and highly complexed nucleic acid are observed (Tranchant, I. *et al.*, 2004, Desigaux, L. *et al.*, 2007). Although pDNA and siRNA follow the same three-zone model, the charge ratio at which these zones occur varies between the two nucleic acids (Zhang, Y. *et al.*, 2010). In addition the pH and salt concentration influence these physical properties as at high ionic strength complexes are unstable and tend to form large aggregates (Boffi, F. *et al.*, 2002, Rejman, J. *et al.*, 2004, Wiethoff, C.M. *et al.*, 2004, Gopal, V. *et al.*, 2006).

## **1.5. Challenges of gene delivery**

Gene delivery is a multi-step process in which a number of barriers must be overcome including internalisation and intracellular barriers such as cell entry, endosomal escape and nuclear entry (Morille, M. *et al.*, 2008, Wasungu, L. and D. Hoekstra, 2006). siRNA has an advantage over pDNA in that it does not require nuclear localization for its action as it acts in the cytoplasm. The challenges of cationic lipid-mediated pDNA/siRNA delivery are considered below.

### **1.5.1. Cellular binding and internalisation**

Due to their polyanionic and macromolecular nature, nucleic acids cannot enter the cells freely. The polyanionic characteristic limits cellular entry and interferes with uptake via endocytosis. The bulky nature of the nucleic acid hinders uptake via passive diffusion. Both issues can be surmounted by the use of cationic carriers (Grayson, A.C. *et al.*, 2006), which as described earlier, effectively condense the nucleic acid into small positively charged complexes. It is generally accepted that binding to cells occurs via an interaction between the positive headgroup of the cationic lipids and the negatively charged cell surface components (Pires, P. *et al.*, 1999, Labatmoleur, F. *et al.*, 1996). Passive fusion of complexes with the cellular membrane has been suggested as a first pathway to deliver nucleic acid directly into the cytoplasm with endocytosis and endocytosis-like pathways being proposed as the main cellular internalisation pathways (Elouahabi, A. and J.M. Ruyschaert, 2005).

### **1.5.2. Endosomal escape**

Once inside the cells the complexes will follow the endocytic pathway and endosomal escape should occur rapidly before the nucleic acid passes into lysosomes and degraded by lysosomal nucleases (Wattiaux R, L.N., Wattiaux-De Coninck S, Jadot M, 2000). As a consequence the main challenge to date for gene delivery has been to get the nucleic acid out of the endosome (Wasungu, L. and D. Hoekstra, 2006) and de-assembly of the complex to release the nucleic acid.

A mechanism for endosomal escape for cationic lipid/DNA complexes has been described by Xu and Szoka (1996) and consists of the formation of ion pairs between complexes and the anionic endosomal membrane, which leads to disruption of the endosomal membrane. The ion pair formation weakens the electrostatic interaction between nucleic acid and the cationic lipid and promotes the formation of non-bilayer hexagonal structures, which in return enhances endosomal disruption and facilitates the release of the nucleic acid from the complex (Koltover, I. *et al.*, 1998, Hafez, I.M. *et al.*, 2001). Elouahabi et al (2005) proposed another endosomal escape mechanism whereby endosomal escape occurs through a detergent-like destabilisation mechanism of the endosomal membrane and the dissociation of complexes after interaction with the cytosolic network. This idea came from the assumption that not all pDNA could be dissociated and released into the cytoplasm during endosomal escape (verified by electron microscopy showing undissociated complexes in the cytoplasm).

### **1.5.3. Nuclear translocation and entry**

The last physical barrier to nucleic acid delivery is translocation to, and entry into, the nucleus. Overcoming this barrier is only necessary for pDNA, which unlike siRNA that exerts its effects in the cytoplasm requires entry into the nucleus in order to be transcribed. The stability of DNA in the cytoplasm is threatened by the presence of nucleases (Lechardeur, D. *et al.*, 1999). It is thus not surprising that the nuclear translocation efficiency of pDNA is low with an estimate of 1 of 1000 plasmids making it into the nucleus (Pollard, H. *et al.*, 1998).

Endocytosis may play a role in the transport of DNA from near the plasma membrane to the perinuclear zone. Another possibility is that the positively charged lipoplex-containing endosomes might interact and eventually fuse with the endoplasmic reticulum resulting in the release of DNA into the lumen of the reticulum. The DNA could then easily access the nucleus through the continuous network existing between nuclear and reticulum membranes. Kamiya et al (2002) suggested that complexes delivered into the cytoplasm of cells fused directly with the nuclear membrane to release DNA into the nucleus.

In terms of nuclear entry, the nuclear membrane is known to contain highly regulated transport structures known as nuclear pores with a diameter of approximately 25 nm. The small diameter of the pores is expected to constrain the entry of pDNA as only small molecules ( $\leq 40$  KDa) can enter via passive diffusion through the nuclear pores. Therefore two pathways for nuclear entry have been proposed; either via a passive entry into the nucleus during cell division when the nuclear membrane is temporarily

disintegrated (Escriou, V. *et al.*, 2001) or via an active transport of DNA through the nuclear pores (Pires, P. *et al.*, 1999).

#### **1.5.4. Stability of the complexes**

Efficient delivery complexes require both chemical and physical stability. The complexes need to be chemically stable to protect the nucleic acid from enzymatic degradation until taken up by cells, but also susceptible to dissociation in the endosomal compartment to allow release of the nucleic acid in the cytoplasm. In terms of physical stability, highly charged complexes tend to form aggregates in presence of polyelectrolytes and physiological salt due to reduced repulsive forces, this needs to be minimised either by electrostatic or steric stabilisation. *In vivo*, the main disadvantage of cationic lipid/DNA complexes is their instability in the presence of negatively charged serum proteins. Several studies used serum, which contains a large number of plasma proteins, to mimic the *in vivo* situation (Zhang, Y. and T.J. Anchordoquy, 2004). The binding of serum proteins to cationic lipid/DNA complexes can cause structural reorganization, aggregation and dissociation of the complexes (Li, S. *et al.*, 1998, Nchinda, G. *et al.*, 2002). Aggregation will lead to reduced binding of the complexes with cellular membrane, rapid clearance of the complexes and increased toxicity. Complex de-assembly can also lead to DNA degradation by serum nucleases, and decreased association of the complexes with the target cells (Yang, J.P. and L. Huang, 1998, Sakurai, F. *et al.*, 2001). The strong inhibitory effect of serum has been observed to affect gene expression efficiency of cationic lipid/pDNA complexes *in vitro* (Escriou, V. *et al.*, 2001), whereas others reported contradictory results in which serum did not inhibit transfection efficiency

*in vitro* (Zuhorn, I.S. *et al.*, 2002a, Zuhorn, I.S. *et al.*, 2002b, Han X, L.S., Qiangyi Fang, Dongxiao Li, Xianghui Gong, Yuyin Wu, Shengli Yang, Bing Q. Shen, 2007). These differences could be due to the fact that different lipidic systems were used in each study and suggests that the susceptibility to serum inhibition is related to the type of cationic lipid used as cationic lipid. In addition, (Yang, J.P. and L. Huang, 1998) reported that at high charge ratios DOTAP:DOPE and DC-Cholesterol:DOPE complexes were more resistant to serum inhibition compared to lower charge ratios. Several strategies have been developed to surmount the inhibitory effect of serum including modification of charge ratios, using alkaline pH and salt during preparation and reducing interaction with negatively charged molecules by including pegylated lipids (Rejman, J. *et al.*, 2004, Schroeder, A. *et al.*, 2010) or neutral lipid such as cholesterol (Zhdanov, R.I. *et al.*, 2002, Hong, K. *et al.*, 1997, Bennett, M.J. *et al.*, 1995) in the formulation.

#### **1.5.5. Toxicity**

Although cationic lipids are not immunogenic like viral vectors, they are not without any toxicity. They can be cytotoxic and the extent to which this is manifested differs between different reagents and cell types. The prospect of toxicity is determined by the nature of the cationic carrier as well as the cationic lipid/nucleic acid complex (Lv, H.T. *et al.*, 2006). In terms of cationic lipid/nucleic acid complexes, the toxicity may, in part, be caused by the large size of the complexes, and the high positive zeta potential required for their uptake (Li, S. *et al.*, 1998, Lv, H.T. *et al.*, 2006). Therefore the toxicity is also associated with the charge ratio between the cationic lipid species and the nucleic acids, as well as the dose of

lipoplexes administered. Higher +/-charge ratios are generally more toxic due to the high positive zeta potential as well as the presence of free (i.e., empty) liposomes (Xu, Y. *et al.*, 1999). Free liposomes are present at high charge ratios when lipid is in excess to nucleic acid but their role in transfection efficiency remains unclear. However, Xu et al (1999) showed that their removal did not increase transfection efficiency but did allowed prevention of a decrease in transfection-associated toxicity. Free liposomes may also compete with nucleic acid complexes for interaction with negatively charged membranes and uptake in cells.

## **1.6. Cellular uptake mechanisms**

The analysis of the uptake pathways for non-viral gene delivery vectors has mainly been focussed on studies with DNA complexes, with endocytosis being established as the main uptake pathway (Labatmoleur, F. *et al.*, 1996, Zuhorn, I.S. *et al.*, 2002a, Zuhorn, I.S. *et al.*, 2002b, Friend, D.S. *et al.*, 1996). However non-endocytic pathways have also been suggested as an alternative route for the internalisation of delivery vectors.

### **1.6.1. Endocytic uptake pathways**

Endocytosis is a broad term that covers multiple distinct pathways used by cells to internalize a variety of macromolecules and can be classified into two categories; phagocytosis and pinocytosis. Phagocytosis is only performed by specialized cells such as macrophages, neutrophils and monocytes and is used to eliminate large molecules including cellular debris and large pathogens such as bacteria and yeast (Conner, S.D. and S.L. Schmid, 2003). The second pathway is

called pinocytosis and is present in almost all mammalian cells and includes several pathways; so far four pathways have been identified, their common feature being the uptake of macromolecules in transport vesicles. However, they differ in the protein composition and size of the vesicles as well as the intracellular trafficking (Conner, S.D. and S.L. Schmid, 2003, Lamaze, C. and S.L. Schmid, 1995). As most of these pathways share several characteristics, it remains difficult to identify which pathway the delivery vectors follow especially since the endocytic pathways themselves are not well understood. Endocytosis-interfering drugs have been used to distinguish between the different pathways and to determine the type of pathway involved. However cautious interpretation of data is recommended, as there are concerns about specificity of these drugs as well as their effect on cell viability.

#### 1.6.1.1. Clathrin-mediated endocytosis

The major and best characterized pathway is clathrin-mediated endocytosis (Takei, K. and V. Haucke, 2001, Lamaze, C. and S.L. Schmid, 1995), which commonly mediates the uptake of plasma membrane receptors such as receptors of transferrin, epidermal growth factor (EGFR) and low density lipoproteins (LDLR) (Ivanov, A.I., 2008). This uptake process is receptor-mediated as it involves specific receptors located in invaginations of the plasma membrane known as clathrin-coated pits. These vesicles are characterized by the presence of a polyglonal clathrin coat and range in size from approximately 100 to 150 nm (Takei, K. and V. Haucke, 2001). They carry ligand-bound receptors inside the cell involving GTPase dynamin activity (Benmerah, A. and C. Lamaze, 2007) and they are transformed into early endosomes where the ligand is separated from the receptor. The ligand is then transferred to late endosomes for potential degradation in lysosomes. The receptors



are recycled and transported back to the cellular membrane (Khalil, I.A. *et al.*, 2006). Genes internalized through the clathrin pathway end up in lysosomes for potential degradation, thus for a successful delivery of biologically active genes, lysosomal escape and release in the cytoplasm is crucial. This receptor-mediated endocytosis is energy-dependent and can be strongly inhibited by lowering temperature (Haylett T, T.L., 1991, Wiliam A. Dunn, A.L.H., And Nathan N. Aronson, 1980) or by depletion of the ATP pool using metabolic inhibitors (Khalil, I.A. *et al.*, 2006). In addition reagents that prevent the assembly of the clathrin lattice on the membrane specifically inhibit this pathway. Such treatments include potassium depletion (Larkin, J.M. *et al.*, 1983, Ivanov, A.I., 2008), hypertonicity, cytosol acidification and the cationic amphipathic drug chlorpromazine (Wang, L.H. *et al.*, 1993, Khalil, I.A. *et al.*, 2006, Ivanov, A.I., 2008).

#### 1.6.1.2. Caveolin-mediated endocytosis

Similar to the clathrin-coated vesicles, caveolae vesicles also originate from cholesterol-enriched invaginations of the plasma membrane. They invaginated as flask-shaped vesicles within the plane of the plasma membrane, or as detached vesicles. In addition, caveolae can fuse to form grape-like structures and tubules with sizes larger than 100 nm (Smart, E.J. *et al.*, 1999, Pelkmans, L. *et al.*, 2001). Caveolae are mainly composed of cholesterol and sphingolipids and accumulate cholesterol binding-proteins known as caveolins, on the cytosolic face of the vesicles (Smart, E.J. *et al.*, 1999, Matveev, S. *et al.*, 2001, Harris, J. *et al.*, 2002). Caveolae play a role in endocytosis of certain viruses such as simian virus 40 (SV40), as well as some bacteria and bacterial toxins such as cholera toxin (Khalil, I.A. *et al.*, 2006)

and like the clathrin pathway, caveolae require GTPases activity for the pinch off of vesicles.

After internalisation, caveolae-derived vesicles fuse with caveosomes (Nichols, B.J. and J. Lippincott-Schwartz, 2001, Pelkmans, L. *et al.*, 2002), which are pre-existing, stable, organelles with a neutral pH and it is believed that this uptake mechanism does not lead to lysosomal degradation (Parton, R.G., 2004). Macromolecules internalized via this route are transported to the endoplasmic reticulum (ER) (Pelkmans, L. *et al.*, 2001) or to the trans-Golgi network (TGN) (Norkin, L.C. and D. Kuksin, 2005) and therefore avoid lysosomal degradation. Due to its non-degradative nature (Ferrari, A. *et al.*, 2003, Harris, J. *et al.*, 2002), caveolar endocytosis represents an attractive pathway for gene delivery, even though this process is considered slow and has a small phase volume making it unlikely to be a primary uptake route. This uptake is also energy dependent so it can be inhibited by lowering temperature or by ATP depletion. In addition, drugs that specifically bind, sequester, or deplete cholesterol such as filipin, nystatin, and methyl- $\beta$ -cyclodextrin, respectively, inhibit internalization by the caveolae (Lamaze, C. and S.L. Schmid, 1995, Schnitzer, J.E. *et al.*, 1994). The caveolae pathway is actin-dependent and therefore drugs that affect the actin cytoskeleton such as cytochalasins are used to inhibit caveolae pathway without affecting the clathrin-mediated endocytosis, although these drugs do also inhibit macropinocytosis (Parton, R.G., 2004).

#### 1.6.1.3. Macropinocytosis

Unlike clathrin and caveolae pathways, macropinocytosis is not a receptor-dependent mechanism. It involves the formation of large, irregular endocytic

vesicles generated from actin-driven membrane ruffles known as macropinosomes (Swanson, J.A. and C. Watts, 1995, Amyere, M. *et al.*, 2002). These vesicles are not coated and their intracellular trafficking is not very clear and depends on cell type. For example in macrophages the macropinosomes merge with lysosomes (Meier, O. and U.F. Greber, 2003), whereas in other cell lines they do not interact with other endosomal compartments (Swanson, J.A. and C. Watts, 1995). The macropinosomes vary in size and can reach up to 5  $\mu\text{m}$  in diameter (Khalil, I.A. *et al.*, 2006) and therefore they represent an efficient route for non-selective endocytosis of large solutes (Conner, S.D. and S.L. Schmid, 2003). In addition the vesicles are leaky in nature, which facilitates the escape or release of gene delivery vectors. The ruffling is dependent on actin cytoskeleton and on protein kinase C. Thus, drugs that inhibit the  $\text{Na}^+/\text{K}^+$  exchanged in the plasma membrane such as amiloride and its analogues can be used to block this pathway (Hewlett, L.J. *et al.*, 1994). Actin cytoskeleton depolymerising drugs such as cytochalasins inhibit the uptake through macropinocytosis (Parton, R.G., 2004). Other drugs have also been used to inhibit this pathway, such as genestein (another kinase inhibitor) but with low specificity (Fishman, P.a.O.a.P.H., 1998) and wortmannin, a phosphatidyl inositol-3-phosphate inhibitor.

#### 1.6.1.4. Caveolae and clathrin-independent endocytosis

Receptor-mediated pathways that do not involve clathrin coats or caveolae proteins have been suggested as possible entry routes (Khalil, I.A. *et al.*, 2006). These pathways are still poorly characterised, it has been suggested that each of these pathways could have a specific function in the cell and vary in the vesicles they

form, type of macromolecules they transport, intracellular fate and how the entry is regulated. Targeting receptor-mediated endocytosis holds a promising strategy for delivering genes to defined cell populations. An example of this is transferrin, an iron-binding glycoprotein, which is highly expressed in rapidly dividing cells and has been used to target tumour cells for gene delivery systems (Kakudo, T. *et al.*, 2004, Wagner, E. *et al.*, 1990). The folate receptor is another example of receptors overexpressed in tumour cells, and it can be used for targeting (Lee, E.R. *et al.*, 1996, Cho, K.C. *et al.*, 2005). However, most of the currently used ligands are internalized by clathrin-mediated endocytosis, and the poor intracellular trafficking associated with this significantly limits the transfection activities of the systems. Therefore, identifying and investigating new receptors that can be internalized by clathrin-independent endocytosis might provide more efficient delivery.

### **1.6.2. Non-endocytic pathways**

Work has suggested that pDNA/lipid complexes enter cells via fusion with the cellular membrane and direct release of pDNA into the cytosol before entering the endosomal compartment (Felgner, J.H. *et al.*, 1994). This mechanism has an advantage over endocytosis in that it can avoid lysosomal degradation. However fusion has been found to only participate minimally in the uptake of gene delivery vectors (Friend, D.S. *et al.*, 1996, Brooks, H. *et al.*, 2005). Another non-endocytic process is an energy-independent direct penetration of the lipid bilayer, which has been used as an internalisation route for pDNA/peptides complexes (Thoren, P.E. *et al.*, 2003, Trehin, R. and H.P. Merkle, 2004). Recently Lu and colleagues (2009) suggested that although 95% of siRNA/lipid complexes entered the cells via

endocytosis, they were not functional in inducing gene silencing and it was the 5% of complexes that entered via a different mechanism that resulted in efficient gene silencing. They suggested that the mechanism followed by the functional complexes was passive diffusion across the cellular membrane.

## **1.7. Formulation strategies to improve delivery of nucleic acids**

### **1.7.1. Helper lipids**

The inclusion of the helper lipid DOPE with cationic lipids has been shown to improve transfection efficiency of pDNA (Legendre J, S.F., 1992, Gao, X. and L. Huang, 1991, Farhood, H. *et al.*, 1995)) and decreased the toxicity. Electron microscopy showed that DOPE has the ability to induce fusion and endosomal disruption by changing the membrane bilayer packing from lamellar to hexagonal, which facilitates DNA entry into the cell and release into the cytosol after endocytosis (Zhdanov, R.I. *et al.*, 2002). The lamellar phase binds stably to anionic lipids while the unstable hexagonal phase fuse easily with anionic membranes and facilitates endosomal escape. The transition to non-bilayer structures does not occur upon inclusion of DOPE in the cationic lipid system, but upon charge neutralization by salts or upon ion pairing with the anionic endosomal membrane as this decreases surface charge (Elouahabi, A. and J.M. Ruyschaert, 2005). DOPE shields some of the positive charge of the cationic lipid and may lead to looser binding of the cationic lipid with the nucleic acid compared to DOPE-devoid complexes as reflected by ethidium bromide intercalation into DOPE-containing complexes even upon complete pDNA binding. The weak binding facilitates complex disassembly.

Therefore DOPE can be used to enhance transfection *in vitro* (Gustafsson, A. and P. Sonesson, 1995), whereas cholesterol has more commonly been used as a helper lipid *in vivo* as it provides resistance to serum inhibition (Zhdanov, R.I. *et al.*, 2002, Hong, K.L. *et al.*, 1997, Bennett, M.J. *et al.*, 1997).

### **1.7.2. Polyoxyethylene glycol polymers**

Polyoxyethylene glycol is a flexible hydrophilic polymer that extends approximately 3-5 nm from liposomal surfaces depending on the length and concentration (Vp, T., 1994). In addition it is non-ionic, water-soluble and is usually associated with phosphatidylethanolamines such as DSPE or DMPE serving as a bilayer anchor (Webb, M.S. *et al.*, 1998). The addition of a polymer such as polyethylene glycol is known to improve the stability of nucleic acid complexes and increase their *in vivo* half-life (Rejman, J. *et al.*, 2004, Schroeder, A. *et al.*, 2010). When they are added to a conventional liposome they form a steric barrier on the surface of the complexes, which inhibits opsonisation and thus prolongs the circulation time of the liposomes in the blood (Harvie, P. *et al.*, 2000). These pegylated-lipid/pDNA complexes have also been shown to be stable and to protect DNA from nuclease degradation in the plasma (Harvie, P. *et al.*, 2000, Song, L.Y. *et al.*, 2002). In addition incorporation of a PEG lipid prevents aggregation during storage and it preserves their transfection activity (Kim, J.K. *et al.*, 2003). Sanders *et al.* (2002) showed that exposure of the conventional DOTAP:DOPE lipoplexes to cystic fibrosis mucus components (albumin, mucin, DNA and phospholipids) reduced their transfection activity *in vitro* and this was associated with lipoplex aggregation, but it did not affect the transfection efficiency or activity of the pegylated complexes. However the hydrophilic nature of pegylated-lipid may

present a disadvantage in terms of transfection efficiency as it can reduce cell binding and membrane fusion (Harvie, P. *et al.*, 2000, Song, L.Y. *et al.*, 2002). However, it has been shown that the reduction in transfection caused by pegylated-lipid is concentration dependent, and efficient transfection can still occur with complexes prepared with less than 2 mol% of pegylated-lipid. In addition, the length of the PEG chain is also a factor and it was shown that by using short length chains there was less inhibition of transfection (Harvie, P. *et al.*, 2000).

### **1.7.3. Pre-condensation with a polycation**

Many studies have shown that the pre-condensation of DNA with polycationic peptides such as protamine sulphate and poly-(L)-Lysine, enhances cationic lipid-mediated gene transfer (Birchall, J.C. *et al.*, 1999, Zhdanov, R.I. *et al.*, 2002). These small polycations are known to condense DNA in a small and stable structure via charge-charge interactions. The commonly used condensing agent, protamine sulphate, is transfection inefficient on its own therefore the addition of cationic lipids is necessary. The high proportion of amine groups of these polypeptides make them able to neutralize a number of charge sites on the DNA molecule, and therefore facilitating condensation by cationic lipids. These lipid-polycation-DNA (LPD) systems are stable at lower cationic lipid to DNA charge ratios and are small, homogenous (small polydispersity in size) and less susceptible to aggregation that can occur with the conventional cationic lipid/DNA complexes. It has been reported that the transfection activity of LPD complexes was higher than that of those formed in the absence of protamine, especially after storage (1-2 months) as compared to freshly prepared complexes (Hong, K. *et al.*, 1997). Moreover in another study it was revealed that pre-condensation of DNA with protamine (3:2 mass ratio) resulted

in smaller compact and homogeneous lipoplexes whose structure remained unchanged by jet nebulisation, even when compared to high ratio (12:1) DOTAP:DOPE/DNA complexes (Gill, D.R. *et al.*, 2004). The LPD system displayed better protection of DNA during nebulisation.



## **1.8. Aims and objectives of the thesis**

The aim of this thesis was to investigate formulation strategies reported for the delivery of pDNA for the delivery of siRNA and identify what adaptations were required for optimal delivery of the shorter nucleotide sequences. Three formulations for DNA delivery were characterised before they were adapted for the formulation of siRNA. The mechanism by which these formulations delivered of siRNA into cells was investigated. Finally, the requirement to formulate the siRNA delivery system for pulmonary delivery was considered.

The specific objectives addressed in this thesis were to:

- Optimise three cationic lipid-based formulations for complexing pDNA by systematically varying the charge ratio and measuring the physicochemical properties of the formulations and their transfection efficacy.
- Formulate siRNA using the systems characterised for pDNA delivery and measure the effect of charge ratio on the physicochemical properties of the formulations and their efficacy in gene silencing,
- Investigate the mechanism of cellular uptake of siRNA lipoplex systems by respiratory epithelial cells.

## **Chapter 2. The effect of physicochemical characteristics on cationic lipid-mediated DNA delivery *in vitro***

## 2.1. Introduction:

Cationic lipids have received considerable attention as potential gene delivery agents and reached clinical trials stage (Gene Therapy Clinical Trials Worldwide, 2011). However, despite the large amount of research in cationic lipid mediated gene delivery, with literally thousands of different formulations examined the efficiency of these carriers is still lower than desirable as compared to their counterpart viral vectors. The optimization of these systems remains a result of trial and error and in order to improve the clinical efficacy of cationic lipid formulations, it is necessary to comprehend the role of the parameters that affect the physicochemical properties of these systems, which in turn affect their biological activity.

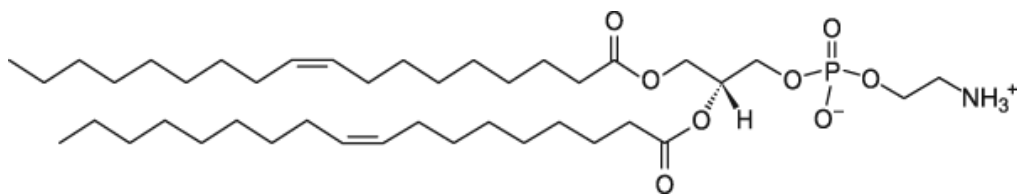
Since the interaction between cationic liposomes and pDNA is of an electrostatic nature, it is expected that the biophysical characteristics of the lipid/pDNA complexes formed would depend significantly on the apparent charge ratio (+/-) of the cationic amines on the liposomes and the negative phosphates groups on pDNA. Mixing pDNA and cationic lipids at different charge ratios will result in the formation of complexes with distinct size, surface charge and colloidal stability (Boffi, F. *et al.*, 2002, Zuidam Nj, B.Y., 1998, Hirsch-Lerner, D. and Y. Barenholz, 1999, Zuidam, N.J. *et al.*, 1999).

Although several studies have examined the effect of physicochemical properties on efficient pDNA delivery and some generalisations were made (Yang, J.P. and L. Huang, 1998, Zuhorn, I.S. *et al.*, 2002a, Zuhorn, I.S. *et al.*, 2002b, Ross, P.C. and S.W. Hui, 1999b) (Ross, P.C. and S.W. Hui, 1999a, Simberg, D. *et al.*, 2001), a detailed comparison between different works is difficult because of the

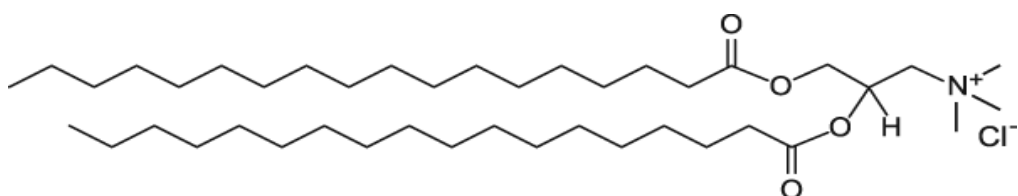
different experimental conditions and different cell lines used. This is particularly so when taking into account that even within a group of structurally related compounds within one class a small change in structure may lead to a dramatic change in activity. In this study the transfection efficiency and toxicity of three different cationic lipid -based vectors were investigated comparatively using the same experimental conditions and the same cell line in an attempt to determine a relationship, if any, between the physicochemical properties and transfection efficiency.

### **2.1.1. Cationic lipid formulation used in this study**

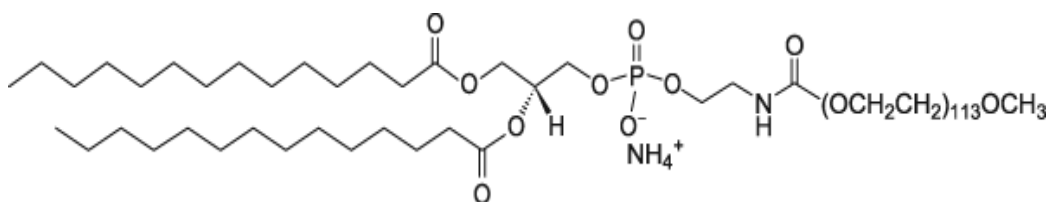
The equimolar combination of cationic lipid DOTAP and neutral lipid DOPE liposomes was used in this study; because this cationic lipid/neutral lipid combination is one of the most widely used lipidic systems for pDNA delivery (Ciani, L. *et al.*, 2004) and extensively described in terms of their physical properties, examination of the basis of their relative transfection efficiencies may provide further insight into the physical basis of effective gene delivery. DOTAP:DOPE was also modified by incorporating either a polycation such as protamine sulphate or a polyethylene glycol-associated lipid both of which have been shown to enhance the stability and transfection efficacy of DOTAP (Kim, J.K. *et al.*, 2003, Rejman, J. *et al.*, 2004, Birchall, J.C. *et al.*, 1999, Sanders Nn, D.S.S., Cheng Sh, Demeester J, 2002, Hong, K.L. *et al.*, 1997). The structure of the lipids used in the study is shown in Figure 2.1. The formulations are summarised in Table 2.1.



DOPE



DOTAP



DMPE-PEG<sub>5000</sub>

**Figure 2.1** Chemical structures of the neutral lipid (DOPE), cationic lipid (DOTAP) and the PEG associated phospholipid (DMPE-PEG<sub>5000</sub>). Avanti Polar Lipids, Inc website (<http://www.avantilipids.com/>).

**Table 2-1** A summary of the formulations used in this study.

Formulation	Components	Abbreviation
DOTAP:DOPE (1:1 molar ratio)/pDNA	Cationic lipid:neutral lipid	LD
DOTAP:DOPE:DMPE- PEG <sub>5000</sub> (1:1:0.05)/pDNA	Cationic lipid:neutral lipid:Pegylated lipid	LpegD
DOTAP:DOPE (1:1)/ Protamine:pDNA (2:1 mass ratio)	Cationic lipid:neutral lipid/Polycation-pDNA	LPD

### 2.1.2. Physicochemical characterization of pDNA complexes

It has been reported that the composition of the suspending medium in particular the ionic strength, affected the physicochemical properties including size and charge of the nucleic acid/lipid complexes (Eastman, S.J. *et al.*, 1997). However it is common that, the physicochemical properties of the complexes are determined in water or in weak electrolyte solutions and the transfection experiments are carried out using cell culture media (transfection media) of physiological salt concentration (Kim, J.K. *et al.*, 2003, Spagnou, S. *et al.*, 2004, Zhang, Y. *et al.*, 2010, Wiethoff, C.M. *et al.*, 2004);(Birchall, J.C. *et al.*, 1999)). Therefore this study also aimed at illustrating the effect of type of media used on the complexation efficiency as well as the physical properties of the cationic lipid/pDNA complexes.

### **2.1.3. Transfection of respiratory epithelial cells by pDNA**

The respiratory epithelium is the first target for gene delivery to the lungs because it is the surface encountered by inhaled particles in the conducting airways of the lungs (trachea, bronchi and respiratory bronchioles) as well as the alveolar region (Forbes, B. and C. Ehrhardt, 2005, Florea, B. *et al.*, 2003)). This is why most efforts have been concentrated on optimising gene transfer to epithelial cells by making it more efficient, less immunogenic and less inflammatory and having prolonged expression. In order to develop suitable gene delivery vectors, an *in vitro* model that correlates with the *in vivo* situation is required. The airway epithelium comprises three major cell types: ciliated cells, secretory (mucous, goblet, serous or clara) and basal cells (Mathias, N.R. *et al.*, 1996). The alveolar epithelium is composed of a monolayer of two types of cells Type I and Type II cells that display different morphologies (Mathias, N.R. *et al.*, 1996). These different cell types with distinct properties make the epithelium a complex barrier to pulmonary delivery. A simpler *in vitro* model of the epithelium would consist of a monoculture of the cell line that contributes to the majority of the epithelial surface area (Forbes, B. and C. Ehrhardt, 2005). Several human-derived cell lines are currently utilized as *in vitro* models of the airway epithelium. These include the bronchial epithelial cells Calu-3, 16HBE14o- and BEAS-2B, and the type II like alveolar epithelial cells, A549 (Steimer, A. *et al.*, 2005).

#### **2.1.3.1. Calu-3 cells**

This cell line derived from a bronchial adenocarcinoma of the airway has been considered to be an appropriate *in vitro* model of the bronchotracheal airway

epithelium (Forbes, B. and C. Ehrhardt, 2005, Florea, B. *et al.*, 2003) These cells were found to be the only cell type derived from a lung cancer to have mRNA and protein content similar to the airway epithelium, which indicated that they are one of the well differentiated cell lines (Mathias, N.R. *et al.*, 1996). Calu-3 cells have been shown to possess many of the features relevant to drug absorption and metabolism as those found in the native epithelium. These features include the formation of tight junctions, secretion of mucus, expression of transport and efflux pumps and the development of apical ciliated cells. These cells also express the cystic fibrosis transmembrane conductance regulator (CFTR) protein (Mathias, N.R. *et al.*, 1996, Foster, K.A. *et al.*, 2000, Florea, B.I. *et al.*, 2002). Moreover Calu-3 cells are readily available and differentiate in monolayers of polarized cells of different phenotypes (Florea, B. *et al.*, 2003). Because of these properties, Calu-3 cells have been extensively evaluated for use as a tool to study drug transport, metabolism and toxicity (Foster, K.A. *et al.*, 2000). However little work has been done in terms of investigating the use of this cell line for gene delivery studies.



#### **2.1.4. Aim and objectives**

The ultimate aim of this work was to characterize formulations for the delivery of pDNA and develop methods for their characterization, which could subsequently be adapted for the delivery of siRNA. Specific objectives related to pDNA delivery were:

- Measure the impact of using biorelevant media (HBSS vs water) on the physicochemical properties of the formulations,
- Investigate the effect of charge ratio on the formulation properties and transfection efficacy in Calu-3 respiratory epithelial cells,
- Compare the physicochemical properties of the formulations with their transfection efficacy in respiratory cells *in vitro*.

## 2.2. Materials

Material	Supplier
Plasmid pGL3-control vector, Bright Glo luciferase assay kit and Glo lysis buffer 1X	Promega, Southampton, UK
Endofree Plasmid Mega Kit, GelPilot loading dye 5X	Qiagen West Sussex, UK
Quant-iT <sup>TM</sup> PicoGreen dsDNA Reagent and kit, Bright Glo <sup>TM</sup> Luciferase assay, Lipofectamine 2000	Invitrogen Paisley, UK
DOPE, DOTAP, DMPE-PEG <sub>5000</sub>	Avanti Polar Lipids, Inc Alabama, USA
Agarose gel	Bioline London, UK
The Bio-Rad DC protein assay	Bio-Rad Laboratories Hertfordshire, UK
GelRed (100001x in DMSO)	Biotium Inc Cambridge, UK
Luria-Bertani (LB) agar	Fluka BioChemica Buchs, Switzerland
Black 96-well microplates	PerkinElmer, UK
Calu-3 cells	ATCC Rockville, USA
L-glutamine (200mM), Penicillin-Streptomycin solution (100x), non-essential amino acids, Dulbecco's modified Eagle's medium/Nutrient Mixture F-12 HAM (DMEM), Trypsin-EDTA (0.25%), Hank's balanced salt solution (HBSS), Foetal bovine serum	Sigma-Aldrich Ltd, Dorset, UK

(FBS), Protamine Sulphate, MTT [3-(4, 5- dimethylthiazol-2-yl)-2, 5-diphenyl tetrazolium bromide), Dimethylformamide (DMF) and SDS (sodium dodecyl sulphate)	
--	--

## 2.3. Methods:

### 2.3.1. Plasmid DNA preparation

#### 2.3.1.1. Plasmid pDNA amplification and purification

The pGL3 control vector encoding for luciferase gene was amplified using an electro-competent *E.coli JM109* strain cultured on Ampicillin LB (Luria-Bertani) agar for 8 h and then subcultured in LB broth for 12-16 h. The bacterial cells were harvested and the pDNA yield was then extracted and purified using a Qiagen Endofree Plasmid Mega Kit according to the manufacturer's instructions (appendix 1). The resulting DNA was stored in 1X TE buffer (10 mM Tris (pH 8), 1 mM EDTA)

#### 2.3.1.2. Plasmid pDNA verification and quantification

**Sequencing:** The presence of the luciferase gene was verified by gene sequencing (Lark Company). The samples were sent to Lark Pharmaceuticals that used Applied Biosystems 3730xl sequencing instrument. Results confirmed the gene sequence of the prepared plasmid pDNA.

**UV spectroscopy:** The purified DNA was also characterized quantitatively by UV spectrophotometry (measurement was taken at a wavelength of 260 nm ( $A_{260}$ ) and 280 ( $A_{280}$ ) using a Perkin Elmer UV/Vis Spectrophotometer Lambda 2S). The ratio between absorbance at 260 nm and absorbance at 280 nm ( $A_{260}/A_{280}$  ratio) was used as a measure of purity of the pDNA sample. This ratio needs to be  $\geq 1.8$  to indicate purity.

**Gel electrophoresis:** The pDNA purity was assessed by agarose gel (1%) electrophoresis stained with Gel Red dye (5%) in 1X TAE buffer and the gel was subjected to 110 V for 75 min, and the DNA bands were viewed under UV light.

**Picogreen assay:** Picogreen dsDNA quantitation reagent is a very sensitive fluorescent nucleic acid stain for quantitating double-stranded DNA (dsDNA). It determines DNA concentration as low as the picogram range. This assay was also used to quantitate pDNA. A standard curve was prepared as follows: 2 µg/ml stock solution of purified pGL3 control vector was used to prepare the following concentrations (0, 0.001, 0.01, 0.1 to 1 µg/ml).

Qaunt-iT PicoGreen reagent (1 ml) was added to each sample and mixed well. After 2-5 min incubation, fluorescence was measured using a spectrofluorometer and fluorescein wavelengths (excitation 480 nm, emission. 520 nm). (The instrument's gain was set at 38 for all measurements). The fluorescence value of the reagent blank was subtracted from that of each of the samples. The corrected data was then used to generate a standard curve of fluorescence versus pDNA concentration. The sample DNA concentration was then calculated from the standard curve (Appendix).

### **2.3.2. Liposome preparation**

The lipids used in this work were DOTAP, DOPE and DMPE-PEG<sub>5000</sub> (Figure 1). DOTAP and DOPE were used at a molar ratio of 1:1. Many studies have shown that maximal gene expression is obtained when DOPE is mixed with DOTAP at this ratio and thus it was adopted for this work (Ciani, L. *et al.*, 2004, Felgner, P.L. *et al.*, 1987). The two lipids were dissolved in a chloroform/methanol 1:1 (v/v) mixture to obtain a final total lipid concentration of 1 mg/ml. 1ml of each component were

aliquoted in a glass vial using a glass syringe and thoroughly mixed to obtain a 2mg/ml total lipid concentration. The solvents were carefully evaporated by air blowing in a fume hood to produce a thin lipid film. Residual solvent was removed via freeze-drying the samples under vacuum (Edwards, UK), by first placing the lipid cake containers in -70°C freezer for 30 min and then placing the frozen lipid cake on a vacuum pump for 4 h. After removal of all traces of solvent the dry lipid film was re-suspended in sterile water to a final total lipid concentration of 2 mg/ml and the dispersion was vortexed for 5 min and the liposomes were left to stand overnight prior to downsizing to make sizing easier and improve the homogeneity of the size distribution. The hydration step was carried out at a temperature above the gel-liquid transition temperature of the lipids used (DOTAP ~ -0°C and DOPE ~ -16°C). To obtain liposomes of around 100 nm particle size the hydrated lipid dispersion was extruded at room temperature 10 times through an Avanti mini-extruder (Avanti Polar Lipids, USA) containing a 0.1 µm filter membrane. The DOTAP:DOPE:DMPE-PEG<sub>5000</sub> complexes were prepared in the same way but at the molar ratios of 1:1:0.05 respectively. The particle sizes of the liposomes were measured after extrusion using a Brookhaven instrument ZETApplus (particle sizer software).

### **2.3.3. Preparation of cationic liposomes and pDNA complexes**

In this study three lipidic systems were used to complex plasmid DNA as described in table 2-1. Plasmid DNA and liposomes were mixed at room temperature and were incubated for 30 min to allow complexation. DOTAP:DOPE and DOTAP:DOPE:PEG<sub>5000</sub> complexes were formed by the addition of pDNA to

sterile water for 5 min, and then the appropriate amount of liposome was added to obtain the different charge ratios. To calculate the mean theoretical charge ratio, it was assumed that 1 µg pDNA is 3 nmol of negatively charged phosphate and that 1 positive charge is displayed by DOTAP.

LPD complexes were prepared by the addition of protamine (1 mg/ml) to pDNA at a 2:1 mass ratio with 10 min incubation, followed by the addition of DOTAP:DOPE. For the three systems, different amounts of lipids were added to DNA to obtain cationic lipid/pDNA charge ratios ranging from 1 to 4.

#### **2.3.4. Physicochemical characterization of cationic liposome/pDNA complexes**

##### **2.3.4.1. Assessment of complexation efficiency**

**Picogreen assay.** The accessibility of the fluorescent intercalating reagent Picogreen to the pDNA associated with cationic liposomes was evaluated to determine the amount of complexed pDNA (Ferrari, M.E. *et al.*, 2001). Picogreen assay was applied as described in section 2.3.1.2. The fluorescence scale was calibrated such that the initial fluorescence of Picogreen (100 µl of 1:200 solution added to wells containing 100 µl of water) was set as background fluorescence. The fluorescence obtained upon addition of pDNA in 100 µl (20 µg/100 µl) minus background fluorescence was set as the control and reference fluorescence value (100% free pDNA). 100 µl of cationic lipid complexes containing 20 µg pDNA were prepared in water and added to each well containing 100 µl of Picogreen solution. The amount of pDNA available for intercalation with the Picogreen was

calculated by subtracting the values of background fluorescence from those obtained for each measurement, and expressed as a percentage of the control according to the following formula: % free pDNA= fluorescence of complexes/fluorescence of control\*100. In order to investigate the effect of high ionic strength on complexation, the complexes were also incubated in HBSS for 1 hour before performing picogreen assay as described above.

**Gel electrophoresis.** Agarose gel electrophoresis of cationic lipid/pDNA complexes was used to assess the complexation of lipid and DNA as a function of the cationic lipid/pDNA charge ratio.

Cationic lipid/pDNA (2 µg pDNA per sample) complexes were prepared at the different charge ratios in 100 µl water. After 1 h incubation, 1 µl of the loading buffer was added to each sample and mixed. Each sample (5µl) was then electrophoresed on a 1% Agarose gel stained with Gel Red dye (5%) in 1X TAE buffer at 110V for 75 min. The stained pDNA bands were then visualized and photographed on a UV transilluminator (Herolab, Germany).

#### 2.3.4.2. Light scattering and zeta potential measurements

Particle sizes of the complexes were determined within one hour of their preparation using a Brookhaven instrument ZETAplus (particle sizing software). ZETAplus uses electrophoretic light scattering and the Laser Doppler Velocimetry (LDV) method to determine particle velocity and, from this, the zeta potential. It also offers the option of particle size analysis in the same instrument. Measurements were made in water. In order to determine the effect of ionic solution on the particle size of the lipoplexes, the prepared liposome/DNA complexes were incubated in



Hank's balanced salt solution (HBSS) 15 min before measuring their particle size. HBSS is the medium in which the lipoplexes would be added to cells in the transfection experiments. The size distribution of the complexes at the different charge ratios was also determined in water and HBSS. Five measurements with 10 s intervals between each measurement were taken for each sample; the measurements were performed on three separate occasions (n=3).

The zeta potential of the lipoplexes was evaluated in both water and HBSS, using a Brookhaven instrument ZETApus, Zeta potential analyzer. Five measurements with 10 s intervals between each measurement were taken for each sample; the measurements were performed on three separate occasions (n=3).

### **2.3.5. Cell culture**

Calu-3 cells, passage number 38-48, were grown in 162 cm<sup>2</sup> flasks in Dulbecco's modified Eagle's medium/Nutrient Mixture supplemented with penicillin-streptomycin solution (5%), L-Glutamine (5%), non-essential amino acids (5%), and foetal bovine serum (50%) at 37°C in a humid atmosphere containing 5% CO<sub>2</sub>. The cell culture medium was changed every 2 days and the cells were observed under a microscope to assess the degree of confluency and to confirm the absence of contaminants. Once the cells reached 80-90% confluency, they were trypsinised using Trypsin-EDTA (0.25%), and either passaged to new flasks or plated in 96-well plates for transfection and toxicity experiments.

### 2.3.6. Transfection experiments

One day before the transfection experiment, cells were seeded into 96-well plates at a density of  $1 \times 10^4$  cells per well in standard cell culture media (plating volume 100  $\mu$ l) and cultured overnight at 37°C. Just before transfection, the medium was removed and 100  $\mu$ l of HBSS buffer was added to each well. After 30 min HBSS was removed and an equal volume of the complexes LD, LpegD and LPD of different charge ratios (0.5, 1, 2, 3, 4) were added to each well in filtered HBSS. The final DNA concentration was 0.2  $\mu$ g per well. The cells were transfected for 6 h before removal of the complexes and each well was then supplied with 100  $\mu$ l standard cell culture medium. Cells were incubated for 48 h to allow gene expression to proceed. The negative control group consisted of naked DNA alone in HBSS. Lipofectamine (0.05  $\mu$ l/well) complexed to DNA (0.2  $\mu$ g/well) was used as a positive control because of its reported high transfection activity. This commercial transfection reagent is suitable for *in vitro* transfection of suspended or adherent cells and it has been optimised for the delivery of both DNA and siRNA in a wide range of cell lines including Calu-3.

#### 2.3.6.1. Luciferase activity

After 48 h incubation, the medium was removed and the cells were lysed by adding 100  $\mu$ l of Glo lysis buffer, 1X, to each well for 5 min. The cells lysate (5  $\mu$ l) was assayed for protein content using the Bio-Rad DC protein assay kit I. The rest of the cell lysate was transferred to a white 96-well plate and the luciferase activity was measured using the Bright-Glo™ Luciferase Assay System (according to the manufacturer's protocol) and the Microtiter plate luminometer (Dynex technologies,

UK). An excitation/emission wavelength of 560 nm was used to measure luciferase activity (a luciferase expressed will oxidise the added luciferin, which will emit photons at 560 nm). All the luminescence values expressed as relative light units (RLU) were normalized per amount of protein.

#### 2.3.6.2. Protein Assay

A standard curve was constructed using a protein standard (bovine gamma-globulin standard) between the concentration range of 0.32 and 1.32 mg/ml. The standards (5 µl) were pipetted into a 96-well plate (6 replicates for each concentration) followed by 25 µl of the reagent A (provided with the kit) and then followed by 200 µl of reagent B. The plate was agitated to mix the reagents. The same procedure was applied to the samples obtained from the cell lysis step of the transfection experiment. After 15 min, absorbance of both the standards and the samples were read at 750 nm using the SpectraMax 190 Microplate Spectrophotometer (Molecular Devices, USA). The amount of protein expressed by the cells was determined from the calibration curve (Appendix).

#### 2.3.6.3. MTT toxicity studies

A relatively simple assay for cytotoxicity is the MTT (3[4, 5-dimethylthiazol-2-yl]-2, 5-diphenyltetrazolium bromide) test. The MTT is a tetrazolium dye that is reduced by mitochondrial enzymes and its colour changes from yellow to blue. This reaction takes place only in cells with viable mitochondria; therefore the colour intensity is directly related to the viability of the cell. This is a useful test to detect cytotoxic compounds.

#### 2.3.6.4. Calibration curves for MTT test

**Cell counting:** Under sterile conditions 100 µl of cell suspension was mixed with an equal volume of Trypan blue dye by gentle pipetting. Trypan blue dye only stains dead cells. The number of viable cells was counted in a pre-cleaned haemocytometer and the concentration of viable cells was determined using the following equation:

$$\text{Concentration of viable cells (cells/ml)} = A \times B \times C$$

Where A is the mean number of viable cells counted, B is the dilution factor and C is the correction factor ( $10^4$ ).

Before performing an MTT test, calibration curves were constructed to determine the optimal cell seeding density for the experiment. The cells were seeded into a 96-wells plate at concentrations of  $5 \times 10^5$ ,  $2.5 \times 10^5$ ,  $1.25 \times 10^5$ ,  $6.25 \times 10^4$ ,  $3.125 \times 10^3$ ,  $1.56 \times 10^3$ ,  $7.81 \times 10^2$ ,  $3.91 \times 10^2$  and  $1.95 \times 10^1$  cells/ml. The experiment blank consisted of 100 µl of medium only. The cells were incubated for 24hrs at 37 °C, 5% CO<sub>2</sub>.

**Solutions:** A 1 mg/ml MTT solution was made by dissolving 40 mg of MTT powder in 40 ml sterile PBS (the mixture was sonicated for a few seconds to aid dissolution) and stored in the fridge (2-8 °C). SDS solution was prepared by dissolving 4g of SDS powder in 20 ml pure water. After sonication, 20ml of DMF was added to the SDS solution to give a final concentration of 10% SDS. After 24 hr incubation, 25 µl of filtered MTT solution (1mg/ml) mixed with 25µl medium was added to each well and the cells re-incubated for 4hrs. Normally the dissolved MTT is converted to insoluble purple formazan crystals by cleavage of the tetrazolium ring

by dehydrogenase enzymes in viable cells. This water insoluble formazan is solubilized using SDS. At the end of the incubation period, the medium was removed from the plate and the converted dye was solubilized by the addition of 100  $\mu$ l of SDS solution to each well (including the blank). The cultures were incubated overnight and absorbance was measured at two wavelengths; 570 and 650 nm. A calibration curve was constructed by plotting number of cells against the mean absorbance (Appendix).

#### 2.3.6.5. Cytotoxicity of pDNA/lipid complexes

After determining the optimal seeding density of Calu-3 cells by calibration curves, cells were seeded into a 96-well plate at  $1 \times 10^4$  cells/ well then incubated for 24 hr (100  $\mu$ l plating volume). At the end of the incubation period the medium was removed, and lipoplexes were added at different lipid:DNA charge ratios (0.5:1, 1:1, 2:1, 3:1, 4:1). After 6 hr incubation, MTT assay was carried out as described above.

#### **2.3.7. Statistical tests**

A statistical package for social sciences (SPSS version 11.0) software was used to perform Independent samples t-test, One-way ANOVA and Post-Hoc Tukey's tests. Statistically significant differences were assumed when *p* values were less than 0.05.

Independent samples t- test was performed to compare the difference in the size and zeta potential at between measurements made in water and HBSS for each system.

One-way ANOVA and Post-Hoc Tukey's tests were performed to determine whether there was a significant difference in luciferase production at the different charge ratios for each lipidic system including the control lipofectamine and to compare the level of luciferase expression between the three lipidic systems at the different charge ratios.

## 2.4. Results

### 2.4.1. pDNA characterization

All pDNA preparations showed a major band of circular DNA and a minor band of nicked plasmid DNA (Figure 2.2) and the bands of the sample pDNA were similar to the marker (pure pGL3 control vector).

The concentration of pDNA was determined using both UV spectroscopy and picogreen assay. One unit of UV absorbance was equivalent to 50 µg plasmid DNA per ml. All DNA samples were obtained in concentrations ranging between 0.8-1.5 mg/ml. This result was confirmed by picogreen assay as the sample DNA concentration was calculated from the standard curve (Appendix) and was found to be in the same range. The pDNA purity was assessed by the A260/A280 ratio, and all preparations had an  $A_{260}/A_{280} \geq 1$ .

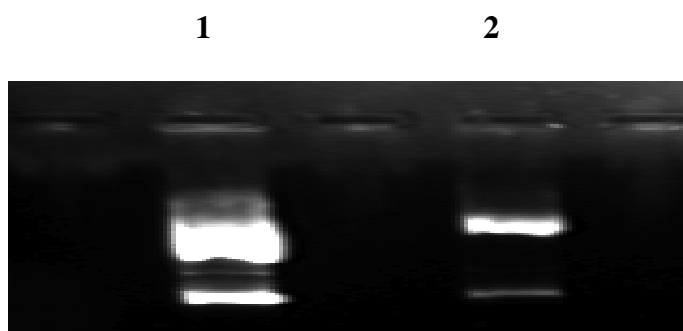


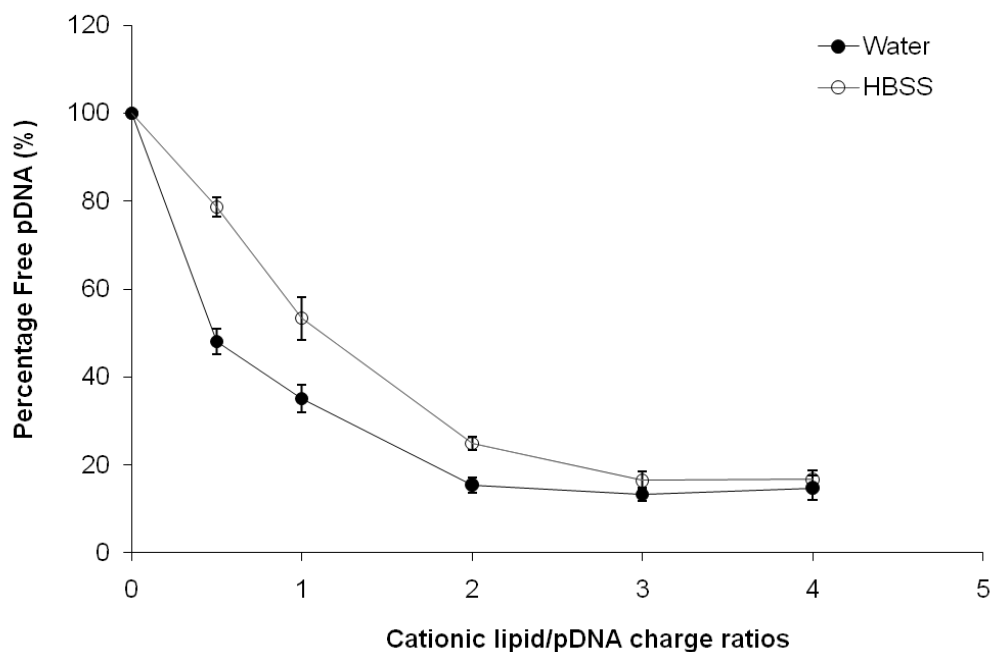
**Figure 2.2** Gel electrophoresis of a sample of pGL3 control vector after extraction and purification using Qiagen Endofree Plasmid Mega Kit. 1) Pure pGL3 obtained from (Sigma Pharmaceuticals) was used as a marker, 2) sample pGL3 control vector.

#### **2.4.2. Complexation efficiency as a function of charge ratio**

The influence of +/- charge ratio on the complexation of pDNA by cationic lipid was investigated using picogreen intercalation assay and agarose gel electrophoresis. The extent of picogreen intercalation depended on the cationic lipid/pDNA charge ratios. Upon addition of DOTAP:DOPE (LD) to pDNA a significant decrease in fluorescence intensity of picogreen was detected with approximately 50% remaining pDNA available for intercalation, which indicated association of 50% pDNA with the cationic lipid (Figure 2.3A). This correlated with the presence of faint fluorescent bands on agarose gel at charge ratio 0.5 corresponding to the ones observed in naked pDNA lane (Figure 2.3B) At charge ratios  $\geq 2$ , high pDNA condensation was achieved with less than 20% pDNA was available for intercalation. However, gel electrophoresis showed absence of fluorescent bands at ratios  $\geq 1$ , which indicated that all pDNA was bound to the lipidic system. . Although picogreen data showed that less than 40% free pDNA was available at charge ratio 1, agarose gel electrophoresis showed absence of free pDNA at this ratio. Picogreen data after incubation of the complexes in HBSS, showed an increase in fluorescence intensity (represented by % free pDNA) suggesting greater dissociation of pDNA from the lipid in particular at low charge ratios (0.5 to 2) compared to incubation in water. High pDNA condensation was achieved at high charge ratios 3-4 with only 20% remaining free pDNA (Figure 2.3A).



A)



B)

M pDNA 0.5 1 2 3 4

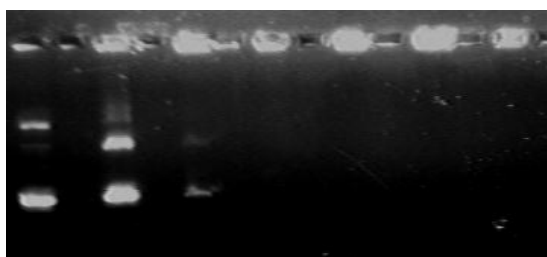
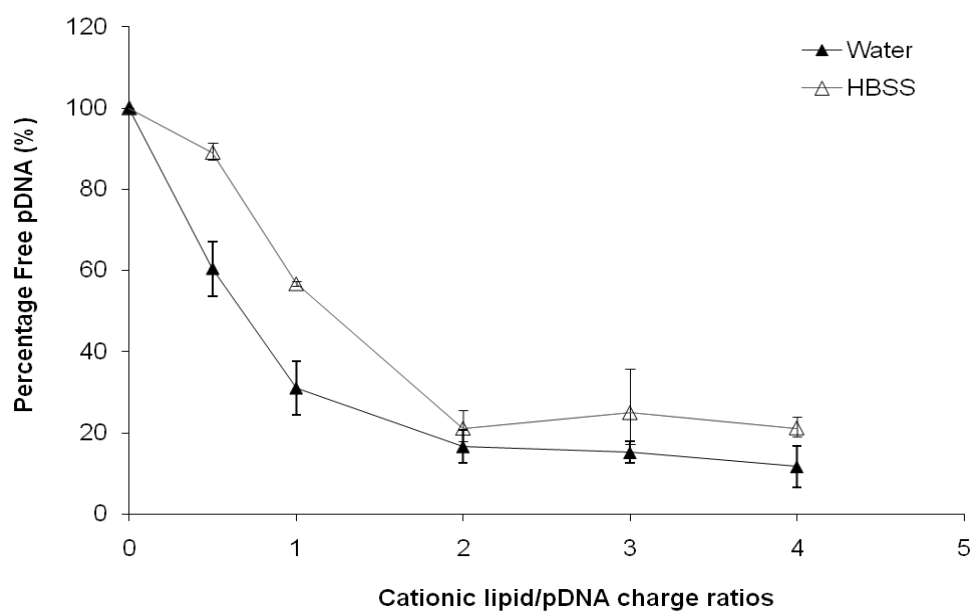


**Figure 2.3** A) Picogreen intercalation assay of LD complexes in water and HBSS. The percentage free pDNA represent the fraction of pDNA in the sample available for intercalation with picogreen reagent (n=3, mean  $\pm$ SEM). B) Gel electrophoresis of LD complexes prepared at different charge ratios in water; pure pGL3 control vector was used as a marker (M).

LpegD complexes showed more or less similar complexation profile as LD complexes both in water and HBSS. In water the fluorescence intensity of picogreen decreased significantly after addition of DOTAP:DOPE:DMPE-PEG<sub>5000</sub> (LpegD) to pDNA as shown by the decrease of percentage free pDNA from 100% to ~ 60% at the 0.5 charge ratio. Increasing the charge ratio caused a further decrease in percentage free pDNA to approximately 10% at charge ratio 4 (Figure 2.4A). Incubation of LpegD complexes in HBSS caused an increase in the fluorescence intensity of picogreen and therefore an increase in percentage free pDNA at low charge ratio (0.5 to 2) indicating dissociation or less effective condensation of pDNA. As the charge ratio increased the percentage of free pDNA was comparable to the one observed in water. In agarose gel, free DNA bands were observed in the until a charge ratio of 2:1 (Figure 3B), after this ratio no bands were observed indicating complexation of pDNA.

A)



B)

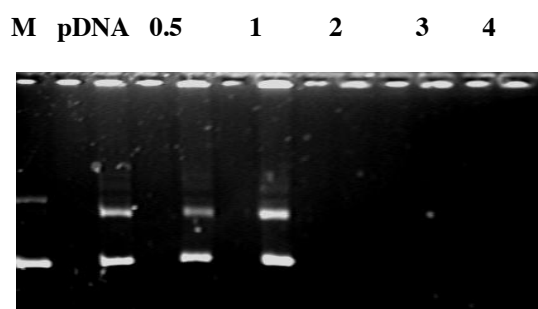
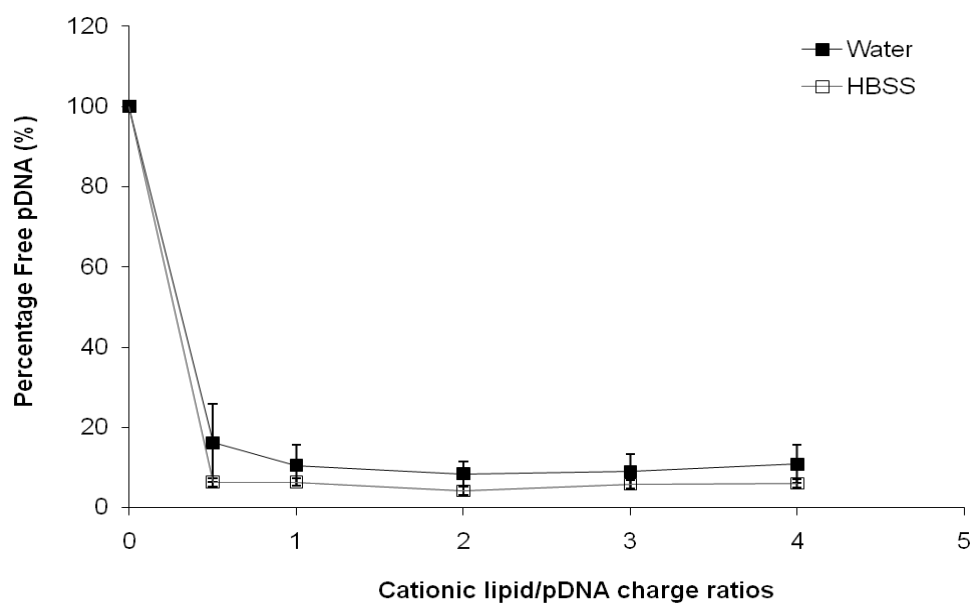


**Figure 2.4** A) Picogreen intercalation assay of LpegD complexes in water and HBSS. The percentage free pDNA represent the fraction of pDNA in the sample available for intercalation with picogreen reagent (n=3, mean  $\pm$ SEM). B) Gel electrophoresis of LpegD complexes prepared at different charge ratios in water; purre pGL3 control vector was used as a marker (M)

In the case of LPD complexes, the percentage of pDNA available for intercalation decreased by 90% at charge ratio 0.5 and remained the same despite increasing the lipid/pDNA charge ratios (Figure 2.5A) indicating complexation at low charge ratios. Unlike the LD and LpegD other complexes, incubation of the LPD complexes in HBSS had no significant effect on the percentage of free pDNA. This data was supported by gel electrophoresis where LPD complexes showed complexation at all charge ratios indicated by the absence of free pDNA bands on the agarose gel (Figure 2.5B).

A)



B)

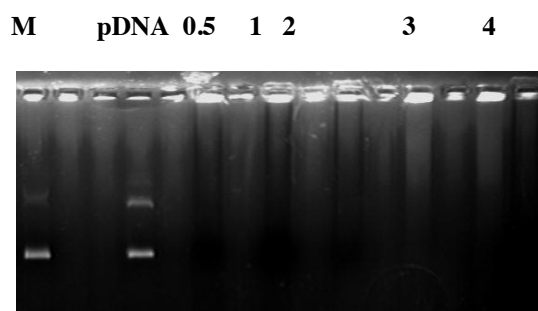
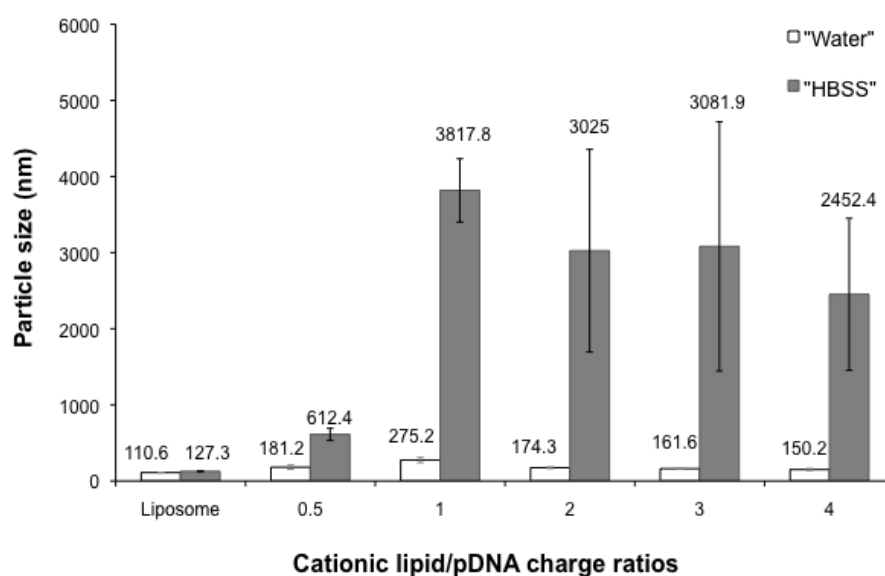


**Figure 2.5** A) Picogreen intercalation assay of LPD complexes in water and HBSS. The percentage free pDNA represent the fraction of pDNA in the sample available for intercalation with picogreen reagent (n=3, mean  $\pm$ SEM). B) Gel electrophoresis of LPD complexes prepared at different charge ratios in water; pGL3 control vector was used as a marker (M)

### **2.4.3. Changes in particle size and zeta potential as a function of charge ratio**

The particle size of LD complexes varied as a function of charge ratios. When DNA was mixed with the liposomes, the mean size of the formed complexes increased from that of the original liposomes. The largest particles were obtained at a charge ratio of 1 and smaller particles were obtained at charge ratios below or above 1 (Figure 2.6A). The smallest diameter (150.2 nm) was observed at charge ratio 4. Zeta potential was negative (-22.91 mV) when pDNA was in excess at the charge ratio of 0.5, then became positive (20-28 mV) at charge ratio  $\geq 1$  (Figure 2.6B). After incubation in HBSS, there was a significant increase in size of the LD complexes at all charge ratios with up to a 10-fold increase at the charge ratio of 1 ( $\sim 3.8 \mu\text{m}$ ) (Figure 2.6A). The trend of particle size as a function of charge ratio was not observed in HBSS as the variability in size increased between different measurements. LD complexes prepared at charge ratio 0.5 were the smallest complexes and their diameters remained in the nano range ( $\sim 500 \text{ nm}$ ). The zeta potential of the LD complexes in HBSS showed a similar profile to the one observed in water; the zeta potential was negative at ratio 0.5 then became positive at charge ratio charge ratios  $\geq 1$  to reach 35 mV at ratio 4 (Figure 2.6B). However as with the particle size, variability in zeta potential between different measurements increased.

(A)



(B)

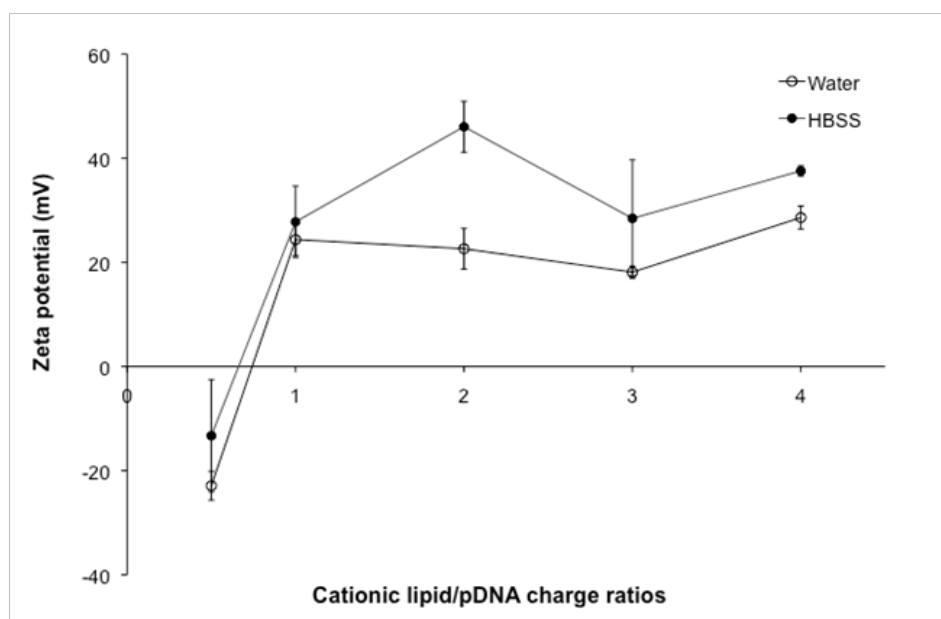
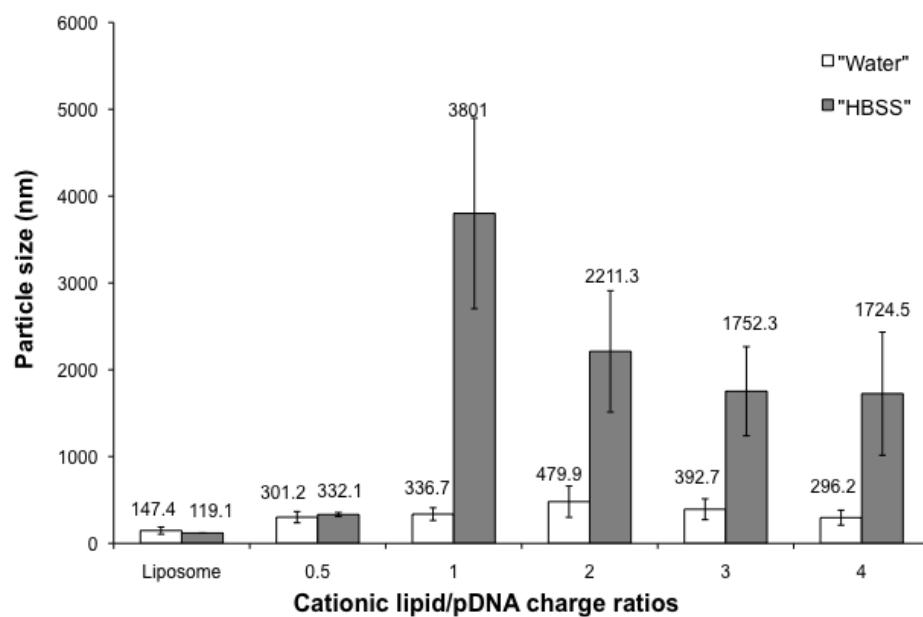


**Figure 2.6** (A) Particle size, and (B) zeta potential of LD complexes prepared at the indicated charge ratios. The particle size (diameter) and zeta potential of the complexes was determined in water (clear) or after incubation in HBSS (filled) (n=3, mean  $\pm$  SEM).

DOTAP:DOPE:DMPE-PEG<sub>5000</sub> had a particle size of  $\sim 150$  nm which increased upon addition upon mixing with pDNA. The LpegD complexes appeared larger than LD complexes with diameters reaching 500 nm or more. However there was high variance in size (Figure 2.7A). The LpegD complexes had a negative zeta potential (-38 to -6 mV) at charge ratios  $\leq 2$ , which became positive as the charge ratios increased. A zeta potential close to zero (charge neutrality) was obtained at charge ratio 2 (Figure 2.7B). Similar to particle size measurements, high variability was also observed between different zeta potential measurements. Incubation of the LpegD complexes in HBSS also resulted in a significant increase in particle size as compared to measurements in water, and the diameters of the complexes went from the nano range to the micro range except complexes at charge ratio 0.5 where the complexes remained small ( $\sim 300$  nm) (Figure 2.7A). Incubation in HBSS significantly increased the positive charge of the LpegD complexes (Figure 2.7B). However similar trends as in water were obtained, the zeta potential shifted from negative to positive at charge ratios greater than 1 to become highly positive at charge ratio  $\geq 2$  ( $\sim 39$ -40 mV) when lipids were in excess. A zeta potential close to zero (neutrality) was observed at charge ratio 1.



(A)



(B)

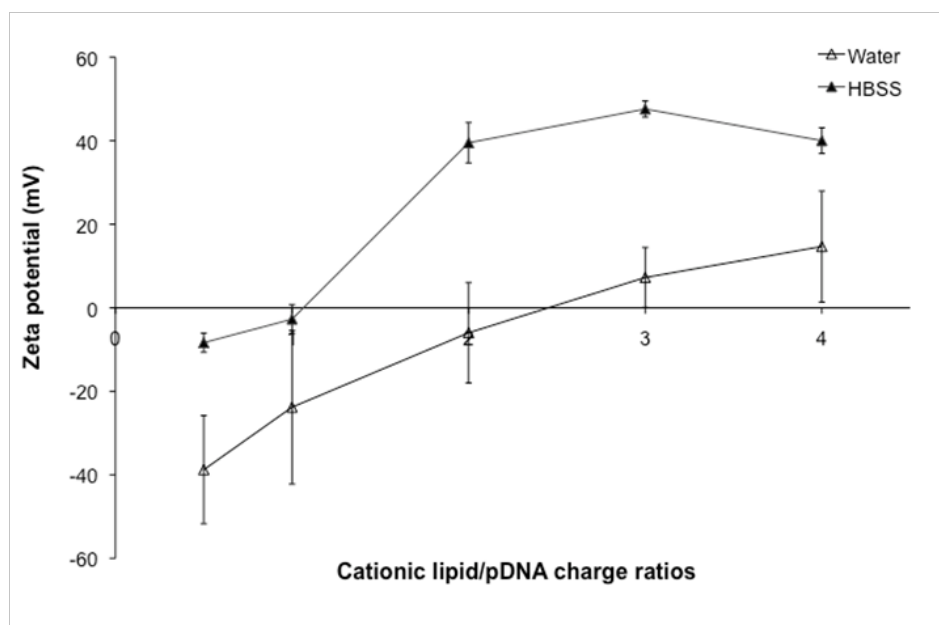
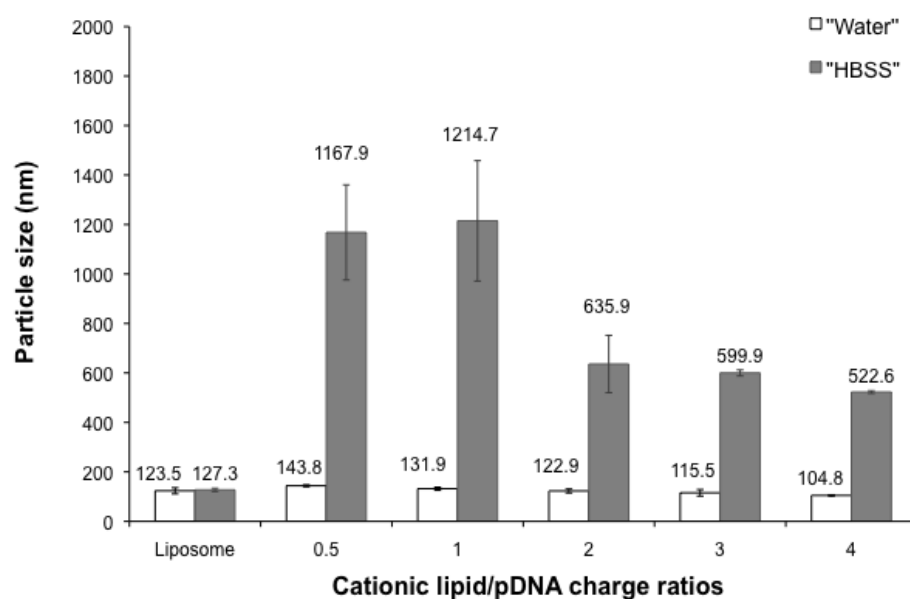


**Figure 2.7** A) Particle size, and B) zeta potential of LpegD complexes prepared at the indicated charge ratios. The particle size (diameter) and zeta potential of the complexes was determined in water or after incubation in HBSS (n=3, mean  $\pm$  SEM).

(A)



(B)

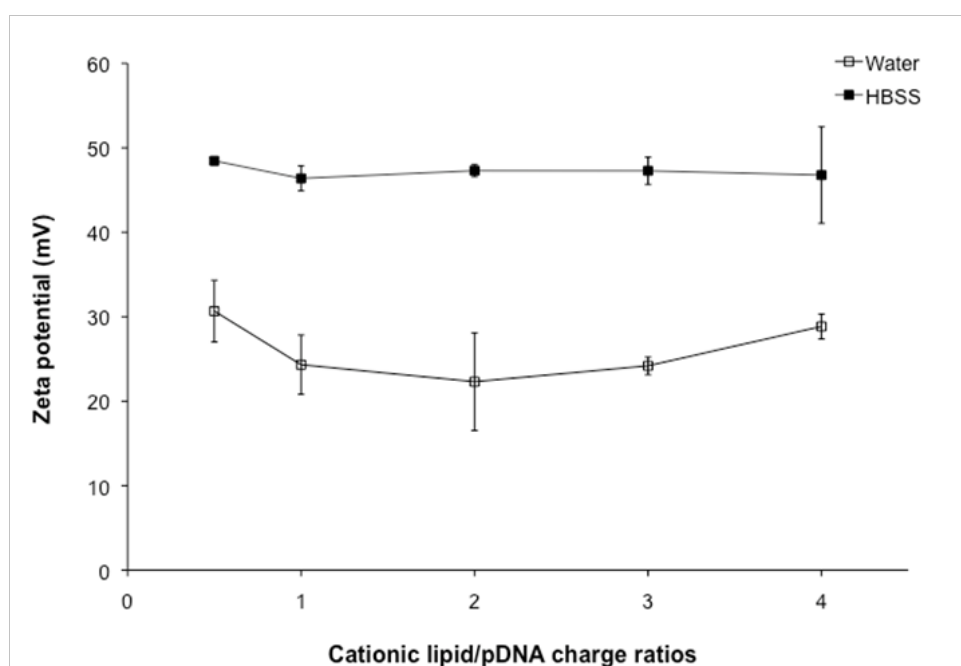


**Figure 2.8** A) Particle size, and B) zeta potential of LPD complexes prepared at the indicated charge ratios. The particle size (diameter) and particle size of the complexes was determined in water or after incubation in HBSS (n=3, mean  $\pm$  SEM).

The exception to the changes in particle size as a function of charge ratio was the LPD complexes. The particle sizes of the LPD complexes were similar to the size of the original DOTAP:DOPE liposomes (~100-120 nm) and remained fairly constant despite the increase in +/- charge ratios (Figure 2.8A). Unlike LD and LpegD complexes, the zeta potentials of the LPD complexes were highly positive (~25-30 mV) at all charge ratios tested. Incubation in HBSS resulted in a significant increase in particle size in particular at low charge ratios 0.5 and 1 (Figure 2.8B). LPD complexes at higher ratios (3-4) were smaller and remained in the nano range (500-600 nm). An important increase in the zeta potential values of the LPD complexes (~45-50 mV) was observed at all ratios as compared to measurements made in water.

#### **2.4.4. Transfection efficacy**

To assess the transfection efficiency of the three lipidic systems, the levels of luciferase gene expression were measured 48 h after delivery of LD, LpegD and LPD complexes at different charge ratios and normalised per amount of protein. Cells transfected with LD complexes showed a significant increase in luciferase expression as compared to naked pDNA ( $p < 0.05$ , ONE-WAY ANOVA and Tukey tests) (Figure 2.9). Luciferase expression induced by LD was dependent on charge ratio with those prepared at  $\leq 2$  (+/-) producing significantly greater gene expression ( $p > 0.05$ , ONE-WAY ANOVA and Tukey tests) than complexes prepared at ratios above this ratio. The LD complexes prepared in the charge ratio range of 0.5 to 2 were as effective as the control lipofectamine/pDNA complexes in inducing luciferase expression

( $p > 0.05$ , ONE-WAY ANOVA and Tukey tests). However at higher charge ratios 3 and 4, a significantly lower gene expression was obtained, almost half of that achieved with lipofectamine, ( $p < 0.05$ , ONE-WAY ANOVA and Tukey tests).

In the case LpegD complexes, a significant luciferase expression was obtained at all ratios as compared to transfection with naked pDNA. ( $p < 0.05$ , ONE-WAY ANOVA and Tukey tests) (Figure 2.10). Again gene expression was determined by charge ratio with maximal expression at charge ratios 0.5 and 1 where the complexes were as effective as the positive control lipofectamine/DNA complexes ( $p > 0.05$ , ONE-WAY ANOVA). On the other hand At charge ratios  $\geq 3$  gene expression levels were significantly lower than those achieved at charge ratio 1 and those obtained with cells transfected with lipofectamine/pDNA complexes ( $p < 0.05$ , ONE-WAY ANOVA and Tukey tests).

As with LD and LpegD complexes, cells transfected with LPD complex showed a significant increase in luciferase expression as compared to naked DNA irrespective of the charge ratio tested ( $p < 0.05$ , ONE-WAY ANOVA and Tukey tests) (Figure 2.11). The complexes at all charge ratios were as effective as lipofectamine/DNA complexes in inducing gene expression ( $p > 0.05$ , ONE-WAY ANOVA and tukey).

When the transfection efficiency of the three complexes were compared, there was no significant difference in gene expression between the three systems at low charge ratios 0.5 to 2 ( $p > 0.05$ , ONE-WAY ANOVA and tukey). However, at charge ratios 3 and 4, the LPD complexes resulted in significantly higher gene expression than both the LD (~3 fold) and LpegD (~5 fold) complexes ( $p < 0.05$ ).

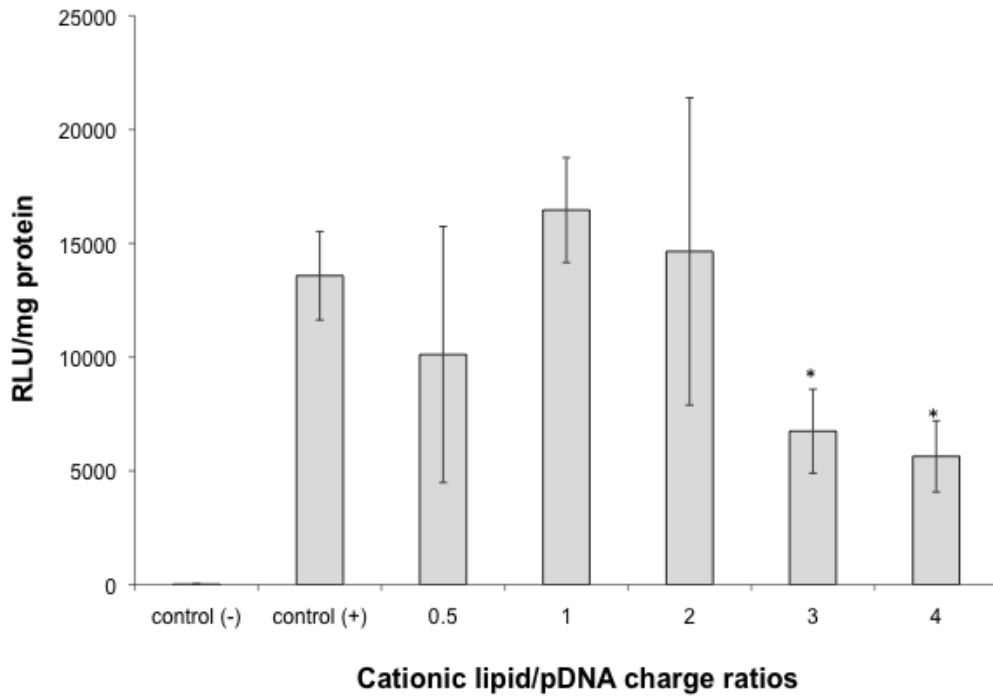


**Figure 2.9** Transfection of Calu-3 cells with LD complexes containing luciferase pDNA prepared at the indicated cationic lipid/pDNA charge ratios. Luciferase activity was measured 48 h post-transfection and luminescence (RLU/mg) represents the level of luciferase gene expression. Lipofectamine/pDNA complexes were used as a (+) control and naked pDNA (charge ratio= 0) represent (-) control. (n=3, mean  $\pm$ SEM). \*Significant ( $p < 0.05$ ) difference from positive control.

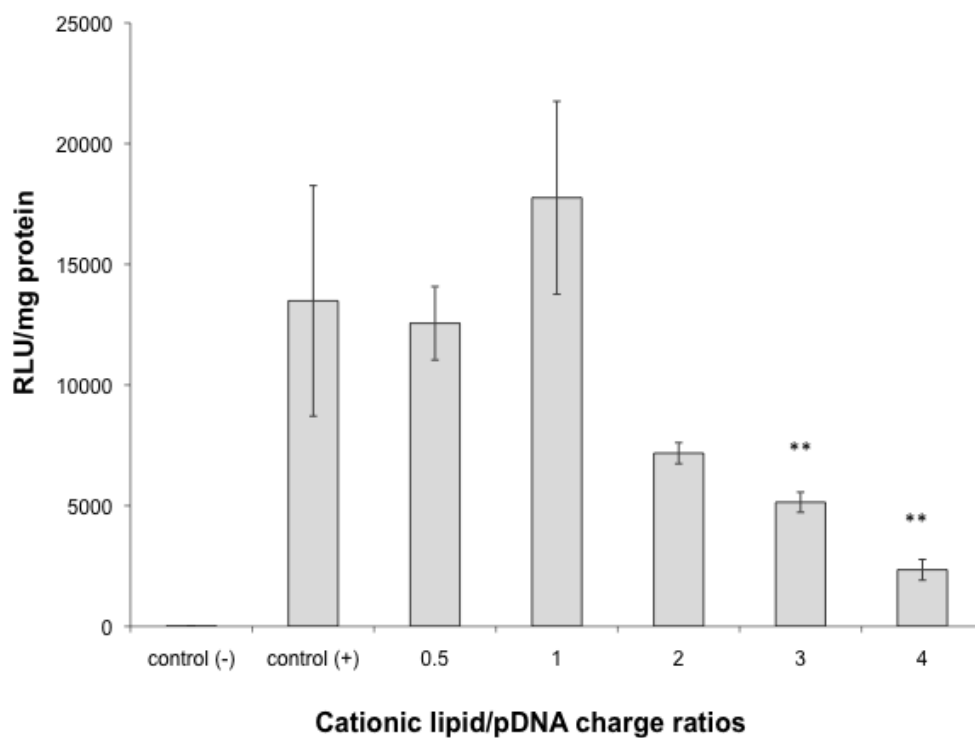


**Figure 2.10** Transfection of Calu-3 cells with LpegD complexes containing luciferase pDNA prepared at the indicated cationic lipid/pDNA charge ratios. Luciferase activity was measured 48 h post-transfection and luminescence (RLU/mg) represents the level of luciferase gene expression. Lipofectamine/pDNA complexes were used as a (+) control and naked pDNA (charge ratio= 0) represent (-) control. (n=3, mean  $\pm$ SEM). \*\*Significant ( $p < 0.01$ ) difference from positive control.

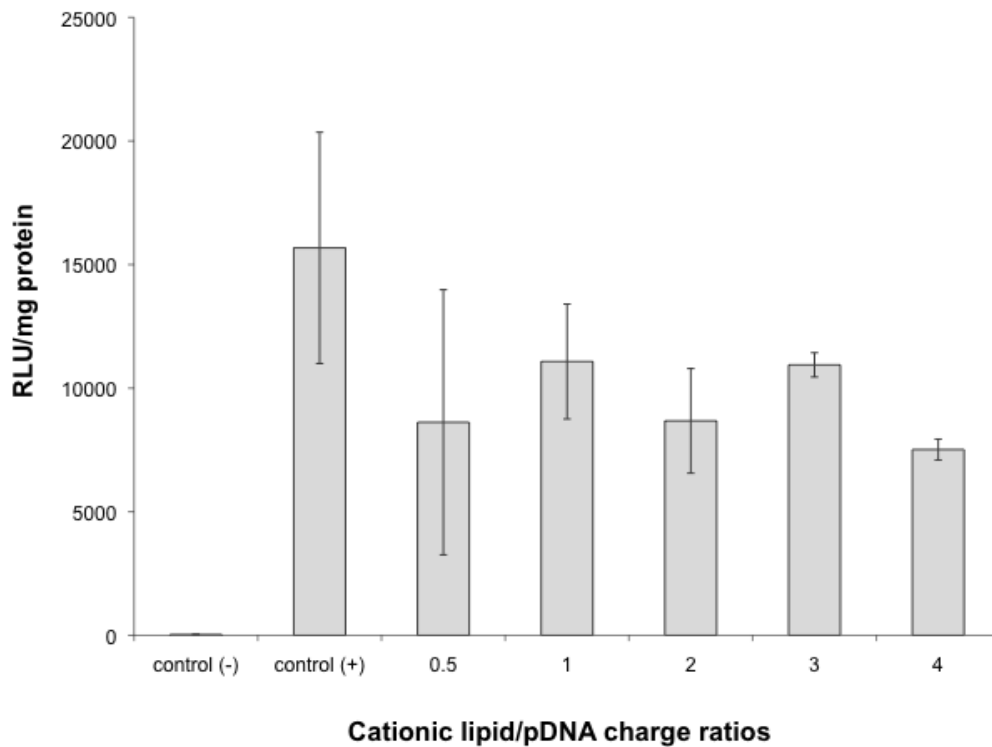


**Figure 2.11** Transfection of Calu-3 cells with LPD complexes containing luciferase pDNA prepared at the indicated cationic lipid/pDNA charge ratios. Luciferase activity was measured 48 h post-transfection and luminescence (RLU/mg) represents the level of luciferase gene expression. Lipofectamine/pDNA complexes were used as a (+) control and naked pDNA (charge ratio= 0) represent (-) control (n=3, mean  $\pm$ SEM).

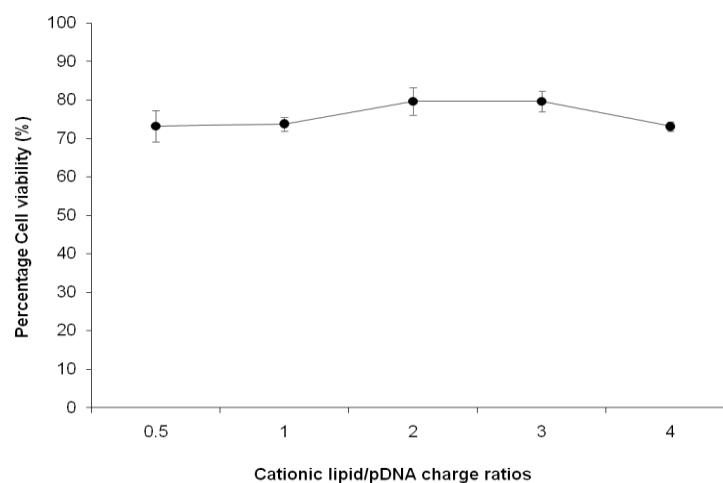
#### 2.4.5. MTT toxicity study

MTT test was carried out to determine the effect of increasing cationic lipid/pDNA charge ratio i.e. amounts of cationic liposomes, on the viability of Calu-3 cells. Untreated cells were considered as having 100% cell viability. The cell viability remained above 70% for all three systems irrespective of the charge ratios

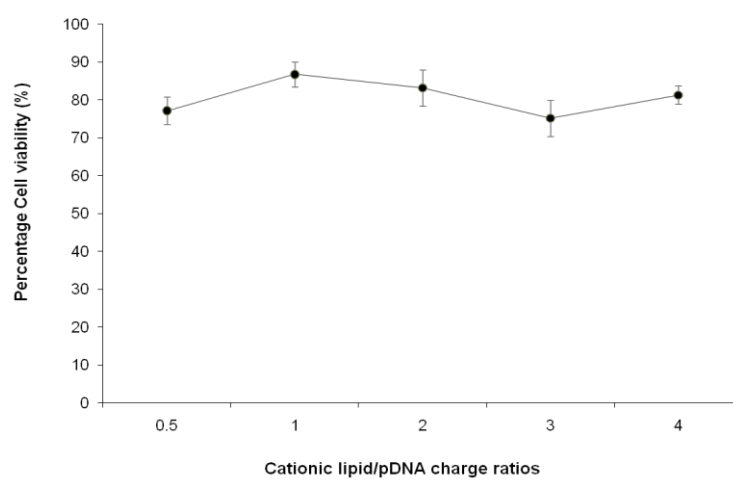
tested. Both LD and LpegD complexes resulted in about 20-30% reduction in cell viability irrespective of the charge ratio used. There was no significant difference in cell viability between low and high charge ratios (Figure 12A&B). LPD complexes on the other hand showed no reduction in cell viability at lipid/pDNA charge ratio 0.5 and resulted in less than 10% reduction at charge ratio 1 (Figure12C). However, a further reduction in cell viability was observed at higher charge (20-30% at charge ratios 2-4)



(A)



(B)



(C)

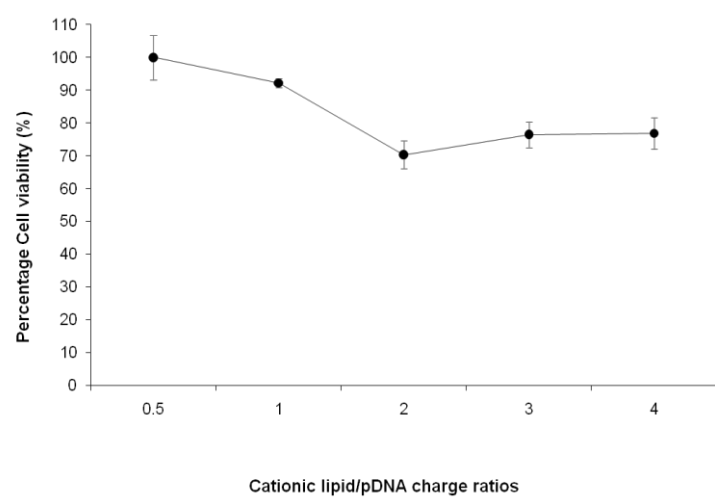


**Figure 2.12** Cytotoxicity of LD (A), LpegD (B) and LPD (C) complexes in Calu-3 as assessed by MTT assay. The relative cell viability as compared to untreated cells is presented as a function of charge ratios ( $n=3$ , mean  $\pm$ SEM).

## **2.5. Discussion**

### **2.5.1. Effect of charge ratio on physicochemical properties of pDNA complexes**

Transfection efficiency of pDNA complexes is known to depend on many factors, among the main ones are complexation efficiency, size and surface charge of complexes. Therefore prior to exploring transfection efficiency, these parameters were determined both in water and in bio-relevant media at different cationic lipid to pDNA charge ratios.

#### **2.5.1.1. Characterization in water**

A strong correlation between complexation efficiency, size and zeta potential data was observed and displayed a consistent trend as a function of charge ratio. Previously, it has been suggested that when liposomes are titrated into pDNA, the vesicles encounter excess pDNA and become coated with pDNA, which leads to the formation of negatively charged small complexes where pDNA was protruding from the surface (Eastman, S.J. *et al.*, 1997). This suggestion is consistent with the data from this study; at low +/- charge ratios where pDNA was in excess (0.5), LD complexes had a negative zeta potential indicating that charge neutralization did not occur, which was confirmed by the picogreen assay where more than half of pDNA was still available for intercalation with picogreen reagent and by the presence of free pDNA bands on agarose gel. At these ratios LD complexes had small diameters (150-180 nm) because the repulsion by the negative charges prevented the formation of aggregates. Larger LD complexes was observed when the charge ratio

approached neutrality because at this ratio there is almost an equal amount of negative *versus* positive charges and the interaction between complexes could occur easily due to the small zeta potential leading to the formation of aggregates and this is known as the colloidal instability zone (Sakurai, F. *et al.*, 2000a). In a previous study, Atomic Force Microscopy (AFM) images of DOTMA:DOPE:DNA complexes, showed that very large and heterogeneous aggregates were formed when the net charge became zero (Sakurai, F. *et al.*, 2000a). After the neutrality zone (charge ratios  $\geq 1$ ) and where cationic lipid is in excess complete condensation of pDNA by the cationic carrier occurred and this was accompanied by the significant fall in the percentage free pDNA, reduced particle size and the shift from negative to positive zeta potential indicating the formation of more stable complexes. In the report by Sakurai and co-workers, AFM images demonstrated that at high +/- charge ratios when cationic lipid was in excess pDNA complexes appeared compact and the pDNA completely shrunk.

In the case of LpegD complexes, picogreen intercalation data showed that pegylation did not significantly affect complexation efficiency as LpegD system showed similar percentage free pDNA trends as LD complexes. However, unlike with LD complexes, LpegD gel electrophoresis data showed the presence of free pDNA at charge ratio 1, suggesting that the LpegD complexes required higher cationic charge ratio than LD complexes to achieve full charge neutralization. The complexation data also correlated with changes in zeta potential, with a high percentage of free pDNA when the zeta potential was negative and then a reduction in the percentage of free pDNA when the zeta potential became positive, indicating negative charge neutralization. This agrees with a study where it was found that

stabilization by the addition of 1% PE-PEG did not much change the morphology of freshly prepared complexes (Sternberg, B. *et al.*, 1998). In addition, Shi and co-workers showed that the inclusion of 5-10% mole pegylated lipids (DSPE-PEG or Ceramide-PEG) did not affect oligonucleotide (ODN) association with cationic lipids (Shi F, W.L., Nomden a, Stuart M C a, Polushkin E, Engberts J and Hoekstra D, 2002). However, LpegD complexes appeared larger (300-500 nm) than LD complexes (150-300 nm) probably due to external PEG chains as reported by Sanders and co-workers who illustrated that the addition of Pegylated-lipid resulted in an increase in size of GL67-pDNA complexes as compared to non-pegylated LD complexes (Sanders Nn, D.S.S., Cheng Sh, Demeester J, 2002). Surprisingly, the presence of PEG chains increased the heterogeneity of the system as compared to LD complexes, although it was difficult to distinguish any trend in particle size as a function of charge ratio because the differences in particle diameter were not statistically significant.

The physicochemical properties of LPD complexes were completely different from those of LD and LpegD complexes. Protamine sulphate is recognized as an effective condensing agent of pDNA (Collins, E. *et al.*, 2007). The pre-condensation of pDNA with the polycation before the addition of the lipid resulted in charge complete charge neutralisation even at low cationic lipid/DNA charge ratio very little pDNA was available for intercalation with picogreen. Similarly on agarose gel, there were no free pDNA bands apparent at all charge ratios. This was matched by a small particle size (100-150 nm) and a positive zeta potential indication the formation of stable complexes irrespective of the cationic lipid +/- charge ratio used. Sternberg and co-workers showed that pre-condensation leads to the formation of new

structures with a size of one or two liposomes (100-200 nm) (Sternberg, B. *et al.*, 1998). The high proportion of amine groups in these polypeptides reduces the number of charge sites for interaction with cationic liposomes, therefore pDNA complexes formed by pretreatment with protamine sulphate were stable at lower cationic lipid to pDNA charge ratio without aggregation as observed with LD and LpegD complexes (Zhdanov, R.I. *et al.*, 2002) (Hong, K.L. *et al.*, 1997). Birchall and co-workers used negative stain transmission microscopy to show that pre-condensation of pDNA resulted in the formation of small spherical complexes as compared to the larger ‘‘fingerprint-like’’ complexes formed by LD complexes (Birchall, J.C. *et al.*, 1999).

#### 2.5.1.2. Characterization at physiological salt concentration

Due to the electrostatic nature of the pDNA/lipid interaction, the presence of salt was expected to alter the dynamics for the formulations. However many physicochemical characterization of pDNA/lipid complexes are reported in water or at low strength media as reported in section 2.1.2 which does not correlate with cell culture media *in vitro* or physiological environment *in vivo*. Therefore in this study it was considered crucial to characterize the complexes in the media in which the transfection experiments were performed (HBSS). The change in the properties of the different lipidic systems after incubation in high salt medium was measured.

**Complexation efficiency.** Eastman and co-workers reported that high ionic strength increased the accessibility a fluorescent dye to pDNA by decreasing association and compaction of pDNA (Eastman, S.J. *et al.*, 1997). The picogreen intercalation data indicated that this occurred for the LD and LpegD complexes as

incubation in HBSS increased percentage of pDNA available for intercalation at charge ratios (0.5 -2). Mechanistically, this may be explained by the ionic strength reducing the release of counter ions from pDNA and cationic lipid, which are the driving force for complex assembly (Kawashima, T. *et al.*, 2006). However, in this study the decrease in binding efficiency was mainly apparent at low charge ratios while at higher ratios (3-4), there was no significant change in complexation as compared to water. This indicated that at high charge ratios pDNA remained condensed and was not affected by the presence of anions. Whietoff and co-workers reported that positively charged LD complexes (at high charge ratios) are generally more resistant to poly-anion mediated disassembly than those at low charge ratios (Wiethoff, C.M. *et al.*, 2004). In this study, the LPD complexes were not significantly affected by the high salt concentration even at low cationic lipid/pDNA charge ratios. This is due to the presence of a constant amount protamine, which increased the pDNA compaction and made the complex more stable.

**Particle size.** The addition of ions extends the aggregation zone and changes the structure of the complex (Tranchant, I. *et al.*, 2004). Other work reported that pDNA/lipid complexes form compact lamellar structures in water but after exposure to high salt concentration, the complexes are more likely to form non-bilayer structures, which are believed to promote transfection (Sternberg, B. *et al.*, 1998). In this work, the size of all three systems increased significantly after incubation at physiological salt concentration irrespective of the charge ratio tested except at charge ratio 0.5, where the increase in particle size was less marked. The low aggregation at this ratio with LpegD complexes can be explained by the effective shielding of cationic charges by the negatively charged free pDNA as well as the

steric barrier caused by PEG chains in the case of LpegD complexes. However with LPD complexes the negative charge of pDNA was already neutralized by the polypeptide and therefore aggregation was observed from charge ratio 0.5. Despite the increase in size, the LPD complexes were less heterogeneous than LpegD and LD complexes due to the pre-compaction with a constant amount of the polypeptide. Interestingly, although the high ionic strength had no significant effect on the complexation efficiency of the LPD system, but it did cause a significant increase in particle size and formation of large aggregates. This was due to the fact that the presence of electrolytes causes agglomeration of like-charged nanoparticles due to reduced screening of repulsive forces (Gary, D.J. *et al.*, 2007).

**Zeta potential.** In terms of surface charge (zeta potential), the findings of this study were contradictory to what has been reported previously (Eastman, S.J. *et al.*, 1997) where it was shown that as the high salt concentration shields some of the positive charge of liposomes and therefore lowers the zeta potential of the complexes. Here, the zeta potential stayed the same or became slightly more positive for all three systems after incubation in HBSS as compared with measurements in water in particular with the LPD and LpegD complexes where the increase was significant. Nonetheless, the trends of zeta potential as a function of charge ratio in HBSS remained similar to those observed in water. The increase in zeta potential with LPD can be explained by the presence of more free liposomes. With the LpegD system the reason for the increase in zeta potential is unclear.

### **2.5.2. Relationship between physicochemical properties and transfection**

With the exception of LPD complexes, there was a marked influence of the cationic lipid to DNA charge ratio on transfection efficiency and a tendency to a higher transfection at low charge ratios. The influence of this parameter on transfection is related to the effect on either the size of the complexes, surface charge or complexation efficiency or on all of them. LD complexes at low charge ratios 0.5-2 were more effective in inducing luciferase expression in Calu-3 cells than complexes formed at charge ratios of 3-4. This is in agreement with the work done by Masotti and co-workers who showed that a charge ratio 1 maximized transfection efficiency of LD complexes and that this was because at this ratio the particle size was greatest (Masotti, A. *et al.*, 2009). However other work has shown that LD complexes were most effective at high charge ratios (3-4) in C6 cell line (Esposito, C. *et al.*, 2006). These differences are probably due to different experimental conditions and cell lines used.

Similar results were obtained with LpegD complexes, which produced higher gene expression at low charge ratios (0.5-2) when compared to higher ratios (3-4). Several studies support the assumption that transfection efficiency is determined by particle size of the complexes and that large complexes (micron-range) favour transfection (Esposito, C. *et al.*, 2006, Boussein, N.F. *et al.*, 2007, Ross, P.C. and S.W. Hui, 1999a). Although, the findings of the current study confirmed that large pDNA complexes (micron range) can transfect cells efficiently, the difference in luciferase expression between high and low charge ratios was not directly associated with the particle size because incubation in HBSS prior to transfection resulted in the



formation of very heterogeneous systems and there was no significant difference in particle diameters of the complexes prepared at the different charge ratios. Wiethoff and co-workers reported that although LD complexes showed no differences in particle size, they produced different levels of gene expression and concluded that size is not a controlling variable in gene expression (Wiethoff, C.M. *et al.*, 2004). This agrees with the results of the current study. In addition, LPD dependence on charge ratio was apparent as the same level of gene expression at almost all charge ratios was observed despite differences in diameters of the complexes as a function of charge ratio. Thus it can be concluded that large pDNA complexes (micron range) resulted in efficient transfection *in vitro*, but particle size was not the only determinant of transfection efficiency and other factors in addition to size play a role in transfection.

It has been assumed that a positive surface charge is necessary for the interaction of lipoplexes with cellular membrane and therefore entry into cells (Brown, M.D. *et al.*, 2001). In addition, the interaction of positively charged pDNA complexes with endosomal membrane anionic lipids through formation of ion pairs, lateral diffusion, and lipid mixing are mechanisms that have been speculated to facilitate the DNA release (Xu, Y. and F.C. Szoka, Jr., 1996). However, there is evidence that neutral or negatively charged complexes are effective in transfection and result in high gene expression (Wiethoff, C.M. *et al.*, 2004, Patil, S.D. *et al.*, 2004). The data presented here, showed an increased gene expression at low charge ratios where LD or LpegD complexes had a negative or small zeta potential (close to neutrality) and a decrease in gene expression at higher charge ratios where zeta potential was positive. This supports the contention that a positive surface charge is

not essential for transfection efficiency, which may be because negatively charged LD complexes trigger internalization via a different endocytic pathway than positively charged complexes as suggested by Wiethoff and co-workers. Their work showed that when cholesterol was used instead of DOPE as the neutral lipid, negatively charged pDNA complexes did not disrupt the negatively charged cellular membrane due to either an inability to attain close proximity between negatively charged liposomes and negatively charge surface of pDNA complexes to initiate fusion or an inability to adopt the non-bilayer structure needed for fusion. Therefore, even if the complexes were taken-up by cells, they may not escape endosomal compartments. Incorporation of DOPE into the formulation resulted in a significant increase in membrane disruption, which correlated with an increase in gene expression. This indicated that the presence of the fusion lipid DOPE has a more significant role in interaction with cellular membranes and transfection efficiency than the surface charge of the complexes (Wiethoff, C.M. *et al.*, 2004). Guo and Lee also demonstrated that the fusigenic lipid DOPE was crucial for the endosomal escape and therefore transfection efficiency of anionic complexes (Guo, W. and L. Rj, 2000).

Another important observation is that although pDNA is not fully neutralized or condensed by the cationic lipid at low charge ratios (percentage pDNA available for interaction with the picogreen reagent was 50-80% with LD and 60-90% with LPegD), high gene expression was obtained whereas at higher complexation rate (less than 20% available pDNA at charge ratio 3-4) gene expression was lower. Although it is believed that full condensation of pDNA is necessary for efficient transfection, Sakurai and co-workers reported that the release

of pDNA from the complexes once inside the cell is one of the most crucial steps in determining optimal cationic lipid to pDNA charge ratio as it might be difficult for pDNA to be released from very compact complexes especially at high charge ratios. This theory could explain the low gene expression at high charge ratios for LD and LpegD complexes but does not justify the high gene expression for LPD complexes in which pDNA is well condensed at all charge ratios as shown by picogreen intercalation and light scattering data.

### **2.5.3. Transfection *versus* toxicity**

In order to assess the relationship between toxicity and transfection efficiency, the cytotoxic effect of LD, LpegD and LPD complexes were determined at different charge ratios using MTT test. Cellular damage caused by the three systems was relatively small compared to untreated cells as cell viability remained above 70% even at high charge ratios. It had been reported that toxicity is closely related to cationic lipid/pDNA charge ratios (Lv, H.T. *et al.*, 2006) and is more pronounced at high charge ratios due to the high positive zeta potential of the complexes (Sakurai, F. *et al.*, 2000b)

However, the cell viability data of LD and LpegD complexes showed no significant difference in cell viability between complexes prepared at different lipid/pDNA charge ratios, which implied that the reduced gene expression at high charge ratios was not due to toxicity. Slightly higher cell viability was observed with LpegD complexes (75-85%) compared to LD complexes, perhaps because the presence of PEG chains shifted some of the positive charge of the cationic lipid. In contrast to LD and LpegD, LPD complexes were associated with a trend to lower

cell viability (albeit still not beyond the 70% viability level) with an increase in cationic lipid/pDNA charge ratios, possibly due to the presence of free liposomes in sample at high charge ratios (Lv, H.T. *et al.*, 2006). Xu and co-workers showed that removal of free liposomes from LD complexes prepared at high charge ratios resulted in reduction of toxicity (Xu, Y. *et al.*, 1999). However in another study, the purification of LPD complexes from free liposomes resulted not only in reduced toxicity, but also reduced transfection efficiency (Li, S. *et al.*, 1998). In terms of transfection efficiency, the reduction in cell viability at high charge ratios did not seem to affect the level of gene expression as cell viability remained above 70% (Masotti, A. *et al.*, 2009). Overall, the charge ratios selected for this study did not cause excessive cellular damage.

#### **2.5.4. Conclusion**

In conclusion, the trends in gene expression achieved using LD and LpegD complexes were similar with lower pDNA condensation at low (+/-) charge ratio giving higher gene expression, which was attributed to ready release of pDNA from the complex once inside the cells. In contrast, LPD complexes showed similar gene expression as LD and LpegD complexes despite the high compaction of pDNA at all charge ratios. Complexes prepared at (+/-) charge ratio 1 appeared to give the highest transfection efficiency except for the LPD system, which was effective at all charge ratios. For LD and LpegD systems formation of stable complexes after charge ratios 1-2 resulted in reduction in transfection efficiency. The parameters that may affect transfection such as size, charge and complexation efficiency were

specific to the lipid composition used and it was not possible to determine the main parameter that governs transfection.

The data presented in this chapter illustrated the importance of characterising pDNA complexes at physiological salt concentration as the presence of high ionic strength resulted in a remarkable change in the physicochemical properties of the complexes. The lipids used here will be used to compare the differences between pDNA and siRNA formulation in terms of physicochemical characteristics and transfection efficiency in the next chapter.

# **Chapter 3 *In vitro* delivery of siRNA using cationic lipid delivery vectors**

### 3.1. Introduction:

siRNA targets have been identified in various diseases such as cancer, viral infections, and neurodegenerative disease (Shrivastava, N. and A. Srivastava, 2008) and as the attractiveness of siRNA as a therapeutic tool is increasingly recognised, there is an imperative need to develop efficient delivery systems for clinical application. When searching for potential siRNA delivery carriers, it is only logical to first investigate those with proven efficacy in delivering pDNA. Among those are cationic lipids, which show great promise as carriers due to their low toxicity and ease of production (Wu, S.Y. and N.A. Mcmillan, 2009).

Although both pDNA and siRNA are polynucleotides and therefore face similar physical barriers to their delivery, structural differences between siRNA and DNA as well as differences in their method of action, are likely to be responsible for differences in formulation (Gary, D.J. *et al.*, 2007, Spelios, M. *et al.*, 2010, Marty, R. *et al.*, 2009b). The size and electrostatic charge of siRNA are much lower than that of pDNA, and siRNA is more susceptible to degradation by nucleases (Mahon, K.P. *et al.*, 2010). siRNA acts primarily in the cytoplasm (Morille, M. *et al.*, 2008, De Fougères, A. *et al.*, 2007), it does not require nuclear targeting which is an important barrier in pDNA delivery (Wasungu, L. and D. Hoekstra, 2006, Thomas, M. *et al.*, 2007). The physicochemical differences between siRNA and pDNA may affect the interaction between the nucleic acid with the delivery vectors and this, along with the different site and mechanism of action, may affect their functionality.

The previous chapter described the physicochemical properties of three cationic lipid/pDNA complexes; LD, LpegD and LPD and attempted to define the

relationship between the properties of the formulations and gene transfection efficacy. No single physicochemical property (size, charge or condensation efficiency) was predictive of gene expression efficiency, but it is possible that the characteristics of the dominating population of complexes (detectable by the characterization methods) might not be the biologically active component.

### **3.1.1. siRNA assays using respiratory epithelial cells *in vitro***

In addition to the Calu-3 cell line utilised in Chapter 2, the A549 cell line was used to assay gene knockdown, to determine whether there is a difference in transfection efficiency between different cell lines. This cell line is one of the most characterised and widely used *in vitro* systems for studying the alveolar epithelial function. This human adenocarcinoma-derived cell line forms cell layers with characteristic alveolar type II cell morphology. Type II cells are more numerous than Type I cells, and have distinct functions such as oxidative metabolism of drugs in the lung and production of surfactant (Foster, K.A. *et al.*, 2000). They are believed to differentiate into Type I pulmonary epithelial cells, which cover 96% of the surface area of the pulmonary epithelium (Steimer, A. *et al.*, 2005). Their endocytic properties have been well characterized which makes them a potential target for drug delivery of macromolecules. A549 cell lines have been shown to have many type II cell characteristics and they have been widely used to study alveolar drug uptake, metabolism, and gene delivery (Steimer, A. *et al.*, 2005). They are also considered as an accepted model in pulmonary toxicity studies, and unlike Calu-3 cells they have been extensively used for gene delivery studies



At the time of this thesis, only one study compared transfection efficiency of pDNA and siRNA using the CDNA:DOPE lipidic formulation in Hela cell line (Spagnou, S. *et al.*, 2004). The findings of this study showed that pDNA and siRNA required different (+/-) charge ratios for optimal transfection, but this has not been investigated systematically with the formulation physicochemical properties linked to functional transfection. In addition the media in which the particle size of siRNA complexes was determined was different from the media used in transfection. Therefore, in this work, it was hypothesized that the factors that influence transfection efficiency such as formulation type, charge ratio, physicochemical properties might have a different effect on pDNA and siRNA transfection efficiency.

### **3.1.2. Aim and objectives**

The aim was to compare the siRNA formulations with equivalent formulations using pDNA using the same three systems characterized for pDNA delivery. Formulations were evaluated in terms of their physicochemical properties and their delivery to obtain a biological effect. The specific objectives of this chapter were to:

- Measure the physicochemical properties of cationic lipid-siRNA formulations and compare these to the results obtained for the same formulations with pDNA,
- Develop assay methodology to measure the effect of siRNA delivery *in vitro* by measuring GADPH knockdown,
- Measure the transfection efficiency of cationic lipid-siRNA formulations,
- Compare the efficacy of the formulations in two cell lines,

### 3.2. Materials

Material	Supplier
Glyceraldehyde-3-phosphate dehydrogenase (GAPDH) siRNA, Cy3-GAPDH siRNA, 1# negative control siRNA and KDalert assay kit	Ambion (UK)
A549 cells (p112-120)	ATCC (Rockville, USA).
RPMI-1640	Sigma-Aldrich Ltd, Dorset, UK
DAPI	Sigma-Aldrich Ltd, Dorset, UK
SYBR green II reagent	Invitrogen (UK)

### **3.3. Methods**

#### **3.3.1. GAPDH siRNA and negative control siRNA**

GAPDH (glyceraldehyde 3-phosphate dehydrogenase) siRNA, which targets the abundant ubiquitously expressed housekeeping gene GAPDH was used to determine gene knockdown in cell cultures. This siRNA efficiently reduces both the mRNA and protein levels of GAPDH in human, mouse and rat cell lines. A non-specific negative control siRNA, which is a non-targeting sequence, was used as baseline from which to determine the siRNA silencing effect. The control was employed to identify nonsequence-specific effects of GAPDH siRNA as well as the toxicity of the delivery vectors.

#### **3.3.2. Preparation of cationic liposomes/siRNA complexes**

Cationic liposomes were prepared in the same way as described in 2.3.2. The three cationic liposomes based systems were used to complex siRNA; DOTAP:DOPE (1:1 molar ratio), DOTAP:DOPE:DMPE-PEG<sub>5000</sub> (1:1:0.05 molar ratio), and DOTAP:DOPE (1:1) Protamine to form LR, LpegR and LPR, complexes, respectively.

siRNA and cationic liposomes complexes were prepared by sequentially diluting siRNA in non-supplemented cell culture media, then adding appropriate amounts of liposomes. After vortexing, the mixtures were incubated for 30 min at room temperature to allow complex formation. The amount of liposomes added was based on the desired +/- charge ratios (0.5, 1, 2, 3, 4, 6, 10, 12). The +/- charge ratio was calculated as total number of positive charges on the DOTAP molecules divided

by the total number of negative charges on the nucleic acid (assuming 1  $\mu$ g siRNA contains 3nmol negatively charged phosphate groups and one DOTAP molecule contains one positive charge). LPR complexes were prepared by the addition of protamine (1 mg/ml) to siRNA at a 2:1 mass ratio with 10 min incubation, followed by the addition of DOTAP:DOPE liposomes and incubation for 30 min to allow complexation.

### **3.3.3. Characterization of cationic liposome/siRNA complexes**

#### **3.3.3.1. SYBR green II intercalation assay**

SYBR green II reagent is a very sensitive fluorescent nucleic acid stain, which is more sensitive to dsRNA than dsDNA. This reagent intercalates between nucleic acid base pairs and emits fluorescence at 497/520 nm and is used to quantify dsRNA at concentration as low as the picogram range. The accessibility of this reagent to intercalation with siRNA base pairs in the lipid complexes was determined and used as a measure of degree of siRNA condensation in the cationic liposome.

siRNA and cationic liposomes complexes were prepared at different charge ratios as described in 3.3.2. SYBR green II 3X solution was prepared by diluting SYBR green II reagent 10000X 1 in 3000 times in HEPES buffer. SYBR green II (100  $\mu$ l, 3X solution) was added to 100  $\mu$ l of the formed complexes in water or non-supplemented cell culture media and the fluorescence was measured in sterile black 96-well microplates at an excitation wavelength of 497 nm and emission wavelength of 520 nm using a Spectra Max Microplate spectrophotometer set at gain 40). The fluorescence scale was calibrated such that the initial fluorescence of SYBR green II

(100 µl of 3X solution added to the well containing 100 µl water or non-supplemented media) was set as background fluorescence. The fluorescence obtained upon addition of naked siRNA in 100 µl non-supplemented media (50 nM/100 µl; control) minus background fluorescence was set as the positive control (reference fluorescence). The amount of siRNA available for intercalation with the SYBR Green II was calculated by subtracting the values of background fluorescence from those obtained for each measurement, and expressed as a percentage of the control according to the following formula: % free siRNA = 100 x (fluorescence of cationic lipid:siRNA complexes/fluorescence of control).

#### 3.3.3.2. Light scattering and zeta potential

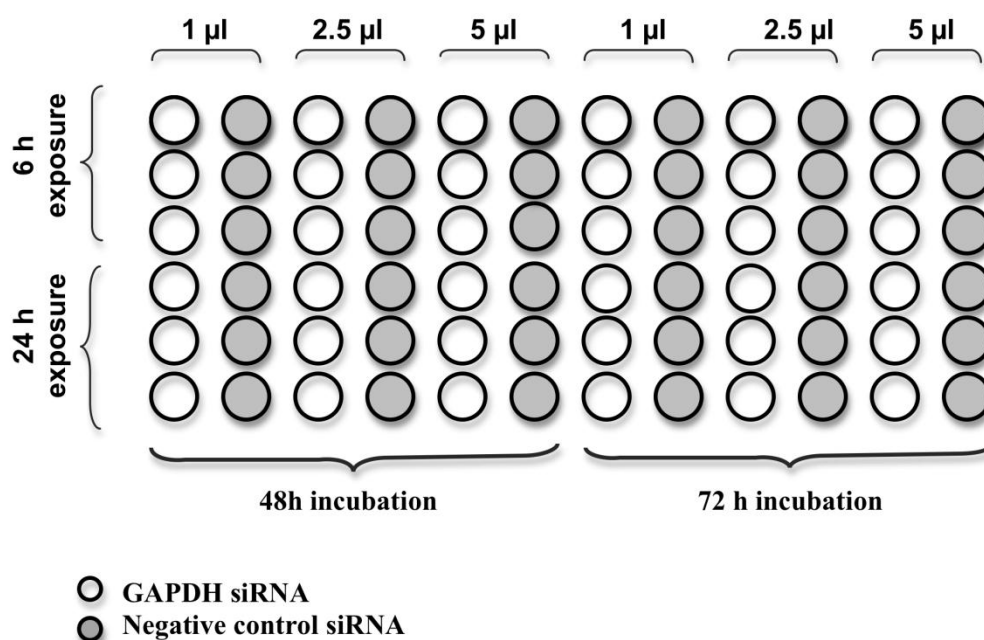
The prepared siRNA complexes were placed into UV cuvettes containing phenol red-free non-supplemented cell culture media and then inserted in Brookhaven instrument ZETApus particle sizer to measure the particle size and zeta potential. The reported hydrodynamic diameters and zeta potentials represent the average values of five readings taken at 10 s intervals.

For the zeta potential measurements, inconsistent readings were obtained, probably due to the low concentration of the complexes in the sample and due to high cost of siRNA higher concentrations could not be increased. Therefore the particle size and polydispersity of the complexes in DMEM were determined only in phenol red-free non-supplemented cell culture media.

### **3.3.4. The optimisation of transfection conditions for the positive control**

The commercial transfection agent, Lipofectamine employed as a positive control for pDNA transfection experiments (section 2.3.6) has not been optimised for siRNA delivery in Calu-3 cells. Therefore the aim of this experiment was to determine the transfection conditions that will provide maximum gene silencing while maintaining an acceptable level of cell viability. The critical parameters that were optimized included the amount of transfection reagent, the duration of complex exposure to cells and the time allowed for protein knockdown to occur (incubation time).

Calu-3 cells were cultured as described in section 2.3.5 with the incubation conditions in the following experiments being 37°C and 5% CO<sub>2</sub>. siRNA/lipofectamine complexes were prepared by diluting siRNA in non-supplemented cell culture media then adding the indicated amounts of lipofectamine. After vortexing, the mixtures were incubated for 30 min at room temperature to allow complex formation. Cells that were seeded in a 96-well plate at a seeding density of  $1 \times 10^4$  cells per well in normal media (10% FBS), and that were incubated for 24 hours before the transfection experiments were performed. The medium was removed from these cells and siRNA/lipofectamine (50 nM siRNA per well) complexes made in serum free DMEM-12 medium at different concentrations were added to the cells. At appropriate times, the complexes were removed and replaced with normal growth medium (10% FBS) to maximize cell growth and prevent potential cytotoxicity. The cells were then incubated for either 48 or 72 h, before measuring GAPDH knockdown and cell viability using the KDalert assay.



Cells were exposed to the complexes prepared using different amounts of lipid for either 6 or 24 h. GAPDH silencing was determined at both 48 and 72 hours post-transfection.

### 3.3.5. Determining protein knock down and toxicity using KDalert assay kit

The KDalert GAPDH assay measures the conversion of NAD<sup>+</sup> to NADH by GAPDH in the presence of phosphate and glyceraldehyde-3-phosphate (G-3-P). The production of NADH under these conditions results in a fluorescence increase and a colour change in the samples. Under the recommended assay conditions, the rate of NADH production is proportional to the amount of GAPDH enzyme present. Thus the assay can be used to determine accurately the amount of GAPDH protein in a sample.

The culture medium was aspirated from transfected cells and the KDalert Lysis Buffer (200  $\mu$ l) was added to each well for 20 min at 4°C. Cell lysate (10  $\mu$ l) was transferred to the wells of a black 96-well plate and 90  $\mu$ l of KDalert Master Mix was added to each sample at approximately the same time. The increase in fluorescence of the samples over 4 min was measured at room temp (excitation/emission wavelengths of 520/585 nm). Efficiency of transfection was expressed as 'percent gene silencing' with respect to controls (cells treated with the same amount of transfection reagent complexed to negative Control #1 siRNA to ensure that the decrease in protein levels was due to specific gene silencing not to the toxicity of the transfection agent). Other controls included untreated cells and cells treated with naked siRNA. The percent remaining gene expression for a given transfection condition was determined from the ratio of the fluorescence increase for samples transfected with GAPDH siRNA to the fluorescence increase for samples transfected with Negative Control #1 siRNA. The level of gene knock down was calculated from the % remaining expression, according to the equation: % knockdown= 100 - (100 x  $\Delta$ fluorescence GAPDH /  $\Delta$ fluorescence Negative control siRNA)

### **3.3.6. Transfection of bronchial epithelial cell line, Calu-3**

GAPDH siRNA or negative control siRNA/lipid complexes LR, LPR and LpegR were prepared in DMEM-12 at different charge ratios (0.5 to 12) as described above. Complexes were then added to the Calu-3 cells for 6 hours (final siRNA concentration 50 nM/100  $\mu$ l). After that time, complexes were removed and replaced with serum containing media and the cells were then incubated for 72 hours before measuring GAPDH enzyme activity using the KDalert assay.



### **3.3.7. Transfection of alveolar epithelial cell line, A549**

A549 cells (passages 104-120) were subcultured in 162 cm<sup>2</sup> flasks in RPM-1640 media supplemented with gentamycin (0.1% v/v), L-glutamine (5% v/v), non-essential amino acids (5% v/v), and foetal bovine serum (10% v/v). Cells were left to grow at 37°C in a humid atmosphere containing 5% CO<sub>2</sub>. Every second day the medium was changed and once the cells reached 80-90% confluency, they were trypsinised using 1 ml of trypsin-EDTA (0.25%) solution before being passaged on or plated for experimentation. The A549 cells were transfected as described above and the level of GAPDH activity was measured 72 hours after transfection using the KDAlert assay.

### **3.3.8. The effect of serum on gene silencing efficiency**

In order to investigate the stability of the siRNA complexes in the presence of serum, A549 cells were transfected with LPR and LpegR complexes prepared at charge ratio of 10:1 in the presence and absence of foetal bovine serum. Transfection was carried out as described above, except that after the preparation of the complexes in serum-free media, 5% or 20% FBS was added to the complex mix, which was then added to A549 cells.

### **3.3.9. Data analysis and statistics**

A statistical package for social sciences (SPSS version 11.0) software was used to perform Unpaired t-test and One-way ANOVA and Post-Hoc Tukey's tests. Statistically significant differences were assumed when p values were less than 0.05.

Unpaired t- test was performed to compare the difference in gene silencing between complexes containing GAPDH siRNA and complexes containing negative control siRNA.

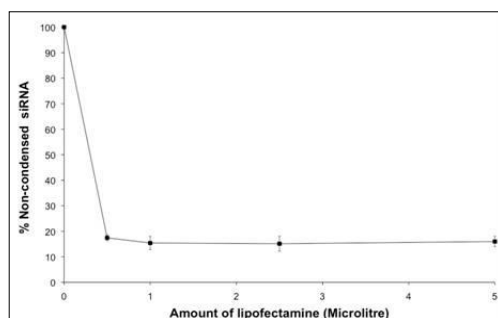
One-way ANOVA and Post-Hoc Tukey's tests were performed to determine whether there was a significant difference in gene silencing between the three lipidic formulations at each charge ratio and the control lipofectamine

### **3.4. Results**

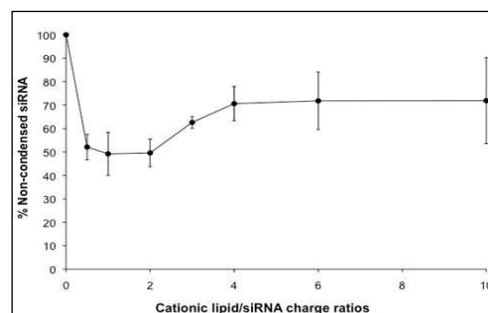
#### **3.4.1. SYBR green II intercalation assay**

SYBR green II intercalation assays were employed to determine the degree of complexation of siRNA by the cationic vectors in LR, LpegR and LPR complexes prepared in transfection media DMEM. Complexation efficiency of lipofectamine a commercial transfection reagent was used as a positive control. Upon addition of lipofectamine to siRNA significant quenching of SYBR green II fluorescence was observed as compared with naked siRNA, which indicated efficient complexation and formation of stable complexes as shown with a decrease in percentage free siRNA from 100% (naked siRNA) to 15% and remained constant despite the increase in the amount of lipid (Figure 3.1A). LR complexes caused a significant decrease in percentage of free siRNA at ratios ranging from 0.5 to 2 (down to ~50% at ratios  $\leq 2$ ). However, at higher ratios (6-10) the percentage of free siRNA available for intercalation increased (Figure 3.1B). LpegR complexes displayed low complexation efficiency at all ratios (Figure 3.1C). In the case of LPR complexes, a significant decrease in percentage free siRNA was observed at charge ratio 0.5 (down to  $\leq 20$  % free siRNA), which then increased to 40-50% and remained constant at all ratios (Figure 3.1A)

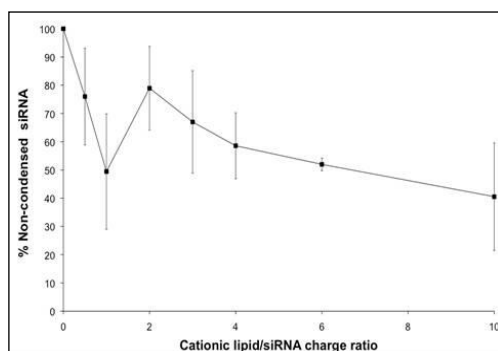
(A)



(B)



(C)



(D)

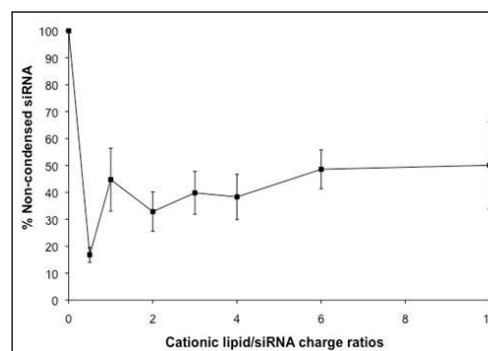


**Figure 3.1** SYBR green II intercalation assay for A) Lipofectamine/siRNA B) LR C) LpegR and D) LPR complexes prepared in DMEM. Complexes were prepared at the indicated charge ratios and the percentage of siRNA in the sample that is available for intercalation with SYBR Green II gel stain was determined. Naked siRNA was used as control and represents 100% free siRNA (n=3, mean  $\pm$  SEM).

### 3.4.2. Particle size and polydispersity of siRNA complexes

After the addition of the cationic lipids to siRNA, the mean particle size generally increased from that of the original DOTAP:DOPE liposomes which was typically 150-160 nm to reach a maximum at charge ratio 2 (~600 nm) then decrease with the increasing charge ratio (down to 200 nm at charge ratio 10) (Figure 3.2). The smallest complexes were observed at ratios ranging between 6 and 12 (<200 nm). High particle size polydispersity was observed at low charge ratios then decreased as the charge ratio increased but the decrease was only significant at ratios ranging between 6 and 12.

LpegR complexes had similar particle size and polydispersity compared to LR complexes, with an initial increase in the particle size after the addition of the cationic lipids to siRNA, from 130-140 nm (size of the original liposome) to reach a maximum of 400-450 nm at the charge ratios 1-2, and then the size decreased with the increasing charge ratios down to a minimum of 100 nm at ratios ranging between 6 to 12 (Figure 3.3). The polydispersity of the system was high at low ratios (0.5-4) then significantly decreased from charge ratio of 6 upwards. The LPR complexes had a fairly stable particle size (200-250 nm) irrespective of the change in cationic lipid/siRNA charge ratios (Figure 3.4). However, the polydispersity displayed a trend similar to the one observed with LR and LpegR, i.e., it was high at low charge ratios then significantly decreased at charge ratios  $\geq 6$ .

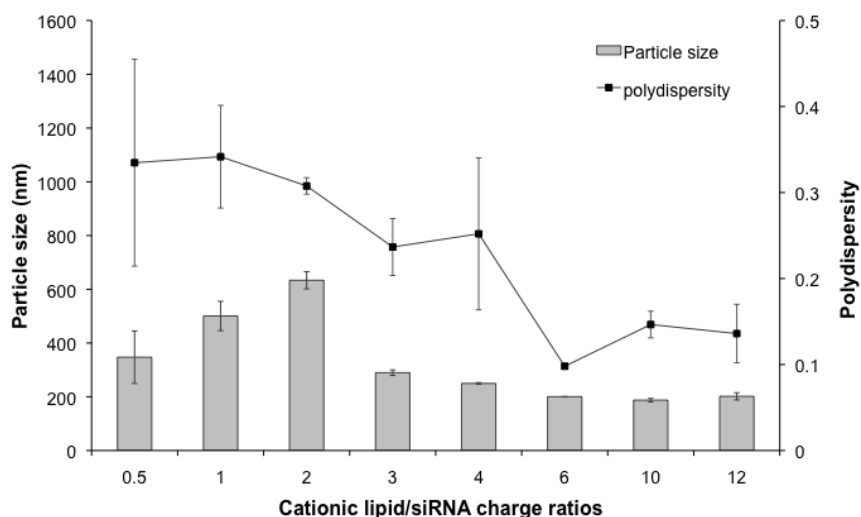


**Figure 3.2** The changes in the particle size and size distribution of LR complexes as a function of the cationic lipid:DNA/siRNA charge ratio. The diameters (nm) and polydispersity of the complexes were determined 45 min after their preparation in serum-free cell culture media. (n=3, mean  $\pm$ SEM).

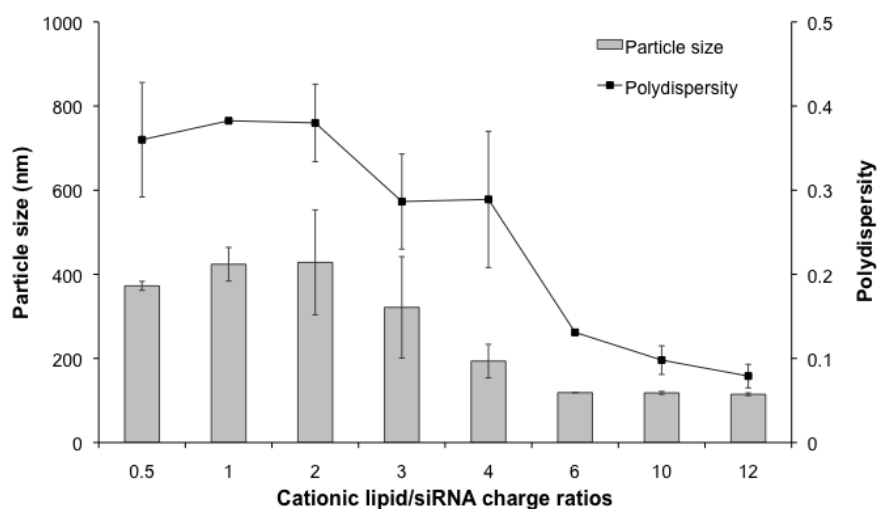


**Figure 3.3** The changes in the particle size and size distribution of LpegR complexes as a function of the cationic lipid:DNA/siRNA charge ratio. The diameters (nm) and polydispersity of the complexes were determined 45 min after their preparation in serum-free cell culture media. (n=3, mean  $\pm$ SEM).

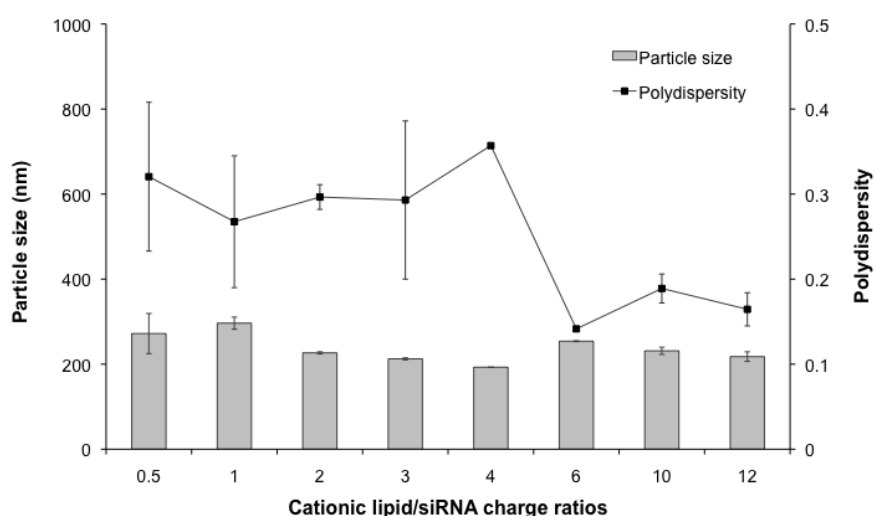


**Figure 3.4** The changes in the particle size and size distribution of LPR complexes as a function of the cationic lipid:DNA/siRNA charge ratio. The diameters (nm) and polydispersity of the complexes were determined 45 min after their preparation in serum-free cell culture media. (n=3, mean  $\pm$  SEM).

### 3.4.3. Optimisation of the transfection conditions

As GAPDH activity reduction might be reduced not only by the silencing effects of the GAPDH siRNA but also by non-specific silencing and cell death, a non-specific siRNA (negative control) was used to normalise the gene silencing induced by GAPDH. GAPDH activity in arbitrary fluorescence units was determined in cells transfected with either GAPDH siRNA or negative control siRNA complexes. After determining GAPDH activity in cells treated with GAPDH siRNA relative to negative control siRNA, the percentage specific GAPDH knockdown was determined at charge ratios where the reduction in GAPDH activity was significant as described in 3.3.5.

When Calu-3 cells were transfected with complexes containing 1  $\mu$ l Lipofectamine, no significant gene silencing was observed regardless of the exposure time or incubation time (Figure 3.5). No significant gene silencing compared to negative control siRNA was observed with either lipofectamine 2.5 or 5  $\mu$ l when the cells were exposed to the complexes for only 6 hours and then incubated for 48 hours to allow gene silencing to occur (Figure 3.5A). Increasing the exposure time to 24 hours resulted in 50-60% gene silencing at both amounts of Lipofectamine, but was associated with 70-90% cell viability when 2.5  $\mu$ l Lipofectamine was used and less than 50% cell viability when 5  $\mu$ l Lipofectamine was used. With 2.5  $\mu$ l Lipofectamine, significant gene silencing (50%) was achieved after 72 hours post-transfection (Figure 3.5B) regardless of the exposure time and cell viability remained above 80%. On the other hand when 5  $\mu$ l was used the results were unexpected with 6 hours incubation time resulting in insignificant gene silencing with approximately 70% cell viability and 24 hour exposure resulted in significant gene silencing (more than 50%) but with less than 60% cell viability. Therefore it was assumed that the reduction in GAPDH activity was associated with some level of toxicity. From the above data it appeared that using 2.5  $\mu$ l, 72 hours transfection duration gave the most favorable results regardless of the exposure time 6 or 24 hours. However, when selecting the suitable experimental condition, 6 hours exposure time was favored for practical reasons.



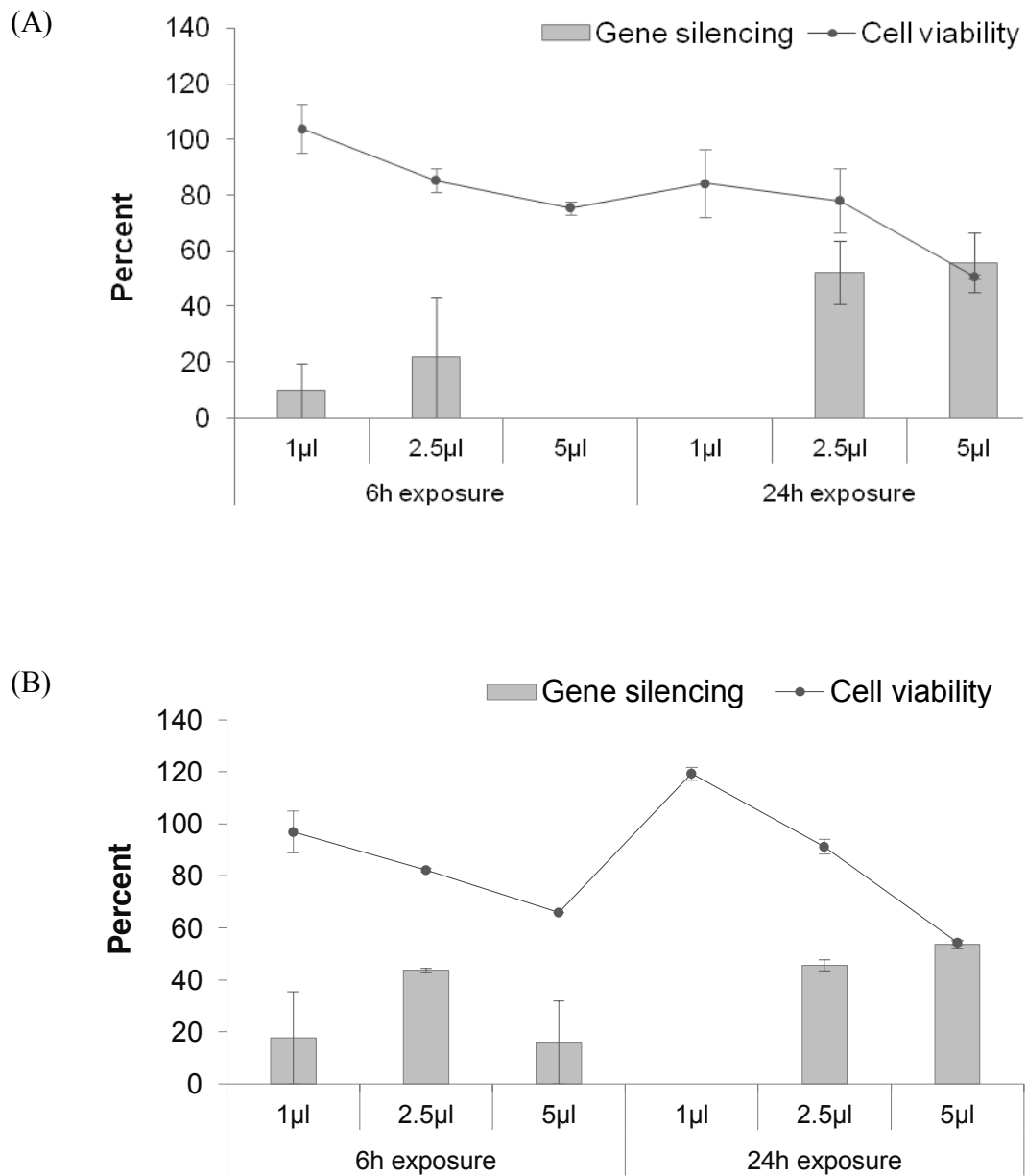
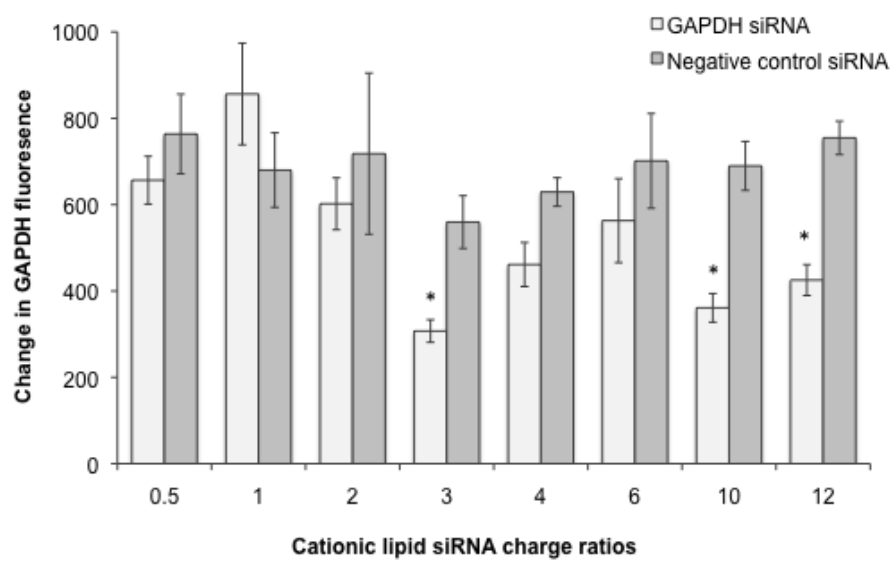


**Figure 3.5** The optimization of siRNA transfection in Calu-3 cells using Lipofectamine. GAPDH gene silencing (bar) and cell viability (line) were determined using KDalert assay either (A) 48 hours or (B) 72 hours post-transfection (n=3, mean±SEM).

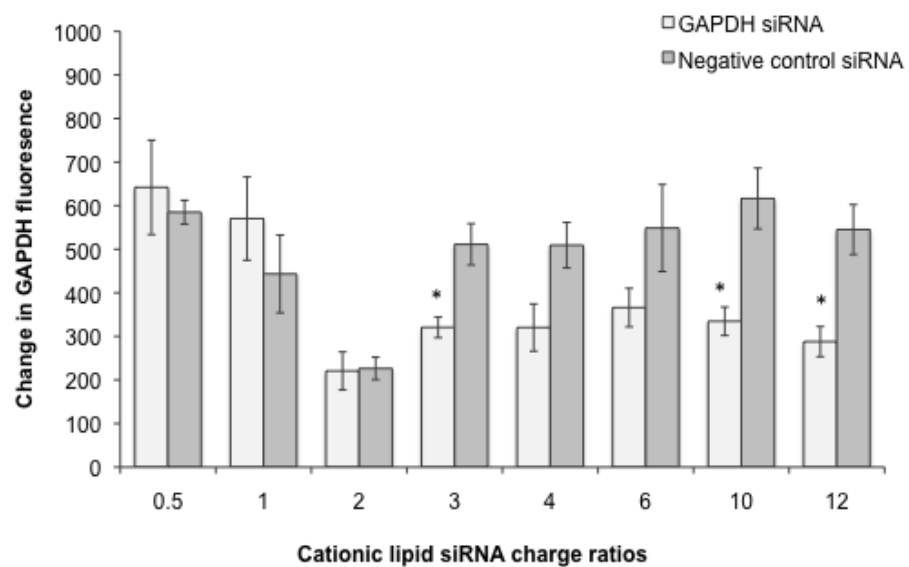
#### **3.4.4. Transfection of Calu-3 cells with siRNA**

Calu-3 cells transfected with LR (Figure 3.6A) or LpegR complexes (Figure 3.6B) at low charge ratios ranging from 0.5 to 6, showed no significant difference in GAPDH fluorescence between GAPDH siRNA and negative control siRNA indicating inefficient GAPDH silencing (Unpaired-t-test,  $p>0.05$ ) except at charge ratio 3. At higher charge ratios 10 to 12 a significant reduction in fluorescence was observed in cells treated with GAPDH siRNA relative to cells treated with negative control siRNA (Unpaired-t-test,  $p<0.05$ ). With the LPR complexes, a significant reduction in fluorescence in cells treated with GAPDH siRNA as compared to those treated with negative control was observed starting from charge ratio of 6 upwards (Figure 3.6C). The percentage GAPDH knockdown was determined at charge ratios where reduction in GAPDH activity was significant (Figure 3.6D). The percentage GAPDH silencing obtained with either LR or LpegR complexes at charge ratios 3, 10 and 12 was comparable (Unpaired-t-test,  $p<0.05$ ) to that obtained with Lipofectamine complexes (positive control) and (up to 50%). On the other hand, LPR complexes were as effective as Lipofectamine complexes in inducing GAPDH silencing starting from a charge ratio of 6 with 45-50% knockdown (Figure 3.6D). Using One-way Anova test, there was no significant difference ( $p>0.05$ ) in the levels of GAPDH knockdown between the three systems at each charge ratio except at charge ratio of 6 where only LPR complexes were effective in inducing gene silencing.

(A)



(B)



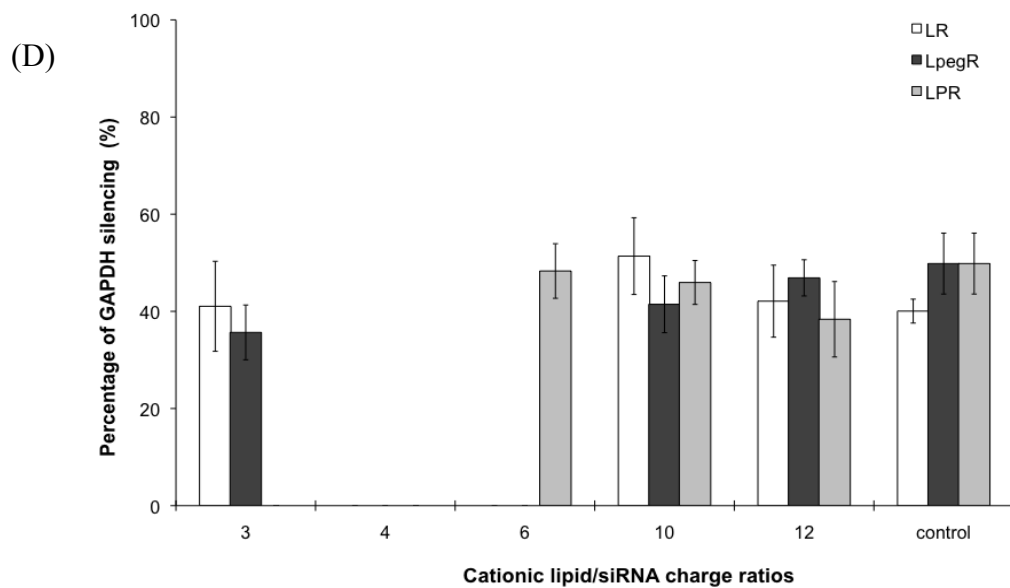
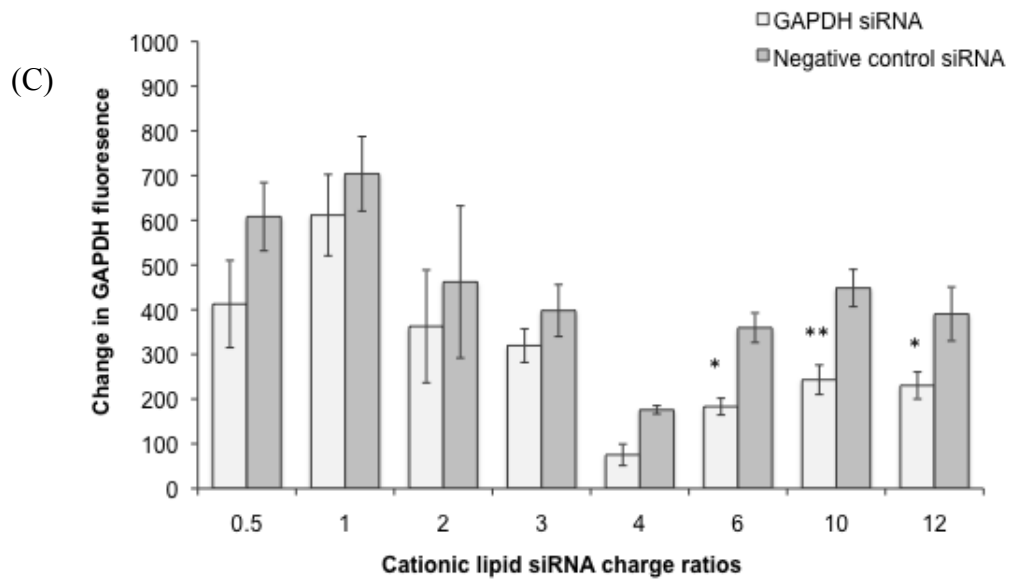
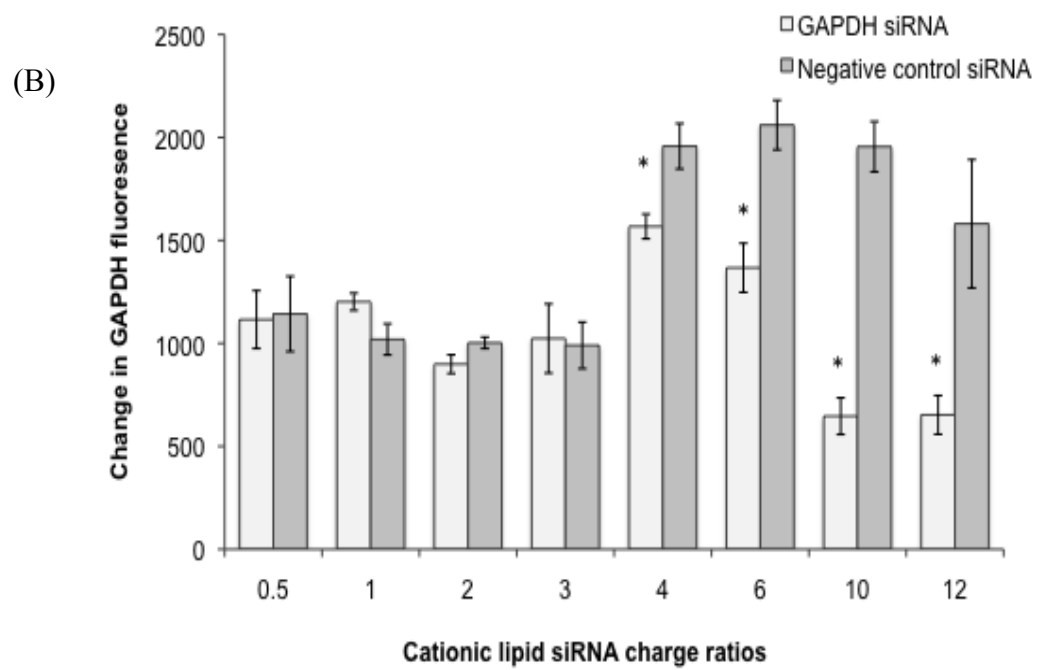
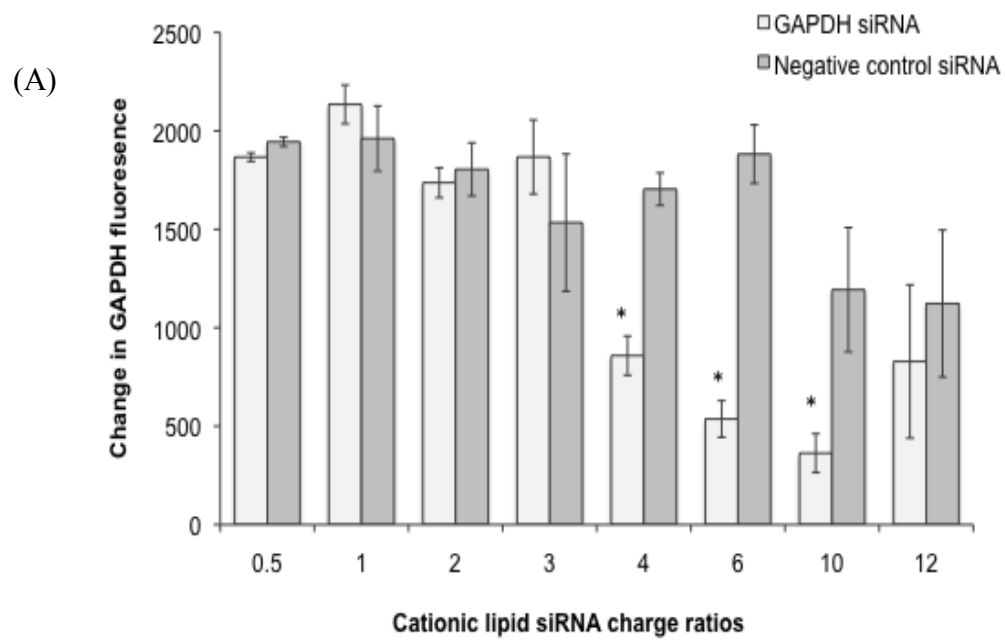


**Figure 3.6** GAPDH activity in arbitrary fluorescence units in Calu-3 cells measured 72h post-transfection with GAPDH and negative control siRNA complexes; A) LR, B) LpegR, C) LPR, D) Percentage specific GAPDH silencing for the three complexes (n=3, mean  $\pm$  SEM). \*Statistical significance as per independent t-test ( $p < 0.05$ ) \*\*( $p < 0.01$ ).

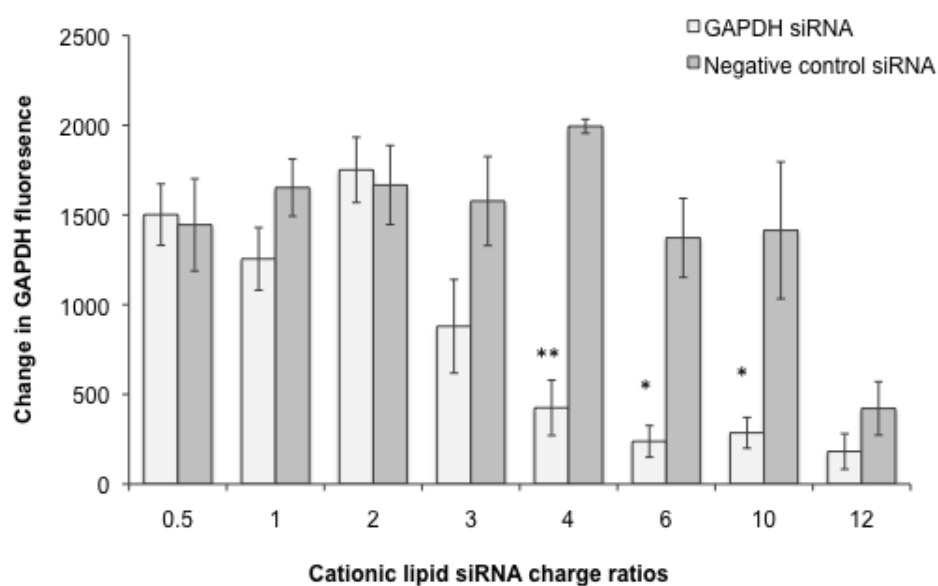
### **3.4.5. Transfection of A549 cells with siRNA**

LR (Figure 3.7A) and LpegR complexes (Figure 3.7B) at charge ratios ranging from 4 to 10 produced significant (Unpaired-t-test,  $p < 0.05$ ) reduction in fluorescence in A549 cultures treated with GAPDH siRNA compared to those exposed to negative control siRNA. At other charge ratios, GAPDH siRNA and negative control siRNA resulted in similar levels of fluorescence indicating no specific GAPDH silencing (Unpaired-t-test,  $p > 0.05$ ). LPR complexes at charge ratios 4-12 resulted in an important decline in fluorescence in cells treated with GAPDH siRNA compared to negative control siRNA suggesting specific GAPDH knockdown (Figure 3.7C).

When percentage GAPDH silencing was determined, LR complexes showed the highest GAPDH silencing at charge ratios 6 and 10 with (up to 70%) and were as effective as the positive control (Lipofectamine/siRNA complexes) (Figure 3.7D). Whereas the LpegR complexes achieve the same levels of gene silencing at charge ratios ranging from 10 to 12 and much lower gene silencing was observed at charge ratios of 4 and 6 (20-30%). LPR complexes on the other hand, displayed high GAPDH silencing at all charge ratios ranging from 4 to 10 with up to 80% knockdown. When the three systems were compared in terms of GAPDH silencing efficiency at each charge ratio, both LPR and LR complexes induced significantly higher GAPDH silencing than LpegR complexes at charge ratios 4 and 6 ( $p < 0.05$ , One-way Anova). In addition LPR complexes had a higher GAPDH knockdown than LR complexes at charge ratio 4.



(C)



(D)

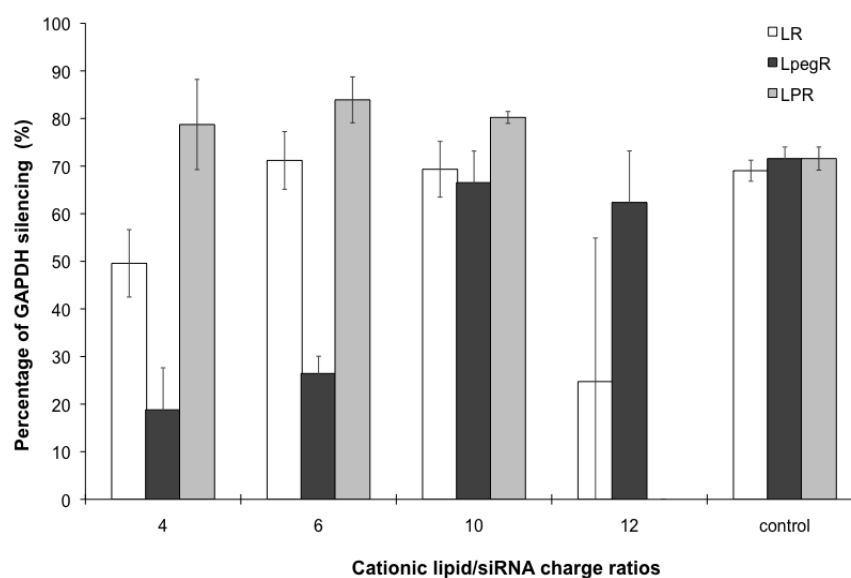


**Figure 3.7** GAPDH activity in arbitrary fluorescence units in A549 cells measured 72h post-transfection with GAPDH and negative control siRNA complexes; A) LR, B) LpegR, C) LPR, D) Percentage specific GAPDH silencing for the three complexes (n=3, mean  $\pm$  SEM). \*Statistical significance as per independent t-test ( $p < 0.05$ ) \*\*( $p < 0.01$ ).

### 3.4.6. Cell viability

Since the levels of GAPDH activity per cell are constant in untransfected cells and in cells transfected with negative control siRNA, GAPDH activity in negative control siRNA-transfected cells ( $\Delta$ fluorescence Negative) can be used as an indicator of cell number, or of relative viability, under the influence of transfection carriers (cationic lipids). Therefore, in cells transfected with negative control siRNA, the higher the fluorescence (GAPDH activity) the less toxic the transfection conditions. Toxicities of the effective formulations were calculated using the following equation:

$$\% \text{ Cell viability} = 100 \times (\Delta \text{fluorescence Negative control} / \Delta \text{fluorescence untreated cells}).$$

In both cell lines, LR complexes there was no significant reduction in cell viability in comparison to untreated cells at the effective charge ratios (3, 10 and 12 in Calu-3 cells, 6 and 10 in A549 cells) (Figure 3.8A). Similarly, LpegR complexes did not cause a decrease in Calu-3 cell viability at the effective charge ratios (3, 10 and 12 for Calu-3 cells, 4-12 for A549 cells) (Figure 3.8B). In the case of LPR complexes, there were no significant toxicity at the effective charge ratios (6-12 in Calu-3 cells, 4-10 for A549 cells) not toxic except at charge ratios 4 (Calu-3 cells) and 12 (A549 cells) (Figure 3.8C). Significant reduction in cell viability was observed with LPR complexes at charge ratio 12.



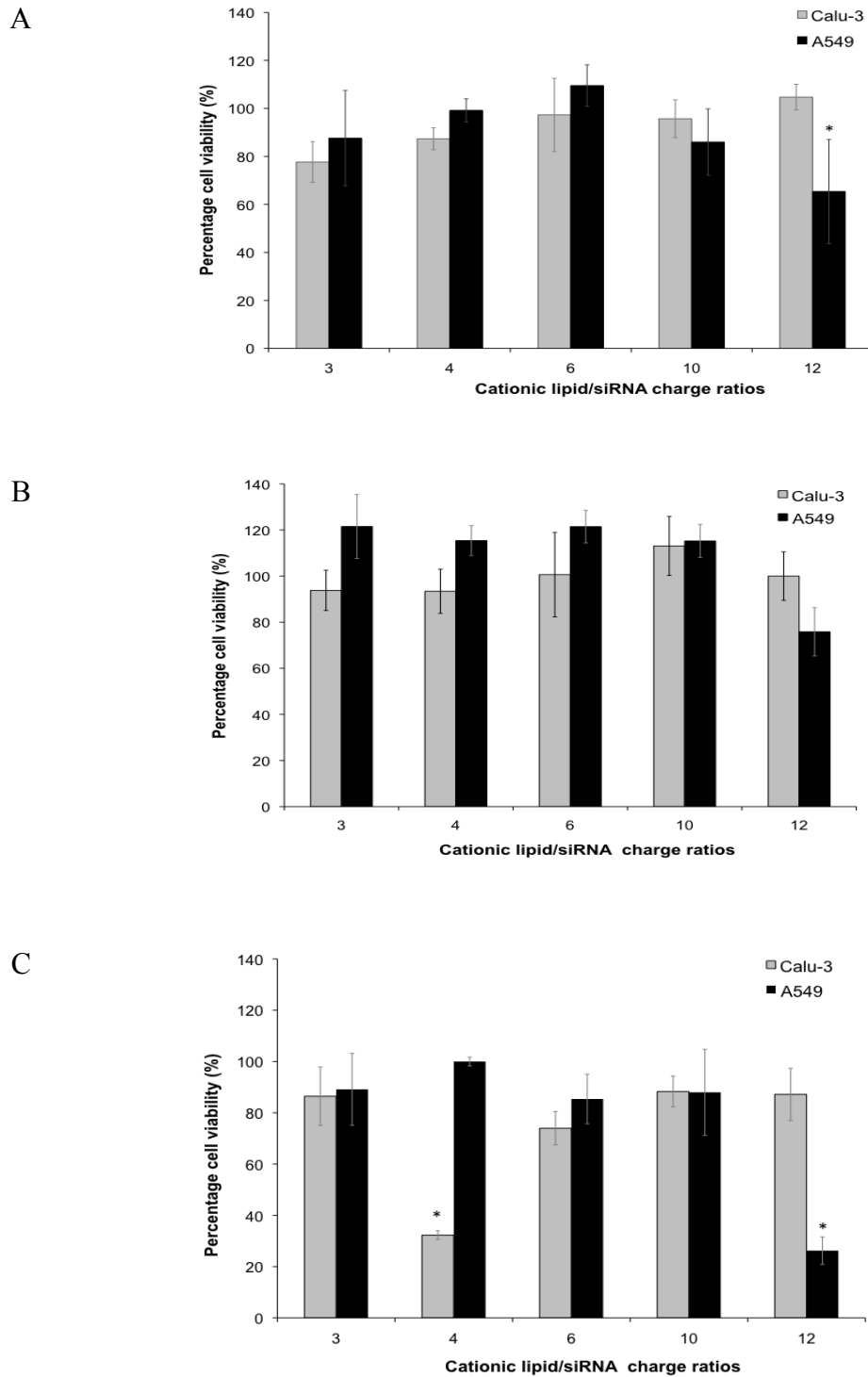


**Figure 3.8** The percentage of cell viability in Calu-3 and A549 cells after transfection with A) LR, B) LpegR, and C) LPR complexes prepared at the indicated cationic lipid/siRNA charge ratios. Data represent the mean of 3 experiments with 3 replicates in each experiment (n=3, mean±SEM). \*Significant difference from control (100% cell viability) as per t-test ( $p < 0.05$ ).

### 3.4.7. The effect of serum on the gene silencing efficiency

The addition of 5% FBS had no effect on the gene silencing efficiency of LpegR complexes, but it resulted in 29% reduction in GAPDH silencing induced by LPR complexes (Figure 3.9). When transfection was performed in the presence of 20% FBS, there was approximately 40-45% decrease in GAPDH silencing induced by either LpegR or LPR complexes. However despite the significant reduction in gene silencing in comparison to 0% FBS, LPR complexes maintained acceptable levels of gene silencing (40-45%) even at high serum concentration (20% FBS).

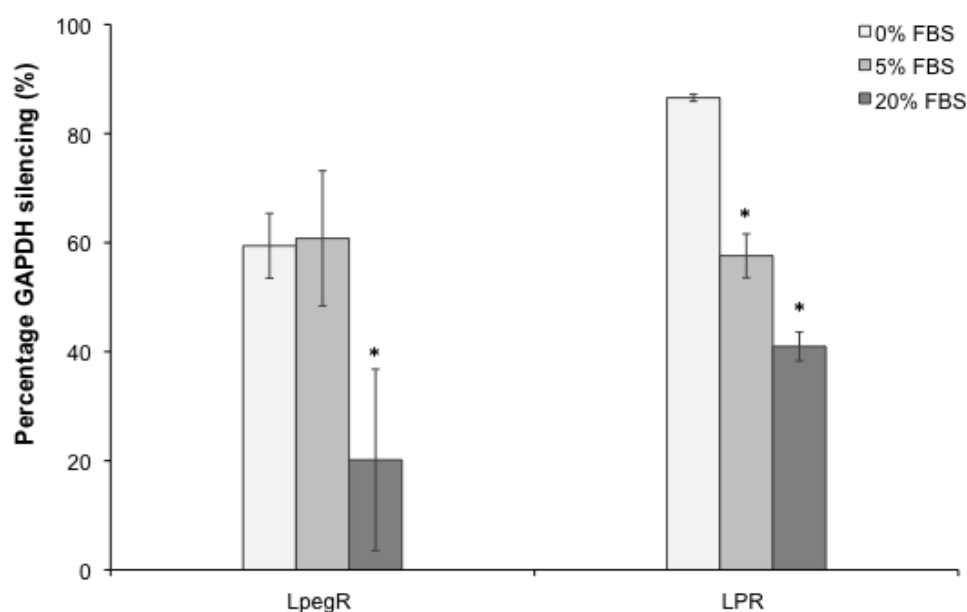


**Figure 3.9.** GAPDH activity measured after 72h exposure of A549 cells transfection with GAPDH and negative control siRNA complexes: LpegR and LPR at the indicated FBS concentrations. Data was presented as percentage GAPDH silencing (n=3, mean±SEM). \*Significant difference from control (0% serum) as per t-test ( $p < 0.05$ ).

### **3.5. Discussion**

Cationic lipid-mediated delivery of siRNA faces many of the same challenges as delivery of pDNA, from internalization to endosomal escape (Grayson, A.C. *et al.*, 2006) and once inside the cell the complexes should dissociate to release the nucleic acids from the vector system (Gary, D.J. *et al.*, 2007). Despite these similarities, formulation with siRNA might be quite different to pDNA formulation. Although both self-assemble by electrostatic forces, pDNA is more than a few hundred-fold larger than siRNA, suggesting that they might have different optimal formulations. In this study several properties of cationic lipid/siRNA complexes that might affect the gene silencing activity were evaluated in comparison with the properties of cationic lipid/pDNA with the objective of identifying an optimal system for siRNA delivery.

#### **3.5.1. Complexation efficiency as a function of charge ratio**

An essential feature for transfection efficiency is complexation and packaging of nucleic acid to result in small particle size and protect from nuclease attack (Collins, E. *et al.*, 2007). SYBR green II intercalation data revealed that a significant portion of siRNA in the complex formulations was accessible to intercalation with the dye indicating low binding. The three lipidic systems were less efficient in complexing siRNA as compared to pDNA. Lipofectamine/siRNA complexes were used as a control to confirm the suitability of the SYBR green II intercalation assay for determining condensation efficiency. Indeed Lipofectamine efficiently bound the siRNA (more than 85% bound siRNA was observed) and despite increasing the amount of lipid, percentage free siRNA. The LPR system

resulted in the highest complexation (85%) at charge ratio 0.5, which decreased to 40-50% at higher ratios. Interestingly, when condensation efficiency of siRNA/protamine complexes without the cationic lipid was determined, up to 85% compaction was obtained which was similar with compaction obtained with the LPR complex at charge ratio 0.5, but as more lipid was added the condensation efficiency decreased to 50% and remained constant all charge ratios. The reason of this was unclear. With the LPD system in the previous chapter, pDNA condensation by protamine was not affected as more lipid was added.

The difference in complexation efficiency between pDNA and siRNA can be explained by the differences in structure and distribution of negative counter ions around the nucleic acid. Li and co-workers (2011) showed that double stranded siRNA was more resistant to condensation compared with double stranded pDNA and this was due to differences in the geometry of charge arrangement. In another study it was found that for siRNA complexes, a larger (+/-) charge ratio than that used for pDNA delivery was required to achieve efficient gene silencing (Spagnou, S. *et al.*, 2004, Zhang, Y. *et al.*, 2010). This was associated with resistance to complex formation due the rotational and translational degrees of freedom associated with siRNA in the bulk being greater than that of long DNA which created a large barrier for complex formation as the siRNA shifts from the bulk state to the confined complexed state. In addition, siRNA has lower adhesion energy per unit length than pDNA, plus there are differences in electrostatic repulsion between pDNA compared to siRNA strands. Other studies reported that the much more rigid and shorter structure of siRNA (21-23 nucleotides *versus* several kilobases for pDNA) prevented lipid-induced condensation (Spelios, M. *et al.*, 2010) and that siRNA requires much

higher +/- charge ratio to achieve the degree of compaction that can be achieved with pDNA complexes at much lower ratios (Zhang, Y. *et al.*, 2010, Marty, R. *et al.*, 2009b). Surprisingly, in the current study, it was shown that despite increasing +/- charge ratio, there was no significant improvement in condensation and siRNA was assumed to be bound to the cationic carrier in a such a way that parts of it remained exposed to intercalation with the SYBR green II reagent.

### **3.5.2. Particle size as a function of charge ratio**

siRNA formed smaller particle size complexes than pDNA under physiological salt conditions. Unfortunately, direct comparison cannot be made because siRNA complexes were prepared in high ionic strength solution while pDNA complexes were prepared in water then transferred into high ionic strength solution. This variation in method of preparation was adopted because it has been shown previously that using cell culture medium rather than water for siRNA/lipid complex formation significantly enhanced gene silencing (Spagnou, S. *et al.*, 2004). The major difference observed in particle size between the two complexes may be either due to the small size of the siRNA molecule and low tendency to aggregation (Li, L. *et al.*, 2011) or simply due to difference in the preparation method.

LR and LpegR complexes displayed relatively large particle size and polydispersity at low charge ratios in particular 1-2 zone, which then decreased as the charge ratio increased. LPR was the only exception where the particle size remained fairly constant despite the change in cationic lipid/pDNA charge ratio. This was attributed to the use of a constant protamine/siRNA mass ratio to condense siRNA before the addition of the cationic lipid. This correlated with SYBR green II

data, as the percentage of condensation was the same at all charge ratios. The significant decrease in the polydispersity at charge ratios  $\geq 6$  for all three systems indicated a fairly homogenous size distribution was formed under these conditions; this accords with previous studies which showed that high ratio cationic lipid/siRNA complexes, the system becomes more homogenous due to complete neutralization of the negative charge of siRNA. However, in the current study, decrease in the particle size and polydispersity data didn't correlate with the low complexation data. There was no clear explanation for this but it is possible that SYBR-green II assay method did not give a clear description of the siRNA/cationic lipids complexation and should be combined with another technique such as gel electrophoresis to have an accurate complexation assay. Similarly, Zhang and co-workers (2010) also reported that PEGylated DC-Chol/DOPE could not cause full siRNA gel retardation even at a (+/-) charge ratio of 15 where the complexes had a small particle size (<500 nm) and positive surface charge. Unfortunately, due to lack of suitable equipment in our laboratory, the zeta potential of siRNA complexes wasn't measured and it was assumed based on previous studies (Desigaux, L. *et al.*, 2007, Zhang, Y. *et al.*, 2010) that at high +/- charge ratios siRNA/cationic lipid complexes will be mainly positively charged.

### **3.5.3. Gene silencing efficiency of siRNA complexes:**

After the physicochemical characterization of the siRNA complexes, their gene silencing activity was determined in two different cell lines. Use of the bronchial epithelial Calu-3 cell line, which was used for pDNA transfection studies in the previous chapter, allowed direct comparison between pDNA and siRNA complexes.

Transfection conditions of Calu-3 cells using the commercial transfection reagent lipofectamine have not been determined previously, therefore, prior to the use of the LR, LPegR and LPR complexes to deliver siRNA, transfection of siRNA using the positive control formulation Lipofectamine was optimized. The second cell line used was the alveolar epithelial cell line A549, which has been commonly used for pDNA transfection experiments and has also used in siRNA transfection studies (Lu, J.J. *et al.*, 2009). Optimisation of the positive control Lipofectamine was not necessary as the manufacturer provides a recommended protocol.

#### 3.5.3.1. Gene silencing efficiency and physical properties of the complexes

This study showed that siRNA complexes were most effective at high charge ratios where they had a homogenous size distribution, small particle size (~200-300 nm) and in which siRNA was not efficiently condensed. Generally, it is believed that the size of the complexes should be 50 nm to 200 nm for efficient internalization by endocytic processes (Gao, H. *et al.*, 2005). However, despite that LR and LpegR complexes prepared at lower charge ratios of 4 to 6 had a similar size as complexes prepared at higher ratios (10-12), the former complexes were inactive in GAPDH silencing whereas the latter resulted in significant knockdown. Spagnou et al (2004), using a different cationic lipid, also demonstrated that there was no significant difference in GAPDH knockdown between complexes of small size (50-100 nm) and larger aggregates (200-600 nm). Similarly LPR complexes showed no significant difference in size at the different charge ratios, but a significant difference in gene silencing was observed. All these observation indicated that the gene silencing function of siRNA complexes is not dependent on the particle size of the complexes.

Once inside the cell the complexes should be able to release siRNA from the vector system to exert its function (Gary, D.J. *et al.*, 2007). Therefore the less efficient binding of siRNA observed in this study even at high charge ratios could be beneficial in facilitating siRNA dissociation from the lipidic system and enhancing gene silencing activity. On the other hand, it could present a disadvantage of exposing siRNA to interaction with polyanions as well as attack by nucleases *in vivo*. In addition, despite having low complexation efficiency, at low charge ratios, siRNA complexes were still inactive at these ratios, which suggested that even if low complexation could be beneficial in enhancing gene silencing efficiency, it is not a major determinant of successful gene silencing.

#### 3.5.3.2. Gene silencing and cytotoxicity in Calu-3 vs A549 cells

GAPDH silencing induced by LR, LPR and LpegR complexes in A549 cells, showed similar trends to Calu-3 cells in terms of protein knockdown activity increasing with the increase in (+/-) charge ratios. For all three lipid formulation systems, protein silencing was more potent in A549 cells at high charge ratios (10-12) cpercentage GAPDH knockdown was higher in A549 cells than in Calu-3 cells. For example, LPR complexes prepared at charge ratio 10 resulted in more than 80% GAPDH silencing in A549 cells in comparison with 50% in the Calu-3 cell line. Electrostatic neutralization between the cationic lipids of siRNA complexes and anionic lipids of the endosome is believed to be involved in the release of the nucleic acid in the cytoplasm after the cationic lipid fuse with the cell membrane of the endosome. Thus difference in the number of negative charges on endosomal membrane in different cell lines might explain differences in optimal charge ratio (Sakurai, F. *et al.*, 2000b).



With cationic lipid/pDNA complexes, reduction in cell viability was minor because the +/- charge ratios used were lower than the ones used in siRNA studies and therefore cytotoxicity did not play a major role in determining the optimal charge ratio (2.5.3). With siRNA, the +/- charge ratios used were much higher than those used with pDNA, which enhanced gene silencing efficiency but could be a cause for concern for cell viability. In both cell lines none of the three systems were toxic at the effective charge ratios. In contrast, significant toxicity was observed with LR complexes at charge ratio 12 in A549 cells; this was probably the cause of the reduced GAPDH silencing at those ratios. Toxicity at high cationic lipid/nucleic acid charge ratio was attributed to an increase in the amount of free cationic liposomes (empty liposomes).

#### 3.5.3.3. Effect of serum on gene silencing

Although low compaction of siRNA even at high ratios was beneficial *in vitro* transfection and didn't seem to inhibit the gene silencing activity, it was important to see how these systems will behave under transfection conditions similar to *in vivo*. Serum has been associated with inhibition of transfection efficiency of pDNA and siRNA complexes (Zhang, Y. and T.J. Anchordoquy, 2004, Simberg, D. *et al.*, 2005). Serum proteins interact with the charged transfection complexes and may either result in the dissociation of the nucleic acid from the carrier or block association with cellular membrane as the complexes become negatively charged. As a result, most transfection studies are done in the absence of serum (Aljaberi, A. *et al.*, 2005, Salvati, A. *et al.*, 2006). The presence of serum *in vivo* is inevitable therefore the gene silencing efficiency of siRNA complexes was also investigated in the presence of serum. This is especially pertinent for siRNA as it's phosphodiester

backbone is considered to be more sensitive to hydrolysis than pDNA and therefore more susceptible to nucleases (Mahon, K.P. *et al.*, 2010, Ming, X. *et al.*, 2011).

Zhang and co-workers (Zhang, Y. *et al.*, 2010) reported that the presence of 10% FBS did not affect the uptake and gene expression activity of pDNA/DC-Cholesterol:DOPE complexes, while it completely inhibited the gene silencing efficiency of siRNA delivered using the same system. In this study, LPR and LpegR complexes were selected to investigate the effect of serum, as they are known to be more stable than the LR complexes in the presence of anionic molecules. Pegylation has been used to reduce interaction between negatively charged molecules in serum and the siRNA complexes and it has been shown to improve the *in vivo* circulation time of siRNA (Zimmermann, T.S. *et al.*, 2006, Santel, A. *et al.*, 2006). Gene silencing data showed that LpegR complexes were not affected by the presence of 5% serum, but as the amount of serum increased to 20% gene silencing was reduced by 40%. On the other hand gene silencing of LPR complexes decreased in the presence of 5 and 20% but remained relatively high (60% silencing at 5% FBS, and 40% at 20% FBS) compared to LpegR complexes although this was not due to more resistance to serum but to the higher gene silencing efficiency of LPR complexes. This data indicated that LpegR and particularly LPR are promising formulations for gene delivery *in vivo*, as the complexes were not completely deactivated by the presence of high concentration of serum (20%).

#### **3.5.4. Delivery of pDNA versus siRNA**

Luciferase expression in Calu-3 cells induced by LD and LpegD complexes was found to decrease as the +/- charge ratio increased and was highest at low ratios

0.5-2 (2.4.4). At these ratios, pDNA complexes formed large polydisperse aggregates (3-4  $\mu\text{m}$ ) that had low condensation efficiency (~50-80% non-condensed pDNA). In contrast, at the same charge ratios, LR and LpegR were completely inactive in inducing GAPDH silencing and only became active at higher charge ratios tested (10-12). The active siRNA complexes had a very small particle size (<200 nm) and had very low complexation efficiency. The LPD complexes resulted in similar levels of luciferase expression irrespective of the charge ratio, which correlated with high condensation (<20 % non-condensed) at all ratio, whereas LPR complexes gene silencing efficiency was dependent on increasing charge ratios despite similar condensation efficiency at all ratios. Overall these data showed that pDNA and siRNA need to be formulated differently as the compositions that worked for pDNA didn't work for siRNA. In agreement with the recently reported findings of Zhang and co-workers (2010), increasing the +/- charge ratio increased the uptake of siRNA/lipid complexes until it reached plateau at ratio of  $\geq 5$  whereas with pDNA increasing charge ratios ( $\geq 4$ ) resulted in a drop in internalization efficiency and was associated with poor endosomal escape of pDNA. Thus pDNA transfection was effective at low charge ratios while siRNA was more effective when delivered using high ratios.

### **3.5.5. Conclusion**

In conclusion, the data presented here elucidated the parameters that affect siRNA versus pDNA delivery *in vitro* using three different cationic-lipidic systems. It was found that what the optimal physicochemical characteristics for pDNA delivery were not optimal for siRNA and that these characteristics varied between

the different cationic carriers tested. This dissimilarity in optimal formulation could be associated with the possibility that different formulations enter the cells through diverse pathways, which will be investigated in the next chapter. The other explanation could be that there is a minor population of complexes not detected by physical characterization that are responsible for the biological activity, as it is assumed that only the pDNA of a small percentage of complexes reaches the nucleus to exert its effect. Similarly with siRNA it has been shown that only a small fraction of the dose is sufficient to almost completely inhibit protein expression (Spelios, M. *et al.*, 2010). In terms of siRNA formulation, LPR and LpegR complexes, which to our knowledge haven't been investigated previously for siRNA delivery, were found to be effective carriers for potent GAPDH knockdown at their optimal charge ratios. These non-toxic carriers could also function in the presence of serum and therefore have the possibility to be explored for *in vivo* application.

## **Chapter 4. The mechanism of cellular uptake of functional siRNA/lipid complexes**

## 4.1. Introduction

Recently it became evident that the mode of internalisation of siRNA has a major influence on the kinetics of its intracellular trafficking and biological effectiveness (Rejman, J. *et al.*, 2005, Detzer, A. *et al.*, 2008). In order to optimise and improve the efficacy of transfection using non-viral vectors such as cationic lipids, it is therefore important to define fully the mechanisms by which cell entry and intracellular trafficking of these complexes occur. There are few published studies that address the uptake mechanism of siRNA-cationic lipid complexes (lipoplexes) and these studies do not provide conclusive findings regarding the exact uptake pathway. A variety of factors have been reported to be influential, including the cell type (Douglas, K.L. *et al.*, 2008), particle size (Rejman, J. *et al.*, 2004, Lai, S.K. *et al.*, 2008), surface charge (Harush-Frenkel, O. *et al.*, 2008, Resina, S. *et al.*, 2009) and the chemistry of the delivery vector (Elouahabi, A. and J.M. Ruyschaert, 2005, Khalil, I.A. *et al.*, 2006). Thus, there is limited knowledge about the uptake mechanisms and the intracellular processing that lead to gene silencing by siRNA. In this Chapter, the LPR and LpegR lipoplexes, which were identified as promising systems in the preceding work, were investigated to try to elucidate their delivery mechanisms.

To date, most data on the uptake mechanism of non-viral delivery complexes comes from studies using DNA. It is generally considered that DNA delivery mediated by lipoplexes or polyplexes is via endocytosis (Felgner, J.H. *et al.*, 1994, Hoekstra, D. *et al.*, 2007, Labatmoleur, F. *et al.*, 1996, Zuhorn, I.S. *et al.*, 2002a, Khalil, I.A. *et al.*, 2006, Friend, D.S. *et al.*, 1996, Godbey, W.T. *et al.*, 1999). Although it is recognized (through the work presented in this thesis and that of

others) that pDNA complexes have different physicochemical properties from those of siRNA complexes, it may be hypothesized that siRNA entry would also be taken up through endocytosis. Endocytosis is a broad term as multiple endocytotic pathways have been described (Conner, S.D. and S.L. Schmid, 2003, Lamaze, C. and S.L. Schmid, 1995), but the common feature of all such pathways is the uptake of macromolecules in transport vesicles. These endocytotic vesicles differ in the composition and size as well their intracellular trafficking and are subcategorised into three well-described endocytic pathways that are distinguished according to their differential sensitivity to pharmacological inhibitors (Table 4-1).

In terms of DNA delivery, the clathrin-mediated pathway has been shown to be the main route for entry of DNA lipoplexes (Rejman, J. *et al.*, 2005, Zhou, X.H. and L. Huang, 1994), whereas the caveolae pathway has been involved in the uptake of DNA/polypeptides complexes (Rejman, J. *et al.*, 2005)) and protein transduction domains such as trans-activator of transcription protein (TAT) (Ferrari, A. *et al.*, 2003, Fittipaldi, A. *et al.*, 2003). It is important to consider that genes internalised through the clathrin-mediated pathway end up in lysosomes, which provide a degradative environment, thus for successful delivery of biologically active genes, lysosomal escape and release in the cytoplasm is crucial. In this context, caveolae-mediated endocytosis represents a more attractive pathway for gene delivery due to the absence of lysosomal internalization, thus avoiding this degradative route (Ferrari, A. *et al.*, 2003, Harris, J. *et al.*, 2002). However, this process is considered slow and the caveolae have a small phase volume meaning that it is limited as a primary uptake route. The third major endocytosis route is macropinocytosis and this is gaining increased interest as a route for gene delivery because it allows higher

levels of uptake, avoidance of lysosomal compartments and, due to the leaky nature of the macropinosomes, escape into the cytosol is easier (Wadia, J.S. *et al.*, 2004). This mechanism has been demonstrated to be involved in the uptake of pDNA complexed to peptides (Kaplan, I.M. *et al.*, 2005, Nakase, I. *et al.*, 2004).



**Table 4-1** Description of the three major endocytic pathways and the chemicals used to inhibit them.

Uptake pathways	Clathrin-mediated endocytosis	Caveolae-mediated endocytosis	Macropinocytosis
Vesicle characteristics	Clathrin-coated (100-150 nm) Receptor mediated	Caveosomes (10-200 nm) Receptor mediated	Irregular shape >1µm Non-receptor mediated
Intracellular fate	Endosomes then lysosomes	Endoplasmic reticulum, transGolgi apparatus or endosomal compartment	Different fates cytoplasm, lysosomes, recycled to cell membrane
Inhibitors	Chlorpromazine Cellular K <sup>+</sup> depletion	Nystatin Cytochalasin D	Amiloride Cytochalasin D
Mode of action of the inhibitor	Prevent assembly of the clathrin lattice	Cholesterol sequestration Actin depolymerisation	Na <sup>+</sup> /K <sup>+</sup> exchange inhibition Actin depolymerisation

#### **4.1.1. Aim and objectives**

The aim in this Chapter was to elucidate which of the endocytosis pathways was involved in the uptake of the best performing formulations in terms of gene silencing efficiency, toxicity profile and reproducibility (3.5.3.2). To achieve this, methodologies originally designed to study the uptake of DNA complexes were used. The objectives of the chapter were to:

- Visualise the intracellular localization of LPR and LpegR lipoplexes in A549 cells. This was studied using fluorescently labelled siRNA and lipids.
- Interrogate the transfected A549 cells for co-localization of the lipoplexes with fluorescent markers of the individual internalization pathways,
- Evaluate the effect of endocytosis inhibitors on gene silencing efficiency mediated by LPR and LpegR complexes.

## 4.2. Materials

Material	Supplier
Cy3-glyceraldehyde-3-phosphate dehydrogenase (Cy3-GAPDH) siRNA	Ambion
1,2-dioleoyl- <i>sn</i> -glycero-3-phosphoethanolamine-N-(carboxyfluorescein) (DOPE-CF)	Avanti lipids
Alexa Fluor-488 and 633 transferrin	Invitrogen Ltd, UK
BODIPY-Lactosylceramide (BODIPY-LacCer)	Invitrogen Ltd, UK
Endocytosis inhibitors: chloropromazine, nystatin, amiloride, cytochalasin D	Sigma-Aldrich Ltd, Dorset, UK
DAPI	Sigma-Aldrich Ltd, Dorset, UK
NaCl, HEPES, pH 7.4, CaCl <sub>2</sub> , MgCl <sub>2</sub> , D-glucose, sodium borohydride, Triton-X-100, paraformaldehyde	Sigma-Aldrich Ltd, Dorset, UK

### **4.3. Methods:**

#### **4.3.1. siRNA complex localization studies**

To follow the cellular internalization of LPR and LpegR complexes in A549 cells, either a fluorescent Cy3-GAPDH siRNA or DOPE-N-carboxyfluorescein was included in the initial siRNA/lipid complex formulation to identify location of siRNA or liposome respectively. Cells were incubated with the formed fluorescent siRNA complexes at a (+/-) ratio of 10 (as described in chapter 3) for 2 h, following which internalization and subcellular localization were examined by confocal microscopy as described below.

Glass microscopy coverslips were sterilized in 60% hydrochloride acid in ethanol, and then washed three times with ultrapure water before a wash in 100% ethanol and drying in a laminar flow cabinet. Once dry the coverslips were placed into each well of a 24-well plate. A549 cells were seeded on top of the coverslips at a seeding density of  $1 \times 10^5$  cells per well and incubated overnight (37°C, 5% CO<sub>2</sub>). On the day of experiment, the complexes LPR and LpegR were prepared as described in chapter 3 (siRNA: 500 nM, N/P ratio: 10/1). However, either fluorescent red Cy3-GAPDH siRNA or fluorescent green DOPE-N-carboxyfluorescein liposomes were substituted in order to form fluorescent complexes. Cell culture media was removed and replaced with 500 µl of fluorescent LPR or LpegR complexes in RPMI-1640 for 2 h (37°C, 5% CO<sub>2</sub>). After this time the media was removed and the cells washed with PBS solution before fixing with 500 µl of 4% paraformaldehyde (PFA) in PBS for 15 min. PFA was then removed and 500 µl of 0.2% Triton-X-100 was added for 15 min to permeabilise the

membrane before replacement with 500  $\mu$ l 1mg/ml sodium borohydride for 15 min. Finally, 500  $\mu$ l of 0.001 mg/ml DAPI was added to stain the nucleus, which was left for 2 min, removed then washed three times with PBS. To mount the coverslips, 10 $\mu$ l Mowiol was added to the glass slides, and the cover slips were carefully removed from each well with tweezers, dipped in clean water and then placed on the Mowiol with care to avoid air bubble formation. After leaving to dry overnight at room temperature, the coverslips were examined using a Leica TCS SP2 Confocal Microscope at different magnification using an oil immersion objective (40x and 60x). These methods were performed in the dark.

#### **4.3.2. Temperature adjustment**

To determine whether the delivery of siRNA lipoplexes is an energy-dependent process, the effect of lowering the temperature on the uptake of siRNA lipoplexes was examined. A549 cells were pre-cooled to 4°C before for 1 h before transfection with Cy3-labeled LPR and LpegR complexes for 2 h at the same temperature. After removal of the complexes, cells were fixed and observed under a confocal microscope as described above.

The effect of lowering the temperature on gene silencing efficiency was also determined. One hour before transfection, A549 cells were incubated at different temperatures (4°C, 10°C, 37°C) then exposed to fluorescent LPR and LpegR complexes for 6 h at these temperatures. After removal of complexes, the cells were incubated (37°C, 5% CO<sub>2</sub>) in RPMI-1640 media for 72 h and assayed for GAPDH protein levels and cell viability using the KDalert assay as described in 3.3.5.

### **4.3.3. Colocalization of siRNA complexes with Alexa Fluor 488-transferrin and BODIPY-LacCer**

#### 4.3.3.1. Colocalization with Alexa Fluor 488-transferrin

Colocalization studies were performed to investigate whether fluorescent LPR and LpegR complexes colocalized with Alexa Fluor 488-transferrin, hence demonstrating clathrin-mediated uptake. Red Cy3-GAPDH siRNA was used to prepare fluorescent LPR and LpegR complexes (500 nM GAPDH siRNA, (+/-) ratio of 10). A549 cells were seeded on microscopy coverslips in 24-well plates overnight (37°C, 5% CO<sub>2</sub>). After incubation, the media was removed and the cells were co-incubated with 300 µl of fluorescent LPR or LpegR complexes (500 nM GAPDH siRNA, N/P: 10/1) and 20 µl of Alexa Fluor 488-transferrin (1 mg/ml) for 2 h (37°C, 5% CO<sub>2</sub>). A 5 min gap was allowed between the addition of the complexes and transferrin. After incubation, cells were washed with PBS before fixation and examination by confocal microscopy.

#### 4.3.3.2. Colocalization with BODIPY-LacCer

Co-localisation studies were performed to investigate whether fluorescent LPR and LpegR complexes colocalised with BODIPY-LacCer, hence demonstrating caveolae-mediated uptake. The experiment was carried out as described in section 4.3.3.1 except that the cells were first washed with cold media and exposed to 1 ml of 1.5 µM Bodipy LacCer for 30 min at 10°C to enhance accumulation of BODIPY-LacCer on the cell membrane. LPR and LpegR complexes in warm media were then

added to the cells and incubated for 2 h (37°C, 5% CO<sub>2</sub>) before fixation and examination by confocal microscopy.

#### **4.3.4. Optimisation of endocytosis inhibitors concentrations**

Endocytosis inhibitors were chosen for their reported selectivity for each of the pathways under study. However under the experimental conditions, the concentration of each inhibitor to be used was optimized based upon efficiency of pathway disruption and toxicity. Hence the most efficient and least toxic concentrations of inhibitors were determined according to the MTT toxicity assay and markers of the major endocytosis pathways.

##### **4.3.4.1. MTT screening of the endocytosis inhibitors**

A549 cells were seeded at a seeding density of  $1 \times 10^4$  cells/well in a 96-well plate and incubated for 24 h (37°C, 5% CO<sub>2</sub>). On the day of the experiment, the medium was removed and 100 µl mixtures of serum free-RPMI-1640 media and inhibitor test solutions at different concentrations, was added to each well as follows: chlorpromazine (1-50 µg/ml) for 30 min and 1 h, nystatin (1-100 µg/ml) and amiloride (1-20 µg/ml) for 1 and 2 h. The control wells were treated identically without the inhibitors. For each concentration 6 replicates were performed per experiment. After the incubation time, the inhibitor solutions were removed and 100 µl of 0.5 mg/ml MTT solution was added to the wells for 3 h (37 °C, 5% CO<sub>2</sub>). After this time, the MTT solution was then removed and replaced by 100 µl of isopropanol and stored at 4°C for approximately 90 min. The absorbance of the

resulting samples was measured at 570 and 650 nm using a SpectraMax Microplate Spectrophotometer.

The effect of potassium depletion on cell viability was also determined by performing potassium depletion as described by Larkin et al (1983). Briefly, A549 cells were washed with potassium-free buffer (140 mM NaCl, 20 mM Hepes, pH 7.4, 1 mM CaCl<sub>2</sub>, 1 mM MgCl<sub>2</sub> and 1 mg/ml D-glucose), followed by a wash with hypotonic buffer (potassium-free buffer diluted with ultrapure water 1:1 v/v). The cells were then washed three times with potassium-free buffer. The cells were then exposed to potassium depleting buffer for 2, 4 and 6 h after which time the MTT assay was carried out as described above. The control represented cells treated with potassium containing buffer.

#### 4.3.4.2. Inhibition of transferrin uptake via the clathrin-mediated endocytosis

In order to determine the minimum concentration of chlorpromazine that would inhibit the clathrin-mediated pathway Alexa Fluor 633-transferrin, known for being internalised via this pathway, was added to A549 cells pre-treated with increasing concentrations of chlorpromazine (0, 4, 8 and 10 µg/ml). A549 cells were seeded at a seeding density of  $1 \times 10^5$  cells/well into a 24-well plate containing sterilized glass microscopy coverslips and incubated overnight (37°C, 5% CO<sub>2</sub>). After this time, the media was removed and replaced with a 1 ml mixture of cell culture medium and chlorpromazine solution to give a final concentration of 4, 8 and 10 µg/ml chlorpromazine per well. The control well contained RPMI-1640 media without the inhibitors. The plate was then incubated for 1 h (37°C, 5% CO<sub>2</sub>), after which time the inhibitor solutions were removed and then replaced with 300 µl of 20



µg/ml fluorescently labeled transferrin solution in RPMI-1640. The cells were incubated for 1 h (37°C, 5% CO<sub>2</sub>) before cell fixation and evaluation of fluorescent transferrin uptake by confocal microscopy. The same experiment was carried out to examine the effect of the endocytosis inhibitors; nystatin (25µg/ml), amiloride (3mM) and Cytochalasin D (10 µg/ml) on the internalization of fluorescently labeled transferrin.

To determine if the clathrin-mediated pathway was inhibited by potassium depletion, the internalization of Alexa Fluor 633-transferrin was examined following potassium depletion as described in section 4.3.4.1. As a control, cells were treated with a buffer containing 10 mM KCl. Alexa Fluor 633-transferrin (20 µg/ml) was then incubated with cells for 1 h (37°C, 5% CO<sub>2</sub>), before fixation and analysis by confocal microscopy.

#### 4.3.4.3. Inhibition of BODIPY-LacCer via caveolae-mediated endocytosis

To optimise the concentration of the caveolar endocytosis inhibitor nystatin, a BODIPY labeled lactocylceramide (BODIPY-LacCer) was used. It has been reported that this sphingolipid is mainly internalised via a caveolae-mediated mechanism (Singh et al., 2003). The experiment was conducted as described in section 4.3.4.2, except that nystatin at different concentrations; 10, 20 and 25µg/ml, was used. After incubation, the nystatin solutions were removed and the cells washed with cold RPMI-1640 media, before the addition of 1 ml of 2 µM BODIPY-LacCer solution and incubation for 1 h at 10°C. After this time the cells were incubated at 37°C for 5

min to stimulate uptake of BODIPY-LacCer followed by fixation and examination using confocal microscopy.

#### 4.3.4.4. Effect of endocytosis inhibitors on the cell viability after 7 h exposure.

The MTT was performed to assess the toxicity of the selected effective concentration of endocytosis inhibitors (see above) that would be used for the transfection experiments. The cells were exposed to the inhibitors for 7 hours (equivalent to the duration of the whole transfection experiment) and then assayed for cell viability. The endocytosis inhibitors; nystatin (25 µg/ml), cytochalasin D (10 µg/ml) and amiloride (8 µg/ml) at the concentrations used showed more than 85% cell viability.

### **4.3.5. Gene silencing in A549 cells with siRNA complexes after inhibition of endocytic pathways**

#### 4.3.5.1. Inhibition of the clathrin-mediated endocytosis

A549 cells were seeded into 96-well plates at a seeding density of  $1 \times 10^4$  cells per well and incubated overnight (37°C, 5% CO<sub>2</sub>). The cells were then exposed to chlorpromazine 7.5 µg/ml for 1 h and transfected with LPR or LpegR complexes (50nM siRNA, N/P charge ratio 10/1) for 6 h (37°C, 5% CO<sub>2</sub>). In order to rule out the possibility that inhibitors might disturb complexation of siRNA with lipids when it is present in transfection solution, the transfection was carried out in two ways; in the presence or absence of the inhibitor. After incubation, the complexes were removed and replaced with supplemented RPMI-1640 (10% FBS) with or without

the inhibitor solution. The cells were incubated for 3 days (37°C, 5% CO<sub>2</sub>) before measurement of gene silencing and cell viability using the KDAlert assay.

For potassium depletion, A549 cells were treated as described above. LPR and LpegR complexes in potassium-free buffer were added to the cells for 6 h incubation (37°C, 5% CO<sub>2</sub>). After incubation, the complexes were removed and replaced with supplemented RPMI-1640 (10% FBS) and the cells cultured for 72 h before measurement of gene silencing and cell viability.

#### 4.3.5.2. Inhibition of caveolae and macropinocytosis

Using similar methods to those described in the preceding section, the cells were pretreated with inhibitors of non-clathrin pathways (i.e. caveolae and macropinocytosis): nystatin (25 µg/ml), amiloride (8 µg/ml) and cytochalasin D (10 µg/ml) in serum-free culture media for 1 h (37°C, 5% CO<sub>2</sub>). Cells were then transfected with LPR or LpegR complexes (per well 50 nM siRNA, (+/-) charge ratio of 10) for 6 h (37°C, 5% CO<sub>2</sub>) in the presence or absence of the inhibitor. After incubation, the complexes solutions were removed and replaced with supplemented RPMI-1640 (10% FBS) and cells cultured for 72 h (37°C, 5% CO<sub>2</sub>) before measurement of gene silencing and cell viability.

#### **4.3.6. Gene silencing in A549 cells after combined inhibition of endocytic pathways**

A549 cells were treated with combinations of two or three endocytosis inhibitors for 1 h (for clathrin and non-clathrin pathways); (7.5µg/ml chlorpromazine + 25µg/ml nystatin), (7.5µg/ml chlorpromazine + 8µg/ml amiloride), (25µg/ml

nystatin + 8µg/ml amiloride) and (7.5µg/ml chlorpromazine + 25µg/ml nystatin + 8µg/ml amiloride). Chlorpromazine was used at a lower concentration (7.5µg/ml) due to the high toxicity caused by the 10µg/ml chlorpromazine combined with the other inhibitors. Subsequently, LpegR complexes (50nM siRNA, N/P charge ratio 10/1) were added to the cells and incubated for 6 h in the presence of the combinations of inhibitors (37°C, 5% CO<sub>2</sub>). After incubation, the complexes were removed and replaced with supplemented RPMI-1640 (10% FBS) and cells cultured for 3 days (37°C, 5% CO<sub>2</sub>) before measurement of gene silencing and cell viability.

#### **4.3.7. Data analysis and statistics**

All data is expressed as mean ± standard error of the mean SEM. Statistical analysis was performed in SPSS, version 16.0, using One-way ANOVA and Student (unpaired) t-test with the chosen level of significance at  $p < 0.05$ .

## **4.4. Results**

### **4.4.1. siRNA complexes subcellular localization**

Both LPR and LpegR complexes effectively delivered siRNA to the cytoplasm of A549 cells (Figure 4.1). Two hours post-transfection, Cy3-labelled GAPDH siRNA delivered by both lipidic formulations accumulated in the cytoplasm and specifically formed a spot like pattern of distribution at the periphery of the nucleus. There was no apparent difference between the localization pattern of LPR or LpegR complexes.

The localization of red fluorescence in the perinuclear region raised the question whether the fluorescence represents the siRNA on its own or associated with the lipid. For this LPR and LpegR complexes were prepared using both labeled siRNA (Cy3-GAPDH) and labeled lipid (Carboxyfluorescein-DOPE:DOTAP) and the distribution of red and green fluorescence were observed. Confocal images showed that in as little as 2 hours post-transfection some of the free siRNA was detected while the rest of siRNA and lipid co-localised giving rise to a yellow fluorescence (Figure 4.2).

### **4.4.2. Functional siRNA complexes uptake is temperature-dependent**

Confocal microscopy images (Figure 4.3) showed that the uptake of the fluorescently labeled LpegR (A) and LPR (B) complexes was inhibited at low temperatures (4°C). In cells transfected at 37°C (Figure 4.1), red dots which represent fluorescent siRNA complexes were observed in the cytoplasm in the perinuclear region whereas when transfected at 4°C the red dots appeared on the cell

membrane rather than the cytoplasm while when transfected at 4°C the red dots seemed to be on the cell membrane not the cytoplasm.

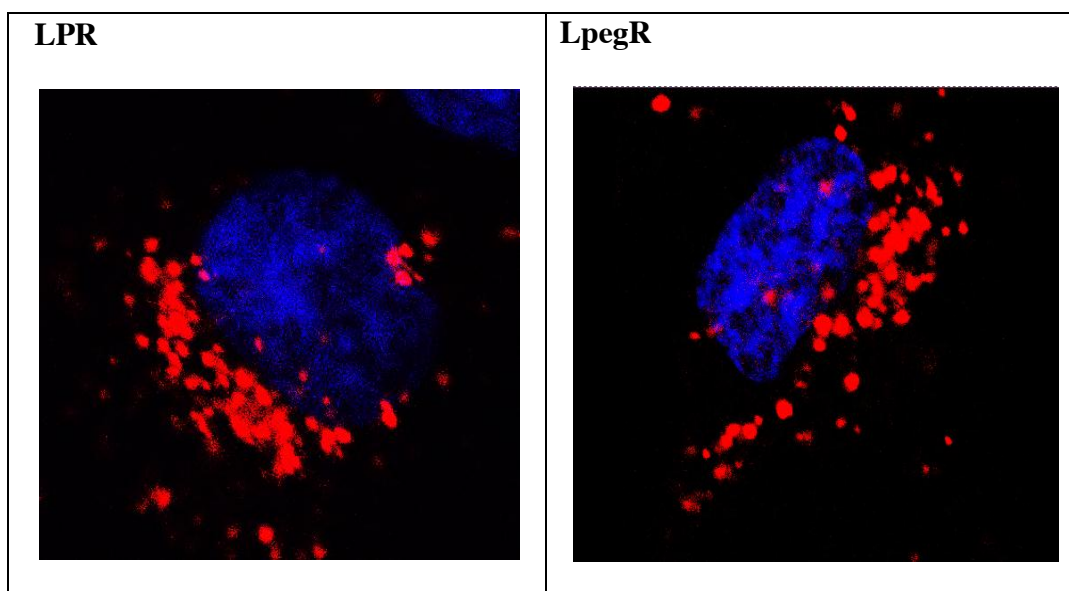


**Figure 4.1** Confocal images of fluorescent LPR and LpegR complexes in A549 cells 2 h post-transfection. Red fluorescence represents Cy3-GAPDH siRNA in the complexes. Blue DAPI stain was employed to highlight the nucleus.

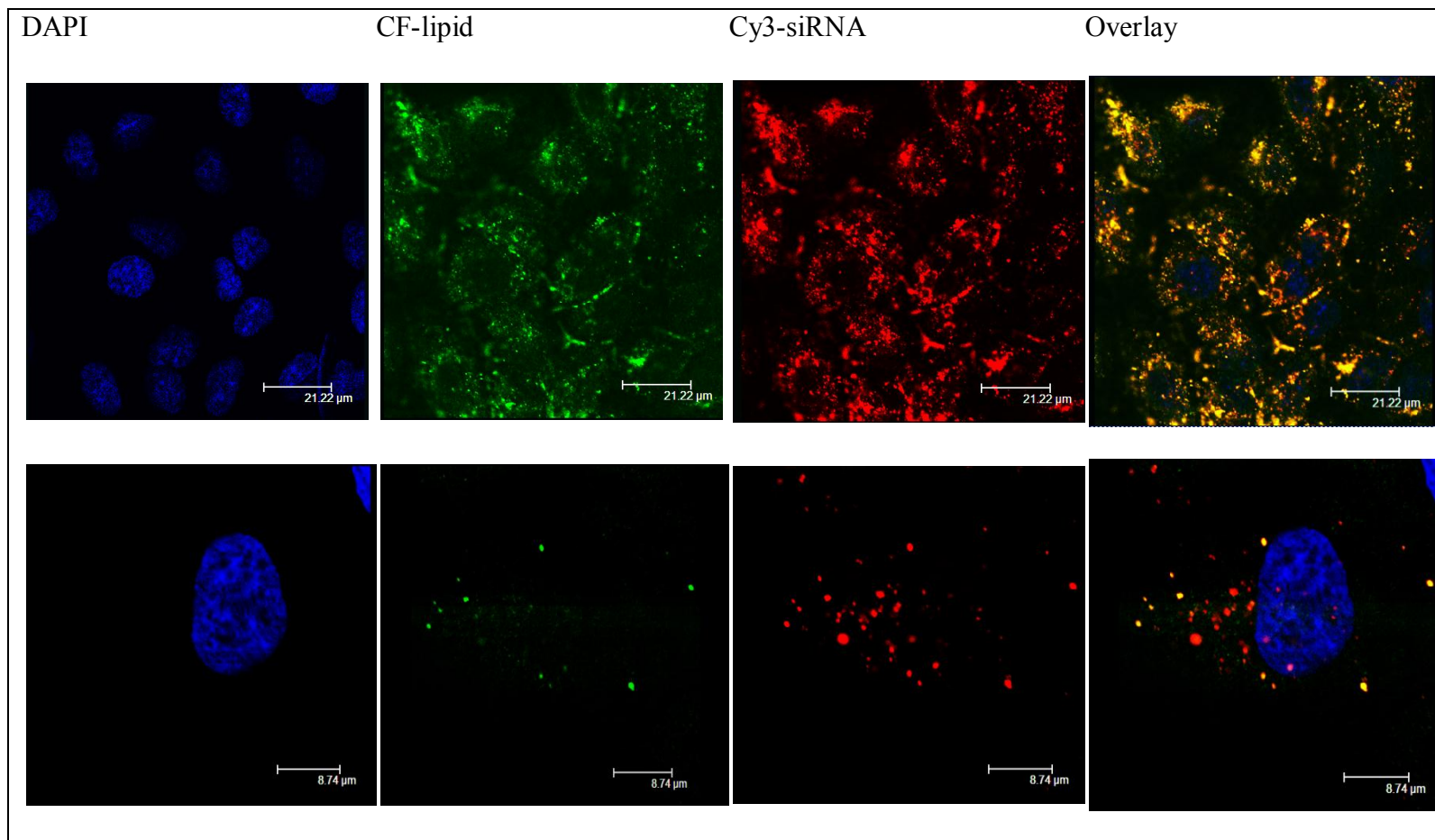


**Figure 4.2** Colocalization of Cy3 siRNA (red) and CF-DOTAP:DOPE (green) in A549 cells after 2 hour incubation with fluorescent LPR complexes. DAPI (blue) was used to stain the nucleus. Images on the lower panel are an enlarged version of images on the upper panel.

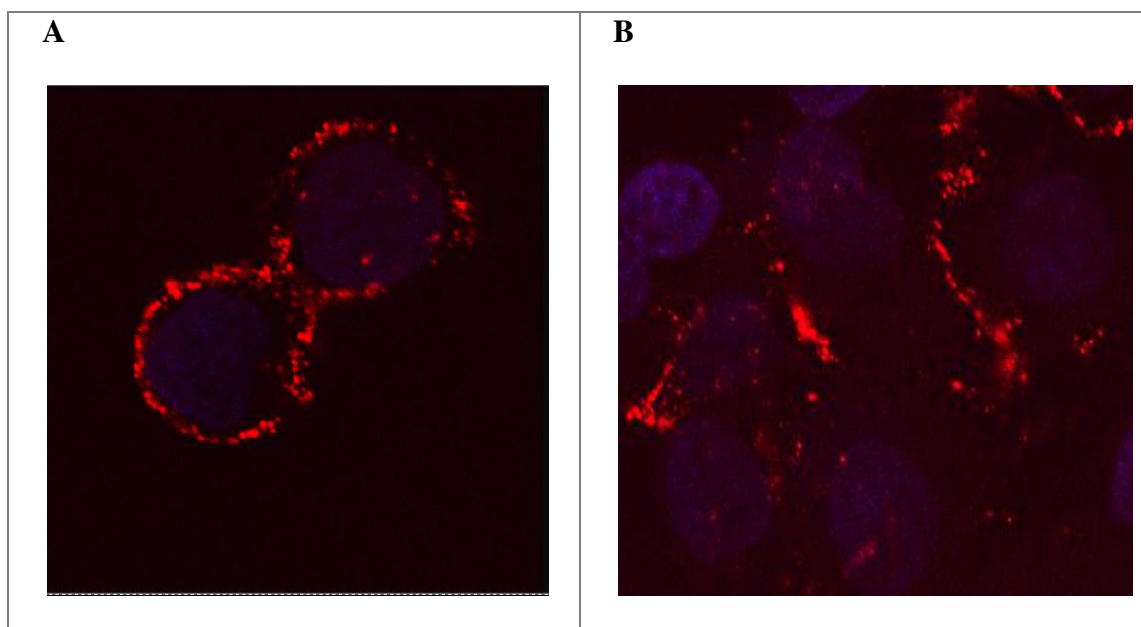


**Figure 4.3** Confocal images of Cy3-GAPDH siRNA in A549 cells at 4°C. A549 cells were transfected with LpegR (A) and LPR (B) complexes for 2 hours at 4°C. The fluorescent complexes were prepared using red Cy3-GAPDH and blue DAPI was used to highlight the nucleus.

In order to investigate the effect of lowering temperature on gene silencing efficiency, A549 cells were transfected with LPR and LpegR complexes at decreasing temperatures to inhibit the energy-dependent endocytosis. The level of GAPDH gene silencing mediated by either LPR or LpegR complexes was significantly ( $p < 0.05$ , student t-test) reduced at 10°C and 4°C as compared to control (37°C), with more than



80% reduction at 4°C (Figure 4.4A). Cell viability (Figure 4.4B) under any of these conditions was unaffected as compared to control ( $p>0.05$ , unpaired t-test).

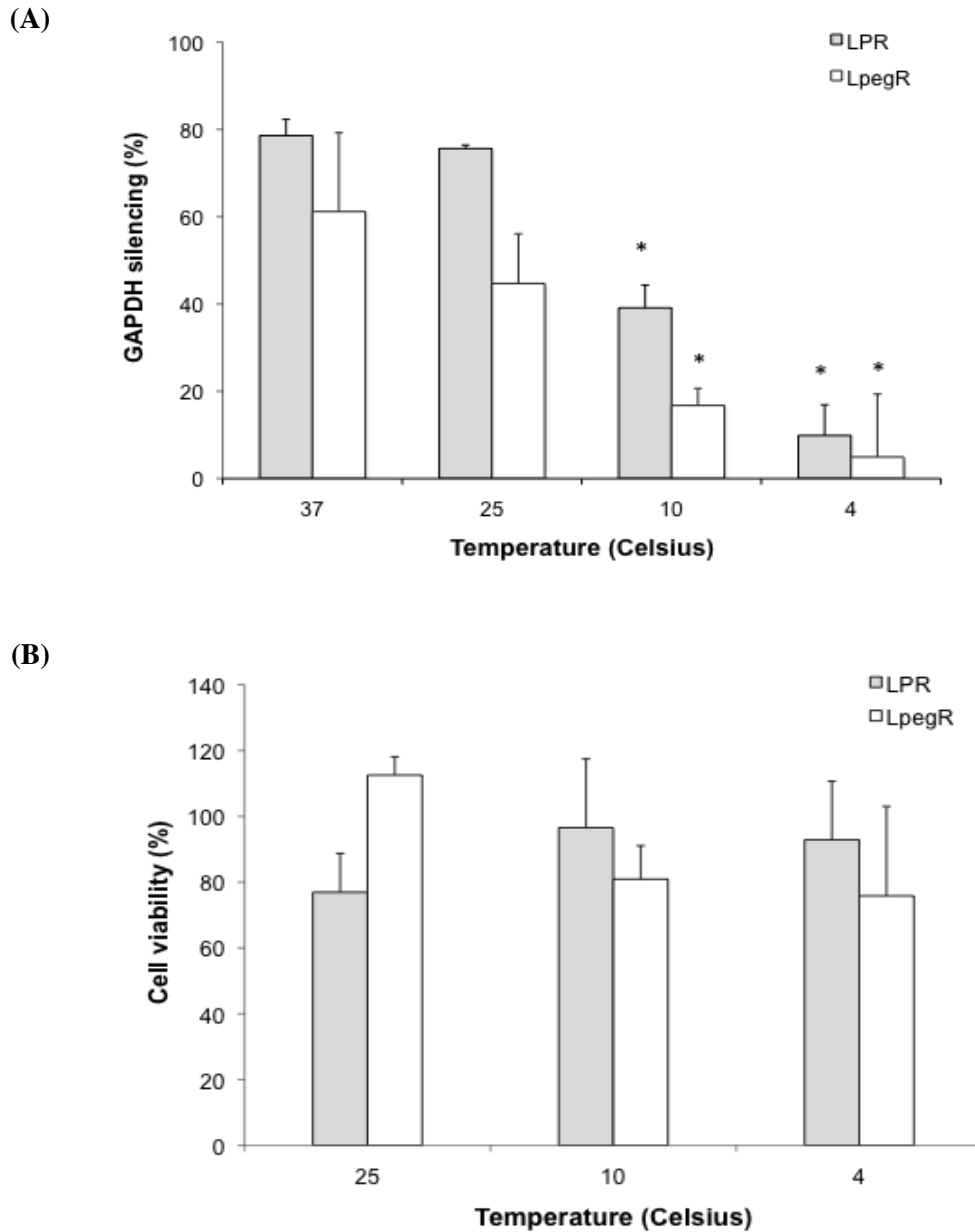


**Figure 4.4** A) Gene silencing efficiency and B) cell viability of A549 cells incubated with LPR and LpegR complexes at different temperatures for 6 h. Cells were incubated at the indicated temperatures for 1 h pre-transfection and during transfection then incubated at 37°C post-transfection. Gene silencing and cell viability were measured after 72 h using KDalert assay ( $n=3$ , mean $\pm$ SEM). \* Statistical significance ( $p<0.05$ , unpaired t-test).

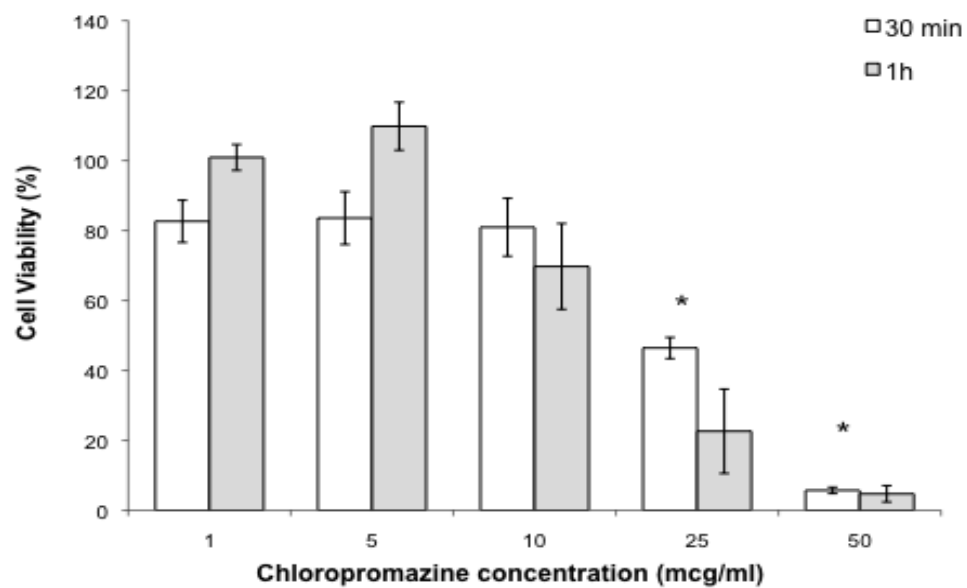
### **4.4.3. Optimisation of endocytosis inhibitors concentrations**

#### **4.4.3.1. MTT screening of endocytosis inhibitors**

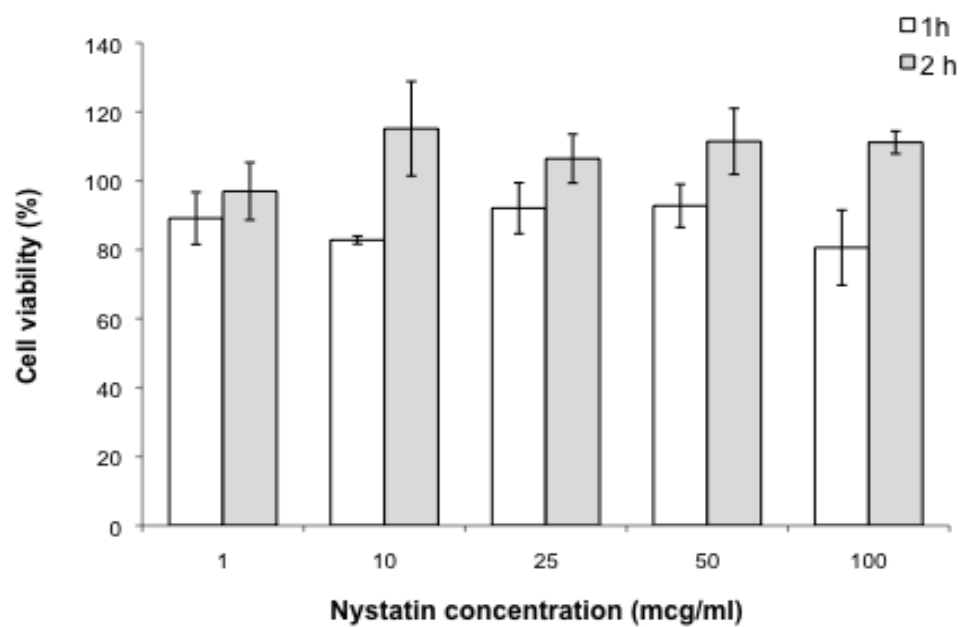
When A549 cells were exposed to chlorpromazine at different concentrations for 30 or 60 min, a concentration dependent toxicity was observed, with chlorpromazine concentrations  $\leq 10$   $\mu\text{g/ml}$  for either 30 or 60 minutes exposure maintaining good cell viability compared to control (Figure 4.5A). However, higher concentrations (25 and 50  $\mu\text{g/ml}$ ) significantly reduced cell viability to less than 40% ( $p < 0.05$ , unpaired t-test). There was no significant increase in toxicity between the 30 min and 1 hour exposure time for all concentrations ( $p > 0.05$ , unpaired t-test). Similarly when A549 cells were exposed to nystatin (Figure 4.5B) and amiloride (Figure 4.5C) for 1 or 2 h, cell viability remained above 80% at the concentration range used. No significant difference was observed between cell viability after 1 or 2 h exposure for all concentrations ( $p > 0.05$ , paired t-test).

Depleting cells from potassium for different durations (2, 4 and 6 h) did not have any effect on cell viability when compared to control cells ( $p > 0.05$ , paired t-test) treated with potassium containing buffer (Figure 4.5D).

(A)



(B)



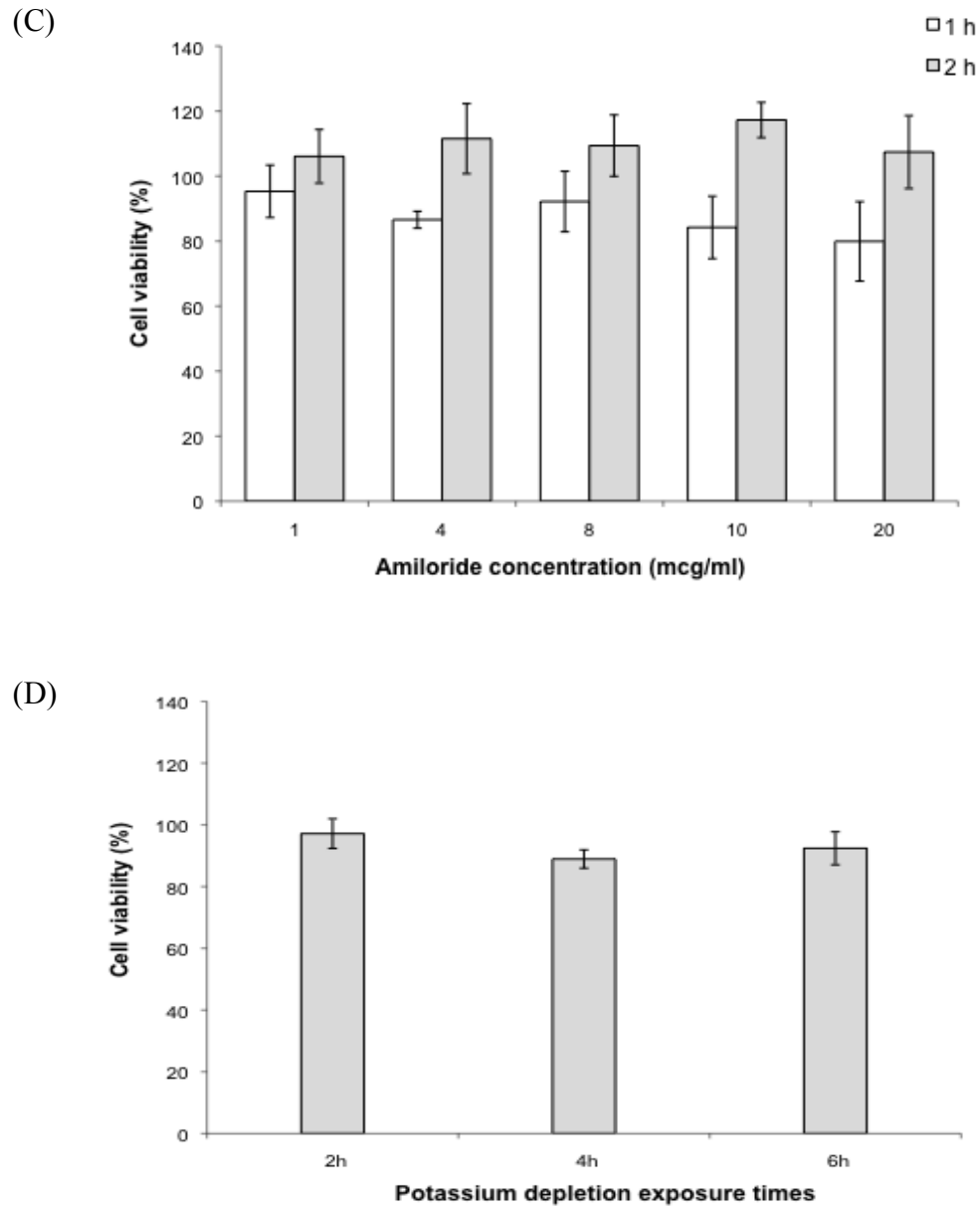


**Figure 4.5** Percentage viability of A549 cells after incubation with different concentrations of inhibitors; A) chlorpromazine, B) nystatin, C) amiloride and D) potassium depletion. Results are expressed as a percentage of the viability of untreated cells or cells treated with potassium containing buffer in the potassium depletion experiment (Data represent mean $\pm$ SEM, n=3). \*Statistically significant ( $p<0.05$ , unpaired t-test).

#### 4.4.3.2. Inhibition of transferrin uptake via the clathrin-mediated pathway

In A549 cells treated with 4  $\mu\text{g/ml}$  chlorpromazine (Figure 4.6B), transferrin internalization was similar to that observed in untreated cells (Figure 4.6A) marked by a similar amount of red fluorescence. However as the concentration of chlorpromazine was increased to 8  $\mu\text{g/ml}$ , there was a reduction in transferrin internalization as seen by the reduced red fluorescence in comparison with untreated cells (Figure 4.6C). Strong inhibition of transferrin internalization was observed when cells were treated with 10  $\mu\text{g/ml}$  chlorpromazine (Figure 4.6D). Based on these findings and the MTT test results, chlorpromazine at 10  $\mu\text{g/ml}$  concentration was selected as the optimal concentration to inhibit clathrin-mediated endocytosis without causing significant toxicity. This comes in accordance with the literature as most studies used chlorpromazine at this concentration to effectively inhibit clathrin pathways (Rejman, J. *et al.*, 2004, Lu, J.J. *et al.*, 2009, Lai, S.K. *et al.*, 2008). In A549 cells treated with non-clathrin inhibitors nystatin, cytochalasin D and amiloride, transferrin internalization was indistinguishable from that observed in untreated cells (Figure 4.7). This confirms that the uptake of transferrin via the clathrin pathway is specifically inhibited by chlorpromazine at the concentrations tested.

Depletion of cellular potassium that specifically inhibits uptake via clathrin-mediated endocytosis reduced the uptake of transferrin in A549 cells following 2 h exposure, as compared to control cells treated with potassium containing buffer (Figure 4.8). Therefore this method can be effectively and safely used to inhibit the uptake via the clathrin-mediated pathway.

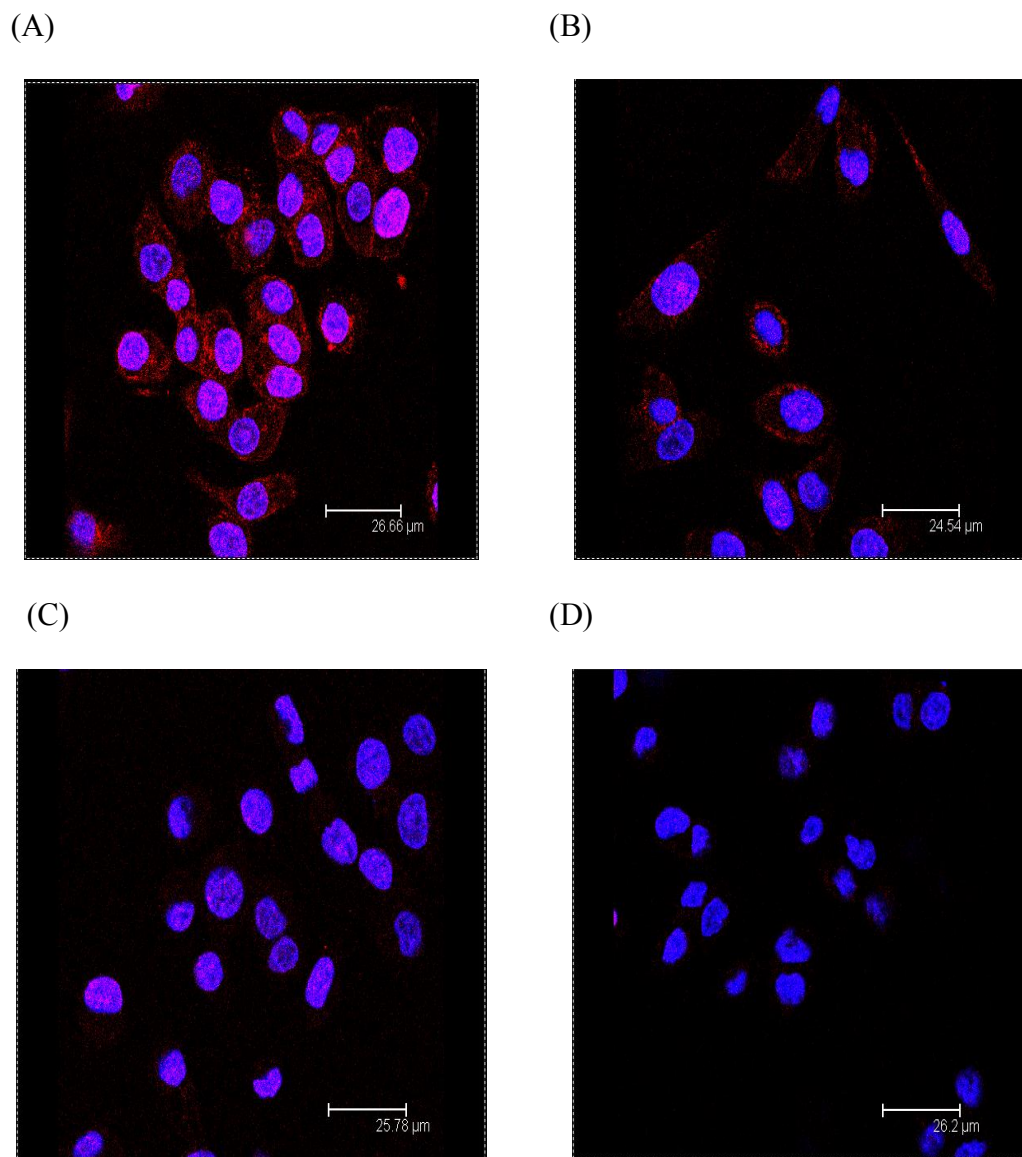


**Figure 4.6** Uptake of Alexa Fluor 633-transferrin in A549 cells pre-treated with chlorpromazine. Confocal microscopy analysis following cell exposure to chlorpromazine at different concentrations: A) 0  $\mu\text{g/ml}$ , B) 4  $\mu\text{g/ml}$ , C) 8  $\mu\text{g/ml}$ , D) 10  $\mu\text{g/ml}$ . Cells were incubated with the inhibitor for 1 h before the addition of transferrin. Blue DAPI stain was used to highlight the nucleus.

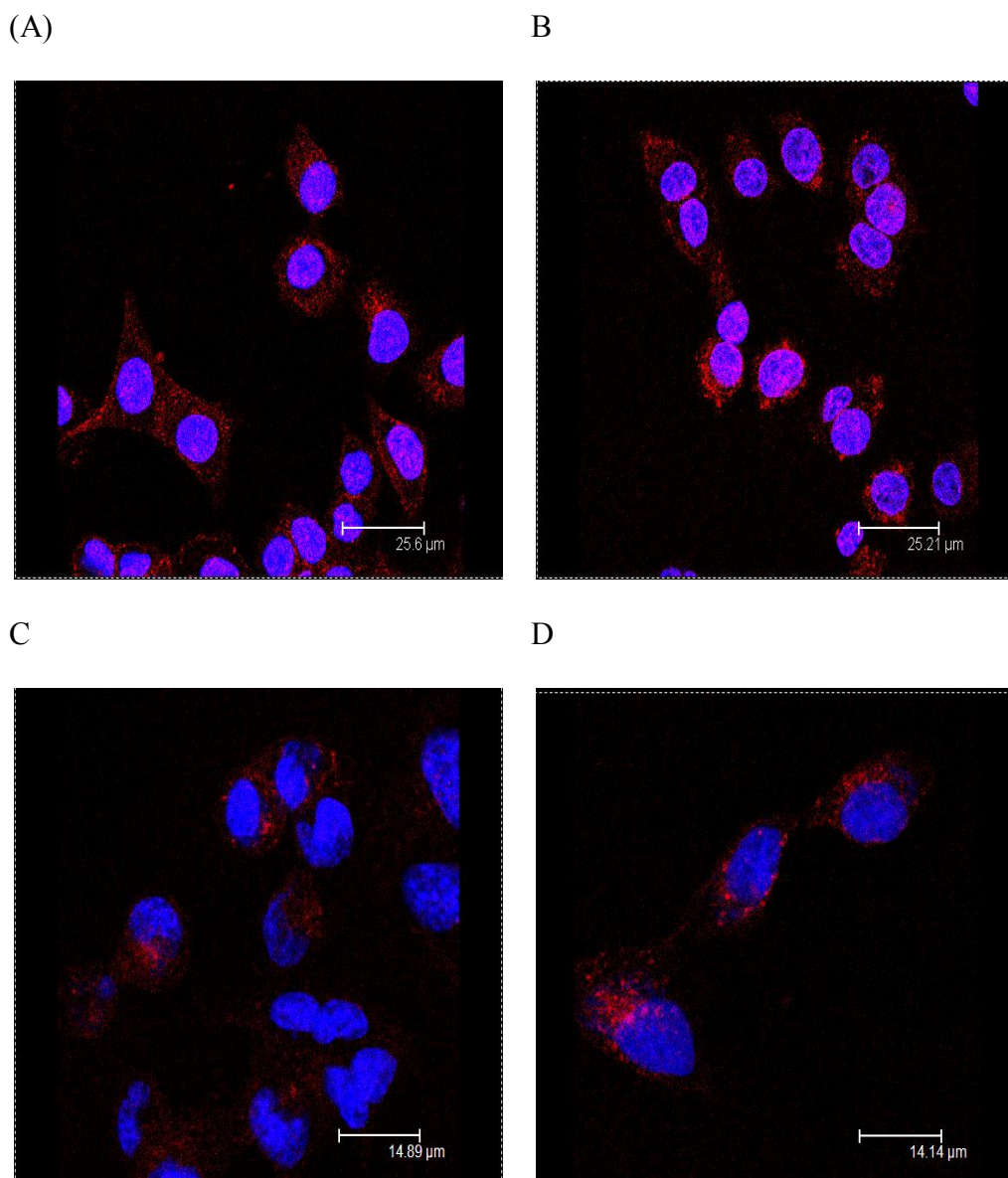


**Figure 4.7** Uptake of Alexa Fluor 633-transferrin in A549 cells pre-treated with non-clathrin inhibitors: Confocal microscopy analysis following cell exposure to A) no inhibitors, B) 25  $\mu\text{g/ml}$  nystatin, C) 10  $\mu\text{g/ml}$  cytochalasin D, D) 8  $\mu\text{g/ml}$  amiloride. Cells were incubated with the inhibitors for 1 h before the addition of transferrin. Blue DAPI stain was used to highlight the nucleus.

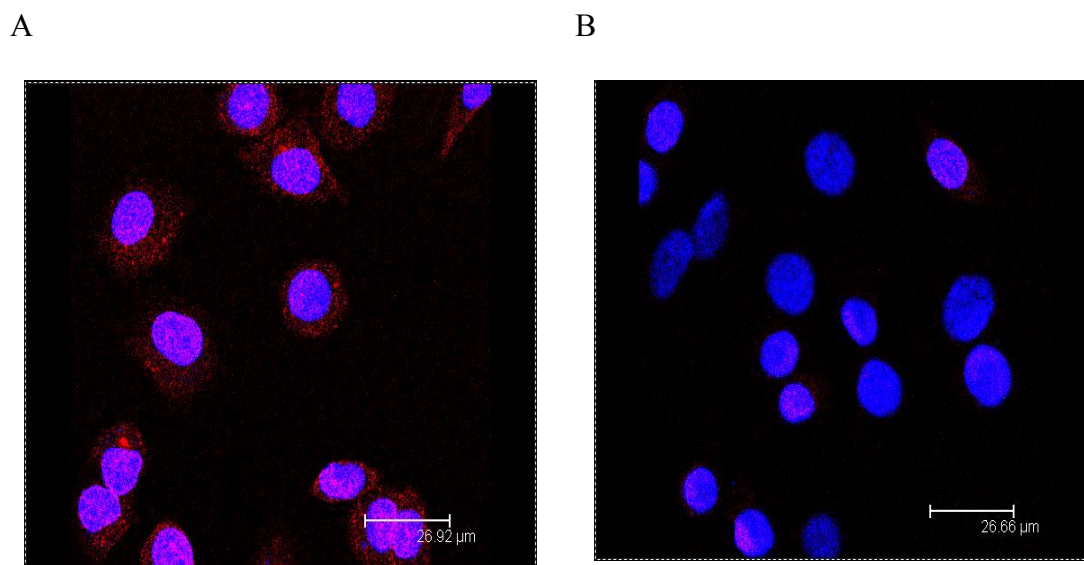


**Figure 4.8** Uptake of Alexa Fluor 633-transferrin in A549 cells exposed to (A) potassium containing buffer and (B) potassium depletion. Blue DAPI stain was used to highlight the nucleus.

#### 4.4.3.3. Inhibition of BODIPY-LacCer via the caveolae-mediated endocytosis

Nystatin at 10  $\mu\text{g/ml}$  was ineffective at inhibiting BODIPY-LacCer internalization, when compared to untreated cells (Figure 4.9). However as the concentration was increased to 20  $\mu\text{g/ml}$  or 25  $\mu\text{g/ml}$ , a significant reduction in internalized BODIPY-LacCer was observed. In accordance with these findings, MTT assay data 25  $\mu\text{g/ml}$  nystatin was used to inhibit the caveolae-mediated pathway.



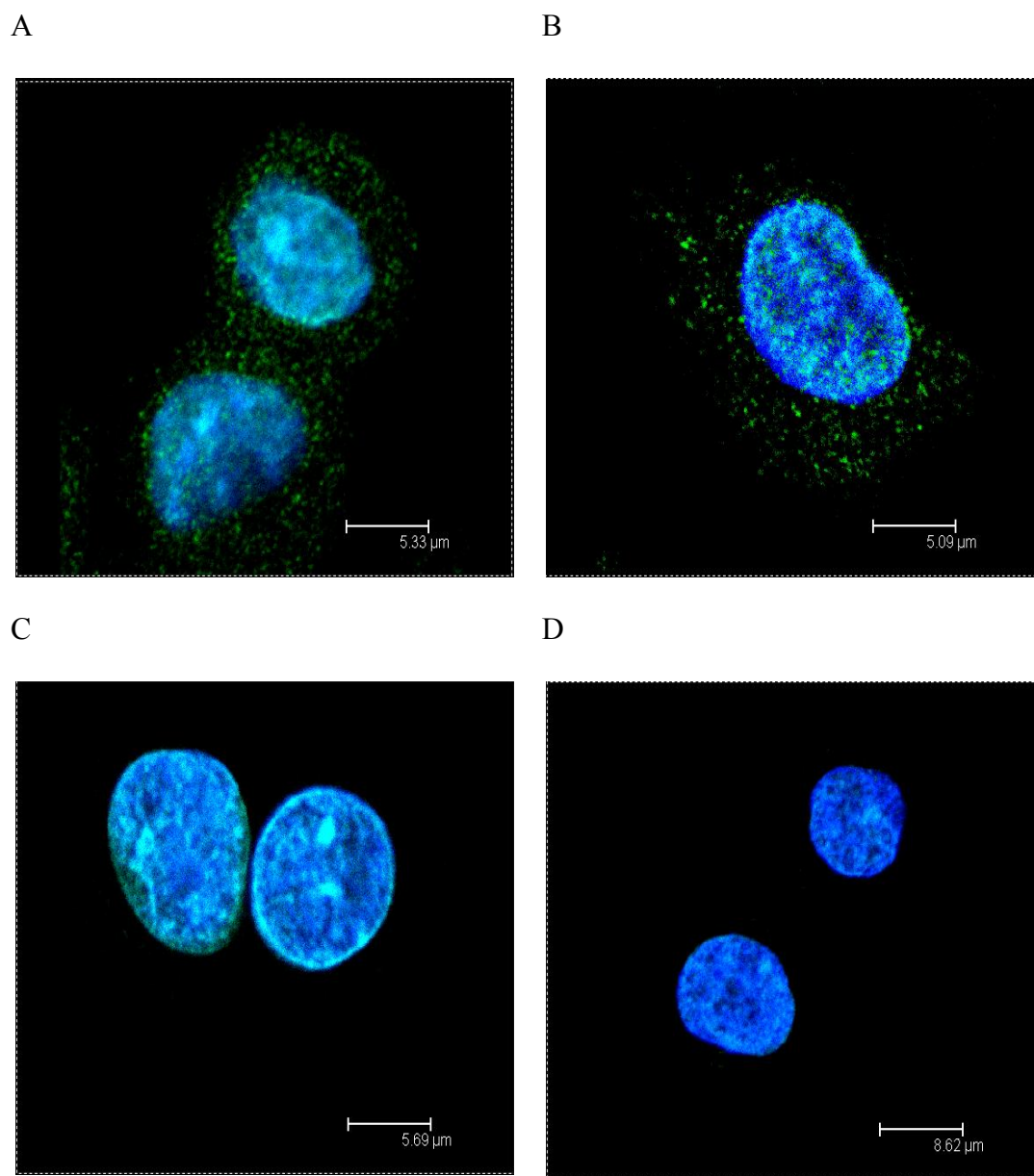


**Figure 4.9** Uptake of BODIPY-LacCer in A549 cells pre-treated with nystatin. Confocal images of uptake in cells treated with different concentrations of nystatin: (A) 0  $\mu\text{g/ml}$ , (B) 10  $\mu\text{g/ml}$ , (C) 20  $\mu\text{g/ml}$ , (D) 25  $\mu\text{g/ml}$ . Cells were incubated with the inhibitor for 1 h before the addition of green BODIPY-LacCer. Blue DAPI stain was used to highlight the nucleus.

#### 4.4.3.4. Effect of endocytosis inhibitors after exposure to cells for a duration equivalent to the duration of transfection experiment

From the previous section, when chlorpromazine 10 µg/ml was incubated with cells for 30 or 60 min, it did not cause a significant effect on cell viability. However after 7 h exposure (i.e., the duration of a transfection experiment), it caused more than 80% reduction in cell viability compared to untreated cells. Chlorpromazine at 7.5µg/ml concentrations appeared less toxic with more than 60 % cell viability after 7 h exposure to cells (Figure 4.10) and was used for the transfection experiments. The other inhibitors were non-toxic even after a 7-hour incubation with cells.

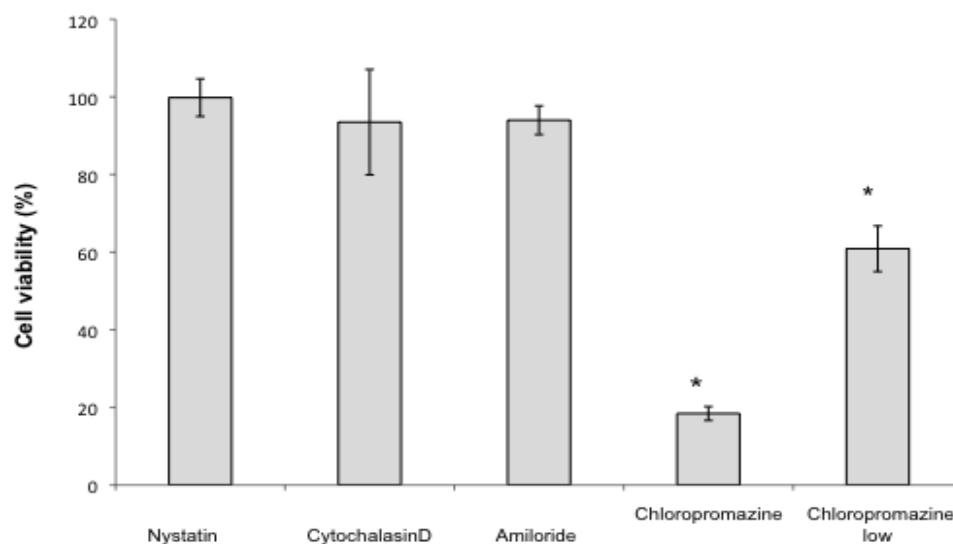


**Figure 4.10** Viability of A549 cells treated for 7 h with endocytosis inhibitors. Treatments were: nystatin (25 µg/ml), cytochalasin D (10 µg/ml), amiloride (8 µg/ml) or chlorpromazine (7.5 µg/ml – low, and 10 µg/ml). Cell viability was measured using the MTT assay and results are expressed as a percentage of the viability of untreated cells (Data represent mean±SEM, n=3). \*Statistically significant (p<0.05, unpaired t-test).

#### **4.4.4. Role of Clathrin-mediated endocytosis in the uptake of functional siRNA**

The colocalization of siRNA complexes with markers of the clathrin-mediated endocytosis was studied. The cellular localization of fluorescent siRNA LpegR complexes was compared to that of fluorescent Alexa Fluor 488-transferrin, which is a selective marker of clathrin-mediated endocytosis. Co-localization of siRNA complexes with the pathway markers would suggest that they share the same uptake pathway. When A549 cells were co-incubated with Cy3-labeled siRNA complexes (LPCy3-R and LpegCy3-R) and Alexa Fluor 488-transferrin, for 2 hours, overlap between the green labeled siRNA complexes and the red labeled transferrin was seen in the cells as yellow-orange fluorescence which indicated co-localization of the both the LPR and LpegR complexes with the clathrin pathway marker (Figure 4.11).

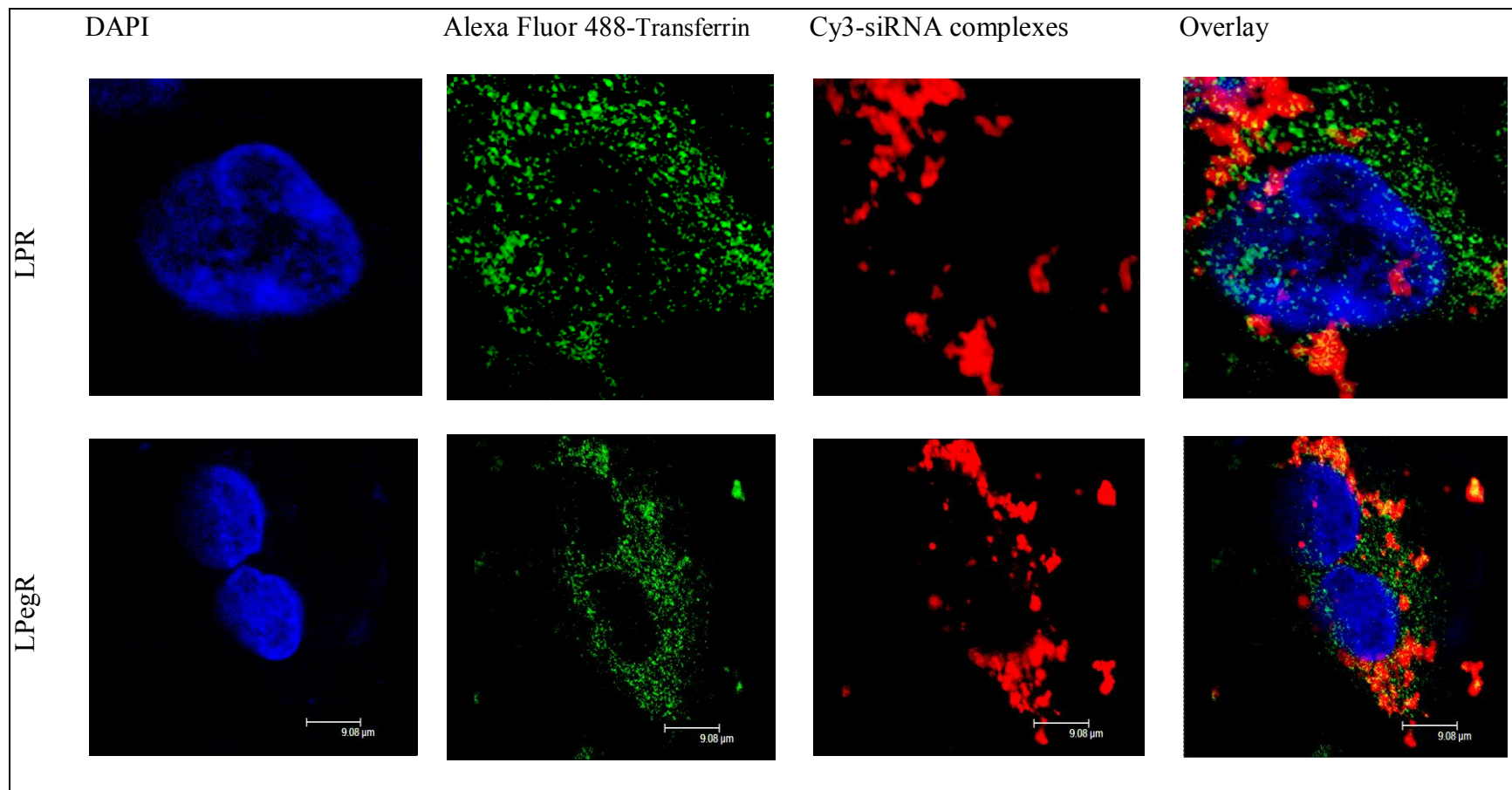


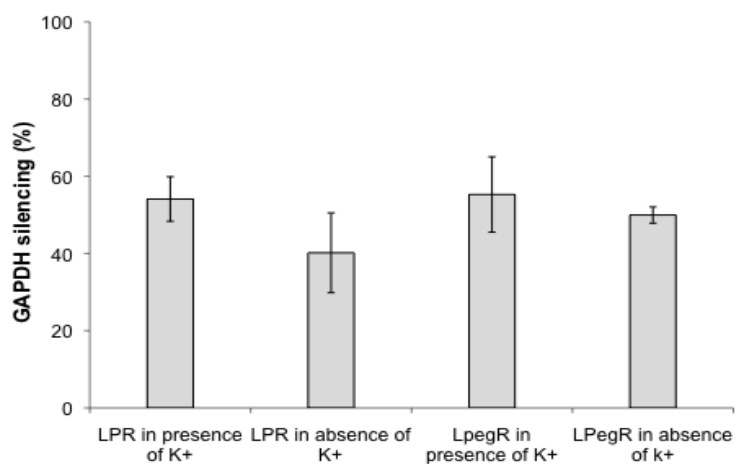
**Figure 4.11** Co-localization of Cy-3 labeled LPR and LpegR complexes with Alexa Fluor 488-transferrin in A549 cells. Cells were co-incubated with fluorescent siRNA complexes and transferrin (green) for 2 h prior to analysis by confocal microscopy. Blue indicates DAPI-stained nucleus.

The inhibition of the clathrin-mediated pathway did not affect gene silencing mediated by LPR and LpegR complexes. The effect of clathrin-mediated endocytosis inhibition on gene silencing was first determined using the potassium depletion method. In A549 cells depleted from potassium, gene silencing mediated by either LPR or LpegR complexes was not affected, as there was not a significant difference in the percentage GAPDH knockdown between cells treated with potassium buffer and cells depleted from potassium (Figure 4.12A). The cell viability of the transfected cells after K<sup>+</sup> depletion was also determined using KDalert assay and was found to be in the range of 75-85% (Figure 4.12B).

The effect of clathrin pathway inhibition on gene silencing was further tested using chlorpromazine. In cells pre-treated with chlorpromazine (7.5µg/ml) for 1 hour then transfected with LPR complexes in the absence of the inhibitor, the gene silencing efficiency was not affected compared to control (no inhibitors) (Figure 4.13A). To confirm the result, the transfection was carried out in the presence of the inhibitor at the same time as the siRNA complexes. Despite getting a significant ( $p < 0.05$ , unpaired t-test) 50% reduction in gene silencing efficiency compared to control, there was more than 80% reduction in cell viability (Figure 4.13B). The same experiments were carried out using a different siRNA complex, LpegR and there was no significant difference in gene silencing efficiency between untreated cells and cells treated with chlorpromazine for 1 hour only or for 7 hours (Figure 4.13C). However, as observed with LPR complexes, cells transfected in the presence of chlorpromazine (7 hours), showed a

significant ( $p < 0.05$ , unpaired t-test) reduction in cell viability (~50%) as compared to the control (Figure 4.13D)

(A)



(B)

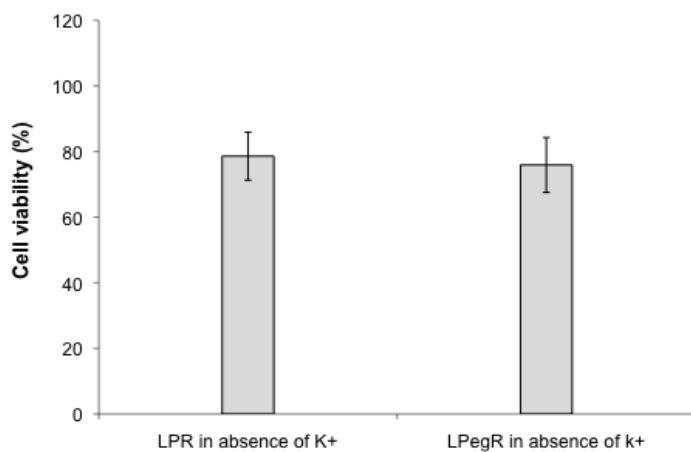
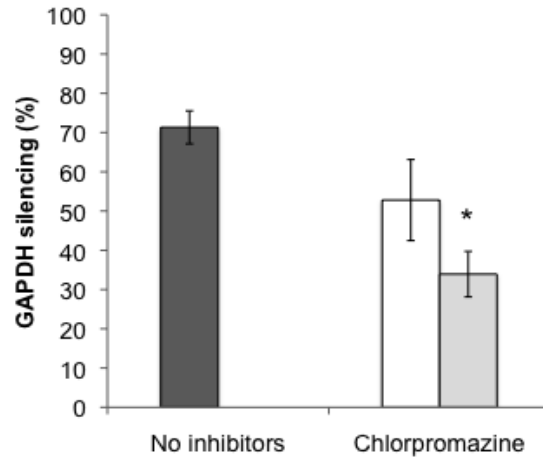
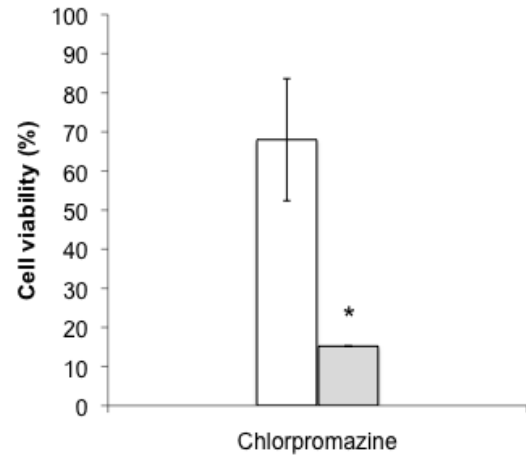


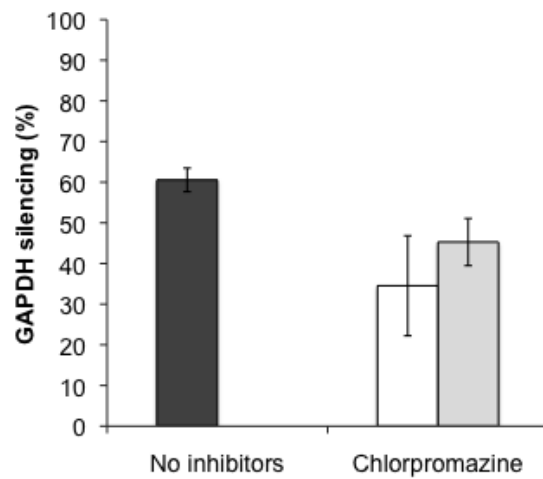
**Figure 4.12** (A) Gene silencing efficiency and (B) cell viability of A549 cells after exposure to potassium depletion and subsequent transfection with LPR and LpegR complexes. Cells transfected in the presence of potassium were used as control. Gene silencing and cell viability were determined 72 h post-transfection by KDalert assay. (Data represent mean $\pm$ SEM, n=3).



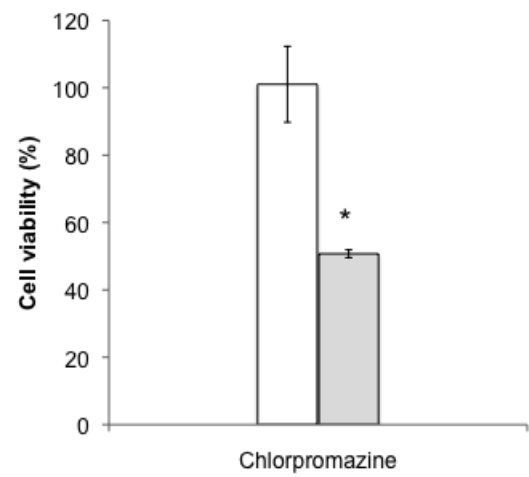
(A)



(B)



(C)



(D)

**Figure 4.13** A) Gene silencing and B) cell viability of A549 cells after pre-treatment with chlorpromazine and subsequent transfection with LPR complexes, as well as C) Gene silencing and D) cell viability after transfection with LpegR complexes. Cells were exposed to chlorpromazine for 1 h, followed by incubation with complexes for 6 h in the absence (grey bars) or presence (white bars) of the inhibitor. Control represent cells transfected with LPR or LpegR complexes without treatment with inhibitors at all (Black bars) (Data represent mean $\pm$ SEM, n=3). \* Statistically significant (p<0.05, unpaired t-test).

#### **4.4.5. Role of Caveolae-mediated endocytosis and macropinocytosis in the uptake of functional siRNA**

siRNA complexes did not co-localize with markers of the caveolae-mediated endocytosis. A549 cells were co-incubated with the marker of the caveolae-mediated endocytosis BODIPY-LacCer and siRNA complexes. Confocal analysis showed that there was no overlap between the red siRNA complexes (LPCy3-R and LpegCy3-R) and the green BODIPY-LacCer (Figure 4.14).

Inhibition of the caveolae and macropinocytosis pathway did not affect gene silencing mediated by LPR and LpegR complexes. In the presence of the caveolae endocytosis inhibitor nystatin (25  $\mu$ g/ml), GAPDH knockdown mediated by both LPR and LpegR complexes and percentage cell viability remained at levels comparable to untreated controls (Figure 4.15A and 4.16A). Similarly, the presence of the macropinocytosis inhibitor amiloride before or during transfection did not diminish gene silencing and did not affect cell viability either. This finding was verified using another drug cytochalasin D, which inhibits both caveolae-mediated endocytosis and macropinocytosis. There was no significant reduction in GAPDH silencing mediated by LPR complexes after treatment with the inhibitor (Figure 4.15A), but a statistically significant ( $p < 0.05$ , unpaired t-test) reduction in cell viability was observed during both 1 and 6 h exposure to the inhibitor (Figure 4.15B). LPegR complexes resulted in ~30% reduction in gene silencing when the inhibitor was present during the whole transfection duration (Figure 4.16A), but it was linked with an 80% reduction in percentage viable cells as compared to cells not treated with cytochalasin D (Figure 4.16B).



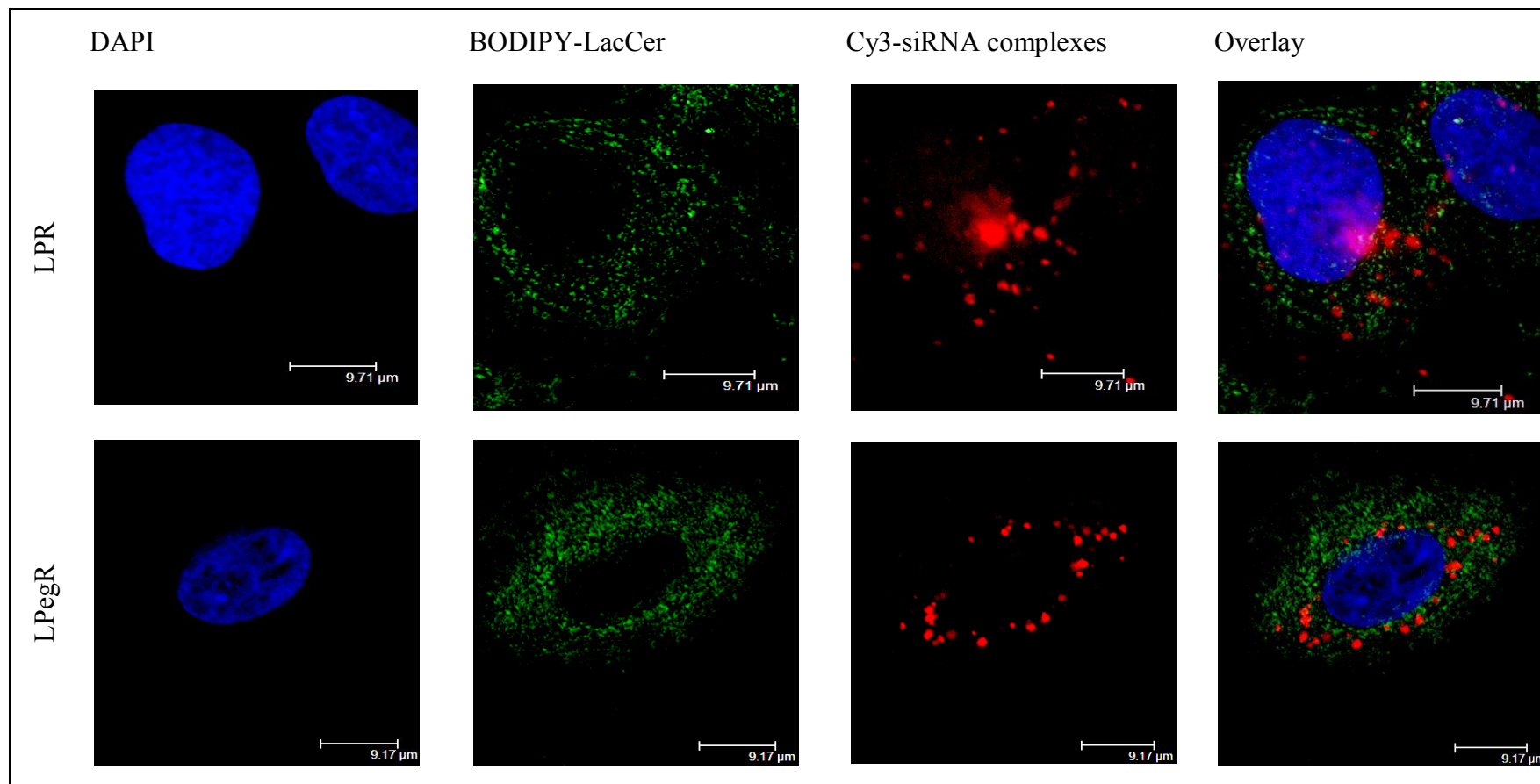


**Figure 4.14** Colocalization studies of LPeg-Cy3-R complexes with BODIPY-LacCer in A549 cells. Cells were first incubated with BODIPY-LacCer (green) for 30 min at 4°C, followed by incubation with LPeg-Cy3-R complexes for another 90 min at 37°C prior to analysis with confocal microscopy. Blue indicates DAPI-stained nucleus.

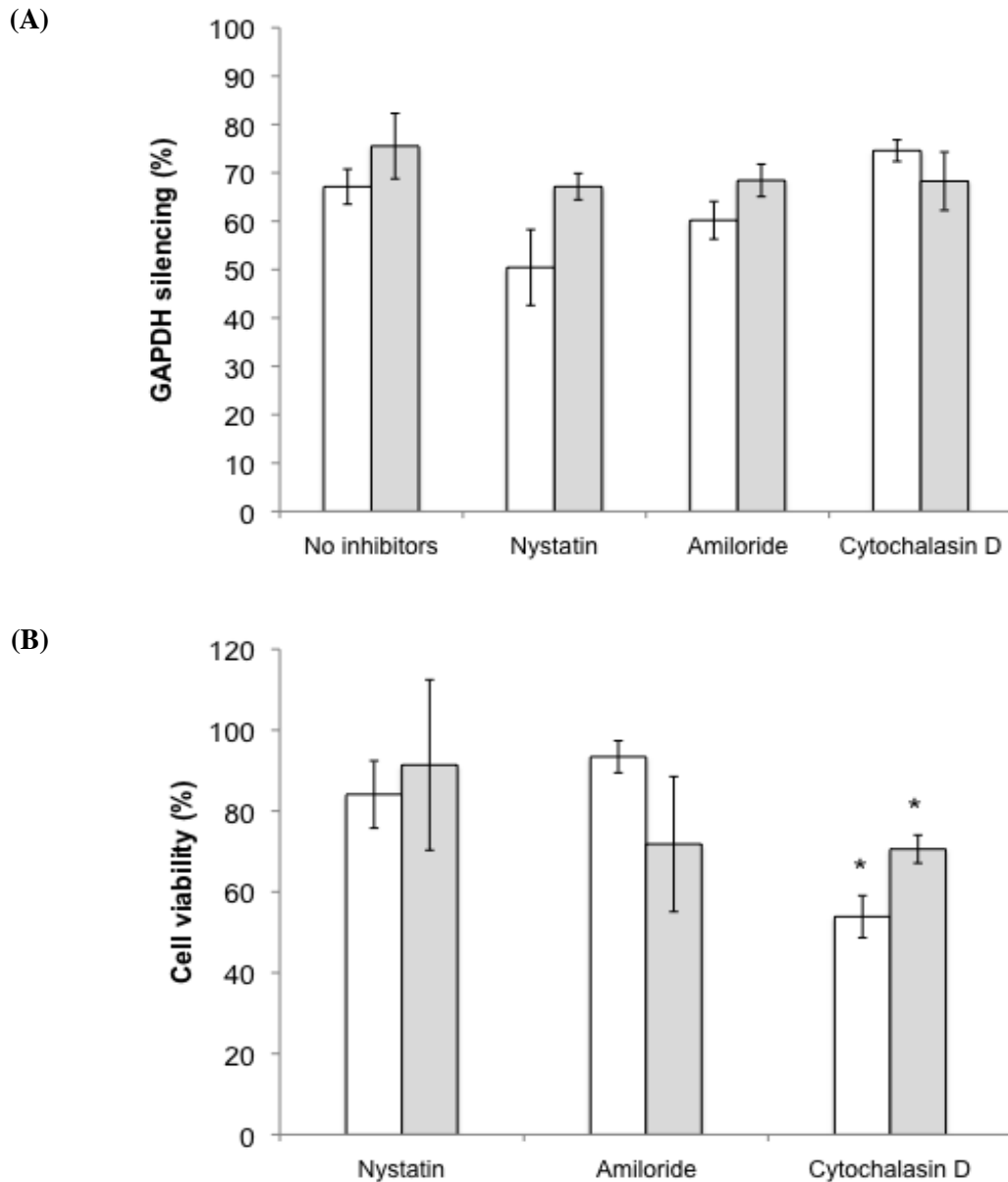


**Figure 4.15** A) Gene silencing and B) cell viability of A549 cells when exposed to LPR complexes after pretreatment with inhibitors of non-clathrin mediated endocytosis. Pre-treatment with nystatin 25  $\mu\text{g/ml}$ , amiloride 8  $\mu\text{g/ml}$  or cytochalasin D 10  $\mu\text{g/ml}$  for 1 h, followed by transfection with LPR complexes in the absence (grey bars) or presence of the inhibitor (white bars) for 6 h. Gene silencing and cell viability were measured 72 h post-transfection using KDaAlert assay. Data represent the mean of three independent experiments (mean $\pm$ SEM). \*Statistically significant (( $p < 0.05$ , unpaired t-test))

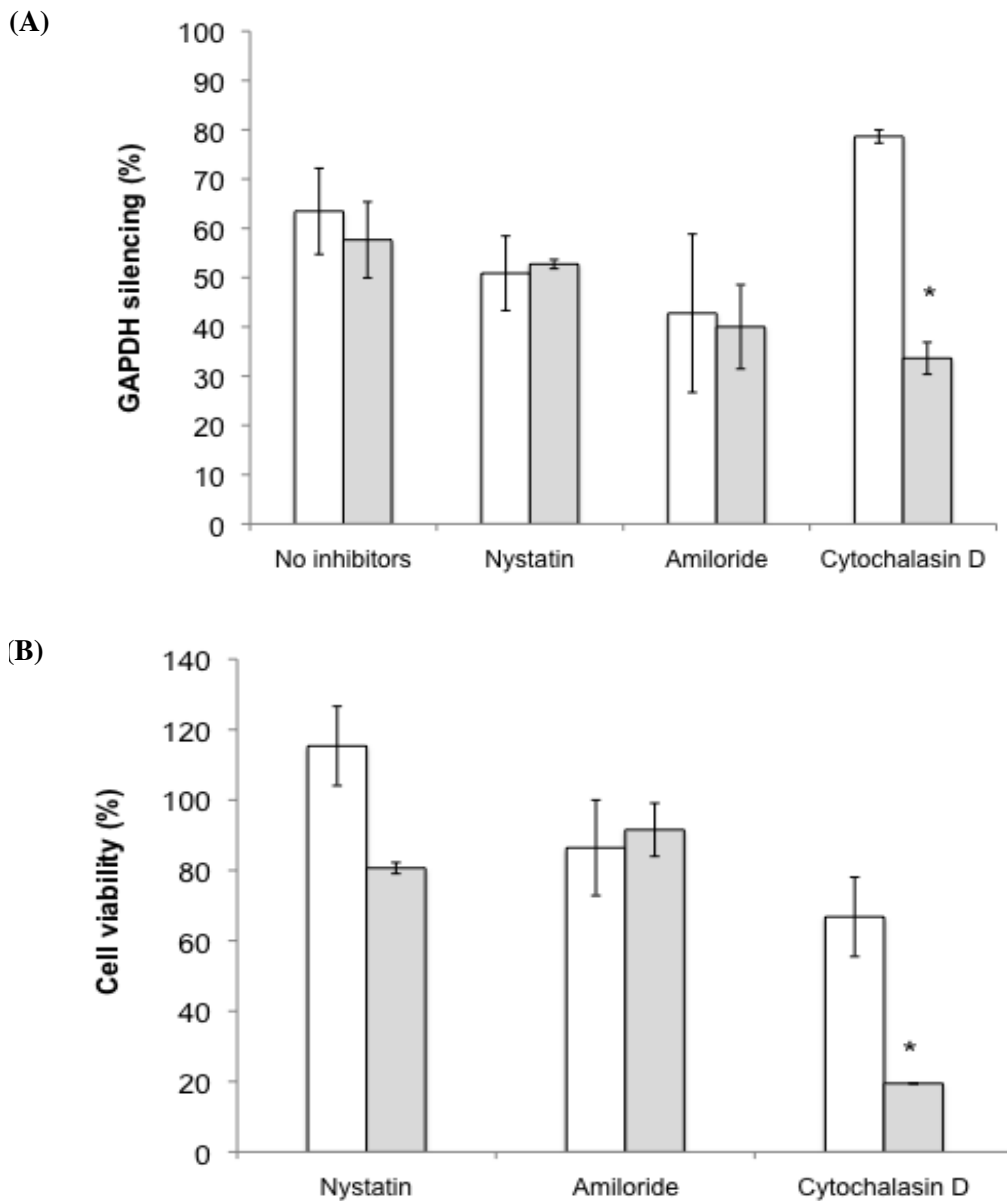


**Figure 4.16** (A) Gene silencing and (B) cell viability of A549 cells when exposed to LpegR complexes after pretreatment with inhibitors of non-clathrin mediated endocytosis. Pre-treatment with nystatin 25  $\mu\text{g/ml}$ , amiloride 8  $\mu\text{g/ml}$  or cytochalasin D 10  $\mu\text{g/ml}$  for 1 h, followed by transfection with LpegR complexes in the absence (grey bars) or presence of the inhibitor (white bars) for 6 h. Gene silencing and cell viability were measured 72 h post-transfection using KDAlert assay. Data represent the mean of three independent experiments (mean $\pm$ SEM). \*Statistically significant (( $p < 0.05$ , unpaired t-test)

#### **4.4.6. The effect of combined inhibition of endocytosis pathways on the gene silencing efficiency of siRNA complexes**

In the previous sections, the effect of a single inhibitor on gene silencing was determined. In this section the combined effect of two or more inhibitors was investigated to determine whether the different endocytosis pathways compensated when one of the pathways was inhibited. A549 cells were exposed to a combination of two or three inhibitors of the endocytosis pathways and subsequently transfected with LpegR complexes in the presence of inhibitors. None of the combinations of two inhibitors showed any significant reduction ( $p > 0.05$ , One-way-Anova, Tukey's) in the gene silencing as compared to untreated cells (Figure 4.17A). However the percentage of viable cells after exposure to two inhibitors was significantly reduced by 50% ( $p < 0.05$ , One-way Anova, Tukey's), except with the nystatin+amiloride combination where the cell viability was not affected (Figure 4.17B).

When A549 cells were exposed to a combination of the three inhibitors chlorpromazine +nystatin + amiloride, there was a significant 40% inhibition of GAPDH gene silencing as compared to control ( $p < 0.05$ , One-way Anova, Tukey's) (Figure 4.17A). However triple inhibitor combination proved to be toxic and significantly decreased cell viability by 60% ( $p < 0.05$ , One-way Anova, Tukey's) (Figure 4.17B). A statistically significant difference in gene silencing between cells treated with nystatin+amiloride and those treated with nystatin+amiloride+chlorpromazine was observed, but again this difference was associated with a considerable decrease in cell viability.

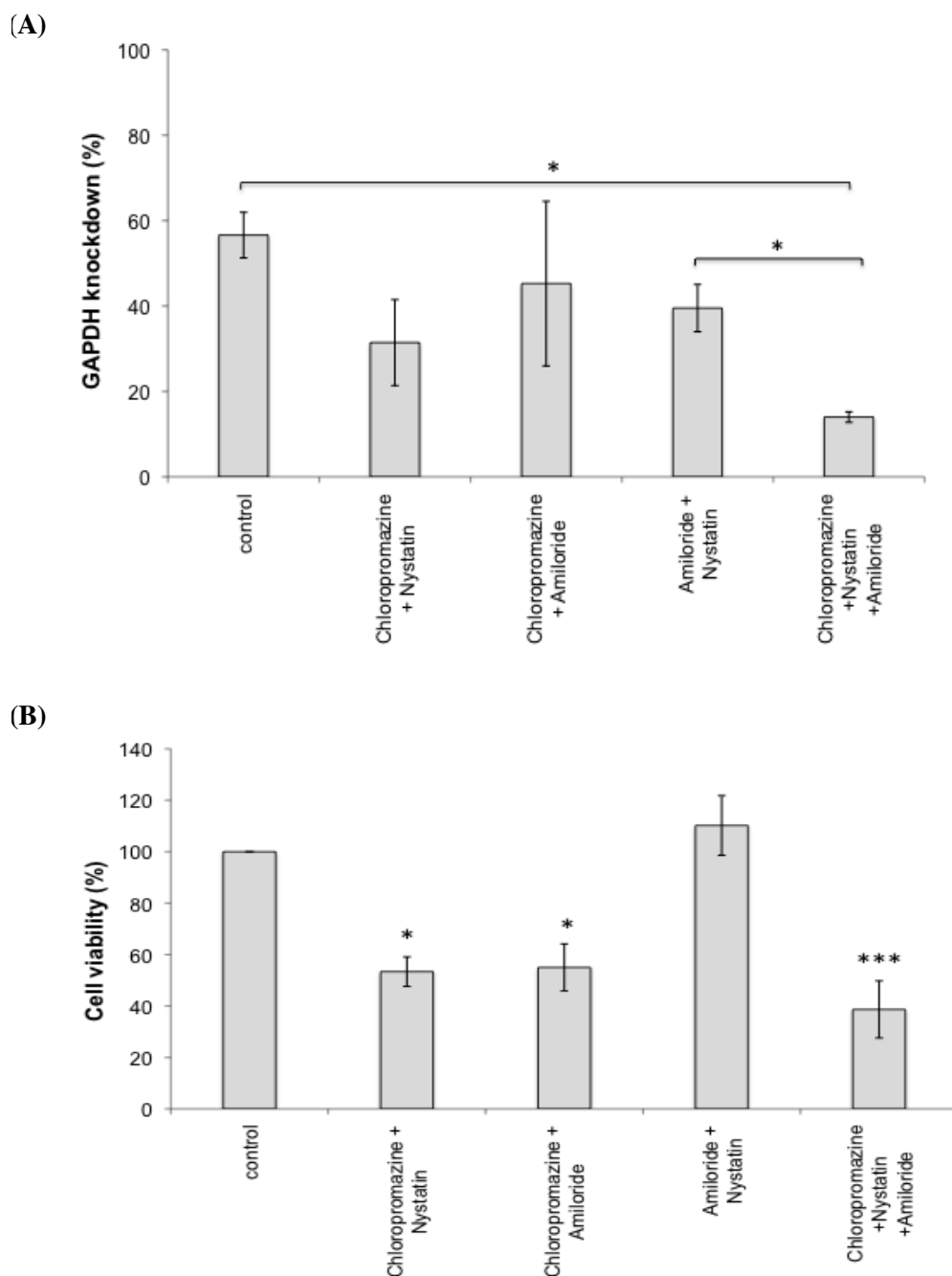


**Figure 4.17** A) Gene silencing and B) cell viability of A549 cells after pre-treatment with combinations of the endocytic inhibitors. Pre-treatment for 1 h, followed by transfection with LpegR complexes in the presence of the inhibitors. Gene silencing and cell viability were measured 72 h post-transfection using the KDalert assay. (Data represent mean $\pm$ SEM, n=3). Statistically significant (\*p<0.05, \*\*\* p<0.001, One-Way Anova, Tukey's test).

## 4.5. Discussion

The first step in gene delivery is the intracellular uptake of the gene delivery complex therefore knowledge of the uptake mechanisms of non-viral gene carriers is essential for the development of improved vectors. Early studies indicated that cationic lipid-mediated pDNA delivery occurs through endocytosis, although there is contradictory evidence regarding the exact endocytic pathways (Khalil, I.A. *et al.*, 2006). Some reports showed that DOTAP:pDNA lipoplexes entered via the clathrin pathway (Rejman, J. *et al.*, 2005, Rejman, J. *et al.*, 2006), while others showed that distinct lipidic formulations follow different endocytic pathways; for example pDNA complexed to the lipid Lipofectamine-LTX entered via the clathrin-mediated endocytosis, while pDNA/DMRIE-C complexes followed the caveolar pathway in the same cell line (Wong, A.W. *et al.*, 2007). However, to date only a few studies have investigated the mechanisms involved in the uptake of siRNA/lipid complexes (Schroeder, A. *et al.*, 2010). Therefore, the aim of this work was to provide a novel insight into the pathways that are involved in the internalization of siRNA lipoplexes and to discern which pathways led to efficient gene silencing, also known as “functional siRNA uptake”.

### 4.5.1. Peri-nuclear localization of siRNA complexes

The first indication of the probable uptake mechanism for siRNA complexes was obtained by confocal microscopy studies; LPR and LpegR complexes were shown to enter the cytoplasm within 2 hours of transfection. This is consistent the gene silencing data in Chapter 3 and indicated that at the effective charge ratios, siRNA uptake was observed. When confocal microscopy was performed using

fluorescently labelled Cy3-GAPDH siRNA in LPR or LpegR complexes, a spot-like distribution of siRNA was observed in the cytoplasm at the periphery of the nucleus. This stippled pattern provides evidence of the entrapment of siRNA in perinuclear vesicles (Lu, J.J. *et al.*, 2009). Furthermore, as early as 2 hours post-transfection some of the siRNA had already dissociated from the cationic lipid and localized in the cytoplasm at the perinuclear region. This localization may represent sites of siRNA processing or sites where the RISC complex resides (Berezghna, S.Y. *et al.*, 2006). Studies have shown that perinuclear localization is associated with high levels of gene silencing suggesting that siRNA is directed to these regions to interact with RISC to induce RNAi (Lavigne, C. and A.R. Thierry, 2007, Veldhoen, S. *et al.*, 2006, Billy, E. *et al.*, 2001, Chiu, Y.L. *et al.*, 2004).

#### **4.5.2. siRNA complexes uptake is temperature-sensitive**

To characterize the uptake mechanism of functional LPR and LpegR complexes further, uptake and transfection experiments were carried out at low temperatures. Confocal analysis showed that at a low temperature (4°C) LPR and LpegR complexes no longer localized to the perinuclear regions but remained on the cellular membrane indicating uptake inhibition. GAPDH silencing greatly decreased when transfection was performed at 4-10°C as compared to 37°C. These findings suggest the involvement of an endocytic uptake pathway as low temperature has been shown to reduce the flexibility and fluidity of cellular membranes and block all of the endocytosis pathways (Haylett T, T.L., 1991, Wiliam A. Dunn, A.L.H., And Nathan N. Aronson, 1980). Studies using a number of different delivery methods have consistently found that siRNA was internalised by some form of endocytosis

(Veldhoen, S. *et al.*, 2008, Lavigne, C. and A.R. Thierry, 2007, Detzer, A. *et al.*, 2008), however, it has not been shown which particular endocytosis pathway leads to successful siRNA delivery i.e. efficient gene silencing.

#### **4.5.3. The uptake of LPR and LpegR complexes is clathrin-dependent**

In order to determine by which routes LPR and LpegR complexes enter the cells, colocalization of internalized complexes with fluorescent uptake pathways markers transferrin and BODIPY-lacCer was investigated. Both LPR and LpegR complexes co-localized with transferrin which is known to be taken up mainly by clathrin-mediated endocytosis. This indicated that both types of complex utilized the clathrin-mediated pathway. This is in agreement with a study by Lu and co-workers, who showed that 95% of siRNA lipoplexes enter the cells via the clathrin pathway (Lu, J.J. *et al.*, 2009). In addition, Rejman and co-workers (2004) showed that the uptake pathway of fluorescent nanoparticles was size dependent and reported that nanoparticles of less than 200 nm diameter entered mainly via the clathrin route; this corresponded with the LPR and LpegR complexes in this study which had particle sizes of less than 200 nm. In contrast, no colocalization was observed between either types of complex with the caveolae pathway marker BODIPY-lacCer, therefore excluding caveolae-mediated endocytosis as an entry route for these siRNA complexes in this cell line.



#### **4.5.4. Functional siRNA uptake is non-clathrin, non-caveolae mediated and does not depend on macropinocytosis**

The uptake and intracellular processing are important factors in transfection efficiency. However, it has been shown recently that effective cellular uptake does not necessarily equate to effective transfection (Ming, X. *et al.*, 2011, Lu, J.J. *et al.*, 2009). This study investigated the uptake pathways that led to the most effective gene silencing, termed here as ‘functional siRNA uptake’. This was done by examining the effect of blocking the major endocytic pathways on the gene silencing efficiency of siRNA complexes using endocytosis inhibitors. Cells were treated with various inhibitors to differentiate clathrin-dependent from clathrin-independent endocytosis. Before these studies were possible, it was necessary to optimize the concentrations of each inhibitor and select the most effective in blocking the uptake pathway with minimal toxicity to the cells.

Despite the supposition that clathrin-mediated endocytosis has been shown to be the major entry pathway for DNA lipoplexes (Rejman, J. *et al.*, 2005, Zhou, X.H. and L. Huang, 1994, Friend, D.S. *et al.*, 1996, Zuhorn, I.S. *et al.*, 2002a), the findings of this study suggested that the uptake of siRNA complexes via this pathway failed to produce functional GAPDH silencing as the gene silencing efficiency was unaffected by the inhibition of the entry pathway by either chlorpromazine or depletion of cellular potassium. Any partial reduction in gene silencing was associated with toxicity due to the combined effect of inhibitors and lipoplexes.

The caveolae pathway is another option for functional siRNA uptake as it has been shown to play a critical role in the uptake of DNA polyplexes (Rejman, J. *et al.*, 2005, Van Der Aa, M.a.E.M. *et al.*, 2007). In addition, Detzer and co-workers (2008)

suggested that phosphothioate-stimulated siRNA uptake may occur through the caveolar pathway. In the present study, functional siRNA delivery was not via the caveolar endocytosis since gene silencing mediated by LPR and LpegR complexes was not impaired in the presence of nystatin. This result is in agreement with the co-localization studies, in which no colocalization was detected between internalised siRNA complexes and the caveolae pathway marker BODIPY-LacCer in A549 cells.

Macropinocytosis is another well-defined non-clathrin uptake pathway and recently has been considered as an entry route for gene delivery vectors in particular peptides such as octaarginine peptide (Khalil, I.A. *et al.*, 2006) and TAT peptide (Kakudo, T. *et al.*, 2004, Kaplan, I.M. *et al.*, 2005, Nakase, I. *et al.*, 2004, Wadia, J.S. *et al.*, 2004). This pathway provides some advantageous aspects such as a higher capacity for the uptake of macromolecules, the avoidance of lysosomal degradation and the ease of escape from macropinosomes because of their relatively leaky nature (Khalil, I.A. *et al.*, 2006). However, in this study, the inhibition of macropinocytosis by amiloride had no effect on the gene silencing efficiency mediated by LPR or LpegR complexes. These results were further confirmed when no effect was seen in the presence of cytochalasin D, which blocks both caveolae and macropinocytosis without affecting clathrin-mediated pathways. Some reduction in gene silencing mediated by LpegR complexes was observed in the presence of cytochalasin D, but this was attributed to toxicity. Thus, neither caveolae nor macropinocytosis could be considered as a main uptake pathway of the functional siRNA/lipid complexes.

As no single endocytotic pathway could be identified as the principal route of functional siRNA delivery by the use of individual inhibitors, the possibility of interaction between the pathways with regard to uptake was investigated. A study by

Luhmann and co-workers (2008) suggested that Poly-L-Lysine-g-PEG-DNA complexes entered cells by several endocytic pathways and that transfection efficiencies were increasingly abolished when two or three pathways are inhibited as compared to inhibition of one pathway. Other investigators have similarly concluded that not one single pathway was responsible for uptake, e.g. several pathways were reported to be involved in the uptake of siRNA mediated by a novel peptide MPG $\alpha$  peptide (Veldhoen, S. *et al.*, 2006). Lu and co-workers (2009) estimated that an siRNA complexed to the commercial lipid Dharmafect was internalized by both clathrin (50%) and caveolar (20%) pathway but that none of the pathways led to functional gene silencing. In the present study, when two inhibitor combinations were used to inhibit two different pathways at the same time, gene silencing mediated by LpegR complexes was not diminished. A strong inhibition of gene silencing was observed when all three pathways (clathrin, caveolae and macropinocytosis) were blocked but this was associated with excessive cellular toxicity (70% cell death) which invalidated the finding; i.e. was not possible to distinguish whether the gene silencing inhibition was due to blockage of the uptake pathways, or as appears more likely, due to significant reduction in cell viability. These findings illustrate that the effect of inhibitors on cell viability is a major limitation to their use in studying uptake mechanisms. Despite using optimized concentrations, there is still a narrow concentration range between effectiveness and toxicity, especially during longer incubation times. Furthermore, the toxicity of inhibitors increased in the presence of siRNA complexes compared to when cells were exposed to inhibitors alone. It is important, therefore, to look at the effect on cell viability as well as the inhibition of uptake to avoid forming misleading conclusions

#### **4.5.5. Conclusion**

The uptake mechanism that led to effective gene silencing was found to be temperature sensitive, indicating that it is probably energy-dependent. In addition, it was shown that entry via the clathrin-mediated pathway occurred, but was not necessary for function, as blockade of this pathway had no effect on gene silencing efficiency. It appeared that the siRNA complexes that led to efficient gene silencing must enter the cells via a pathway that is not clathrin, caveolae nor macropinocytosis-dependent as the inhibition of all the investigated pathways had no effect on gene silencing. This other uptake pathway may be either another unconventional endocytotic pathway or passive diffusion. Recent work by Ming and co-workers (2011) showed that antisense oligonucleotides (ODN) lipoplexes entered the cells via both endocytic and non-endocytic pathways, but it was the latter that accounted for gene silencing activity. Lu and co-workers (2009) showed that despite most siRNA lipoplexes (95%) entering cells via endocytosis it was the 5% that entered through a different pathway that resulted in the majority of functional siRNA. They suggested that the minor uptake pathway was passive diffusion through the cellular membrane as gene silencing was significantly blocked at low temperature and by cholesterol depletion using nystatin. Passive diffusion provides the advantage of avoiding endosomal compartment and therefore siRNA can directly enter the cytoplasm and result in effective gene silencing. The findings of the current study are consistent with these reports, although the gene silencing efficiency was not affected by cholesterol depletion. However, the punctuate distribution and temperature sensitivity do not exclude the involvement of an endocytic pathway which has yet to be characterised. It should be remembered that interpretation of

these findings is problematic because experiments have focused on the three well-characterized types of endocytotic pathways and yet many aspects of these and other pathways remain unclear. Nonetheless this study has provided insights into the uptake pathway of functional siRNA mediated by two cationic lipid systems and supplemented the limited evidence for the mechanism of action of such formulations.

## **Chapter 5. General discussion**

## 5.1. Introduction

The delivery of nucleic acids represents a powerful therapeutic tool for the treatment of a broad range of diseases including those of pulmonary origin (Gill, D.R. *et al.*, 2004). Therefore extensive efforts have been made in order to develop an optimal delivery vector that allows the transfer of these nucleic acids to their target cells.. Non-viral delivery of pDNA has progressed over the years with the continuous discoveries of new delivery agents. So far for pulmonary diseases, there has been a total of eight clinical trials concerning aerosol delivery of gene carriers to the lungs, and all these pertain to cystic fibrosis (Griesenbach, U. and E.W. Alton, 2009) and only very few gene transfer vectors have been aerosolised to the lungs of patients. One of these trials uses the non-viral cationic lipid system Genzyme lipid 67A (GL67A) complexed to pDNA (Alton, E.W.F.W. *et al.*, 1999) and has been shown that cationic-lipid-mediated CFTR gene transfer can significantly influence the underlying chloride defect in the lungs of patients with cystic fibrosis. A more recent one consist of cystic fibrosis gene pGT-1 complexed to DMRI:DOPE lipid but results are still pending (The U.S. National Institutes Health). Although, cationic lipids represent a major class of non-viral delivery vectors and to date more than 100 cationic lipids have been designed, most are under *in vitro* conditions, with a relatively few tested *in vivo* (Marty, R. *et al.*, 2009a) The process of nucleic acid delivery remains unclear and there is ongoing work to develop an optimal system for *in vitro* and *in vivo* use.

As discussed in chapter 1, since the discovery of RNA interference, the popularity of siRNA as a therapeutic agent has increased tremendously and the attention from gene therapy has deviated to gene silencing. siRNA has been

delivered using different cationic lipid carriers, some of which have begun to be evaluated in the clinic (Schroeder, A. *et al.*, 2010). Despite considerable advances in this field, there is still a need to develop safe and effective delivery systems for siRNA. Previously, most of the cationic lipids shown to be effective for pDNA delivery have been used for siRNA delivery. However a study in 2004 showed that optimal lipid-based transfection agents for siRNA differ from those of pDNA (Spagnou, S. *et al.*, 2004). Gary et al (2007) reviewed the differences between polymer-based siRNA and pDNA delivery and highlighted the fact that siRNA delivery approaches can benefit from the wealth of information on pDNA delivery. The limited information regarding transferability of vector design between pDNA and siRNA therefore warrants a study of their physical properties and function in order to help identify the key requirements for siRNA delivery.

Before looking at the differences between siRNA and pDNA formulation, it is essential to understand what the characteristics of an optimal delivery system in general are. Many researchers have investigated the optimal physical properties that lead to efficient lipid-mediated delivery of pDNA as reviewed by Barteaux et al (2008) and a few have looked at siRNA (Spagnou, S. *et al.*, 2004, Desigaux, L. *et al.*, 2007, Zhang, Y. *et al.*, 2010). A review of the available literature so far indicates a lot of contradiction and differences in the optimal characteristics for high transfection efficiency. These variations have been associated with the use of different delivery systems, different cell lines and different characterization media. This study's approach to tackle this issue was to compare three types of cationic lipid-based formulations of pDNA and siRNA, under the same experimental conditions, in order to enable correlation of physicochemical properties and delivery



efficiency, and to determine whether the same rule applies to all types of complexes. A number of unresolved questions arose from the findings of this study and are discussed below.

In addition, investigating the uptake mechanism and the intracellular fate of pDNA and siRNA/lipid complexes allows us to gain further information on how to design a delivery system that will provide optimal results. Much work has been done in the field of uptake mechanisms of pDNA complexes, with debatable results, but generally it is agreed that pDNA/lipid complexes enter the cells via endocytosis (Rejman, J. *et al.*, 2005, Elouahabi, A. and J.M. Ruyschaert, 2005, Luhmann, T. *et al.*, 2008). However, at the time of this study there was only one report by Lu *et al.* (2009) that attempted to characterise the uptake pathway of siRNA/lipid complexes. Research in the field of uptake pathways of siRNA in general, and siRNA/lipid complexes in particular, is still in its infancy. Thus, this thesis investigated the involvement of major endocytic pathways in the uptake of siRNA/lipid complexes.

## **5.2. Correlation between the physicochemical properties and transfection efficiency of pDNA complexes**

The aim of this chapter was to set ground for working with siRNA, as in order to compare between the two nucleic acids it is important to use the same systems, cell line and experimental conditions. Despite some slight modifications to the protocols, the cationic lipid-based systems used in this study have already been employed to deliver pDNA but were not compared directly under one study. Nor have they been prepared and characterised in the same media and at the same +/- charge ratios in previous studies (Yang, J.P. and L. Huang, 1998, Birchall, J.C. *et al.*,

1999, Kim, J.K. *et al.*, 2003, Coulman, S.a.B., David; Anstey, Alexander; Gateley, Chris; Morrissey, Anthony; Wilke, Nicolle; Allender, Chris; Brain, Keith; Birchall, James C, 2006). By taking into consideration all three systems, results showed no obvious correlation between physical properties and gene expression efficiency i.e. transfection efficiency. However if looking at the systems individually, high transfection was related to negative or low zeta potential, low condensation efficiency and a large particle size (micron range) for LD and LpegD complexes. However, when looking at the LPD complexes, high transfection correlated with a high positive charge, high condensation efficiency, and despite showing significant differences in particle size, there was no significant difference in gene expression levels. These differences led to the suggestion that the LPD complexes might have either a different uptake mechanism or a different endosomal escape mechanism and pDNA release mechanism due to the presence of protamine. On the other hand, protamine has not been shown to be involved in transfection as pDNA complexed to protamine is inactive in inducing transfection and this was associated with the inability to enter cells or inability to escape endosomes (Collins, E. *et al.*, 2007). On the other hand, one has to consider the possibility that due to the heterogeneity of the pDNA/lipid complexes in physiological media, the physical characterisation methods used were not detecting a minor population of complexes that is functional and resulted in efficient gene expression. Before incubation in the transfection media, complexes were first made in water and characterised. Results showed that in water the condensation ability, size and charge correlated with the general three-zone colloidal stability pattern discussed in chapter 2. After incubation in physiological media, complexes formed large aggregates and lost the particle size trends observed in water. In addition, the physical characteristics of LPD complexes in water

matched those of gene expression levels, so it can be assumed that the population of complexes that did not form aggregates are responsible for effective transfection.

It is also important to highlight the significance of characterising the complexes in the media used for transfection as characterisation in water or low salt concentration solution might give misleading results. Many studies have characterised pDNA or siRNA complexes in water and performed transfection experiments in cell culture media which has a high ionic strength not taking into account any changes in complex characteristics upon change of media (Eastman, S.J. *et al.*, 1997, Nchinda, G. *et al.*, 2002, Wiethoff, C.M. *et al.*, 2004, Spagnou, S. *et al.*, 2004, Zhang, Y. *et al.*, 2010). For example Birchall *et al.* (2000) who designed the LPD system argued that this system would provide compact, small, homogenous complexes but did not show the effect of high ionic strength of media on the physical characteristics. The use of high ionic strength media reflects the *in vivo* situation, which may lead to a poor control on the stability of the complexes once exposed to physiological conditions.

### **5.3. Difference between siRNA and pDNA complexes**

#### **5.3.1. Physical properties**

In these studies, siRNA was complexed to the same systems as pDNA and showed significantly different physical properties, particularly with the condensation data. siRNA complexes showed much lower condensation than pDNA complexes, especially the LPR system, which contains both a polycation and a cationic lipid. This was explained by the fact that pDNA is much larger than siRNA and possesses

a molecular topography that allows it to condense into nanoparticles, whereas siRNA molecules are only 21-23 nucleotides in length and have a rigid structure and do not condensate even upon interaction with a cationic carrier (Gary, D.J. *et al.*, 2007).

Recent work has shown that by increasing the +/- charge ratio, cationic lipids were able to compact siRNA at ratios higher than those used to condense pDNA, but these studies used different lipidic systems and different methods of characterizing complexation. For example, gel electrophoresis (Zhang, Y. *et al.*, 2010), which reflects binding more than condensation, and the ethidium exclusion assay (Desigaux, L. *et al.*, 2007) can tell you different things. In addition the study by Desigaux and colleagues did not show the standard deviation and did not mention the number of experiments performed so it does not indicate the reproducibility of the system. The findings of the current study contradicted these finding as even with increasing the charge ratio to 20 (data not shown), siRNA was still accessible to the intercalation dye. That raised a suspicion about the suitability of using SYBR-green II intercalation assay to determine complexation efficiency, but when siRNA was complexed to either protamine without lipids, and the commercial transfection reagent Lipofectamine, high condensation was observed. Thus it validates the suitability of the data. Nonetheless, careful interpretation of the intercalation assay is required because exclusion of the intercalating dye not only suggests condensation but can also indicate charge neutralisation. Therefore even if siRNA was not accessible to the dye when complexed to protamine or Lipofectamine, it does not necessarily indicate condensation. With the three lipidic systems studied it is likely that siRNA is loosely bound to the cationic lipids, which makes it easier for the intercalating dye to compete with the lipid and gain access to the nucleic acid. In

addition, the presence of the neutral lipid DOPE might have caused weaker binding between siRNA and the cationic lipid. This weak binding could be beneficial in terms of ease of release of siRNA once the complexes enter the cells, but is also a disadvantage *in vivo* as the complexes might de-asSEMBle easily upon interaction with negatively charged plasma proteins before reaching their target cells.

In terms of particle size, although siRNA complexes were prepared in cell culture media (high ionic strength) the complexes were much smaller than pDNA complexes (nanorange) and followed the three-zone model, when negative or positive charge are in excess the complexes have a small particle size (150-200 nm) and at neutral charge (positive charges almost equal negative charges) large aggregates were observed (500-700 nm). This comes in agreement with recent studies (Desigaux, L. *et al.*, 2007, Zhang, Y. *et al.*, 2010). The only exception to the particle size change was the LPR system that had the same small size regardless of the amount of lipid used (+/-charge ratio), and this can normally be associated with pre-complexation of the nucleic acid with protamine.

### **5.3.2. Transfection efficiency**

The finding of these studies showed that the optimal charge ratios for pDNA transfection in Calu-3 cells were inefficient for siRNA transfection. siRNA complexes for all three systems were only active in inducing protein knockdown at higher charge ratios. The characteristics of the effective siRNA complexes were a small size with low polydispersity, a positive charge and a low complexation efficiency. However, effective gene silencing cannot directly be associated with these physical properties because in the case of the LPR systems, complexes showed

no difference in particle size and complexation at the different charge ratios but displayed differences in gene silencing efficiency. The main conclusion from these studies was that what was effective for pDNA was ineffective for siRNA complexes, regardless of the lipidic system used.

At the effective ratios for each system, about 50% GAPDH protein knockdown in Calu-3 cells was observed. The protein knockdown was also determined in a different cell line, the alveolar A549 cells previously used in the transfection efficiency studies to verify the reproducibility of the results in different cells. Surprisingly, the percentage protein knockdown was higher and reached up to 80-90% at some charge ratios. This showed that A549 cells were more transfectable than Calu-3 cells. One explanation for this is the difference in the negative charge of the endosomal membrane and again this highlights the fact that efficient gene silencing is also dependent on the target cells. Cell lines represent an important tool for screening new therapeutics, which has the advantage of shorter experimental times, and being less labour extensive than primary cultures or animal use. However there is a concern about how well results can be based on cell lines that do not accurately reflect the *in vivo* situation. In order to mimic the *in vivo* situ, this study looked at the effect of serum on the gene silencing efficiency of the complexes. LPR and LpegR complexes at a charge ratio of 10 were judged to be most effective due to the reproducibility of protein knockdown. The presence of protamine and PEG chains has been reported to enhance stability, which may have aided in complex stability in serum (Hong, K. *et al.*, 1997). Data showed that despite some inhibition of protein knockdown at high serum concentration, complexes were still active and

resulted in up to 50% protein knockdown, in particular the LPR complexes. Therefore, these systems might have the potential for *in vivo* use.

Overall all these data led to the conclusion that despite being complexed to identical cationic systems, the resulting siRNA and pDNA complexes were significantly different in terms of complexation efficiency, particle size and biological activity. Therefore what worked for pDNA did not work for siRNA. In addition, factors that affected pDNA transfection efficiency were different from those that affected siRNA delivery. This suggested that although siRNA delivery can benefit from ideas and knowledge developed in the pDNA delivery field, it is better to look to siRNA as a different molecule and aim to further investigate the factors that influence gene-silencing efficiency.

#### **5.4. The involvement of endocytic pathways in the uptake of siRNA complexes**

At the time of this work, there was only one study that investigated the involvement of different endocytic pathways in the uptake of siRNA/lipid complexes. Lu and colleagues used the commercial cationic lipid based siRNA transfection agent called DharmaFECT1, and proposed that even if siRNA complexes were mainly internalised via an endocytic pathway (clathrin and non-clathrin dependent), a small portion of complexes that were biologically active entered via a minor pathway which was affected by changes in temperature and cholesterol depletion. They suggested that this pathway is passive diffusion. The findings of the present study showed that LPR and LpegR complexes were internalised via clathrin-mediated endocytosis, but the inhibition of this mechanism

had no effect on gene silencing efficiency, which correlated with the data reported by Lu and colleagues. Molecules that enter through the endocytic pathway end up in early endosomes maturing into lysosomes where degradation takes place. Therefore there it is possible that most of the complexes are degraded in the endosomes unless they escape, making this uptake process unfavourable for siRNA complexes. However, the protein knockdown activity of both LPR and LpegR was completely inhibited by reduction in temperature suggesting an energy-dependent process (Haylett T, T.L., 1991, William A. Dunn, A.L.H., And Nathan N. Aronson, 1980). Furthermore, in confocal microscopy studies, fluorescent siRNA complexes displayed a punctuate distribution in the peri-nuclear region, suggesting a vesicular entrapment of the complexes. All these findings led to the conclusion that functional siRNA entered cells through a temperature-dependent pathway which was clathrin and caveolae-independent and did not involve macropinocytosis. This pathway could be a yet unknown receptor-mediated endocytosis and complexes that entered through this route avoided the endosomal pathway and therefore remained biologically active. There is a small chance that passive diffusion could be involved as hypothesised by Lu and colleagues, but they justified their theory by the inhibitory effect of both temperature and cholesterol, which affect cellular membrane integrity. However the current data only showed temperature dependence and cholesterol depletion had no effect on protein knockdown efficiency. In addition, the dotted-like distribution of fluorescent complexes suggested a vesicular entrapment. Determining the nature of vesicles in which siRNA was internalised could provide further information on the uptake pathway. The difference in the uptake mechanism between pDNA and siRNA complexes could explain their differences in transfection efficiency.



## 5.5. Future challenges

The above discussion drew attention to a few areas that need further consideration in order to develop an optimal siRNA formulation for *in vivo* use. These include (a) investigating the effect of serum on the physical properties and stability of the LPR and LpegR and the effect of increasing pegylated lipid concentration on serum inhibition, (b) quantitative analysis of the uptake of siRNA complexes would provide a more clear picture on the involvement of each endocytic pathway, (c) differentiating between endosomes from other vesicles by fluorescent staining in order to gain more information on the nature of the vesicles involved in siRNA complexes uptake, (d) optimising the formulation of siRNA into a dry powder for *in vitro* delivery to monolayers of differentiated lung cell lines with extension to *in vivo* delivery to animals.

## **Appendix. Standard Curves**

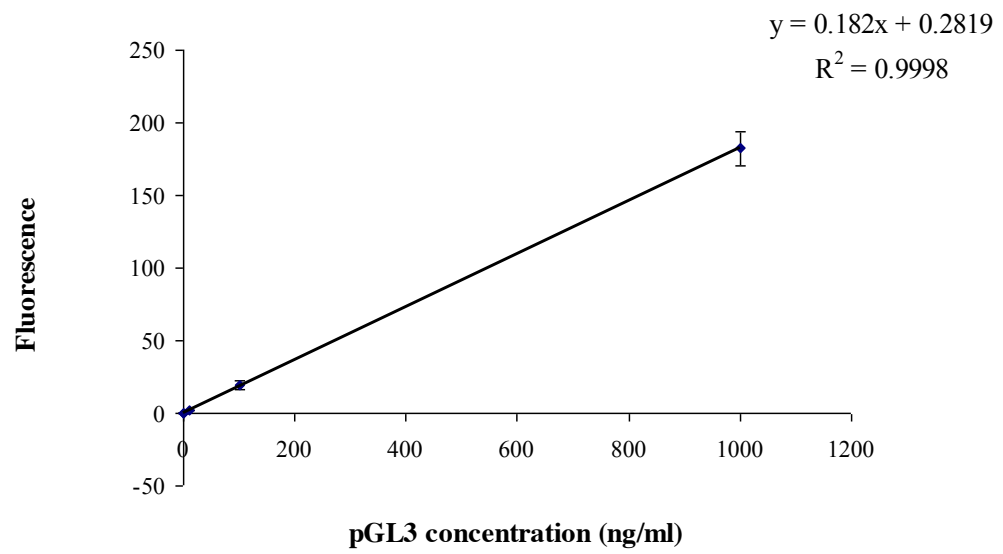


**Figure A.1** Picogreen assay standard curve using pGL3 control vector (n=3, mean  $\pm$  STD).

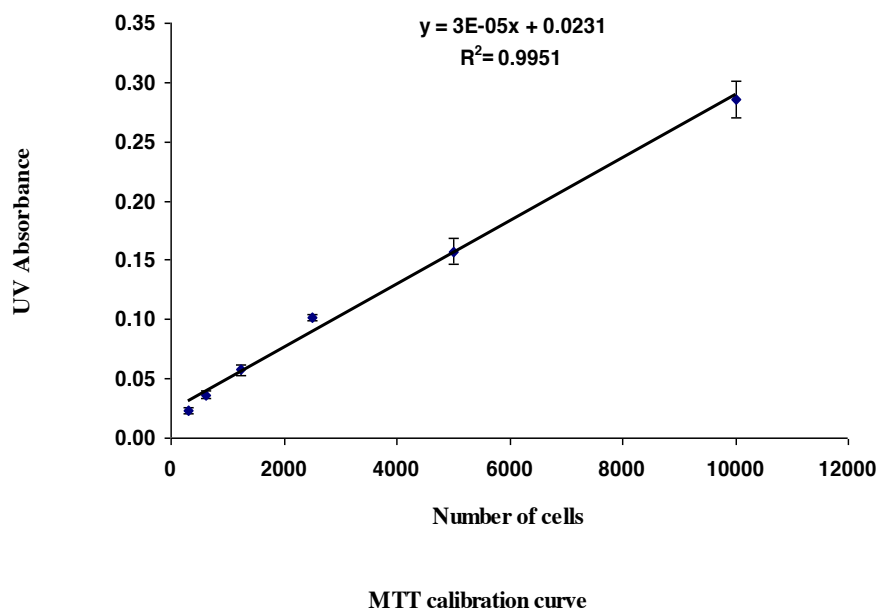


**Figure A.2** MTT calibration curve to determine the optimal Calu-3 cells' seeding density for MTT test. The experiment was carried out three times with n=12 each time (n=3, mean  $\pm$  STD).

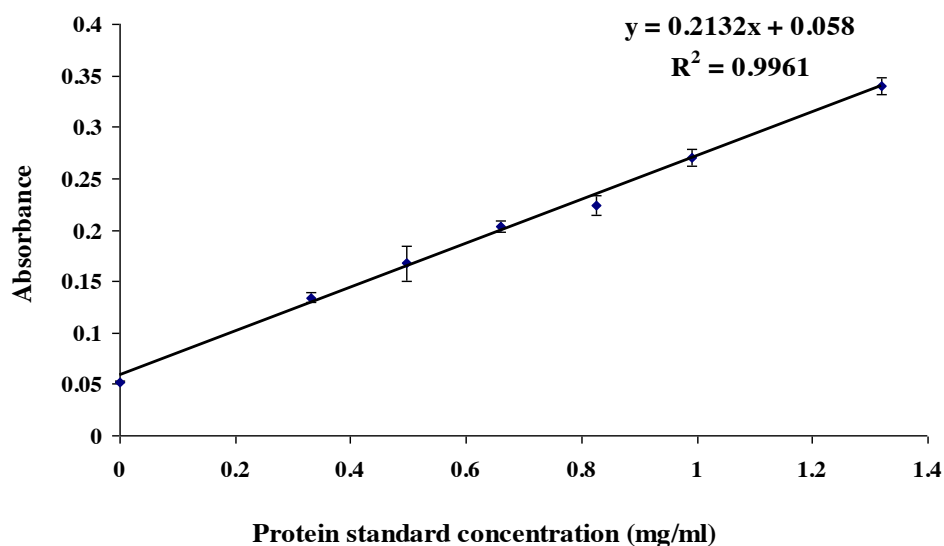


**Figure A.3** Bio-Rad protein assay standard curve using, the standard protein (bovine gamma-globulin). (n=3, mean  $\pm$  STD).

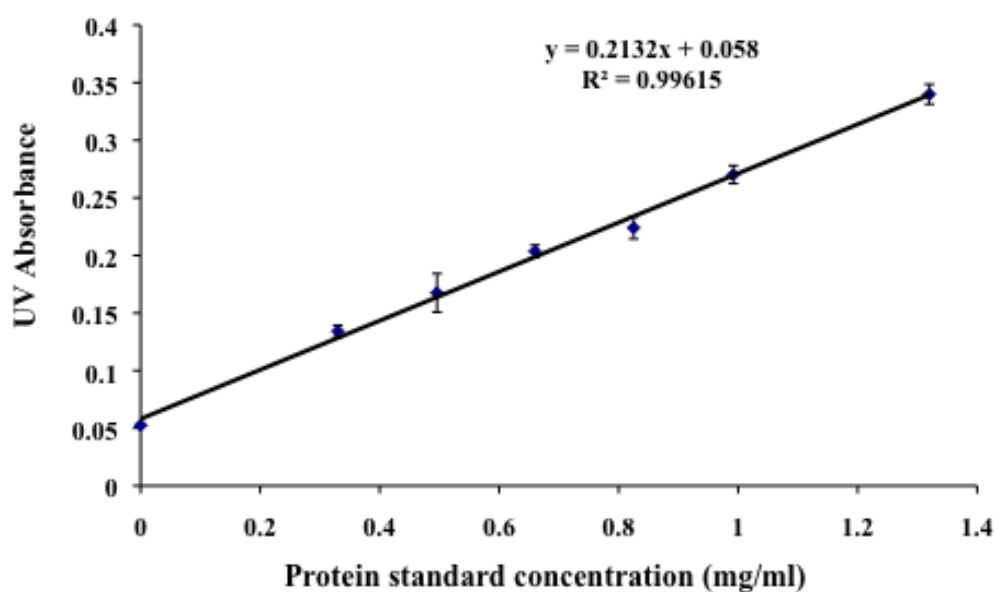


**Figure A.4** GAPDH enzyme standard curve (n=3, mean  $\pm$  STD).

## References

Aigner, A. 2007. Applications of RNA interference: current state and prospects for siRNA-based strategies in vivo. *Appl Microbiol Biotechnol*, 76, 9-21.

Akhtar, S. & Benter, I. F. 2007. Nonviral delivery of synthetic siRNAs in vivo. *Journal of Clinical Investigation*, 117, 3623-3632.

Aljaberi, A., Chen, P. S. & Savva, M. 2005. Synthesis, in vitro transfection activity and physicochemical characterization of novel N,N'-diacyl-1,2-diaminopropyl-3-carbamoyl-(dimethylaminoethane) amphiphilic derivatives. *Chemistry and Physics of Lipids*, 133, 135-149.

Alton, E. W. F. W., Stern, M., Farley, R., Jaffe, A., Chadwick, S. L., Phillips, J., Davies, J., Smith, S. N., Browning, J., Davies, M. G., Hodson, M. E., Durham, S. R., Li, D., Jeffery, P. K., Scallan, M., Balfour, R., Eastman, S. J., Cheng, S. H., Smith, A. E., Meeker, D. & Geddes, D. M. 1999. Cationic lipid-mediated CFTR gene transfer to the lungs and nose of patients with cystic fibrosis: a double-blind placebo-controlled trial. *Lancet*, 353, 947-954.

Amyere, M., Mettlen, M., Van Der Smissen, P., Platek, A., Payraastre, B., Veithen, A. & Courtoy, P. J. 2002. Origin, originality, functions, subversions and molecular signalling of macropinocytosis. *Int J Med Microbiol*, 291, 487-94.

Angaji, S. A., Hedayati, S. S., Poor, R. H., Madani, S., Poor, S. S. & Panahi, S. 2010. Application of RNA interference in treating human diseases. *J Genet*, 89, 527-37.

Barteau, B., Chevre, R., Letrou-Bonneval, E., Labas, R., Lambert, O. & Pitard, B. 2008. Physicochemical Parameters of Non-Viral Vectors that Govern Transfection Efficiency. *Current Gene Therapy*, 8, 313-323.

Behlke, M. A. 2006. Progress towards in vivo use of siRNAs. *Molecular Therapy*, 13, 644-70.

Benmerah, A. & Lamaze, C. 2007. Clathrin-coated pits: vive la difference? *Traffic*, 8, 970-82.

Bennett, M. J., Aberle, A. M., Balasubramaniam, R. P., Malone, J. G., Malone, R. W. & Nantz, M. H. 1997. Cationic lipid-mediated gene delivery to murine lung: Correlation of lipid hydration with in vivo transfection activity. *Journal of Medicinal Chemistry*, 40, 4069-4078.

Bennett, M. J., Nantz, M. H., Balasubramaniam, R. P., Gruenert, D. C. & Malone, R. W. 1995. Cholesterol Enhances Cationic Liposome-Mediated DNA Transfection of Human Respiratory Epithelial-Cells. *Biosci Rep*, 15, 47-53.

Berezhna, S. Y., Supekova, L., Supev, F., Schultz, P. G. & Deniz, A. A. 2006. siRNA in human cells selectively localizes to target RNA sites. *Proc Natl Acad Sci U S A*, 103, 7682-7687.

Bertrand, J. R., Pottier, M., Vekris, A., Opolon, P., Maksimenko, A. & Malvy, C. 2002. Comparison of antisense oligonucleotides and siRNAs in cell culture and in vivo. *Biochem Biophys Res Commun*, 296, 1000-1004.

Billy, E., Brondani, V., Zhang, H. D., Muller, U. & Filipowicz, W. 2001. Specific interference with gene expression induced by long, double-stranded RNA in mouse embryonal teratocarcinoma cell lines. *Proc Natl Acad Sci U S A*, 98, 14428-14433.



Birchall, J. C., Kellaway, I. W. & Mills, S. N. 1999. Physico-chemical characterisation and transfection efficiency of lipid-based gene delivery complexes. *Int J Pharm*, 183, 195-207.

Boffi, F., Bonincontro, A., Bordi, F., Bultrini, E., Cametti, C., Congiu-Castellano, A., De Luca, F. & Risuleo, G. 2002. Two-step mechanism in cationic lipoplex formation as observed by dynamic light scattering, dielectric relaxation and circular dichroism methods. *Physical Chemistry Chemical Physics*, 4, 2708-2713.

Bouxsein, N. F., Mcallister, C. S., Ewert, K. K., Samuel, C. E. & Safinya, C. R. 2007. Structure and gene silencing activities of monovalent and pentavalent cationic lipid vectors complexed with siRNA. *Biochemistry*, 46, 4785-92.

Brooks, H., Lebleu, B. & Vives, E. 2005. Tat peptide-mediated cellular delivery: back to basics. *Adv Drug Deliv Rev*, 57, 559-77.

Brown, M. D., Schatzlein, A. G. & Uchegbu, I. F. 2001. Gene delivery with synthetic (non viral) carriers. *Int J Pharm*, 229, 1-21.

Cejka, D., Losert, D. & Wacheck, V. 2006. Short interfering RNA (siRNA): tool or therapeutic? *Clin Sci (Lond)*, 110, 47-58.

Chan, J. H., Lim, S. & Wong, W. S. 2006. Antisense oligonucleotides: from design to therapeutic application. *Clin Exp Pharmacol Physiol*, 33, 533-40.

Chiu, Y. L., Ali, A., Chu, C. Y., Cao, H. & Rana, T. M. 2004. Visualizing a correlation between siRNA localization, cellular uptake, and RNAi in living cells. *Chemistry & Biology*, 11, 1165-1175.

Cho, K. C., Kim, Jeong & Park, T. G. 2005. Folate receptor-mediated gene delivery using folate-poly(ethylene glycol)-poly(L-lysine) conjugate. *Macromol Biosci*, 5, 512-9.

Ciani, L., Ristori, S., Salvati, A., Calamai, L. & Martini, G. 2004. DOTAP/DOPE and DC-Chol/DOPE lipoplexes for gene delivery: zeta potential measurements and electron spin resonance spectra. *Biochim Biophys Acta*, 1664, 70-9.

Collins, E., Birchall, J. C., Williams, J. L. & Gumbleton, M. 2007. Nuclear localisation and pDNA condensation in non-viral gene delivery. *Journal of Gene Medicine*, 9, 265-274.

Conner, S. D. & Schmid, S. L. 2003. Regulated portals of entry into the cell. *Nature*, 422, 37-44.

Coulman, S. a. B., David; Anstey, Alexander; Gateley, Chris; Morrissey, Anthony; Wilke, Nicolle; Allender, Chris; Brain, Keith; Birchall, James C 2006. Minimally Invasive Cutaneous Delivery of Macromolecules and Plasmid DNA Via Microneedles. *Current Drug Delivery*, 3, 65-75.

Davidson, B. L. & Paulson, H. L. 2004. Molecular medicine for the brain: silencing of disease genes with RNA interference. *Lancet Neurol*, 3, 145-9.

De Fougerolles, A., Vornlocher, H. P., Maraganore, J. & Lieberman, J. 2007. Interfering with disease: a progress report on siRNA-based therapeutics. *Nat Rev Drug Discov*, 6, 443-53.

Desigaux, L., Sainlos, M., Lambert, O., Chevre, R., Letrou-Bonneval, E., Vigneron, J. P., Lehn, P., Lehn, J. M. & Pitard, B. 2007. Self-assembled lamellar complexes of siRNA with lipidic aminoglycoside derivatives promote efficient siRNA delivery and interference. *Proc Natl Acad Sci U S A*, 104, 16534-9.

Detzer, A., Overhoff, M., Mescalchin, A., Rompf, M. & Sczakiel, G. 2008. Phosphorothioate-Stimulated Cellular Uptake of siRNA: A Cell Culture Model for Mechanistic Studies. *Current Pharmaceutical Design*, 14, 3666-3673.

Dorsett, Y. & Tuschl, T. 2004. siRNAs: applications in functional genomics and potential as therapeutics. *Nat Rev Drug Discov*, 3, 318-29.

Douglas, K. L., Piccirillo, C. A. & Tabrizian, M. 2008. Cell line-dependent internalization pathways and intracellular trafficking determine transfection efficiency of nanoparticle vectors. *European Journal of Pharmaceutics and Biopharmaceutics*, 68, 676-687.

Driskell, R. A. & Engelhardt, J. F. 2003. Current status of gene therapy for inherited lung diseases. *Annu Rev Physiol*, 65, 585-612.

Dyckxhoorn, D. M. & Lieberman, J. 2006. Knocking down disease with siRNAs. *Cell*, 126, 231-5.

Eastman, S. J., Siegel, C., Tousignant, J., Smith, A. E., Cheng, S. H. & Scheule, R. K. 1997. Biophysical characterization of cationic lipid: DNA complexes. *Biochim Biophys Acta*, 1325, 41-62.

Elbashir, S. M., Harborth, J., Lendeckel, W., Yalcin, A., Weber, K. & Tuschl, T. 2001. Duplexes of 21-nucleotide RNAs mediate RNA interference in cultured mammalian cells. *Nature*, 411, 494-8.

Elouahabi, A. & Ruyschaert, J. M. 2005. Formation and intracellular trafficking of lipoplexes and polyplexes. *Molecular Therapy*, 11, 336-47.

Escρίου, V., Carrière, M., Bussone, F., Wils, P. & Scherman, D. 2001. Critical assessment of the nuclear import of plasmid during cationic lipid-mediated gene transfer. *Journal of Gene Medicine*, 3, 179-187.

Esposito, C., Generosi, J., Mossa, G., Masotti, A. & Castellano, A. C. 2006. The analysis of serum effects on structure, size and toxicity of DDAB-DOPE and DC-Chol-DOPE lipoplexes contributes to explain their different transfection efficiency. *Colloids Surf B Biointerfaces*, 53, 187-92.

Farhood, H., Serbina, N. & Huang, L. 1995. The role of dioleoyl phosphatidylethanolamine in cationic liposome mediated gene transfer. *Biochim Biophys Acta*, 1235, 289-95.

Felgner, J. H., Kumar, R., Sridhar, C. N., Wheeler, C. J., Tsai, Y. J., Border, R., Ramsey, P., Martin, M. & Felgner, P. L. 1994. Enhanced Gene Delivery and Mechanism Studies with a Novel Series of Cationic Lipid Formulations. *Journal of Biological Chemistry*, 269, 2550-2561.

Felgner, P. L., Gadek, T. R., Holm, M., Roman, R., Chan, H. W., Wenz, M., Northrop, J. P., Ringold, G. M. & Danielsen, M. 1987. Lipofection - a Highly Efficient, Lipid-Mediated DNA-Transfection Procedure. *Proc Natl Acad Sci U S A*, 84, 7413-7417.

Ferrari, A., Pellegrini, V., Arcangeli, C., Fittipaldi, A., Giacca, M. & Beltram, F. 2003. Caveolae-mediated internalization of extracellular HIV-1 tat fusion proteins visualized in real time. *Molecular Therapy*, 8, 284-94.

Ferrari, M. E., Rusalov, D., Enas, J. & Wheeler, C. J. 2001. Trends in lipoplex physical properties dependent on cationic lipid structure, vehicle and complexation procedure do not correlate with biological activity. *Nucleic Acids Res*, 29, 1539-48.

Fishman, P. a. O. a. P. H. 1998. Filipin-dependent inhibition of cholera toxin: evidence for toxin internalization and activation through caveolae-like domains. *J Cell Biol.*, 141, 905-15.

Fittipaldi, A., Ferrari, A., Zoppe, M., Arcangeli, C., Pellegrini, V., Beltram, F. & Giacca, M. 2003. Cell membrane lipid rafts mediate caveolar endocytosis of HIV-1 Tat fusion proteins. *Journal of Biological Chemistry*, 278, 34141-34149.

Florea, B., Tj, M., I, B., In, M., J, K., Tj, V. B., He, J., Ea, B. & G., B. 2003. Identification of an internalising peptide in differentiated Calu-3 cells by phage display technology; application to gene delivery to the airways. *J Drug Target.* , 7, 383-90.

Florea, B. I., Meaney, C., Junginger, H. E. & Borchard, G. 2002. Transfection efficiency and toxicity of polyethylenimine in differentiated Calu-3 and nondifferentiated COS-1 cell cultures. *Aaps Pharmsci*, 4.

Forbes, B. & Ehrhardt, C. 2005. Human respiratory epithelial cell culture for drug delivery applications. *European Journal of Pharmaceutics and Biopharmaceutics*, 60, 193-205.

Foster, K. A., Avery, M. L., Yazdanian, M. & Audus, K. L. 2000. Characterization of the Calu-3 cell line as a tool to screen pulmonary drug delivery. *Int J Pharm*, 208, 1-11.

Friend, D. S., Papahadjopoulos, D. & Debs, R. J. 1996. Endocytosis and intracellular processing accompanying transfection mediated by cationic liposomes. *Biochim Biophys Acta*, 1278, 41-50.

Gao, H., W, S. & Lb, F. 2005. Mechanics of receptor-mediated endocytosis. *Proc Natl Acad Sci U S A*, 102, 9469-74.

Gao, X. & Huang, L. 1991. A Novel Cationic Liposome Reagent for Efficient Transfection of Mammalian-Cells. *Biochem Biophys Res Commun*, 179, 280-285.

Garbuzenko, O. B., Saad, M., Betigeri, S., Zhang, M., Vetcher, A. A., Soldatenkov, V. A., Reimer, D. C., Pozharov, V. P. & Minko, T. 2009. Intratracheal versus intravenous liposomal delivery of siRNA, antisense oligonucleotides and anticancer drug. *Pharm Res*, 26, 382-94.

Gary, D. J., Puri, N. & Won, Y. Y. 2007. Polymer-based siRNA delivery: perspectives on the fundamental and phenomenological distinctions from polymer-based DNA delivery. *Journal of Controlled Release*, 121, 64-73.

Gene Therapy Clinical Trials Worldwide. 2011. Available: <http://www.abedia.com/wiley/index.html> [Accessed Oct 2011].

Gershon, H., Ghirlando, R., Guttman, S. B. & Minsky, A. 1993. Mode of formation and structural features of DNA-cationic liposome complexes used for transfection. *Biochemistry*, 32, 7143-51.

Gill, D. R., Davies, L. A., Pringle, I. A. & Hyde, S. C. 2004. The development of gene therapy for diseases of the lung. *Cell Mol Life Sci*, 61, 355-68.

Godbey, W. T., Wu, K. K. & Mikos, A. G. 1999. Tracking the intracellular path of poly(ethylenimine)/DNA complexes for gene delivery. *Proc Natl Acad Sci U S A*, 96, 5177-5181.

Gopal, V., Prasad, T. K., Rao, N. M., Takafuji, M., Rahman, M. M. & Ihara, H. 2006. Synthesis and in vitro evaluation of glutamide-containing cationic lipids for gene delivery. *Bioconjugate Chemistry*, 17, 1530-1536.

Grayson, A. C., Doody, A. M. & Putnam, D. 2006. Biophysical and structural characterization of polyethylenimine-mediated siRNA delivery in vitro. *Pharm Res*, 23, 1868-76.

Griesenbach, U. & Alton, E. W. 2009. Cystic fibrosis gene therapy: successes, failures and hopes for the future. *Expert Rev Respir Med*, 3, 363-71.

Guo, W. & Rj, L. 2000. Efficient gene delivery using anionic liposome-complexed polyplexes (LPDII. *Biosci Rep*, 20, 419-32.

Gustafsson, A. & Sonesson, P. 1995. [Good surgical care at a county hospital. Evaluation of 5 years of emergency traumatology]. *Lakartidningen*, 92, 4092-4.

Hafez, I. M., Maurer, N. & Cullis, P. R. 2001. On the mechanism whereby cationic lipids promote intracellular delivery of polynucleic acids. *Gene Therapy*, 8, 1188-96.

Hammond Sm, B. S., Caudy Aa, Kobayashi R, Hannon Gj 2001. Argonaute2, a link between genetic and biochemical analyses of RNAi. *Science*, 293, 1146-50.

Han X, L. S., Qiangyi Fang, Dongxiao Li, Xianghui Gong, Yuyin Wu, Shengli Yang, Bing Q. Shen 2007. Transient expression of osteopontin in HEK 293 cells in serum-free culture. *Enzyme and Microbial Technology*, 41, 133-140.

Harris, J., Werling, D., Koss, M., Monaghan, P., Taylor, G. & Howard, C. J. 2002. Expression of caveolin by bovine lymphocytes and antigen-presenting cells. *Immunology*, 105, 190-5.

Harush-Frenkel, O., Rozentur, E., Benita, S. & Altschuler, Y. 2008. Surface charge of nanoparticles determines their endocytic and transcytotic pathway in polarized MDCK cells. *Biomacromolecules*, 9, 435-443.

Harvie, P., Wong, F. M. & Bally, M. B. 2000. Use of poly(ethylene glycol)-lipid conjugates to regulate the surface attributes and transfection activity of lipid-DNA particles. *J Pharm Sci*, 89, 652-63.

Haylett T, T. L. 1991. Endosome-lysosome fusion at low temperature. *J Biol Chem*, 266, 8322-7.

Hewlett, L. J., Prescott, A. R. & Watts, C. 1994. The coated pit and macropinocytic pathways serve distinct endosome populations. *Journal of Cell Biology*, 124, 689-703.

Hirsch-Lerner, D. & Barenholz, Y. 1999. Hydration of lipoplexes commonly used in gene delivery: follow-up by laurdan fluorescence changes and quantification by differential scanning calorimetry. *Biochimica Et Biophysica Acta-Biomembranes*, 1461, 47-57.



Hoekstra, D., Rejman, J., Wasungu, L., Shi, F. & Zuhorn, I. 2007. Gene delivery by cationic lipids: in and out of an endosome. *Biochemical Society Transactions*, 35, 68-71.

Hong, K., Zheng, W., Baker, A. & Papahadjopoulos, D. 1997. Stabilization of cationic liposome-plasmid DNA complexes by polyamines and poly(ethylene glycol)-phospholipid conjugates for efficient in vivo gene delivery. *FEBS Lett*, 400, 233-7.

Hong, K. L., Zheng, W. W., Baker, A. & Papahadjopoulos, D. 1997. Stabilization of cationic liposome-plasmid DNA complexes by polyamines and poly(ethylene glycol)-phospholipid conjugates for efficient in vivo gene delivery. *FEBS Lett*, 400, 233-237.

Ivanov, A. I. 2008. *Exocytosis and Endocytosis*, Totowa NJ 07512 USA, Humana Press.

Juliano, R., Alam, M. R., Dixit, V. & Kang, H. 2008. Mechanisms and strategies for effective delivery of antisense and siRNA oligonucleotides. *Nucleic Acids Res*, 36, 4158-71.

Kakudo, T., Chaki, S., Futaki, S., Nakase, I., Akaji, K., Kawakami, T., Maruyama, K., Kamiya, H. & Harashima, H. 2004. Transferrin-modified liposomes equipped with a pH-sensitive fusogenic peptide: an artificial viral-like delivery system. *Biochemistry*, 43, 5618-28.

Kamiya, H., Fujimura, Y., Matsuoka, I. & Harashima, H. 2002. Visualization of intracellular trafficking of exogenous DNA delivered by cationic liposomes. *Biochem Biophys Res Commun*, 298, 591-7.

Kaneda, Y. 2001. Gene therapy: a battle against biological barriers. *Curr Mol Med*, 1, 493-9.

Kaplan, I. M., Wadia, J. S. & Dowdy, S. F. 2005. Cationic TAT peptide transduction domain enters cells by macropinocytosis. *Journal of Controlled Release*, 102, 247-253.

Karagiannis, T. C. & El-Osta, A. 2005. RNA interference and potential therapeutic applications of short interfering RNAs. *Cancer Gene Therapy*, 12, 787-795.

Kawashima, T., Sasaki, A. & Sasaki, S. 2006. Transition of nanostructure in DNA-cationic surfactant complexes with the added salt. *Biomacromolecules*, 7, 1942-1950.

Kay, M. A. 2007. AAV vectors and tumorigenicity. *Nat Biotechnol*, 25, 1111-3.

Keller, M. 2005. Lipidic carriers of RNA/DNA oligonucleotides and polynucleotides: what a difference a formulation makes! *Journal of Controlled Release*, 103, 537-40.

Khalil, I. A., Kogure, K., Akita, H. & Harashima, H. 2006. Uptake pathways and subsequent intracellular trafficking in nonviral gene delivery. *Pharmacol Rev*, 58, 32-45.

Kim, J. K., Choi, S. H., Kim, C. O., Park, J. S., Ahn, W. S. & Kim, C. K. 2003. Enhancement of polyethylene glycol (PEG)-modified cationic liposome-mediated

gene deliveries: effects on serum stability and transfection efficiency. *J Pharm Pharmacol*, 55, 453-60.

Koltover, I., Salditt, T., Radler, J. O. & Safinya, C. R. 1998. An inverted hexagonal phase of cationic liposome-DNA complexes related to DNA release and delivery. *Science*, 281, 78-81.

Kovesdi, I., Brough, D. E., Bruder, J. T. & Wickham, T. J. 1997. Adenoviral vectors for gene transfer. *Curr Opin Biotechnol*, 8, 583-9.

Labatmoleur, F., Steffan, A. M., Brisson, C., Perron, H., Feugeas, O., Furstenberger, P., Oberling, F., Brambilla, E. & Behr, J. P. 1996. An electron microscopy study into the mechanism of gene transfer with lipopolyamines. *Gene Therapy*, 3, 1010-1017.

Lai, S. K., Hida, K., Chen, C. & Hanes, J. 2008. Characterization of the intracellular dynamics of a non-degradative pathway accessed by polymer nanoparticles. *Journal of Controlled Release*, 125, 107-111.

Lamaze, C. & Schmid, S. L. 1995. The emergence of clathrin-independent pinocytic pathways. *Curr Opin Cell Biol*, 7, 573-80.

Larkin, J. M., Brown, M. S., Goldstein, J. L. & Anderson, R. G. 1983. Depletion of intracellular potassium arrests coated pit formation and receptor-mediated endocytosis in fibroblasts. *Cell*, 33, 273-85.

Lasic, D. D. & Templeton, N. S. 1996. Liposomes in gene therapy. *Adv Drug Deliv Rev*, 20, 221-266.

Lavigne, C. & Thierry, A. R. 2007. Specific subcellular localization of siRNAs delivered by lipoplex in MCF-7 breast cancer cells. *Biochimie*, 89, 1245-51.

Lechardeur, D., Sohn, K. J., Haardt, M., Joshi, P. B., Monck, M., Graham, R. W., Beatty, B., Squire, J., O'brodovich, H. & Lukacs, G. L. 1999. Metabolic instability of plasmid DNA in the cytosol: a potential barrier to gene transfer. *Gene Therapy*, 6, 482-497.

Lee, E. R., Marshall, J., Siegel, C. S., Jiang, C. W., Yew, N. S., Nichols, M. R., Nietupski, J. B., Ziegler, R. J., Lane, M. B., Wang, K. X., Wan, N. C., Scheule, R. K., Harris, D. J., Smith, A. E. & Cheng, S. H. 1996. Detailed analysis of structures and formulations of cationic lipids for efficient gene transfer to the lung. *Human Gene Therapy*, 7, 1701-1717.

Lee, M. & Kim, S. W. 2005. Polyethylene glycol-conjugated copolymers for plasmid DNA delivery. *Pharm Res*, 22, 1-10.

Legendre J, S. F. 1992. Delivery of Plasmid DNA into Mammalian Cell Lines Using pH-Sensitive Liposomes: Comparison with Cationic Liposomes. *Pharmaceutical Research*, 9.

Li, L., Pabit, S. A., Meisburger, S. P. & Pollack, L. 2011. Double-stranded RNA resists condensation. *Phys Rev Lett*, 106, 108101.

Li, S., Rizzo, M. A., Bhattacharya, S. & Huang, L. 1998. Characterization of cationic lipid-protamine-DNA (LPD) complexes for intravenous gene delivery. *Gene Therapy*, 5, 930-937.

Lu, J. J., Langer, R. & Chen, J. Z. 2009. A Novel Mechanism Is Involved in Cationic Lipid-Mediated Functional siRNA Delivery. *Molecular Pharmaceutics*, 6, 763-771.

Luhmann, T., Rimann, M., Bitterman, A. G. & Hall, H. 2008. Cellular uptake and intracellular pathways of PLL-g-PEG-DNA nanoparticles. *Bioconjugate Chemistry*, 19, 1907-1916.

Lv, H. T., Zhang, S. B., Wang, B., Cui, S. H. & Yan, J. 2006. Toxicity of cationic lipids and cationic polymers in gene delivery. *Journal of Controlled Release*, 114, 100-109.

Mahato, R. I., Rolland, A. & Tomlinson, E. 1997. Cationic lipid-based gene delivery systems: Pharmaceutical perspectives. *Pharm Res*, 14, 853-859.

Mahon, K. P., Love, K. T., Whitehead, K. A., Qin, J., Akinc, A., Leshchiner, E., Leshchiner, I., Langer, R. & Anderson, D. G. 2010. Combinatorial approach to determine functional group effects on lipidoid-mediated siRNA delivery. *Bioconjug Chem*, 21, 1448-54.

Malone, R. W., Felgner, P. L. & Verma, I. M. 1989. Cationic Liposome-Mediated Rna Transfection. *Proc Natl Acad Sci U S A*, 86, 6077-6081.

Martin, M. E. & Rice, K. G. 2007. Peptide-guided gene delivery. *AAPS J*, 9, E18-29.

Marty, R., N'soukpoe-Kossi, C. N., Charbonneau, D., Weinert, C. M., Kreplak, L. & Tajmir-Riahi, H. A. 2009a. Structural analysis of DNA complexation with cationic lipids. *Nucleic Acids Res*, 37, 849-57.

Marty, R., N'soukpoe-Kossi, C. N., Charbonneau, D. M., Kreplak, L. & Tajmir-Riahi, H. A. 2009b. Structural characterization of cationic lipid-tRNA complexes. *Nucleic Acids Res*, 37, 5197-207.

Masotti, A., Mossa, G., Cametti, C., Ortaggi, G., Bianco, A., Grosso, N. D., Malizia, D. & Esposito, C. 2009. Comparison of different commercially available cationic liposome-DNA lipoplexes: Parameters influencing toxicity and transfection efficiency. *Colloids Surf B Biointerfaces*, 68, 136-44.

Mathias, N. R., Kim, K. J. & Lee, V. H. L. 1996. Targeted drug delivery to the respiratory tract: Solute permeability of air-interface cultured rabbit tracheal epithelial cell monolayers. *Journal of Drug Targeting*, 4, 79-86.

Matveev, S., Uittenbogaard, A., Van Der Westhuyzen, D. & Smart, E. J. 2001. Caveolin-1 negatively regulates SR-BI mediated selective uptake of high-density lipoprotein-derived cholesteryl ester. *Eur J Biochem*, 268, 5609-16.

Meier, O. & Greber, U. F. 2003. Adenovirus endocytosis. *Journal of Gene Medicine*, 5, 451-62.

Middaugh, C. R. & Ramsey, J. D. 2007. Analysis of cationic-lipid-plasmid-DNA complexes. *Anal Chem*, 79, 7240-8.

Ming, X., Sato, K. & Juliano, R. L. 2011. Unconventional internalization mechanisms underlying functional delivery of antisense oligonucleotides via cationic lipoplexes and polyplexes. *Journal of Controlled Release*, 153, 83-92.

Morille, M., Passirani, C., Vonarbourg, A., Clavreul, A. & Benoit, J. P. 2008. Progress in developing cationic vectors for non-viral systemic gene therapy against cancer. *Biomaterials*, 29, 3477-3496.

Nakase, I., Niwa, M., Takeuchi, T., Sonomura, K., Kawabata, N., Koike, Y., Takehashi, M., Tanaka, S., Ueda, K., Simpson, J. C., Jones, A. T., Sugiura, Y. & Futaki, S. 2004. Cellular uptake of arginine-rich peptides: Roles for macropinocytosis and actin rearrangement. *Molecular Therapy*, 10, 1011-1022.

Napoli, C., Lemieux, R. & Jorgensen, R. 1990. Introduction of a Chimeric Chalcone Synthase Gene into *Petunia* Results in Reversible Co-Suppression of Homologous Genes in trans. *Plant Cell*, 2, 279-289.

Nchinda, G., Uberla, K. & Zschornig, O. 2002. Characterization of cationic lipid DNA transfection complexes differing in susceptibility to serum inhibition. *BMC Biotechnol*, 2, 12.

Nichols, B. J. & Lippincott-Schwartz, J. 2001. Endocytosis without clathrin coats. *Trends in Cell Biology*, 11, 406-412.

Norkin, L. C. & Kuksin, D. 2005. The caveolae-mediated sv40 entry pathway bypasses the golgi complex en route to the endoplasmic reticulum. *Virology*, 2, 38.

Opalinska, J. B. & Gewirtz, A. M. 2002. Nucleic acid therapeutics: a work in progress. *Curr Opin Investig Drugs*, 3, 928-33.

Parton, R. G. 2004. Caveolae meet endosomes: a stable relationship? *Dev Cell*, 7, 458-60.

Patil, S. D., Rhodes, D. G. & Burgess, D. J. 2004. Anionic liposomal delivery system for DNA transfection. *AAPS J*, 6, e29.

Pelkmans, L., Kartenbeck, J. & Helenius, A. 2001. Caveolar endocytosis of simian virus 40 reveals a new two-step vesicular-transport pathway to the ER. *Nat Cell Biol*, 3, 473-83.

Pelkmans, L., Puntener, D. & Helenius, A. 2002. Local actin polymerization and dynamin recruitment in SV40-induced internalization of caveolae. *Science*, 296, 535-9.

Pires, P., Simoes, S., Nir, S., Gaspar, R., Duzgunes, N. & De Lima, M. C. P. 1999. Interaction of cationic liposomes and their DNA complexes with monocytic leukemia cells. *Biochimica Et Biophysica Acta-Biomembranes*, 1418, 71-84.

Pollard, H., Remy, J. S., Loussouarn, G., Demolombe, S., Behr, J. P. & Escande, D. 1998. Polyethylenimine but not cationic lipids promotes transgene delivery to the nucleus in mammalian cells. *Journal of Biological Chemistry*, 273, 7507-11.

Ponnappa, B. C. 2009. siRNA for inflammatory diseases. *Current Opinion in Investigational Drugs*, 10, 418-424.

Prasad, T. K., Gopal, V. & Rao, N. M. 2003. Structural changes in DNA mediated by cationic lipids alter in vitro transcriptional activity at low charge ratios. *Biochimica Et Biophysica Acta-General Subjects*, 1619, 59-69.



Reischl, D. & Zimmer, A. 2009. Drug delivery of siRNA therapeutics: potentials and limits of nanosystems. *Nanomedicine-Nanotechnology Biology and Medicine*, 5, 8-20.

Rejman, J., Bragonzi, A. & Conese, M. 2005. Role of clathrin- and caveolae-mediated endocytosis in gene transfer mediated by lipo- and polyplexes. *Molecular Therapy*, 12, 468-474.

Rejman, J., Conese, M. & Hoekstra, D. 2006. Gene transfer by means of lipo- and polyplexes: Role of clathrin and caveolae-mediated endocytosis. *Journal of Liposome Research*, 16, 237-247.

Rejman, J., Oberle, V., Zuhorn, I. S. & Hoekstra, D. 2004. Size-dependent internalization of particles via the pathways of clathrin- and caveolae-mediated endocytosis. *Biochemical Journal*, 377, 159-169.

Resina, S., Prevot, P. & Thierry, A. R. 2009. Physico-Chemical Characteristics of Lipoplexes Influence Cell Uptake Mechanisms and Transfection Efficacy. *Plos One*, 4.

Ross, P. C. & Hui, S. W. 1999a. Lipoplex size is a major determinant of in vitro lipofection efficiency. *Gene Therapy*, 6, 651-659.

Ross, P. C. & Hui, S. W. 1999b. Polyethylene glycol enhances lipoplex-cell association and lipofection. *Biochimica Et Biophysica Acta-Biomembranes*, 1421, 273-283.

Sakurai, F., Inoue, R., Nishino, Y., Okuda, A., Matsumoto, O., Taga, T., Yamashita, F., Takakura, Y. & Hashida, M. 2000a. Effect of DNA/liposome mixing

ratio on the physicochemical characteristics, cellular uptake and intracellular trafficking of plasmid DNA/cationic liposome complexes and subsequent gene expression. *Journal of Controlled Release*, 66, 255-269.

Sakurai, F., Inoue, R., Nishino, Y., Okuda, A., Matsumoto, O., Taga, T., Yamashita, F., Takakura, Y. & Hashida, M. 2000b. Effect of DNA/liposome mixing ratio on the physicochemical characteristics, cellular uptake and intracellular trafficking of plasmid DNA/cationic liposome complexes and subsequent gene expression (vol 66, pg 255, 2000). *Journal of Controlled Release*, 69, 219-220.

Sakurai, F., Nishioka, T., Yamashita, F., Takakura, Y. & Hashida, M. 2001. Effects of erythrocytes and serum proteins on lung accumulation of lipoplexes containing cholesterol or DOPE as a helper lipid in the single-pass rat lung perfusion system. *European Journal of Pharmaceutics and Biopharmaceutics*, 52, 165-172.

Salvati, A., Ciani, L., Ristori, S., Martini, G., Masi, A. & Arcangeli, A. 2006. Physico-chemical characterization and transfection efficacy of cationic liposomes containing the pEGFP plasmid. *Biophysical Chemistry*, 121, 21-29.

Sanders Nn, D. S. S., Cheng Sh, Demeester J 2002. Pegylated GL67 lipoplexes retain their gene transfection activity after exposure to components of CF mucus. *Gene Therapy*, 9, 363-71.

Santel, A., Aleku, M., Keil, O., Endruschat, J., Esche, V., Durieux, B., Löffler, K., Fechtner, M., Rohl, T., Fisch, G., Dames, S., Arnold, W., Giese, K., Klippel, A. & Kaufmann, J. 2006. RNA interference in the mouse vascular endothelium by systemic administration of siRNA-lipoplexes for cancer therapy. *Gene Therapy*, 13, 1360-1370.

Scherer, L. J. & Rossi, J. J. 2003. Approaches for the sequence-specific knockdown of mRNA. *Nat Biotechnol*, 21, 1457-65.

Schnitzer, J. E., Oh, P., Pinney, E. & Allard, J. 1994. Filipin-Sensitive Caveolae-Mediated Transport in Endothelium - Reduced Transcytosis, Scavenger Endocytosis, and Capillary-Permeability of Select Macromolecules. *Journal of Cell Biology*, 127, 1217-1232.

Schroeder, A., Levins, C. G., Cortez, C., Langer, R. & Anderson, D. G. 2010. Lipid-based nanotherapeutics for siRNA delivery. *Journal of Internal Medicine*, 267, 9-21.

Shi F, W. L., Nomden a, Stuart M C a, Polushkin E, Engberts J and Hoekstra D 2002. Interference of poly (ethylene glycol)-lipid analogues with cationic-lipid-mediated delivery of oligonucleotides; role of lipid exchangeability and non-lamellar transitions. *Biochemical Journal*, 366.

Shrivastava, N. & Srivastava, A. 2008. RNA interference: an emerging generation of biologicals. *Biotechnol J*, 3, 339-53.

Simberg, D., Danino, D., Talmon, Y., Minsky, A., Ferrari, M. E., Wheeler, C. J. & Barenholz, Y. 2001. Phase behavior, DNA ordering, and size instability of cationic lipoplexes - Relevance to optimal transfection activity. *Journal of Biological Chemistry*, 276, 47453-47459.

Simberg, D., Weiss, A. & Barenholz, Y. 2005. Reversible mode of binding of serum proteins to DOTAP/cholesterol lipoplexes: A possible explanation for intravenous lipofection efficiency. *Human Gene Therapy*, 16, 1087-1096.

Sioud, M. & Sorensen, D. R. 2003. Cationic liposome-mediated delivery of siRNAs in adult mice. *Biochem Biophys Res Commun*, 312, 1220-5.

Smart, E. J., Graf, G. A., Mcniven, M. A., Sessa, W. C., Engelman, J. A., Scherer, P. E., Okamoto, T. & Lisanti, M. P. 1999. Caveolins, liquid-ordered domains, and signal transduction. *Mol Cell Biol*, 19, 7289-304.

Smisterova, J., Wagenaar, A., Stuart, M. C., Polushkin, E., Ten Brinke, G., Hulst, R., Engberts, J. B. & Hoekstra, D. 2001. Molecular shape of the cationic lipid controls the structure of cationic lipid/dioleoylphosphatidylethanolamine-DNA complexes and the efficiency of gene delivery. *Journal of Biological Chemistry*, 276, 47615-22.

Song, L. Y., Ahkong, Q. F., Rong, Q., Wang, Z., Ansell, S., Hope, M. J. & Mui, B. 2002. Characterization of the inhibitory effect of PEG-lipid conjugates on the intracellular delivery of plasmid and antisense DNA mediated by cationic lipid liposomes. *Biochimica Et Biophysica Acta-Biomembranes*, 1558, 1-13.

Spagnou, S., Miller, A. D. & Keller, M. 2004. Lipidic carriers of siRNA: differences in the formulation, cellular uptake, and delivery with plasmid DNA. *Biochemistry*, 43, 13348-56.

Spelios, M., Kearns, M. & Savva, M. 2010. From gene delivery to gene silencing: plasmid DNA-transfecting cationic lipid 1,3-dimyristoylamidopropane-2-[bis(2-dimethylaminoethane)] carbamate efficiently promotes small interfering RNA-induced RNA interference. *Biochemistry*, 49, 5753-9.

Steimer, A., Haltner, E. & Lehr, C. M. 2005. Cell culture models of the respiratory tract relevant to pulmonary drug delivery. *Journal of Aerosol Medicine-Deposition Clearance and Effects in the Lung*, 18, 137-182.

Sternberg, B., Hong, K. L., Zheng, W. W. & Papahadjopoulos, D. 1998. Ultrastructural characterization of cationic liposome-DNA complexes showing enhanced stability in serum and high transfection activity in vivo. *Biochimica Et Biophysica Acta-Biomembranes*, 1375, 23-35.

Swanson, J. A. & Watts, C. 1995. Macropinocytosis. *Trends in Cell Biology*, 5, 424-8.

Takei, K. & Haucke, V. 2001. Clathrin-mediated endocytosis: membrane factors pull the trigger. *Trends in Cell Biology*, 11, 385-391.

Takeshita, F. & Ochiya, T. 2006. Therapeutic potential of RNA interference against cancer. *Cancer Sci*, 97, 689-96.

The U.S. National Institutes Health. ClinicalTrials.gov [Online]. Available: <http://clinicaltrials.gov/ct2/home> [Accessed Oct 2011].

Thomas, M., Lu, J. J., Chen, J. & Klibanov, A. M. 2007. Non-viral siRNA delivery to the lung. *Adv Drug Deliv Rev*, 59, 124-33.

Thoren, P. E., Persson, D., Isakson, P., Goksor, M., Onfelt, A. & Norden, B. 2003. Uptake of analogs of penetratin, Tat(48-60) and oligoarginine in live cells. *Biochem Biophys Res Commun*, 307, 100-7.

Tijsterman, M., May, R. C., Simmer, F., Okihara, K. L. & Plasterk, R. H. 2004. Genes required for systemic RNA interference in *Caenorhabditis elegans*. *Curr Biol*, 14, 111-6.

Tijsterman, M., Okihara, K. L., Thijssen, K. & Plasterk, R. H. 2002. PPW-1, a PAZ/PIWI protein required for efficient germline RNAi, is defective in a natural isolate of *C. elegans*. *Curr Biol*, 12, 1535-40.

Tomlinson, E. & Rolland, A. P. 1996. Controllable gene therapy - Pharmaceutics of non-viral gene delivery systems. *Journal of Controlled Release*, 39, 357-372.

Tranchant, I., Thompson, B., Nicolazzi, C., Mignet, N. & Scherman, D. 2004. Physicochemical optimisation of plasmid delivery by cationic lipids. *Journal of Gene Medicine*, 6, S24-S35.

Trehin, R. & Merkle, H. P. 2004. Chances and pitfalls of cell penetrating peptides for cellular drug delivery. *European Journal of Pharmaceutics and Biopharmaceutics*, 58, 209-23.

Tseng, Y. C., Mozumdar, S. & Huang, L. 2009. Lipid-based systemic delivery of siRNA. *Adv Drug Deliv Rev*, 61, 721-31.

Van Der Aa, M. a. E. M., Huth, U. S., Hafele, S. Y., Schubert, R., Oosting, R. S., Mastrobattista, E., Hennink, W. E., Peschka-Suss, R., Koning, G. A. & Crommelin, D. J. A. 2007. Cellular uptake of cationic polymer-DNA complexes via caveolae plays a pivotal role in gene transfection in COS-7 cells. *Pharm Res*, 24, 1590-1598.

Veldhoen, S., Laufer, S. D. & Restle, T. 2008. Recent developments in peptide-based nucleic acid delivery. *International Journal of Molecular Sciences*, 9, 1276-1320.

Veldhoen, S., Laufer, S. D., Trampe, A. & Restle, T. 2006. Cellular delivery of small interfering RNA by a non-covalently attached cell-penetrating peptide: quantitative analysis of uptake and biological effect. *Nucleic Acids Res*, 34, 6561-6573.

Vp, T. 1994. Immunoliposomes and PEGylated immunoliposomes: possible use for targeted delivery of imaging agents. *Immunomethods*, 4, 244-58.

Wadia, J. S., Stan, R. V. & Dowdy, S. F. 2004. Transducible TAT-HA fusogenic peptide enhances escape of TAT-fusion proteins after lipid raft macropinocytosis. *Nature Medicine*, 10, 310-315.

Wagner, E., Zenke, M., Cotten, M., Beug, H. & Birnstiel, M. L. 1990. Transferrin-Polycation Conjugates as Carriers for DNA Uptake into Cells. *Proc Natl Acad Sci U S A*, 87, 3410-3414.

Wang, L. H., Rothberg, K. G. & Anderson, R. G. W. 1993. Mis-Assembly of Clathrin Lattices on Endosomes Reveals a Regulatory Switch for Coated Pit Formation. *Journal of Cell Biology*, 123, 1107-1117.

Wasungu, L. & Hoekstra, D. 2006. Cationic lipids, lipoplexes and intracellular delivery of genes. *Journal of Controlled Release*, 116, 255-64.

Wattiaux R, L. N., Wattiaux-De Coninck S, Jadot M 2000. Endosomes, lysosomes: their implication in gene transfer. *Adv Drug Deliv Rev*, 41, 201-8.

Webb, M. S., Saxon, D., Wong, F. M., Lim, H. J., Wang, Z., Bally, M. B., Choi, L. S., Cullis, P. R. & Mayer, L. D. 1998. Comparison of different hydrophobic anchors conjugated to poly(ethylene glycol): effects on the pharmacokinetics of liposomal vincristine. *Biochim Biophys Acta*, 1372, 272-82.

Wiethoff, C. M., Koe, J. G., Koe, G. S. & Middaugh, C. R. 2004. Compositional effects of cationic lipid/DNA delivery systems on transgene expression in cell culture. *Journal of Pharmaceutical Sciences*, 93, 108-123.

William A. Dunn, A. L. H., And Nathan N. Aronson 1980. Low temperature selectively inhibits fusion between pinocytic Vesicles and lysosomes during heterophagy of <sup>125</sup>I-Asialofetuin by the perfused rat liver. *The Journal of Biological Chemistry*, 255, 5971-5978.

Wolff, J. A. & Rozema, D. B. 2008. Breaking the bonds: non-viral vectors become chemically dynamic. *Molecular Therapy*, 16, 8-15.

Wong, A. W., Scales, S. J. & Reilly, D. E. 2007. DNA internalized via Caveolae requires microtubule-dependent, Rab7-independent transport to the late endocytic pathway for delivery to the nucleus. *Journal of Biological Chemistry*, 282, 22953-22963.

Wu, S. Y. & Mcmillan, N. A. 2009. Lipidic systems for in vivo siRNA delivery. *AAPS J*, 11, 639-52.

Xu, Y., Hui, S. W., Frederik, P. & Szoka, F. C., Jr. 1999. Physicochemical characterization and purification of cationic lipoplexes. *Biophys J*, 77, 341-53.



Xu, Y. & Szoka, F. C., Jr. 1996. Mechanism of DNA release from cationic liposome/DNA complexes used in cell transfection. *Biochemistry*, 35, 5616-23.

Yadava, P., Roura, D. & Hughes, J. A. 2007. Evaluation of two cationic delivery systems for siRNA. *Oligonucleotides*, 17, 213-22.

Yang, J. P. & Huang, L. 1998. Time-dependent maturation of cationic liposome-DNA complex for serum resistance. *Gene Therapy*, 5, 380-387.

Yang, S. T., Marchio, J. L. & Yen, J. W. 1994. A dynamic light scattering study of beta-galactosidase: environmental effects on protein conformation and enzyme activity. *Biotechnol Prog*, 10, 525-31.

Zhang, S., Zhao, B., Jiang, H., Wang, B. & Ma, B. 2007. Cationic lipids and polymers mediated vectors for delivery of siRNA. *Journal of Controlled Release*, 123, 1-10.

Zhang, Y. & Anchordoquy, T. J. 2004. The role of lipid charge density in the serum stability of cationic lipid/DNA complexes. *Biochimica Et Biophysica Acta-Biomembranes*, 1663, 143-157.

Zhang, Y., Li, H., Sun, J., Gao, J., Liu, W., Li, B., Guo, Y. & Chen, J. 2010. DC-Chol/DOPE cationic liposomes: a comparative study of the influence factors on plasmid pDNA and siRNA gene delivery. *Int J Pharm*, 390, 198-207.

Zhdanov, R. I., Podobed, O. V. & Vlassov, V. V. 2002. Cationic lipid-DNA complexes-lipoplexes-for gene transfer and therapy. *Bioelectrochemistry*, 58, 53-64.

Zhou, X. H. & Huang, L. 1994. DNA Transfection Mediated by Cationic Liposomes Containing Lipopolylysine - Characterization and Mechanism of Action. *Biochimica Et Biophysica Acta-Biomembranes*, 1189, 195-203.

Zimmermann, T. S., Lee, A. C. H., Akinc, A., Bramlage, B., Bumcrot, D., Fedoruk, M. N., Harborth, J., Heyes, J. A., Jeffs, L. B., John, M., Judge, A. D., Lam, K., Mcclintock, K., Nechev, L. V., Palmer, L. R., Racie, T., Rohl, I., Seiffert, S., Shanmugam, S., Sood, V., Soutschek, J., Toudjarska, I., Wheat, A. J., Yaworski, E., Zedalis, W., Koteliansky, V., Manoharan, M., Vornlocher, H. P. & MacLachlan, I. 2006. RNAi-mediated gene silencing in non-human primates. *Nature*, 441, 111-114.

Zuhorn, I. S., Kalicharan, R. & Hoekstra, D. 2002a. Lipoplex-mediated transfection of mammalian cells occurs through the cholesterol-dependent clathrin-mediated pathway of endocytosis. *Journal of Biological Chemistry*, 277, 18021-18028.

Zuhorn, I. S., Visser, W. H., Bakowsky, U., Engberts, J. B. & Hoekstra, D. 2002b. Interference of serum with lipoplex-cell interaction: modulation of intracellular processing. *Biochim Biophys Acta*, 1560, 25-36.

Zuidam Nj, B. Y. 1998. Electrostatic and structural properties of complexes involving plasmid DNA and cationic lipids commonly used for gene delivery. *Biochem Biophys Acta*, 1368, 115-128.

Zuidam, N. J., Hirsch-Lerner, D., Margulies, S. & Barenholz, Y. 1999. Lamellarity of cationic liposomes and mode of preparation of lipoplexes affect transfection efficiency. *Biochimica Et Biophysica Acta-Biomembranes*, 1419, 207-220.

